IRE Transactions

on Microwave Theory and Techniques

IEEE transactions on microwave theory and technique

Volume MTT-6 **JANUARY, 1958** Number 1

In This Issue

For complete Table of Contents, see page 1.

PUBLISHED BY THE

essional Group on Microwave Theory and Techniques

IRE PROFESSIONAL GROUP ON MICROWAVE THEORY AND TECHNIQUES

The Professional Group on Microwave Theory and Techniques is an association of IRE members with professional interest in the field of Microwave Theory and Techniques. All IRE members are eligible for membership and will receive all Group publications upon payment of the prescribed annual fee of $3.00. Members of the American Physical Society may become affiliated with PGMTT and receive all Group publications upon payment of the Affiliate fee of $7.50 per year.

PGMTT Chapters

Albuquerque-Los Alamos	H. D. Finch	New York	Saul Rosenthal
Baltimore	W. R. Hom	Northern New Jersey	Nat Evans
Boston	P. D. Strum	Philadelphia	E. J. Forbes
Buffalo-Niagara	Robert E. Kell	San Diego	J. B. Smyth
Chicago	Edward Dervishian	San Francisco	W. H. Thon
Long Island	Henry Jasik	Schenectady	T. R. Bristol
Los Angeles	Dean Anderson	Syracuse	W. T. Whistler
	Washington	Gustave Shapiro	

IRE TRANSACTIONS®

on Microwave Theory and Techniques

Published by the Institute of Radio Engineers, Inc., for the Professional Group on Microwave Theory and Techniques, at 1 East 79th Street, New York 21, New York. Responsibility for the contents rests upon the authors, and not upon the IRE, the Group, or its members. Price per copy: IRE PGMTT members, $2.65; IRE members, $3.95, nonmembers, $7.95. Annual subscription price: IRE members, $8.50; colleges and public libraries, $12.75; nonmembers, $17.00.

Address all manuscripts to K. Tomiyasu, PGMTT Editor, General Electric Microwave Laboratory, 601 California Ave., Palo Alto, Calif. Submission of three copies of manuscripts, including figures, will expedite the review.

IRE Transactions on Microwave Theory and Techniques

Published by the Professional Group on Microwave Theory and Techniques

Volume MTT-6 JANUARY, 1958 Number 1

TABLE OF CONTENTS

CONTRIBUTIONS

CORRESPONDENCE

PGMTT NEWS

Clarence Lester Hogan

Clarence Lester Hogan was born on February 8, 1920, in Great Falls, Mont. He received the B.S. degree in chemical engineering from Montana State College in 1942. While an undergraduate he was elected to Phi Kappa Phi and Tau Beta Pi and received two awards: the American Chemical Society Award, based on an election by the faculty and student body, and given to a junior student showing great promise for professional development, and the Montana Society of Engineers Gold Medal, given to the most outstanding senior in the College of Engineering. Among his extra curricular activities were the offices of editor-in-chief of the college publication, *The Montana Engineer*, and vice-president of Kappa Sigma.

Following his graduation from Montana State College he was employed for one year as a research engineer at Anaconda Copper Mining Company, Great Falls, Mont. He then served as an officer in the United States Navy for three years during which time he was officer-in-charge of the acoustic torpedo shop at Pearl Harbor for two years.

Dr. Hogan pursued his graduate studies at Lehigh University and was awarded the degrees of M.S. and Ph.D. in physics in 1947 and 1950, respectively. His major fields of study were solid-state and electromagnetic theory, and his doctoral dissertation was titled "The Thermal Conductivity of Metals at High Temperature." He became affiliated with Sigma Xi in 1948. Dr. Hogan held a full-time instructorship in the Physics Department at Lehigh University teaching several courses in physics and electronics.

In 1950, Dr. Hogan became a member of the technical staff at Bell Telephone Laboratories, Murray Hill, N. J. Thereafter, he became intrigued with the feasibility of a nonreciprocal element at microwave frequencies. His logic soon led to the combination of electrons immersed in a magnetic field and the problem very rapidly centered on that of a suitable material. Utilizing his knowledge in physics and chemistry, his attention focused on iron oxides in crystalline structures and this resulted in the investigation and development of new ferrite materials.

Dr. Hogan performed experiments which demonstrated nonreciprocity at microwave frequencies and carried out a theoretical analysis substantiating the experiments. This early work, now a classical reference, was published in January, 1952 in the *Bell System Technical Journal* under the title, "The Ferromagnetic Faraday Effect at Microwave Frequencies and Its Applications."

In 1953, Dr. Hogan accepted the position of Associate Professor of Applied Physics at Harvard University, Cambridge, Mass., where he has been actively extending the knowledge of ferrites. By realizing that the basic limitations in the application of ferrites will be due to the material itself, Dr. Hogan and his graduate students at Harvard University studied new single crystals and rare-earth-element ferrites. The investigations contributed to the development of phenomenally low-loss ferrite garnets which greatly lower the operational frequencies of ferrite devices. The extent of the significance of Dr. Hogan's early experiments on nonreciprocity cannot yet be predicted.

Dr. Hogan organized and led the widely acclaimed Symposium on Microwave Properties and Applications of Ferrites which was held at Harvard University on April 2–4, 1956. He later edited the October, 1956 issue of the PROCEEDINGS OF THE IRE which was a special issue featuring the papers presented at this Symposium.

He has published nine articles, presented twenty-five invited seminars and papers, holds two patents, and has consulted for six industrial laboratories. He is a member of the American Physical Society, Technical Panel on Magnetic Materials (Materials Advisory Board for the Department of Defense), Subcommittee on Magnetic Materials (AIEE), Second Vice-President of Harvard Engineering Society, Conference on Electrical Engineering Education (sponsored by National Science Foundation), and the Advisory Council of the Department of Electrical Engineering of Princeton University. He is also a Senior Member of the Institute of Radio Engineers and a member of the Executive Committee of the Boston IRE Section.

In 1957 Dr. Hogan was promoted to Gordon McKay Professor of Applied Physics at Harvard University.

The Pace of Modern Technology

In 1946, J. H. E. Griffiths published in *Nature* the first account of an experimental observation of the phenomenon of ferromagnetic resonance. Naturally enough this paper elicited little interest from electrical engineers, nor did the theoretical work of C. Kittel and D. Polder published during the next three years which gave a quantitative explanation of Griffith's experiment. Now, however, approximately eight years after Polder's rather complete theoretical paper on ferromagnetic resonance this issue of an engineering journal is devoted exclusively to the practical ramifications of this first experimental observation. Many of the devices referred to in this issue are beyond the development stage and are already in widespread use in microwave systems. Although the delay between research and development and between development and production usually seems interminably long to those most actively associated with the development of engineering devices, it appears, in retrospect at least, that in this case the progress has been almost astounding. In fact, it is illuminating to go back to the beginning of the electronic era and look at the basic experiments which led to the development of the vacuum tube in order to see how our technological timetable has been greatly compressed during the last fifty years.

Actually as early as 1725, DuFay discovered that the region surrounding a red-hot body was a conductor of electricity, but the first definitive experiments which showed conclusively that electrons could pass from a hot filament to a cold plate were performed by Edison in 1883 (158 years after DuFay's observation). Even so, it was not until 1905 that Fleming developed the diode and DeForest added a third electrode known as the grid in 1907, 24 years after Edison's experiments. If the same timetable were in effect today, the first practical engineering device based upon the phenomenon of ferromagnetic resonance would not be constructed until sometime after 1968 and this issue of the TRANSACTIONS of the PGMTT could not become a reality until most of us had retired from active engineering practice.

It is not our purpose here to account for the various factors which make this progress possible nor to imagine what our engineering specialty will be like even twenty years from now if this rate of productivity continues to increase. Instead it is sufficient merely to point out the tremendously rapid transition that has been made from fundamental physical research to engineering practice in this particular instance and to contend that this example does not represent an isolated phenomenon but more nearly describes typical creative engineering activity as it exists today. In fact, we sometimes find our profession pressing so hard upon the latest results of the solid-state physicist that engineering demand is becoming a common criterion which the experimental physicist uses to shape the course of his experiments. A natural result of this progress is that we, as engineers, are forced into ever closer alliance with physicists and physical research.

This journal reports the proceedings of a meeting held in May, 1957. That meeting covered as completely as possible the latest advances in the microwave ferrite art. Now, however, approximately six months later, newer and in some respects more exciting applications of ferromagnetic resonance than those described in this issue have been reduced to practice in many laboratories. These newer devices include: 1) harmonic generators; 2) passive microwave amplitude limiters; 3) low-noise microwave amplifiers; and 4) efficient microwave detectors which promise to cover all wavelengths from a fraction of a millimeter to several centimeters. Some of these newer devices are based on the theoretical work of H. Suhl which was first published in the October, 1956 issue of the PROCEEDINGS OF THE IRE. Most of these new devices appear practical because within the last year new materials (the ferromagnetic garnets) have been made available to us. In addition to their obvious engineering potentialities, these materials promise to give a tremendous boom to our fundamental understanding of the properties of ferromagnetic materials and thus, perhaps, give us the knowledge needed to produce a great myriad of engineering devices which we are not able even to conceive of today.

It appears evident, however, that we are only at the beginning of a tremendous revolution in high-frequency communication techniques which has been made possible by mankind's increasing knowledge of the behavior of solid-state materials. We are fortunate to be part of a profession that allows us to take part in this exciting progress.

CLARENCE LESTER HOGAN

Foreword

With the tremendous advances being made in the microwave ferrite field and solid-state microwave devices, and with the success of the Harvard Symposium in April, 1956, it was felt that further symposia were desired on the subject especially at the radio engineers' level. Hence, it was proposed that the Long Island, New York, and Northern New Jersey Chapters of the PGMTT hold a jointly sponsored meeting on the subject during the 1956–1957 season.

The Northern New Jersey Chapter, under the chairmanship of Robert Mac Veety, proposed to the Administrative Committee of the PGMTT that a jointly sponsored meeting be held. Because of the interest in the subject, it was decided that we should make this the subject for the annual meeting of the PGMTT with the committee made up of members of the Long Island, New York, and Northern New Jersey Chapters of the PGMTT.

It therefore was decided to call this the 1957 Annual PGMTT Meeting, and the general plans for this symposium were formulated at a Steering Committee Meeting held in October, 1956. Originally it was hoped that this symposium might be held in January, 1957, but it was felt that this was impossible because of the short schedule and the meeting date was changed to May 9th and 10th. The general plans were formulated by the Steering Committee, composed of the following members:

T. N. Anderson, Airtron, Inc., Linden, N. J.
B. J. Duncan, Sperry Gyroscope Co., Great Neck, N. Y.
R. Mac Veety, RMC Associates, Bogota, N. J.
J. L. Melchor, Microwave Engineering Labs., Palo Alto, Calif.
W. W. Mumford, Bell Telephone Labs., Whippany, N. J.
H. E. D. Scovil, Bell Telephone Labs., Murray Hill, N. J.
E. N. Torgow, Microwave Research Institute, Brooklyn, N. Y.
S. W. Rosenthal, Microwave Research Institute, Brooklyn, N. Y.
S. Weisbaum, Bell Telephone Labs., Murray Hill, N. J.
R. D. Wengenroth, Wheeler Labs., Great Neck, N. Y.

The detail plans and work involved were handled by Subcommittees from the Chapters as follows:

Treasurer—Long Island Chapter
Karle S. Packard, Airborne Instruments Labs., Mineola, N. Y.
Local Arrangements—New York Chapter
Moe Wind, Polytechnic Research and Development Co., Brooklyn, N. Y.
Publicity and Organization—Northern New Jersey
Tore N. Anderson, Airtron, Inc., Linden, N. J.

Three invited papers were selected to preview the state of the art in microwave ferrites, nonreciprocal electromagnetic propagation in ionized gaseous media and in solid-state microwave amplifiers. Then from over thirty papers received, twenty papers were selected as having the most general interest for the purpose of the meeting, and sessions were basically divided into: 1) Material characteristics, 2) theoretical papers showing basic theory and 3) microwave devices.

At the end of this session of the symposium a round table discussion was held by Dr. C. L. Hogan of Harvard University with the following panel members:

Dr. H. Seidel, Bell Telephone Labs., Murray Hill, N. J.
Dr. G. S. Heller, M.I.T., Lincoln Lab., Lexington, Mass.
Dr. R. C. LeCraw, Diamond Ordnance Fuze Labs., Washington, D. C.
Dr. J. O. Artman, Harvard University, Cambridge, Mass.
Dr. P. H. Vartanian, Microwave Engineering Labs., Palo Alto, Calif.
Dr. H. J. Carlin, Microwave Research Institute, Brooklyn, N. Y.
Dr. D. L. Fresh, Trans-Tech, Inc., Rockville, Md.

There was considerable interest in the panel discussion and recordings of the remarks of the panel members and from the floor were made for publication.

Thanks are due to all the members of the Steering Committee for their guidance and help in planning this symposium, and to the Chairmen and Members of the Subcommittees.

We are indebted to the Western Union Company for the use of their auditorium at no charge. The annual PGMTT award for the best paper published in these TRANSACTIONS was announced at a cocktail party and dinner held at the Three Crowns Restaurant.

TORE N. ANDERSON
Chairman, 1957 Annual PGMTT Meeting

The Status of Microwave Applications of Ferrites and Semiconductors*

BENJAMIN LAX†

Summary—The recent developments in the field of ferrite devices are reviewed. Emphasis is placed on the extension of nonreciprocal devices to lower microwave frequencies and high powers. The design considerations and achievements of broad banding also are covered. Fundamental principles leading to the applications of nonlinear properties of ferrites are described briefly. Preliminary experimental accomplishments in the construction of frequency doublers, mixers, and ferromagnetic resonance amplifiers are summarized. The possible role of the new ferrimagnetic garnet material is indicated. Although no significant new semiconductor devices have been developed at microwave frequencies, possibilities are considered for doing this with use of cyclotron resonance and spin resonance phenomena and their related properties in semiconductors.

Introduction

THIS paper's object is to review the developments in the application of ferrites at microwave frequencies during the last two years. The emphasis is placed on the improvements of existing devices, their extension to lower frequencies, to higher power, and the consideration of broad banding these devices. New developments, such as the ferromagnetic amplifier and nonlinear devices, also are discussed in terms of the basic ideas and research which has led to these new devices. The four devices which have received a great deal of attention are the ones using the Faraday rotation phenomenon, the nonreciprocal phase shifter in rectangular waveguide, the resonance isolator, and the field-displacement isolator. The problems taken up in regard to these devices are the considerations of the principles involved in broad banding and in improving performance at lower frequencies and higher power. Some of these problems have been reviewed in previous articles,[1–8] which have shown that one of the most important problems associated with achieving these objectives is the magnetic losses in the ferrite.

One contribution is the low-field loss in the ferrite when it is in the unmagnetized state. This arises from the existence of internal fields consisting of the effective anisotropy field and the magnetic field induced inside the ferrite by the magnetic charges created on the domain walls by the rf field.

The second type of magnetic loss is that associated with ferromagnetic resonance in the ferrite when it is in the magnetized state. One way to minimize the low-field loss has been offered by the synthesis of diluted ferrites with low magnetization[9] and low anisotropy fields. The residual loss then is negligible in the partially magnetized state, the usual one employed in operating ferrite devices with applied dc magnetic fields below resonance. Another solution for avoiding the low-field loss, suggested by R. H. Fox,[10] is the operation of the ferrite in a completely magnetized state with larger dc fields above resonance. This particular scheme has been employed recently by Stern[11] to build a high-power phase shifter at *S* band.

The low-frequency limit of the four classes of devices, however, has been determined primarily by the losses attributed to the ferromagnetic resonance phenomenon in ferrites.[7,12] As is indicated later, the important factor which describes the loss at a given frequency is the resonance line width of the ferrite. It is important that the line width be made as narrow as possible in order to reduce the loss associated with ferromagnetic resonance. Considerable effort has been made to develop ferrites which have narrow resonance lines. The most successful results have been achieved with a new ferrimagnetic material called the yttrium-iron garnet. The synthesis of this material has been reported by Bertaut and Forrat[13] and by Geller and Gilleo.[14] The microwave properties of single crystals of this material have been measured

* Manuscript received by the PGMTT, August 12, 1957. The research reported in this paper was supported jointly by the U. S. Army, Navy, and Air Force under contract with Mass. Inst. Tech., Cambridge, Mass.

† Lincoln Lab., M.I.T., Lexington, Mass.

[1] C. L. Hogan, "The ferromagnetic Faraday effect at microwave frequencies and its applications," *Rev. Mod. Phys.*, vol. 25, p. 253; January, 1953.

[2] J. H. Rowen, "Ferrites in microwave applications," *Bell Sys. Tech. J.*, vol. 32, p. 1333; November, 1953.

[3] M. L. Kales, "Propagation of fields through ferrite loaded waveguides," *Proc. Symp. on Modern Advances in Microwave Techniques*, Polytechnic Inst. of Brooklyn, Brooklyn, N. Y., p. 215; November, 1954.

[4] B. Lax, "Fundamental design principles of ferrite devices," *Proc. Symp. on Modern Advances in Microwave Techniques*, Polytechnic Inst. of Brooklyn, Brooklyn, N. Y., p. 229; November, 1954.

[5] A. G. Fox, S. E. Miller, and M. T. Weiss, "Behavior and applications of ferrites in the microwave region," *Bell Sys. Tech. J.*, vol. 34, p. 5; January, 1955.

[6] C. L. Hogan, "The elements of nonreciprocal microwave devices," PROC. IRE, vol. 44, pp. 1345–1368; October, 1956.

[7] B. Lax, "Frequency and loss characteristics of microwave ferrite devices," PROC. IRE, vol. 44, pp. 1368–1386; October, 1956.

[8] P. J. B. Clarricoats, A. G. Hayes, and A. F. Harvey, "A survey of the theory and applications of ferrites at microwave frequencies," *Proc. IEE*, vol. 104 B, p. 267; October, 1956.

[9] L. G. Van Uitert, J. P. Shafer, and C. L. Hogan, "Low-loss ferrites for applications at 4000 megacycles per second," *J. Appl. Phys.*, vol. 25, p. 925; July, 1954.
L. G. Van Uitert, "Low magnetic saturation ferrites for microwave applications," *J. Appl. Phys.*, vol. 26, p. 1289; November, 1955.

[10] R. H. Fox, "Extension of nonreciprocal ferrite devices to the 500–3000 megacycle frequency range," *J. Appl. Phys.*, vol. 26, p. 128; January, 1955.

[11] E. Stern, private communication.

[12] B. Lax, "A figure of merit for microwave ferrites at low and high frequencies," *J. Appl. Phys.*, vol. 26, p. 919; July, 1955.

[13] F. Bertaut and F. Forrat, "Structure des ferrites ferrimagnetiques des terres rares," *Compt. Rend.*, vol. 242, p. 382; 1956.
F. Bertaut and R. Pauthenet, "Crystalline structure and magnetic properties of ferrites having the general formula $5Fe_2O_3\,3M_2O_3$," *Proc. IEE*, vol. 104 B, p. 261; October, 1956.

[14] S. Geller and M. A. Gilleo, "Structure and ferrimagnetism of yttrium and rare earth-iron garnets," *Acta Cryst.*, to be published.

by Dillon and more recently by others.[15] The magnetic properties and crystal structure of this class of ferrimagnetics have been discussed by Bertaut and Pauthenet.[13] The yttrium garnet, which is the first of a series of such materials, is given by

$$Fe_2^{3+}Y_3^{3+}(Fe^{3+}O_4)_3.$$

This formula can be rewritten as

$$\overset{\uparrow}{B_2}L_3\ (\overset{\downarrow}{A}\ O_4)_3$$

where A and B are the two different types of lattice sites for the magnetic ions and L represents the large rare-earth ions such as yttrium, gadolinium, etc. The arrows above the A and B ions indicate that the magnetic moments of the two sets of spins are oriented oppositely as in the ferrite which gives rise to a net magnetization, $4\pi M_s \approx 1700$ Gauss. This means that the residual loss in the unmagnetized state in this material has an upper frequency limit of about 5000 mc. The garnet also has a very high resistivity of the order of 10^6 ohm-cm. As Dillon reported, the anisotropy of this material at room temperature from the microwave resonance measurements on a single crystal is approximately 90 oersteds, or about half that of the ferrites. This is another advantage of this material since it further minimizes the residual loss in the unmagnetized state and also is partly responsible for the narrow resonance line in polycrystalline material. The latter has been reported to be as low as 50 oersteds when the garnet is made fairly dense. Finally, some single crystals of yttrium garnet have a very narrow resonance line (below 10 oersteds) at room temperature. Unlike the diluted ferrites, the yttrium garnet, with its smaller resonance line width and anisotropy, has a reasonably high Curie temperature of about 300°C.

Nonreciprocal Devices

The Faraday Rotator

Consider the effect on the Faraday rotator of the development of these new materials which possess narrower resonance lines. The resonance loss parameter enters in the following manner. An idealized limit for the figure of merit F from perturbation theory can be written as[7,12]

$$F = \frac{\theta}{\alpha} = \omega T = \frac{2H_r}{\Delta H}, \qquad (1)$$

where F is the ratio of θ, the angle of rotation, to α, the attenuation, and is approximately equal to ω, the angular frequency, times T, the phenomenological relaxation time associated with the precessional motion of the dipole. H_r is the internal field required for resonance at the frequency ω, and ΔH is the width of the resonance line at the half-power point. The relation of (1) indicates that for a given frequency, which fixes H_r, the figure of merit improves as ΔH decreases. Conversely, if the figure of merit is fixed by the system requirements, then one can go to lower and lower frequencies as ΔH becomes smaller. Considering the properties of the garnet, $\Delta H \approx 50$ oersteds for polycrystalline material, the lower frequency limit for the Faraday rotator becomes approximately 1000 mc. If one could obtain single crystals of this material of sufficiently large size, then in principle, the low-frequency limit could be extended down to approximately 200 mc if one assumes $\Delta H \approx 10$ oersteds. Of course, this presupposes the appropriate design considerations which avoid dimensional and other effects observed with single crystal material of required sizes.

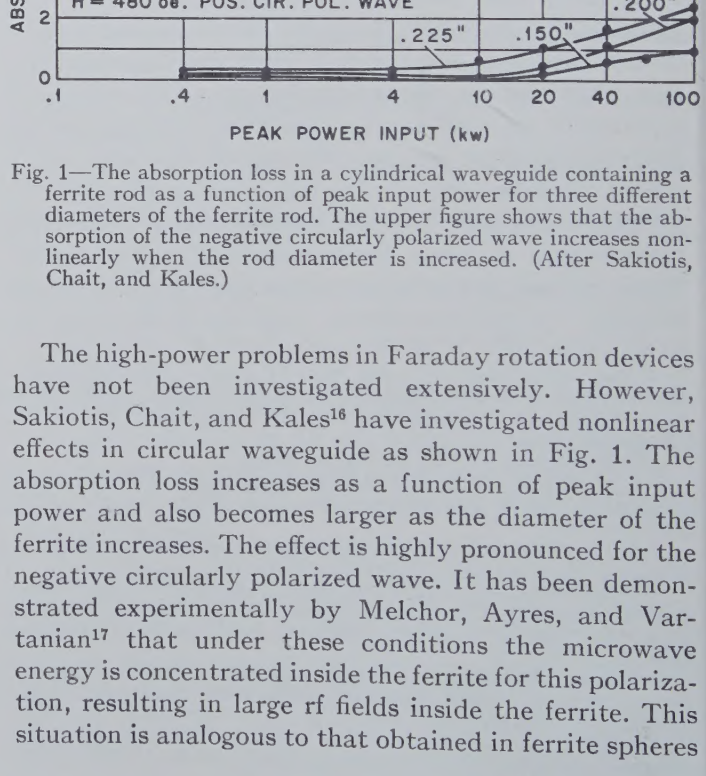

Fig. 1—The absorption loss in a cylindrical waveguide containing a ferrite rod as a function of peak input power for three different diameters of the ferrite rod. The upper figure shows that the absorption of the negative circularly polarized wave increases nonlinearly when the rod diameter is increased. (After Sakiotis, Chait, and Kales.)

The high-power problems in Faraday rotation devices have not been investigated extensively. However, Sakiotis, Chait, and Kales[16] have investigated nonlinear effects in circular waveguide as shown in Fig. 1. The absorption loss increases as a function of peak input power and also becomes larger as the diameter of the ferrite increases. The effect is highly pronounced for the negative circularly polarized wave. It has been demonstrated experimentally by Melchor, Ayres, and Vartanian[17] that under these conditions the microwave energy is concentrated inside the ferrite for this polarization, resulting in large rf fields inside the ferrite. This situation is analogous to that obtained in ferrite spheres

[15] J. F. Dillon, Jr., "Ferrimagnetic resonance in yttrium iron garnet," *Phys. Rev.*, vol. 105, p. 759; January 15, 1957.
C. P. Rodrique, J. E. Pippen, W. P. Wolf, and C. L. Hogan, "Ferrimagnetic resonance in some polycrystalline rare earth garnets," this issue, p. 83.

[16] N. Sakiotis, H. N. Chait, and M. L. Kales, "Nonlinearity of propagation in ferrite media," Proc. IRE, vol. 43, pp. 1011; August, 1955, and "Nonlinearity of microwave ferrite media," IRE Trans., vol. AP-4, pp. 111–115; April, 1956.

[17] J. L. Melchor, W. P. Ayres, and P. H. Vartanian, "Energy concentration effects in ferrite loaded wave guides," *J. Appl. Phys.*, vol. 27, p. 72; January, 1956.

in cavities by Damon[18] and by Bloembergen and Wang;[18] the large losses in these nonlinear effects are associated with instabilities as proposed by Suhl.[19]

A number of schemes has been proposed for broad banding the Faraday rotator. One such scheme, that of surrounding the ferrite rod with a dielectric sleeve, was proposed by Rowen[20] and applied by Ohm[21,22] to develop a broad-band microwave circulator. The effect of such a dielectric sleeve can be seen readily from the results of the perturbation formula which states that the Faraday rotation[7]

$$\theta \sim \sqrt{\epsilon\mu_0 - \frac{(1.84)^2}{\omega^2 R^2}} \qquad (2)$$

where θ is the angular frequency of the rf field, R is the radius of the guide, ϵ is the dielectric constant of the medium surrounding the ferrite, and μ_0 is the permeability of free space. As one increases the dielectric constant, the term containing the frequency becomes relatively smaller, making θ less frequency dependent. Perhaps the best scheme for broad banding the Faraday rotator is that suggested by Chait and reported in Kales' review article,[23] in which he used ridged circular waveguide with a ferrite rod down the center. The experiment shows that in the normal waveguide the Faraday rotation increases with frequency, which is also evident from (2). Evidently, the frequency characteristics of the ridged waveguide compensate for the frequency variation of the Faraday rotation from 8000 to 10,000 mc. Melchor and Vartanian[24] and later Wantuch[25] combined both of these schemes using a dielectric sleeve and a ridged waveguide to give a Faraday rotation of $90° \pm 1$ per cent from 8.5 to 9.6 kmc. Another very interesting technique for broad banding Faraday rotation devices has been developed by Vartanian, Melchor, and Ayres;[26] this also uses a quadruply ridged circular waveguide and two stagger-tuned Faraday rotators in tandem. The first of these gives a 45° rotation at 9.5 kmc and the second, 45° rotation at 12 kmc, as determined by the applied field to each section. This structure was used for an isolator, the characteristics of which are shown in Fig. 2. It provides greater than 30-db isolation from 8.2 to 13 kmc with less than 2-db insertion loss.

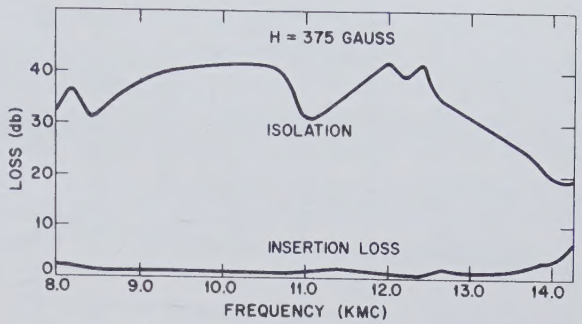

Fig. 2—The reverse and forward attenuation as a function of frequency in a Faraday rotation type isolator which has been broad banded by using both the quadruply ridged circular guide and also two stagger-tuned sections. The two sections were tuned to 9.5 and 12 kmc, respectively. (After Vartanian, Melchor, and Ayres.)

Rectangular Waveguide Phase Shifter

Some of the considerations discussed for the Faraday rotator apply also to the rectangular waveguide phase shifter. The low-frequency limit, when analyzed quantitatively from the perturbation theory as the ratio of differential phase shift to the total loss, becomes the same numerically as that of the Faraday rotator. Similarly, the high-power considerations as studied by Sakiotis, Chait, and Kales[16] show curves similar to those of Fig. 1 in which the nonlinear losses increase with high power and the thickness of the ferrite slabs used. This phenomenon again is associated with the ferrite dielectric modes, which tend to concentrate the electromagnetic energy in the ferrite slab for one direction of propagation.

Several schemes have been proposed for broad banding the phase shifter. The first of these is that suggested by Fox[4] in which he studied the differential phase shift as a function of the position of the ferrite slab for different frequencies. He showed that the minimum frequency variation would not occur at the position where the differential phase shift was a maximum. Recently, this work has been extended by Van Wolfe and co-workers[27] who optimized this technique. Fig. 3 shows the results of their work for the differential phase shift as a function of frequency for different values of position of the ferrite slab in the waveguide. It can be seen that an extremely small variation of differential phase shift of about $2\frac{1}{2}$ per cent is obtained from 8.2 to 10 kmc when the slab is located 0.150 inch from the wall. Another method proposed by Weisbaum and Boyet[28] uses a ferrite slab on each side of the guide, magnetized in the

[18] R. W. Damon, "Relaxation effects in ferromagnetic resonance," *Rev. Mod. Phys.*, vol. 25, p. 239; January, 1953.
N. Bloembergen and S. Wang, "Relaxation effects in para- and ferromagnetic resonance," *Phys. Rev.*, vol. 93, p. 72; January, 1954.
[19] H. Suhl, "Subsidiary absorption peaks in ferromagnetic resonance at high signal levels," *Phys. Rev.*, vol. 101, p. 1437; February, 1956, and "The nonlinear behavior of ferrites at high microwave signal levels," PROC. IRE, vol. 44, pp. 1270–1284; October, 1956.
[20] J. H. Rowen, "Ferrites in microwave applications," *Bell Sys. Tech. J.*, vol. 32, p. 1333; November, 1953.
[21] E. A. Ohm, "A broad-band microwave circulator," IRE TRANS., vol. MTT-4, pp. 210–217; October, 1956.
[22] ——, "A broadband microwave circulator," *Bell. Labs. Rec.*, vol. 35, p. 293; August, 1957.
[23] M. L. Kales, "Propagation of fields through ferrite loaded waveguides," *Proc. Symp. on Modern Advances in Microwave Techniques*, Polytechnic Inst. of Brooklyn, Brooklyn, N. Y., p. 215; November, 1954.
[24] J. L. Melchor and P. H. Vartanian, private communication.
[25] E. Wantuch, private communication.
[26] P. H. Vartanian, J. L. Melchor, and W. P. Ayres, "Broadbanding ferrite microwave isolators," 1956 IRE CONVENTION RECORD, pt. 5, pp. 79–83.
[27] R. Van Wolfe, C. J. Cacheris, and C. Morrison, "The Broadbanding of Microwave Nonreciprocal Ferrite Phase Shifters," Diamond Ordnance Fuze Labs., Washington, D. C., Rep. No. TR-348; April, 1956.
[28] S. Weisbaum and H. Boyet, "Broad-band nonreciprocal phase shifts—analysis of two ferrite slabs in rectangular waveguide," *J. Appl. Phys.*, vol. 27, p. 519; May, 1956.

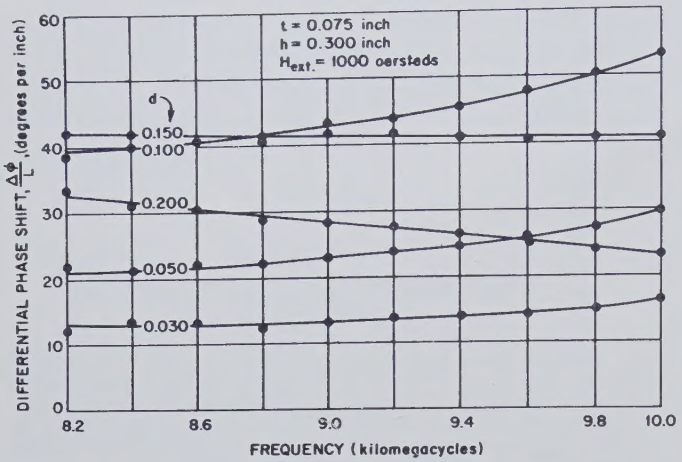

Fig. 3—The differential phase shift as a function of frequency for a transversely magnetized ferrite slab in a rectangular waveguide with the distance, *d*, between the slab and the waveguide wall as a parameter. For a slab 0.075 inch thick placed 0.150 inch from the wall in X-band guide, the differential phase shift is constant within 2.5 per cent over the band. (After Van Wolfe, Cacheris, and Morrison.)

same direction but having different dimensions or magnetic properties. In this case the phase-shift frequency dependences of the two ferrites compensate one another. However, the total differential phase shift is the difference between that of the two ferrites. One can improve on this by operating one of the ferrites above resonance and the other below resonance by using a suitable geometric configuration. In this way, the differential phase shifts of the two ferrites are added and again the frequency variation would compensate. A simple and effective scheme used by Wantuch[25] consists of a ferrite slab and an adjacent dielectric slab, both occupying the full height of the waveguide. As pointed out by Vartanian, Melchor, and Ayres,[26] who use a similar method for a resonance isolator, one of the objectives of using the dielectric is to generate the appropriate elliptical polarization in the region of the ferrite slab adjacent to the dielectric so that the internal field in the ferrite is essentially circularly polarized. The dielectric also minimizes the traversal of the point of circular polarization across the waveguide as a function of frequency. The dielectric loading also minimizes the perturbation in the waveguide due to the presence of the ferrite and reduces the concentration of energy in the ferrite. The optimum position of the slab was determined experimentally,[25] resulting in a 25 per cent bandwidth. The result obtained by dielectric loading of the rectangular waveguide is analogous to that discussed for the Faraday rotator. From the perturbation theory of (2), it was shown that the effect of the dielectric is to broad band the waveguide and to reduce the frequency dependence of the Faraday rotation. Similar arguments show that the same situation is achieved here because, in essence, a dielectric lowers the frequency cutoff of the waveguide and minimizes the shift of the circular polarization of waveguide as a function of frequency. This type of phase shifter, using dielectric loading in rectangular waveguide, has been used in a circulator,[25] which contains two phase shifters between a hybrid-tee junction at one end and a 3-db directional coupler at the other end. The surprising situation is that the ferrite component does not limit the bandwidth of this device but instead the limitation is imposed by the hybrid tee to give a 12 per cent bandwidth in the 9000 mc range with 30-db isolation over the band. This circulator is capable of handling relatively high power of the order of 600 watts average and 600-kw peak.

Resonance Isolators

The resonance isolator has proved to be the most widely used ferrite device at microwave frequencies. In terms of achieving the three objectives of low frequency, high power, and broad bandwidth, the resonance isolator by far is the most successful. First consider the low-frequency problem. In the absence of an exact theory, which is difficult to calculate even for simple geometries, it has been necessary again to resort to the perturbation theory for calculating a theoretical limit for the figure of merit.[7] In this case this is given by the reverse-to-forward loss on resonance or the ratio of the attenuation constant for the negative and positive circularly polarized waves corresponding to the two directions of propagation:

$$R = \frac{\alpha_+}{\alpha_-} = (2\omega T)^2 = \left(\frac{4H_r}{\Delta H}\right)^2. \tag{3}$$

Again ωT, or its equivalent in terms of the resonance line width at the half-power point, determines the lower-frequency limit. To date it has been possible to build this particular type of device at frequencies as low as 1300 mc.[29] With the presently available ferrite materials, Heller[30] also has built an isolator using trough waveguide in the uhf region (~900 mc) with better than 30 to 1 reverse-to-forward ratio of attenuation.

A number of new techniques has made it possible to improve the figure of merit of the resonance isolator so it approaches the values predicted theoretically. One of the important developments is the dielectric loading introduced by Weiss,[31] who used the scheme of placing a dielectric material adjacent to the ferrite slab, preferably on the inner side. For the *E*-plane isolator in which the long transverse dimension of the ferrite slab is parallel to the electric field in the waveguide, Weiss was able to increase the reverse-to-forward ratio of attenuation from 60 to 1 without the dielectric to about 120 to 1 with the dielectric. Fig. 4 shows the reverse and forward loss as a function of magnetic field for an *H*-plane resonance isolator with and without dielectric loading.

[29] G. S. Heller and G. W. Catuna, "Measurement of ferrite isolation at 1300 mc," this issue, p. 97.

[30] G. S. Heller, "*L*-band isolator utilizing new materials," presented at WESCON Convention, San Francisco, Calif.; August 20, 1957, and Quart. Prog. Rep. on Solid State Res., M.I.T. Lincoln Lab., Lexington, Mass.; August, 1957. (Not generally available.)

[31] M. T. Weiss, "Improved rectangular waveguide resonance isolators," IRE TRANS., vol. MTT-4, pp. 240–243; October, 1956.

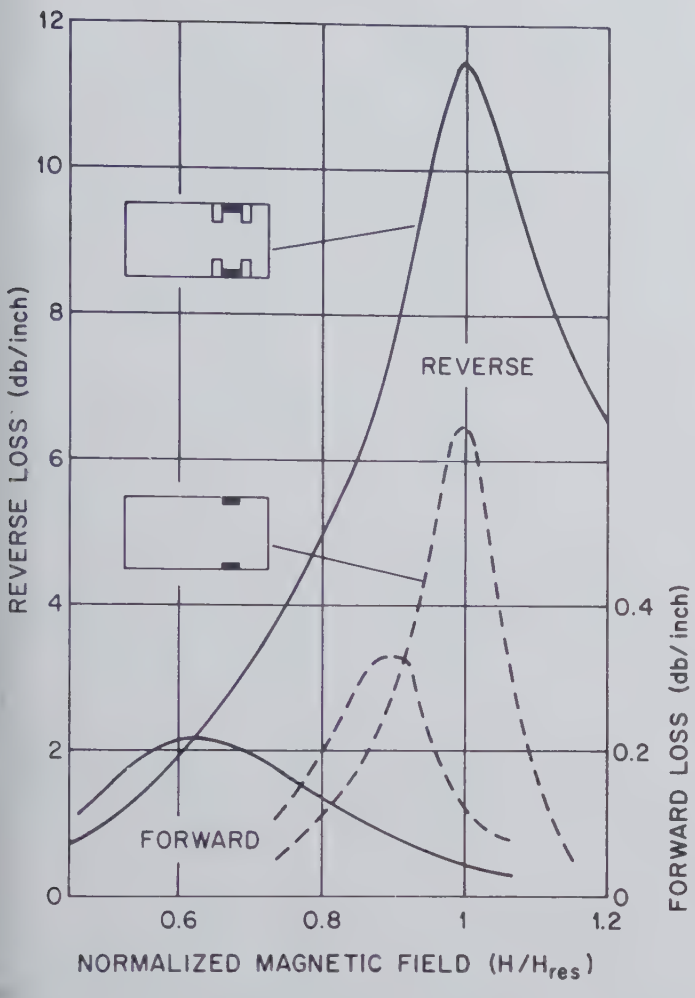

Fig. 4—Experimental curves of the reverse and forward attenuation for a transversly magnetized H-plane ferrite resonance isolator as a function of applied magnetic field. The dashed lines were obtained at a frequency of 10.5 kmc with a flat slab of ferrite placed against the top and bottom walls of X-band waveguide. The solid lines were obtained when dielectric material was placed adjacent to the ferrites as shown in the inset. (From the data of Weiss.)

This time the reverse-to-forward ratio is increased from about 75 to 1 to 150 to 1. This is somewhat better than the E-plane isolator, and one can show from simple reasoning and the analysis of circular polarization in the ferrite and waveguide that this geometry is somewhat more favorable since the position of circular polarization inside the ferrite coincides with that in the waveguide. The importance of dielectric loading and its effect in improving the performance has been demonstrated by Heller[29] in the development of an isolator at 1300 mc, in which he showed progressive improvement in the figure of merit as he went from partial dielectric loading to a ferrite surrounded by a dielectric.

The progress made in the development of high-power isolators also has been impressive. Wantuch[25] has built an H-plane isolator at about 2800 mc in which four ferrite slabs are located appropriately, two at the bottom, two at the top of the guide on either side of the center. These are surrounded with dielectric in a manner similar to that of Heller's isolator. The dc magnetic field is applied in the opposite sense to the ferrites on the left- and right-hand side of the guide. This scheme provides a compact device which reduces the length of the ferrites to about eight inches. Furthermore, this H-plane configuration gives maximum efficiency for heat transfer from the ferrite to the water-cooled wall of the waveguide. One of the considerations in building a high-power isolator is making the thickness of the ferrite of the order of a skin depth on resonance which is

$$\delta = \frac{\lambda}{2}\sqrt{\frac{2}{\epsilon\omega_M T}} \tag{4}$$

in cgs units. For a ferrite having a saturation magnetization of 2000 Gauss, such as Ferramic $R-1$, the skin depth on resonance at S band is about 1 to 2 mm which turns out to be close to the thickness actually used. This particular unit is capable of handling 4000 watts average power and providing 12-db isolation at this level and a reverse-to-forward ratio of almost 50. The insertion loss is $\frac{1}{4}$ db. This low insertion loss is particularly desirable at these high-power levels.

Several procedures have been proposed for broad banding the resonance isolators. One method, used by Weiss,[31] consisted of two ferrites, one above the other, both magnetized in the same direction and with appropriate dielectric loading. Since the saturation magnetization of the two ferrites differed, the internal fields for the two slabs were unequal resulting in resonance at 10.7 and 11.4 kmc. This combines effectively two resonance isolators which have peak absorption at two frequencies, resulting in the broadening of the reverse-to-forward ratio of better than 40 to 1 over a 10 per cent frequency range. Of course, this scheme has reduced the maximum possible value of R. Such a result is consistent with an approximate relation that $\overline{R}\Delta f \approx$ constant, where $\overline{R}$ is the average reverse-to-forward ratio over the frequency range Δf. Thus, in principle, another way of broad banding the resonance isolator, particularly at high frequency, is to select a ferrite with a broad resonance line. Vartanian, Melchor, and Ayres[26] have used dielectric loading adjacent to a thin ferrite slab placed in the E plane of a rectangular waveguide which, for the reasons discussed for the phase shifter, resulted in broad banding the characteristics of the waveguide and of course the resonance isolator. They obtained better than 25 to 1 reverse-to-forward ratio over a band from 8 to 12.5 kmc and, in an S-band isolator, better than 12 to 1 from 2.4 to 4 kmc. Fig. 5 shows results obtained when the two schemes of dielectric loading and stagger tuning are combined.[24,25] This isolator employed two permanent magnets, in tandem, so that the magnetic field applied to two regions of the ferrite differed, providing two resonance frequencies corresponding to the peaks at about 9 and 12 kmc. Experimental location of ferrite and dielectric resulted in 40 per cent bandwidth with a reverse-to-forward ratio greater than 43.

Perhaps one of the most significant recent developments in nonreciprocal devices is the resonance isolator in coaxial waveguide developed by Duncan and co-

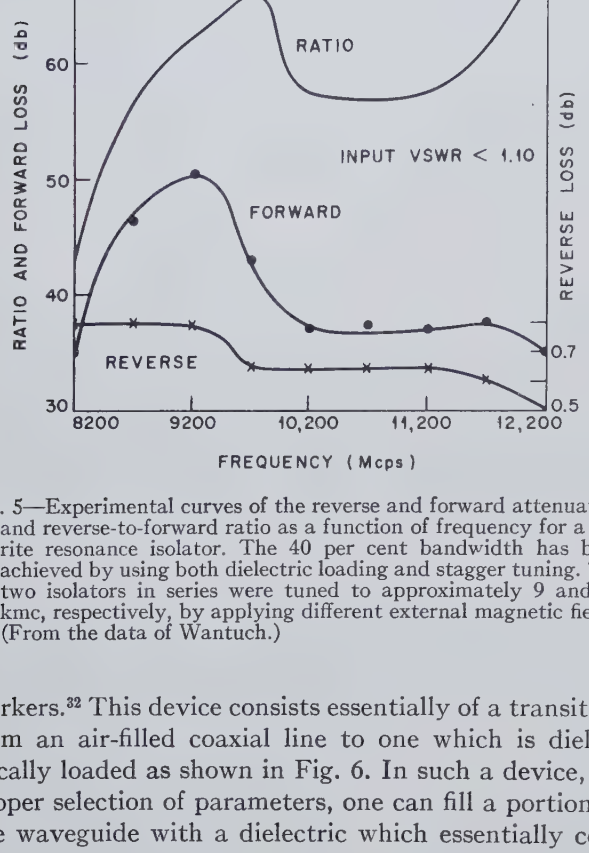

Fig. 5—Experimental curves of the reverse and forward attenuation and reverse-to-forward ratio as a function of frequency for a ferrite resonance isolator. The 40 per cent bandwidth has been achieved by using both dielectric loading and stagger tuning. The two isolators in series were tuned to approximately 9 and 12 kmc, respectively, by applying different external magnetic fields. (From the data of Wantuch.)

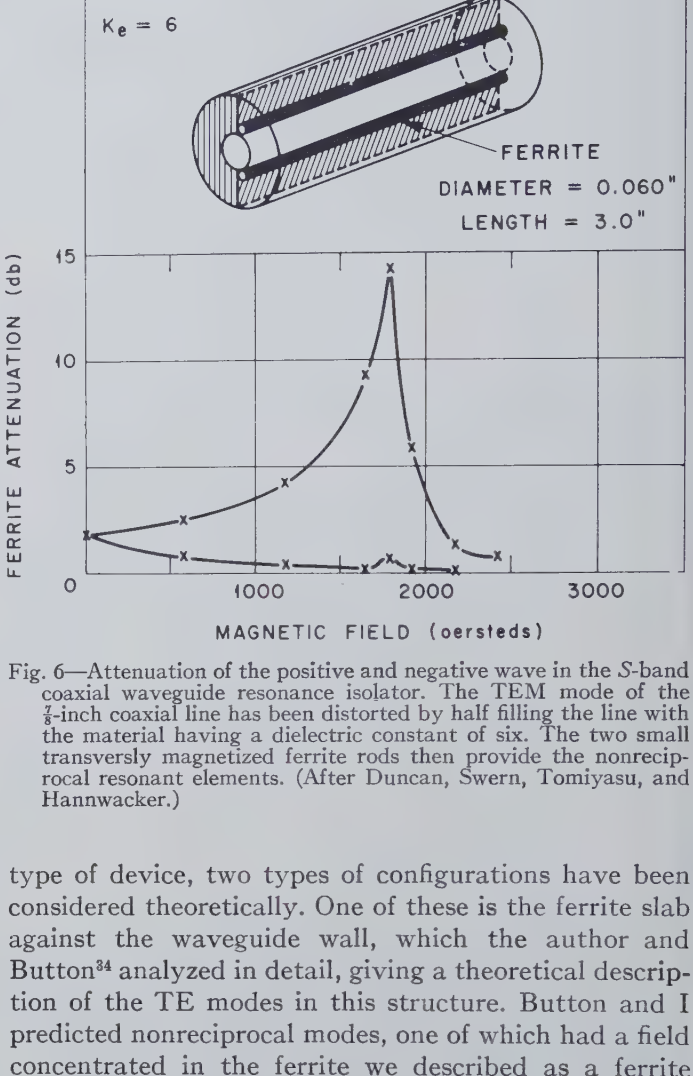

Fig. 6—Attenuation of the positive and negative wave in the *S*-band coaxial waveguide resonance isolator. The TEM mode of the $\frac{7}{8}$-inch coaxial line has been distorted by half filling the line with the material having a dielectric constant of six. The two small transversly magnetized ferrite rods then provide the nonreciprocal resonant elements. (After Duncan, Swern, Tomiyasu, and Hannwacker.)

workers.[32] This device consists essentially of a transition from an air-filled coaxial line to one which is dielectrically loaded as shown in Fig. 6. In such a device, by proper selection of parameters, one can fill a portion of the waveguide with a dielectric which essentially converts the TEM mode to a quasi-TE mode in which there is no longer any angular symmetry of the fields. Consequently, for the configuration shown, there are two positions of circular polarization of the internal rf field in the ferrite at the dielectric interface. If a transverse magnetic field is applied, a coaxial resonance isolator is possible. This is shown by the attenuation curves for the positive and negative waves shown in Fig. 6. Using this basic idea, Duncan, *et al* were able to build a coaxial isolator with more than 10.5-db isolation over the 2- to 4-kmc band with a forward loss of less than 0.8 db. In addition to broad banding, the coaxial configuration has permitted the construction of very compact devices (~four inches long) at this frequency. Obviously, this new development also offers possibilities of other nonreciprocal devices, such as phase shifters in coaxial geometry. A theory of such a device has been discussed by Sucher and Carlin[33] and also has been considered by the group at Lincoln Laboratory.

The Field-Displacement Isolator

The field-displacement isolator is essentially a low-power device which was first discussed by Fox, Miller, and Weiss.[5] In order to understand the operation of this type of device, two types of configurations have been considered theoretically. One of these is the ferrite slab against the waveguide wall, which the author and Button[34] analyzed in detail, giving a theoretical description of the TE modes in this structure. Button and I predicted nonreciprocal modes, one of which had a field concentrated in the ferrite we described as a ferrite "dielectric mode." The general features of this theoretical analysis have been confirmed experimentally by Straus and Heller[35] for the thick slab against the wall as shown in Fig. 7. They used an electric field probe which traversed across the width of the guide and measured the relative rf electric field intensity as a function of position from the far wall of the guide to the ferrite interface. In the forward direction of propagation for external field intensities of 1000 and 2000 oersteds, they clearly demonstrated the existence of the ferrite "dielectric modes." In the reverse direction of propagation, the electromagnetic field was concentrated in the empty portion of the guide in accordance with the theory. At $H=3000$ oersteds for the forward direction, there is a departure from the dielectric mode, and the field becomes less concentrated in the ferrite as one approaches

[32] B. J. Duncan, L. Swern, K. Tomiyasu, and J. Hannwacker, "Design considerations for broad-band ferrite coaxial line isolators," PROC. IRE, vol. 45, pp. 483–490; April, 1957.

[33] M. Sucher and H. J. Carlin, "Coaxial line nonreciprocal phase shifters," *J. Appl. Phys.*, vol. 28, p. 921; August, 1957.

[34] B. Lax and K. J. Button, "Theory of new ferrite modes in rectangular waveguide," *J. Appl. Phys.*, vol. 26, p. 1184; September, 1955, and "New ferrite mode configurations and their applications," *J. Appl. Phys.*, vol. 26, p. 1186; September, 1955.

[35] T. M. Straus and G. S. Heller, "Ferrite dielectric mode—experimental," Quart. Prog. Rep. on Solid State Res., M.I.T. Lincoln Lab., Lexington, Mass., p. 50; February, 1956. (Not generally available.)

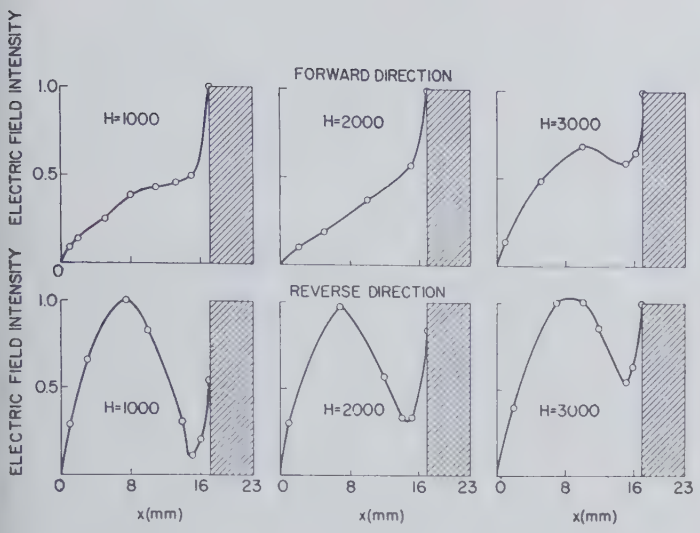

Fig. 7—The experimental electric field configurations in a rectangular waveguide containing a transversly magnetized ferrite slab against the side wall. For an externally applied field of 2000 oersteds at X-band (center figure), the energy is transmitted almost entirely in the ferrite dielectric mode in the forward direction. In the reverse direction, only the distorted waveguide mode exists. (After Straus and Heller.)

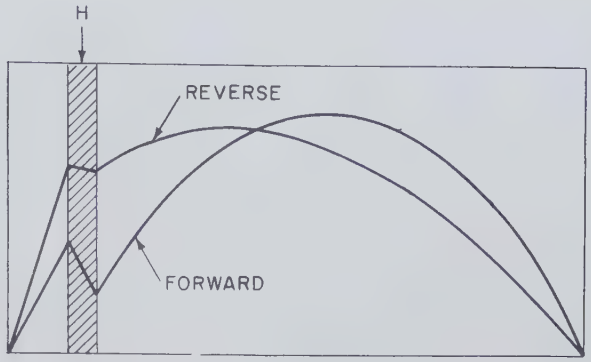

Fig. 8—Theoretical model of the electric field configurations in a ferrite-loaded guide to demonstrate nonreciprocal field displacement. (After Lax, Button, and Roth.)

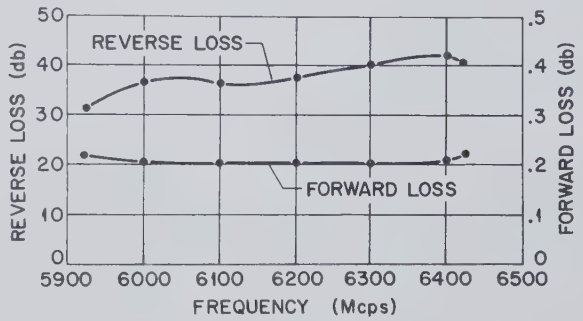

Fig. 9—Experimental curves of the reverse and forward loss as a function of frequency for the single-slab field-displacement isolator. (After Weisbaum and Seidel.)

resonance. This behavior has been demonstrated theoretically by Button.[36]

In analyzing this type of device, the particular electric field configuration used in the literature to explain the principles is that shown in Fig. 8, where a thin ferrite slab is displaced from the wall. The electromagnetic fields for this also have been worked out theoretically[37] and one can show that the null exists for the E field for one direction of propagation.[38] Weisbaum and Seidel[38] carried out their analysis based on this configuration, but their actual device contained a thick slab of ferrite nearly against the wall. Although the analysis used for Fig. 8 predicts the use of a negative effective permeability for the ferrite, the actual experimental devices use the ferrite in a state of positive effective permeability. Button,[39] analyzing this particular case by using the experimental parameters of Weisbaum and Seidel, has shown that the mode configurations for this case are not those of Fig. 8 but, for one direction, involve a "dielectric" mode whose detailed structure has not yet been presented in the literature. The important feature of such a "dielectric" mode is that for one direction of propagation the energy concentration is large within the ferrite and for the other direction it is small. The experimental results of Weisbaum and Seidel definitely involve the existence of two nonreciprocal modes whose field displacement characteristics differ, but their paper does not indicate the nature of the field patterns. Nevertheless, using the empirical approach, they have built such an isolator with a resistance strip or coating across the face of the ferrite whose performance characteristics are shown in Fig. 9. The device operated over the frequency range 5900 to 6400 mc with a reverse-to-forward ratio of attenuation of about 150 to 1 which is better than that achieved by the resonance isolator at this frequency. Weisbaum and Boyet[40] built a field displacement isolator with two ferrite slabs, one on each side of the guide, which were magnetized in the opposite sense. This device had a reverse-to-forward ratio of 70 to 1 from 10.8 to 11.6 kmc and a very low vswr.

A number of other ferrite devices has been developed during the past three years which, although noteworthy, cannot be discussed in detail in this review. The resonance isolator in helical lines was proposed by Cook, Kompfner, and Suhl[41] and further developed by Rich and Webber and also by Enander[42] for use in traveling-wave tubes and related devices. It is not surprising that a phase shifter in a helical line also was developed eventually. A directional coupler using a ferrite was

[36] K. J. Button, "Theory of ferrites in rectangular waveguide," Quart. Prog. Rep. on Solid State Res., M.I.T. Lincoln Lab., Lexington, Mass., p. 47; February, 1956. (Not generally available.)

[37] B. Lax, K. J. Button, and L. M. Roth, "Ferrite phase shifters in rectangular wave guide," *J. Appl. Phys.*, vol. 25, p. 1413; November, 1954.

[38] S. Weisbaum and H. Seidel, "The field-displacement isolator," *Bell Sys. Tech. J.*, vol. 35, p. 877; July, 1956.

[39] K. J. Button, to be published.

[40] S. Weisbaum and H. Boyet, "A double-slab ferrite field displacement isolator at 11 kmc," Proc. IRE, vol. 44, pp. 554–555; April, 1956.

[41] J. S. Cook, R. Kompfner, and H. Suhl, "Nonreciprocal loss in traveling-wave tubes using ferrite attenuators," Proc. IRE, vol. 42, pp. 1188–1189; July, 1954.

[42] J. A. Rich and S. E. Webber, "Ferrite attenuators in helixes," Proc. IRE, vol. 43, pp. 100–101; January, 1955.
B. N. Enander, "A new ferrite isolator," Proc. IRE, vol. 44, pp. 1421–1430; October, 1956.

suggested by Damon[43] and more recently investigated by Berk and Strumwasser.[44] The use of ferrites in cavities for tuning has been treated by Jones, Cacheris, and Morrison,[45] Fay,[46] Nelson,[47] and Burgess,[48] and has been investigated theoretically by Heller and Campbell[49] and Bussey and Steinert[50] for TM modes in a circular cavity containing a cylindrical ferrite rod. The use of ferrites as radiating elements at the end of a waveguide has been discussed by Angelakos and Korman,[51] and ferrites in the form of radiating rods have been described by Reggia, Spencer, Hatcher, and Tompkins.[52] The application of the birefringent properties of ferrites was proposed by Weiss and Fox[53] and has been applied by Karayianis and Cacheris.[54] The single-sideband modulator has been developed for several applications by Cacheris,[55] and switching applications have been discussed by Le Craw.[56] In addition to these, it is important to mention the significant contributions of Seidel[57] in analyzing the anomalous propagation in ferrite-loaded waveguides and their significance in developing new devices and explaining experimentally observed anomalies in existing nonreciprocal components. The possibility of nonreciprocal effects in N-wire transmission lines has been demonstrated theoretically by Boyet and Seidel.[58] Also, attention should be called to the recent reports of Harvey[59] and of Laverick and Rivett-Carnac[60] describing the extension and development of ferrite devices to the millimeter wave region.

Nonlinear Ferrite Devices

Frequency Doublers and Mixers

One of the most interesting developments that promises to provide a new class of devices involving the use of ferrites and related ferrimagnetic materials depends on the nonlinear behavior of the spin system under the action of high rf power. The first of these developments was reported by Melchor, Ayers, and Vartanian,[61,62] who used the ferrite in a waveguide as a frequency doubler to generate power at harmonic frequencies. The phenomenon can be analyzed from the equation of motion of the magnetization vector. This is given in the familiar form

$$\frac{d\vec{M}}{dt} = \gamma(\vec{M} \times \vec{H}) \tag{5}$$

where $\vec{M}$ is the total magnetization, $\vec{H}$ is the total magnetic field, and γ is the gyromagnetic ratio. The total field consists of a dc field and an rf field which can be represented as

$$\vec{H} = \vec{H}_0 + \vec{h}e^{j\omega t}. \tag{6}$$

If the magnetization is written out in a Fourier expansion in the following manner

$$\vec{M} = \vec{M}_0 + \vec{m}_1 e^{j\omega t} + \vec{m}_2 e^{2j\omega t} \tag{7}$$

where $\vec{M}_0$, the dc component of the magnetization is along the direction of the applied dc field, m_1 and m_2 may be determined by substitution of (6) and (7) into (5) and equating terms with the same time dependence. If the resulting equation is linearized no longer, as is usually done in the small-signal theory, then it can be shown that a component of second order along the z direction is given by

$$(\dot{m}_2)_z = \gamma(m_x h_y - m_y h_x) \tag{8}$$

where h_x and h_y are the internal rf magnetic fields within the ferrite in a plane transverse to the dc magnetic field. Obviously, if the rf field is circularly polarized and the first-order magnetization components induced are also circularly polarized, there is no time-dependent z component of the magnetization. However, if either h_x or

[43] R. W. Damon, "Magnetically controlled microwave directional coupler," *J. Appl. Phys.*, vol. 26, p. 1281; September, 1955.
[44] A. D. Berk and E. Strumwasser, "Ferrite directional couplers," Proc. IRE, vol. 44, pp. 1439–1445; October, 1956.
[45] G. R. Jones, J. C. Cacheris, and C. A. Morrison, "Magnetic tuning of resonant cavities and wideband frequency modulation of klystrons," Proc. IRE, vol. 44, pp. 1431–1438; October, 1956.
[46] C. E. Fay, "Ferrite-tuned resonant cavities," Proc. IRE, vol. 44, pp. 1446–1449; October, 1956.
[47] C. E. Nelson, "Ferrite-tunable microwave cavities and the introduction of a new reflectionless, tunable microwave filter," Proc. IRE, vol. 44, pp. 1449–1455; October, 1956.
[48] J. H. Burgess, "Ferrite-tunable filter for use in S band," Proc. IRE, vol. 44, pp. 1460–1462; October, 1956.
[49] G. S. Heller and M. M. Campbell, "Ferrite Loaded Cavity Resonators," presented at Annual PGMTT Meeting, New York, N. Y.; May 9–10, 1957.
[50] H. E. Bussey and L. A. Steinert, "Exact solution for a cylindrical cavity resonator containing a gyromagnetic material," Proc. IRE, vol. 45, pp. 693–694; May, 1957.
[51] D. J. Angelakos and M. M. Korman, "Radiation from ferrite-filled apertures," Proc. IRE, vol. 44, pp. 1463–1468; October, 1956.
[52] F. Reggia, E. G. Spencer, R. D. Hatcher, and J. E. Tompkins, "Ferrod Radiator Systems," Diamond Ordnance Fuze Labs., Washington, D. C., Tech. Rep. No. 357; June, 1956.
[53] M. T. Weiss and A. G. Fox, "Magnetic double refraction at microwave frequencies," *Phys. Rev.*, vol. 88, p. 146; October, 1952.
[54] N. Karayianis and J. C. Cacheris, "Birefringence of ferrites in circular waveguide," Proc. IRE, vol. 44, pp. 1414–1421; October, 1956.
[55] J. C. Cacheris, "Microwave Single-Sideband Modulator Using Ferrites with Transverse Magnetic Fields," Natl. Bur. of Standards, Washington, D. C., Rep. No. 17-77; September, 1952, and "Microwave single-sideband modulator using ferrites," Proc. IRE, vol. 42, pp. 1242–1247; August, 1954.
J. C. Cacheris and H. A. Dropkin, "Compact microwave single-sideband modulator using ferrites," IRE Trans., vol. MTT-4, pp. 152–155; July, 1956.
[56] R. C. LeCraw, "High-speed magnetic pulsing of ferrites," *J. Appl. Phys.*, vol. 25, p. 678; May, 1954.
R. C. LeCraw and H. B. Bruns, "Time delay in high-speed ferrite microwave switches," *J. Appl. Phys.*, vol. 26, p. 124; January, 1955.
[57] H. Seidel, "Anomalous propagation in ferrite-loaded waveguide," Proc. IRE, vol. 44, pp. 1410–1414; October, 1956.
[58] H. Boyet and H. Seidel, "Analysis of nonreciprocal effects in an N-wire ferrite-loaded transmission line," Proc. IRE, vol. 45, pp. 491–495; April, 1957.
[59] A. F. Harvey, "Ferrite structures for millimetre wavelengths," *Proc. IEE*, vol. 104 B, p. 346; October, 1956.
[60] E. Laverick and A. Rivett-Carnac, "Some measurements and applications of the microwave properties of a magnesium-manganese ferrite in the 8–9 mm waveband," *Proc. IEE*, vol. 104 B, p. 379; October, 1956.
[61] J. L. Melchor, W. P. Ayres, and P. H. Vartanian, "Microwave frequency doubling from 9 to 18 kmc in ferrites," Proc. IRE, vol. 45, pp. 643–646; May, 1957.
[62] W. P. Ayres, P. H. Vartanian, and J. L. Melchor, "Frequency doubling in ferrites," *J. Appl. Phys.*, vol. 27, p. 188; February, 1956.

h_y are zero, *i.e.*, the transverse rf field is linearly polarized, then there is a second-order component of m_z which represents the nutational component of the precession at twice the frequency of the applied rf field. One can solve this particular problem directly. However, the expansion scheme used demonstrates the frequency doubling phenomenon rather simply. Furthermore, more complicated situations can be analyzed and interpreted physically by this scheme. Pippin[63] has shown that one can obtain frequency mixing in a manner analogous to the frequency doubling. He used two transverse components of the rf field of different frequencies and the nutational component along the z direction can contain either the sum or the difference frequencies. This situation has been analyzed in detail by Stern and Pershan[64] for both the frequency doubler and the ferrite mixer. They also carried out an experiment in which they demonstrated the mixing phenomenon. At relatively low power levels, of the order of milliwatts, they obtained a conversion factor of about −30 db. It is very likely one can obtain greater efficiency at higher power levels. This was precisely the situation achieved by Melchor, Ayres, and Vartanian,[61] who went up to levels of about 30 kw and obtained a conversion efficiency of about −6 db as indicated in Fig. 10. They carried out their experiments at a peak power level of 30 kw at 9 kmc and obtained 8-kw output at 18 kmc.

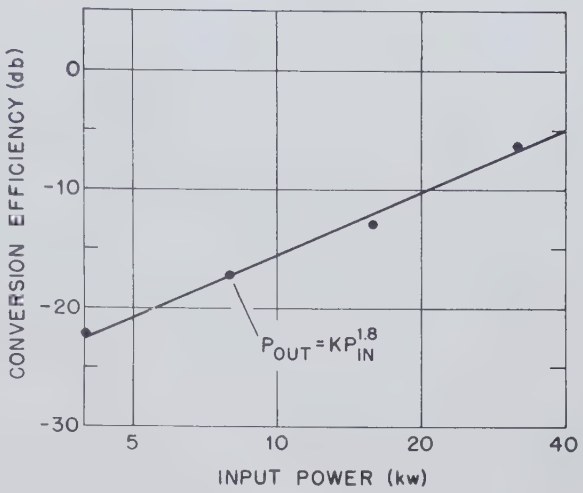

Fig. 10—Conversion efficiency for frequency doubling from 9 to 18 kmc as a function of input power level. These data were taken for a transversly magnetized half disk of ferrite against the side wall of a rectangular waveguide. (After Melchor, Ayres, and Vartanian.)

Ferromagnetic Resonance Amplifier

A relatively new device proposed by Suhl[65] is a ferromagnetic resonance amplifier based on two classes of phenomena in ferrites recently investigated.[66–71] The first of these involves the theoretical interpretation[67] of the observed behavior of ferrites at high powers as investigated by Damon[18] and Bloembergen and Wang.[18] They observed that the susceptibility at high powers was reduced as the power was increased and, concurrently, that the line width became broader as a function of power, indicating an increased loss. They also observed a secondary absorption peak below resonance at high powers. Actually, the onset of these effects occurred at relatively low or intermediate power levels, and they are closely related to the effects observed in a waveguide by Sakiotis, Chait, and Kales.[16] The interpretation of these phenomena was given by Suhl, who showed that the onset can occur at these intermediate power levels because of the existence there of an instability of the nonlinear behavior of ferrites. Suhl[67] also has shown that this instability can be represented very simply for a flat disk by the solution of the z component of the magnetization given approximately by

$$\frac{M_z}{M_0} \approx 1 - \frac{\frac{1}{2}\gamma^2 h^2 rf}{[\omega - \gamma(H - N_z M_z)]^2 + 1/T^2} \qquad (9)$$

where M_0 is the total magnetization which is equal to M_z in the absence of an rf signal, $N_z M_z$ is the demagnetizing field in the z direction, and T is a phenomenological relaxation time inversely proportional to the line width. It can be shown from (9) that, below resonance, when the rf power increases, the precessional angle of the magnetization increases, thus decreasing M_z, the component of the magnetization along the direction of the dc magnetic field. This makes $H_{eff} = H - N_z M_z$ larger since the demagnetizing term is smaller, reducing the magnitude of the term in the brackets. Hence, one can see from (9) that M_z on the left-hand side is reduced further. In this way, the effective field is brought even closer to resonance. There is a critical value of the rf field which leads to feedback or an instability of this type. Basically, this phenomenon is responsible for the rapid development of these nonlinear effects at intermediate power levels. As a matter of fact, Suhl has shown[67] that the critical field for this condition is given by

$$h_{crit} \approx \Delta H \sqrt{\frac{3\Delta H}{4\pi M}} . \qquad (10)$$

[63] J. E. Pippin, "Frequency doubling and mixing in ferrites," Proc. IRE, vol. 44, pp. 1054–1055; August, 1956, and Harvard Univ. Gordon McKay Lab., Cambridge, Mass., Sci. Rep. No. 2, AFCRC-TN-369; May, 1956.

[64] E. Stern and P. Pershan, "Harmonic Generation in Ferrites," presented at Symposium on the Role of Solid State Phenomena in Electric Circuits, Polytechnic Inst. of Brooklyn, Brooklyn, N. Y.; April 23, 1957.

[65] H. Suhl, "Proposal for a ferromagnetic amplifier in the microwave range," *Phys. Rev.*, vol. 106, p. 384; April, 1957.

[66] P. W. Anderson and H. Suhl, "Instability in the motion of ferromagnets at high microwave power levels," *Phys. Rev.*, vol. 100, p. 1788; December, 1955.

[67] H. Suhl, "The nonlinear behavior of ferrites at high microwave signal levels," Proc. IRE, vol. 44, pp. 1270–1284; October, 1956.

[68] ——, "The theory of ferromagnetic resonance at high signal powers," *J. Phys. Chem. Solids*, vol. 1, p. 209; January, 1957.

[69] R. L. White and I. M. Solt, "Multiple ferromagnetic resonance in ferrite spheres," *Phys. Rev.*, vol. 104, p. 56; October, 1956.

[70] L. R. Walker, "Magnetostatic modes in ferromagnetic resonance," *Phys. Rev.*, vol. 105, p. 390; January, 1957.

[71] J. F. Dillon, Jr., "Ferromagnetic resonance in thin discs of manganese ferrite," *Bull. Amer. Phys. Soc.*, ser. II, vol. 1, p. 125; March, 1956.

Such a condition can also exist when the ferrite sample is spherical and involves the existence of spin waves. Since that subject is beyond the scope of this paper, it is sufficient to give the final result for the sphere. The expression for h_{crit} is similar to (10) except that the factor 3 is replaced by the number 2 in the formula for the critical field for the onset of instability. The significance of this work is that values of the critical field $h_{crit} \approx 8$ oersteds are obtained for a ferrite resonance line width of 50 Gauss. Obviously, the critical value becomes lower as the line width decreases. Suhl's analysis also brought out that the susceptibility of a subsidiary absorption peak below the main resonance increased rapidly above the threshold rf field to a maximum susceptibility and subsequently decreased with increasing power. The physical origin of the increased line width with high power above the threshold has to do with the transfer of energy from the usual uniform precessional mode to spin waves whose frequencies are degenerate with the resonant frequency of the particular geometry associated with the uniform precession.

Another phenomenon which must be considered in this ferromagnetic amplifier and which also is related to the spin waves of a low wave number is that discovered by White and Solt[69] and also investigated experimentally by Dillon,[71] namely, the existence of nonuniform precessional modes in a ferrite body of finite size. Fig. 11 shows some of the original results of White and Solt, in which they placed a ferrite sphere in a cavity where the rf magnetic field is not uniform. Under these circumstances, one obtains resonance in the ferrites containing a number of peaks in addition to the main peak. The figure shows four, although Dillon has obtained many more in his experiments. The explanation is seen in the following: there is a spatial distribution of the precessional phase of the spins in the sphere, such that the magnetic dipoles set up on the surface result in a demagnetization in which there is an azimuthal and a polar distribution as well as a radial distribution in the spins. These were analyzed by Mercereau and Feynman[72] and more completely by Walker.[70]

Suhl has proposed that one can use these magnetostatic modes and the nonlinear properties of the ferrites to build an amplifier in one of three ways. The first one involves the coupling of two nonuniform modes of operation of the ferrite through the uniform precession or the lowest mode of precession of the spins in the ferrite. This requires the condition $\omega_1+\omega_2=\omega$, where ω_1 is the frequency of one of the nonuniform or magnetostatic modes, ω_2 is another, and ω is the operating frequency of the uniform precession. The magnetostatic modes are confined to the range of frequencies $\gamma(H-4\pi M)$ to $\gamma(H+2\pi M)$. This particular system may have some difficulties because of the type of in-

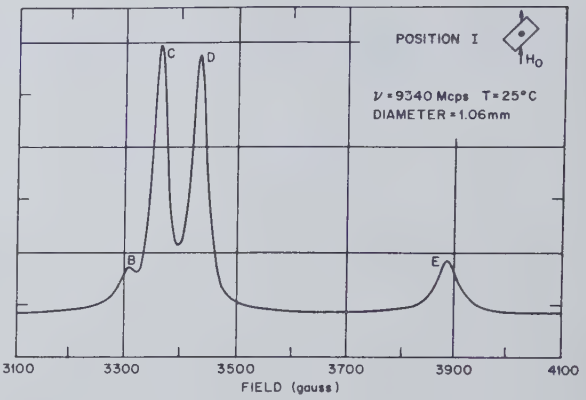

Fig. 11—Multiple ferromagnetic resonances in a single crystal of manganese-zinc ferrite due to nonuniform precessional modes. The ferrite sphere was placed in a cavity in a position of nonuniform rf magnetic field. (After White and Solt.)

stability discussed previously. A second method involves the use of the resonant properties of a cavity and the magnetic modes of the ferrite as follows. The magnetic field is adjusted such that the frequency of no two nonuniform modes add to ω. However, the resonance frequencies ω_1 and ω_2 of the cavity do add to ω. The sample is placed at a position in the cavity where one of the cavity modes has an rf component along the dc magnetic field and the other cavity mode has an rf component transverse to the dc magnetic field. Suhl calls this the "electromagnetic" scheme in which the ferrite couples the modes of the cavity. The third scheme, which is called "semistatic" operation, is a hybrid of the first two. The cavity could supply one mode, ω_1 and the sample, the other, ω_2. In the first system, the critical or threshold field depends on the sample losses. The electromagnetic scheme depends on the cavity losses or the Q of each cavity mode. In the third case, the threshold field depends on both the cavity and the sample losses. The detailed analysis has not yet been presented in the literature. Very recently, Weiss reported[73] on the operation of such a ferromagnetic resonance amplifier and oscillator. He used the "electromagnetic" mode of operation in which the frequencies f_1 and f_2 were both equal to 4500 mc and the pumping, or resonance, frequency was equal to the sum, 9000 mc. The device achieved a gain of 8 db at the lower frequency as an amplifier and yielded 100 watts peak power output as an oscillator. A single crystal of manganese ferrite was used and the high-power source of pumping power was a magnetron which operated at a level of 20-kw peak for oscillation.

Again, in these new devices as well as the old ones, it is desirable to obtain ferrites with narrow resonance line widths. It seems that in both linear and nonlinear devices the operation is enhanced when this is achieved. Hence, the search for new and better materials such as the garnets is an increasingly important aspect of the development of ferromagnetic devices.

[72] J. E. Mercereau and R. P. Feynman, "Physical conditions for ferromagnetic resonance," *Phys. Rev.*, vol. 104, p. 63; October, 1956.

[73] M. T. Weiss, "Microwave ferromagnetic amplifier and oscillator," *Phys. Rev.*, vol. 107, p. 317; July, 1957.

Semiconductors at Microwave Frequencies

The role of semiconductors in microwaves is not new as the first microwave rectifiers built during World War II were made of either silicon or germanium. Not a great deal of development work has been done to improve and extend the use of semiconductors as microwave detectors until recently when Messenger and McCoy[74] took advantage of the know-how obtained from the transistor technology and used single germanium crystals of appropriate resistivity to optimize the properties of microwave detectors at selected frequencies. The possible use of such detectors at low temperatures is receiving some attention and perhaps with the greater understanding of semiconductors which has been achieved, some progress may be made in this direction. The use of the *p-n* junction diode, particularly the depletion layer as proposed by Gärtner,[75] narrow-base devices, graded base diodes, and transistors shows promise of application at higher frequencies, which probably will extend into the microwave region.

The primary reason for including semiconductors in this review is to discuss the close relationship to the behavior of ferrites in electromagnetic fields, which has led to nonreciprocal devices and resonance amplifiers. It is this feature of semiconductors and the two classes of phenomena, namely cyclotron and spin resonance in semiconductors, that is discussed next.

Cyclotron Resonance

The initial experiments have been carried out at Berkeley and at Lincoln Laboratory.[76–78] This phenomenon is a simple one and involves the motion of an electron or a hole in the semiconductor in the presence of a dc magnetic field. One can write very simple equations of motion for such a charged particle as follows:

$$m^*\dot{\vec{v}} = e\vec{E}\exp(j\omega t) + e(\vec{v}\times\vec{B}) \qquad (11)$$

where $\vec{B}$ is the dc magnetic field and m^* is the effective mass which is usually less than that of the free electron mass, m_0. In materials such as InSb where the electron mass is isotropic and represented by a simple scalar quantity, the problem is very similar to that which occurs in the propagation of electromagnetic waves in an ionized gas. This equation can be solved readily to obtain an expression for the conductivity tensor that is very similar to the form of representation of the permeability tensor for ferrites. For the case of interest here the conductivity tensor can be represented in the following form:

$$\sigma = \begin{pmatrix} \sigma_{11} & \sigma_{12} & 0 \\ -\sigma_{12} & \sigma_{22} & 0 \\ 0 & 0 & \sigma_{33} \end{pmatrix}. \qquad (12)$$

These tensor components are given by

$$\sigma_{11} = \sigma_{22} = \sigma_0 \frac{1 + j\omega t}{(1 + j\omega\tau)^2 + (\omega_c\tau)^2}$$

$$\sigma_{12} = -\sigma_{21} = \sigma_0 \frac{\omega_c\tau}{(1 + j\omega\tau)^2 + (\omega_c\tau)^2}$$

$$\sigma_0 = \frac{ne^2\tau}{m^*} \qquad (13)$$

where τ is the mean free time of scattering of a charge carrier, e is the electronic charge, n is the number of charge carriers per cubic meter, and $\omega_c = eB/m^*$ is the cyclotron resonance frequency. To show the analogy between the permeability of ferrites and conductivity of semiconductors, examine the plot in Fig. 12(a) of the scalar permeability quantities used for the positive and negative circular polarized fields. The dispersive and dissipative components are shown in the familiar forms used to explain the basic operation of nonreciprocal devices. For instance, for the Faraday rotation, the dispersive components which are the real parts of the susceptibilities are used below resonance where the differential effects are greatest. The conductivities for circularly polarized waves propagating through a semiconductor are given by $\sigma_\pm = \sigma_{11} \pm \sigma_{12}$ where the complex quantities σ_{11} and σ_{12} are given in (13). The real and imaginary parts of $\sigma_\pm$ have been plotted in Fig. 12(b). In this case, however, the dispersive components are the imaginary parts and exhibit maximum differential effects above resonance. Hence, a device using the Faraday rotation in a semiconductor probably should be operated at values of applied magnetic field above resonance. It is likely this is the most practical type of nonreciprocal device that can be built with semiconductors, because circularly polarized rf electric fields are not obtained very conveniently except in square or circular waveguide. It is evident from Fig. 12(b) that the resonance properties (again in a cylindrical waveguide) could be utilized for constructing a nonreciprocal resonance isolator. This may have some possible advantages over the ferrite isolator at very high microwave frequencies. Firstly, the rotation or absorption per unit volume in a semiconductor can be much larger because the interaction of a single electron with the electric field is much greater than that of a single magnetic dipole with the rf magnetic field by a factor of 10^{13}.

[74] G. C. Messenger and C. T. McCoy, "A Low Noise-Figure Microwave Crystal Diode," Philco Corp., Philadelphia, Pa., unpublished report.
C. T. McCoy, "The 1N263, A Low-Noise Microwave Mixer Diode," presented at Electronic Components Conference, Los Angeles, Calif.; May 26, 1955.

[75] W. W. Gärtner, "Transit Time Effects in Depletion Layer Transistors at Microwave Frequencies," presented at Symposium on the Role of Solid State Phenomena in Electric Circuits, Polytechnic Inst. of Brooklyn, Brooklyn, N. Y.; April 23, 1957.

[76] See, for example, the review of work on silicon and germanium by G. Dresselhaus, A. F. Kip, and C. Kittel, "Cyclotron resonance of electrons and holes in silicon and germanium crystals," *Phys. Rev.*, vol. 98, p. 368; April, 1955.

[77] R. N. Dexter, H. J. Zeiger, and B. Lax, "Cyclotron resonance experiments in silicon and germanium," *Phys. Rev.*, vol. 104, p. 637; November, 1956.

[78] For a recent review of cyclotron resonance and tabulated data on a variety of semiconductors and metals, see B. Lax, "Experimental investigations of the electronic band structure of solids," *Rev. Mod. Phys.*, January, 1958.

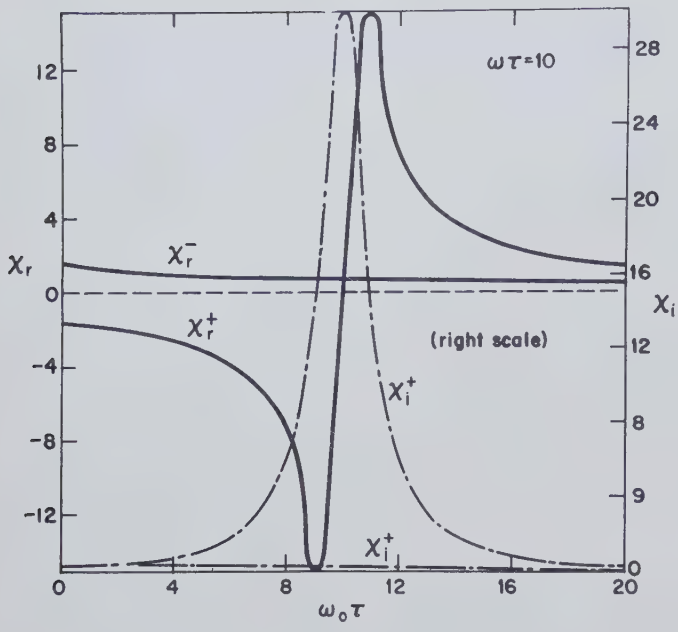

Fig. 12—Components of (a) complex scalar susceptibility and (b) conductivity for the positive and negative circularly polarized waves as a function of applied dc magnetic field. The resonances shown are ferromagnetic and cyclotron resonance, respectively.

Although the number of electrons per unit volume may be less, nevertheless the over-all effect is much greater. The same considerations of line width apply to the semiconductor as to the ferrite. The value of $\omega\tau = 10$ shown in Fig. 12(b) represents that obtained for a pure sample of germanium that could only be achieved at liquid helium temperature and at K-band frequency (or possibly millimeter waves at liquid nitrogen temperature). However, there is an additional definite advantage over the ferrites in the millimeter region because the effective mass of holes and electrons are much smaller than the free electron mass. In germanium the electron mass is about 0.1 m_0 and the light hole mass is about 0.04 m_0; in InSb the electron mass is about 0.013 m_0. This means that cyclotron resonance can be observed in germanium with 4-mm radiation using a dc magnetic field of only 2500 Gauss or 1000 Gauss for n type or p type, respectively. In indium antimonide, only the fairly small field of 400 Gauss would be required.

Germanium is most desirable from the point of view of getting the highest value of $\omega\tau$. At the present time it is not really a very simple medium from the electromagnetic viewpoint. The cyclotron resonance phenomenon has shed a great deal of light on this and Fig. 13 shows just how complicated the situation is. If one orients the magnetic field arbitrarily relative to the crystalline axis, then for the electrons, one can obtain four resonances. This is because there are four sets of electrons, each moving on an ellipsoidal energy-momentum surface, which are directed along the four cube diagonals of the cubic crystal. Thus for n-type material, it is necessary that one direct the magnetic field along the cube axis, in which case all of the electrons appear identical and one obtains only one resonance value. The situation is different for p-type material. There are two kinds of holes, a heavy hole and a light hole. The light hole is nearly isotropic, has a mass of 0.04 m_0, and is less densely populated than the heavy hole which has a mass of $\sim$0.33 m_0. The latter moves on an energy-momentum surface, which is a warped sphere giving rise to nonlinear effects in the presence of a magnetic field. Dexter, Zeiger, and Lax[71] have observed second and third harmonics of the heavy hole resonance due to the existence of warping. Maiman[79] has suggested the possibility of harmonic generation by modulating the cyclotron resonance frequency with an alternating magnetic field.

The electromagnetic problems have been treated, taking into account the complicated anisotropy properties of either the holes or electrons, and the results have been expressed in terms of an effective conductivity which is defined by[80]

$$\Gamma^2 = -\omega^2\epsilon\mu_0 + j\omega\mu_0\sigma_{eff}. \tag{14}$$

The expressions for σ_{eff} for electrons in germanium and silicon have been worked out by Lax and Roth[80] for different orientations of the dc magnetic field and for various electric field polarizations. The simplest is the case where the dc field is parallel both to the direction of propagation and, for germanium, to the cubic or [100] axis of the crystal. In the case of silicon, the magnetic field and the propagation vector should be along the cube diagonal or [111] axis. Then, for both germanium and silicon

$$\frac{\sigma_{eff}}{\sigma_0} = \frac{1 \pm (\rho + 2)jb/(2\rho + 1)}{1 + (\rho + 2)b^2/3\rho} \tag{15}$$

[79] T. H. Maiman, "Solid State Millimeter Wave Generation Study—Second Quarterly Progress Report," Hughes Aircraft Co., Culver City, Calif.; October–December, 1956.

[80] B. Lax and L. M. Roth, "Propagation and plasma oscillation in semiconductors with magnetic fields," *Phys. Rev.*, vol. 98, p. 548; April, 1955

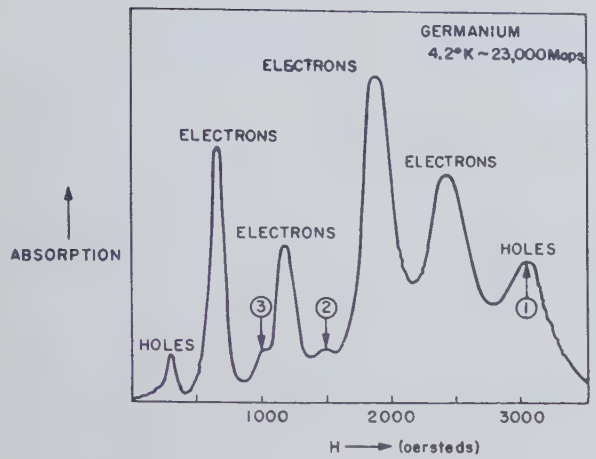

Fig. 13—Experimental cyclotron resonance absorption in germanium at K band and liquid helium temperature as a function of magnetic field. Resonance peaks for the electrons and holes are indicated. (After Dexter, Zeiger, and Lax.)

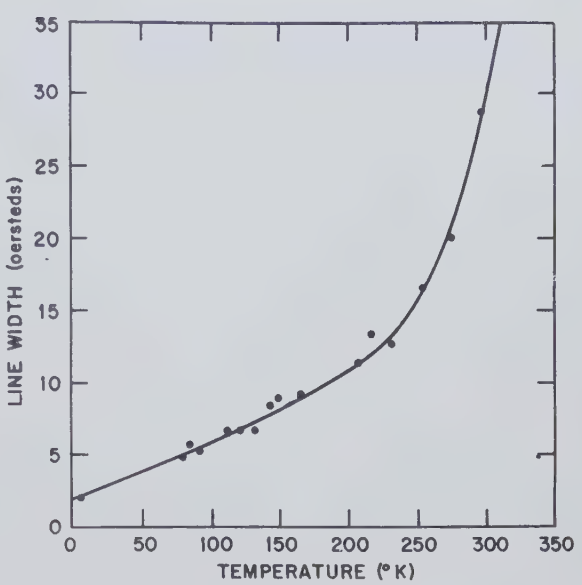

Fig. 14—Electron spin resonance line width in n-type silicon at X band as a function of temperature. (After Portis, Kip, Kittel, and Brattain.)

where

$$\sigma^* = ne^2/m^*(\nu + j\omega),$$
$$m^* = 3m_l m_t/(2m_l + m_t),$$
$$b = eB/m_t(\nu + j\omega),$$
$$\rho = m_l/m_t.$$

σ^* is the rf conductivity in the absence of a magnetic field; m^* the average or conductivity mass expressed in terms of the longitudinal mass m_l and the transverse mass m_t associated with the ellipsoidal energy surfaces; and b is a parameter which is proportional to the magnetic field and involves the collision frequency ν, which is assumed independent of electron energy. The difference between silicon and germanium is that $m_l = 1.64\ m_0$, $m_t = 0.082\ m_0$ for germanium, and $m_l = 0.98\ m_0$, $m_t = 0.019\ m_0$ for silicon. Analogous results for the holes, taking into account the warped surfaces, have been worked out by the Lincoln group for various limiting conditions.

Spin Resonance

The first spin resonance experiments in semiconductors were observed first by the group at Berkeley,[81] which studied the spin resonance in heavily doped n-type silicon, as shown in Fig. 14. An apparent single line was observed in which the line width varied as a function of temperature from about 2 oersteds at liquid helium to about 30 oersteds at room temperature. Since then more extensive work has been carried out, primarily at Bell Laboratories, in which different impurities and different concentrations were used. At high impurity concentrations, one obtains an apparent single line. However, it is shown in Fig. 15 that[82] at lower concentrations, one can observe the splitting due to the presence of the nucleus, *i.e.*, the hyperfine structure, which becomes more complex as the magnetic moment of the nucleus increases from $\frac{1}{2}$ in phosphorus to $\frac{3}{2}$ in arsenic to $\frac{5}{2}$ and $\frac{7}{2}$ in antimony. The narrow lines obtained in these materials indicate interesting possibilities. Furthermore, the very long spin-lattice relaxation times, of the order of seconds as observed by Feher

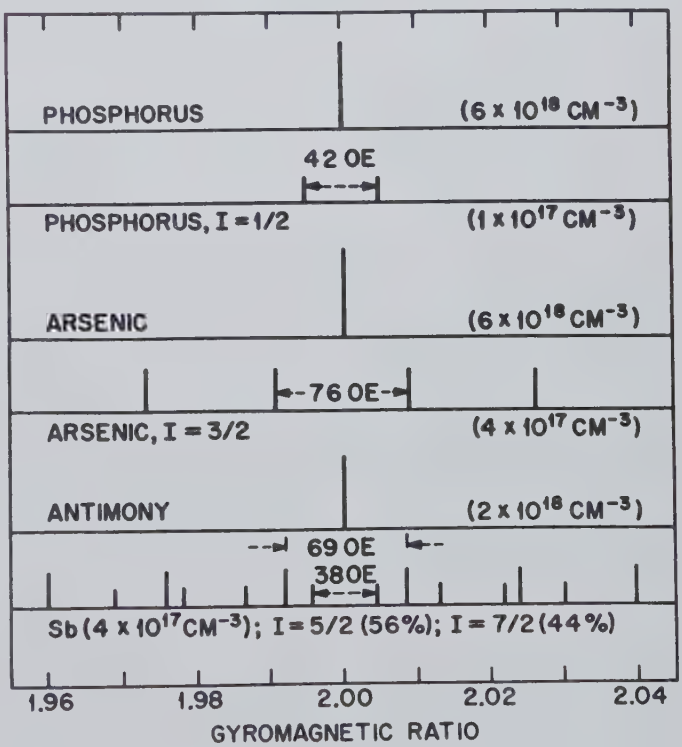

Fig. 15—A schematic representation of the absorption line spectrum for silicon doped with various amounts of phosphorous, arsenic, and antimony. Hyperfine structure is observed in samples with impurity content of the order of 10^{17} per cubic centimeter. (After Fletcher, Yager, Pearson, and Merritt.)

[81] A. M. Portis, A. F. Kip, C. Kittel, and W. H. Brattain, "Electron spin resonance in a silicon semiconductor," *Phys. Rev.*, vol. 90, p. 988; June, 1953.

[82] R. C. Fletcher, W. A. Yager, G. L. Pearson, and F. R. Merritt, "Hyperfine splitting in spin resonance of group V donors in silicon," *Phys. Rev.*, vol. 95, p. 844; August, 1954.

and Fletcher,[83] and sometimes even much longer, suggest possibilities for maser-type devices. The first contribution to the solid-state maser art was made last year by Townes and co-workers[84] in France using silicon. The original work on the maser at Bell Telephone Laboratories considered the use of a single crystal consisting of a silicon-29 isotope as a possible medium for such a device. With such narrow lines and long spin-lattice relaxation times, one can consider new possible devices using nonreciprocal or nonlinear properties of the spin resonance at low temperatures.

Conclusion

It is apparent that some of the recent developments indicate improvement and extension of present devices and the promise of new ones in the field of ferrites. The advent of the ferromagnetic garnet both in polycrystalline and single crystal form indicates the possibility of nonreciprocal ferrite components at lower microwave frequencies extending to the uhf region of the spectrum. The theoretical and experimental work on the nonlinear behavior of ferrites promises practical devices such as harmonic generators,[79] frequency mixers, and detectors.[85] Perhaps the most exciting possibility in this regard is the ferromagnetic resonance maser using ferrites or garnet crystals. However, whether it proves to be superior to existing devices at room temperatures or the paramagnetic maser[86] at low temperature remains to be demonstrated.

Semiconductor microwave applications other than the existing detectors may be realized in the very near future in the form of junction rectifiers and transistors as a result of new developments. The use of the cyclotron resonance properties of holes and electrons in germanium promises practical applications for nonreciprocal devices in the millimeter wavelength region. The spin resonance in silicon and possibly other semiconductors may very well provide us with devices similar to the maser.

Acknowledgment

It is a privilege to acknowledge the invaluable technical contributions of K. J. Button to both the ferrite and semiconductor problems. His assistance in preparing this document is appreciated greatly. The author thanks Dr. G. S. Heller and his group for discussing their current work and giving permission to use their results prior to publication and Dr. E. Wantuch for providing up-to-date information and data on several nonreciprocal ferrite devices developed by him and his group.

The preprint sent by Dr. H. Suhl, describing his work on the ferromagnetic resonance amplifier, was of special value.

Discussions with Dr. G. Birnbaum in connection with the work of his group on the applications of cyclotron resonance for harmonic generation have been very stimulating. The advance copy of the work of Dr. E. Stern on frequency doubling and mixing and the prepublication report of Dr. W. W. Gärtner on the application of transistors at microwave frequencies have been quite helpful.

The author is grateful to the group at the Diamond Ordnance Fuze Laboratories for keeping him abreast of their ferrite research and, in particular, to Dr. J. Cacheris and his co-workers for their recent work on the ferrite detector. He is indebted also to Dr. A. Aden for information regarding the work of his physics group on broad banding of ferrite devices.

[83] G. Feher and R. C. Fletcher, "Relaxation effects in donor spin resonance experiments in silicon," *Bull. Amer. Phys. Soc.*, ser. II, vol. 1, p. 125; March, 1956.

[84] J. Combrisson, C. H. Townes, and A. Honig, "Utilisation de la resonance de spins," *Compt. Rend.*, vol. 242, p. 2421; May, 1956.

[85] D. Jaffe, J. C. Cacheris, and N. Karayianis, "Ferrite Microwave Detector," Diamond Ordnance Fuze Labs., Washington, D. C., Tech. Rep. No. TR-457; May, 1957.

[86] N. Bloembergen, "Proposal for a new type solid state maser," *Phys. Rev.*, vol. 104, p. 324; October, 1956.
H. E. D. Scovil, G. Feher, and H. Seidel, "Operation of a solid state maser," *Phys. Rev.*, vol. 105, p. 762; January, 1957.
A. L. McWhorter and J. W. Meyer, "A Solid State MASER Amplifier," presented at 15th Annual Conference on Electron Tube Research, Berkeley, Calif.; June 26, 1957.

Nonreciprocal Electromagnetic Wave Propagation in Ionized Gaseous Media*

L. GOLDSTEIN†

Summary—**The nonreciprocal propagation of electromagnetic waves in ionized gaseous media is discussed, and experimental observations are reported in this paper. The classical Faraday experiment in the optics of anisotropic media has suggested an analogous phenomenon at microwave frequencies. The anisotropic behavior of the free electron gas which is immersed in a magnetic field and subjected to an incident electromagnetic wave is determined. Guided microwave experiments were performed which confirm the theoretical predictions of nonreciprocal wave propagation in such ionized gases.**

Introduction

THIS PAPER is concerned with propagation of high radio frequency electromagnetic waves in ionized gases. More particularly, we shall be concerned here with those general restricted conditions of the ionized gaseous media under which such wave propagation is nonreciprocal.

Before describing the properties of such media, it appears advisable to review in broad terms the main historical áspects of wave propagation effects which led to the discovery of the conditions of nonreciprocity in em wave propagation. We are referring here to the phenomenon observed by Faraday (in 1845) in the course of his studies of the change in the properties of matter under the influence of magnetic fields. In these investigations Faraday used visible light as a probe. Since visible light was used to investigate the change in the bulk properties of matter, this had to be transparent to the light beam so that true propagation in the medium could take place. This requirement led, first, to the use of glass, a transparent dielectric. As is well known, the effect consists of the rotation of the plane of polarization of the plane polarized light waves that are transmitted through the substance when it is immersed in a longitudinal steady magnetic field. This rotation, in substances isotropic when not immersed in magnetic fields, was found to be maximum when the direction of the light wave propagation was parallel or antiparallel with the direction of magnetization.

In 1884, A. Kundt performed the Faraday type experiment by sending light waves through appropriate thicknesses of ferromagnetic metallic foils that were immersed in longitudinal magnetic field. The Faraday effect in paramagnetic substances was first observed in 1906 by J. Becquerel.

While the first observations were made with visible light, the phenomenon has later been extended to very broad regions of the em spectrum on both sides of the visible. Looking back at these original experiments, among the most significant facts appears to be that which concerns the magnitude of the measured rotations.[1]

The systematic experiments of Verdet with a large number of substances transparent to visible light, performed in 1854 and following years, have indicated, as a rule, the proportionality of the rotation angle with the magnetic field intensity and the total (optical) path of the medium traversed by the light waves.

$$\theta = V_e \cdot H \cdot L \cdot \cos \phi. \tag{1}$$

Here H is the magnetic field, L is the total light path, ϕ is the angle of H with the direction of wave propagation, and V_e is a constant of proportionality characteristic of the substance. This constant is known as the Verdet constant. This relation appears to be valid for all substances which are transparent to the light waves used. The Faraday-Verdet rule, however, loses its validity for light waves whose frequency is close to a proper frequency or absorption band of the substance.

It is another historical fact that the Faraday effect has not been satisfactorily interpreted until the discovery of the Zeeman effect some fifty years after the original Faraday experiments.

The interpretation of the Faraday effect, as is now well known, makes use of the Zeeman effect, and it is based on the Fresnel decomposition of a linearly polarized em wave into two circularly polarized waves where the Fresnel vectors are of equal amplitudes and which rotate in opposite senses, at the frequency of the wave. This mathematical "artifice" introduced by Fresnel was instrumental in interpreting the natural rotation phenomena of plane polarized light that was observed in birefringent crystals prior to Faraday's magnetic rotation discovery.

The oppositely rotating circularly polarized waves propagate in the medium with different velocities (phase and energy). If N_+ is the index of refraction of the wave rotating to the right of an observer looking at the source, and N_- is that of the wave which rotates to the left, while N is the index of refraction in the medium in the absence of the magnetic field, we have

$$N_+ = N - \frac{\theta}{L} \cdot \frac{c}{\omega} \quad \text{and} \quad N_- = N + \frac{\theta}{L} \cdot \frac{c}{\omega}$$

where c is the wave velocity in free space and ω is the angular frequency of the propagated wave.

[1] To give an order of magnitude of the rotation angle θ, in glass about 30,000 times as thick as the wavelength, the maximum rotation observed after one crossing was 12° in a field of several thousand Gauss.

* Manuscript received by the PGMTT, July 30, 1957.
† University of Illinois, Urbana, Ill.

It follows from the above that the angle of rotation

$$\theta = L \cdot (N_- - N_+) \frac{\omega}{2c} \cdot \tag{2}$$

The problem of predicting the magnetic rotation of the plane of polarization of a linearly polarized em wave traversing a certain transparent medium is reduced to the determination of the refractive indices N_- and N_+, that is to say, of the velocities of the two oppositely rotating circular waves which compose it.

This assumes that the medium is equally transparent for these circularly polarized waves. Should the medium be dichroic, however, then the rotated wave becomes elliptical with its large axis in the rotated direction. The angle of rotation remains, in general, little or unaffected. Turning now to the medium of our immediate interest, we shall have to define first the conditions of its transparency for high radio frequency em waves.

The Ionized Gaseous Medium

In an ionized gas there are, of course, free charge carriers of both sign. We shall consider here only those gases in which the free negative charges are free electrons and not negative ions. Electrons in all velocity ranges remain free in the inert monatomic gases and only in certain inert molecular gases such as N_2. For simplicity, we shall consider only the monatomic rare gases. The reason for this is that ions, positive or negative, due to their heavy mass, are not capable of oscillations with any significant amplitude in high-frequency em fields; thus, they do not directly affect high-frequency wave propagation in ionized gaseous media; only electrons are influential in determining propagation.

The region of an ionized gas where the free electron density is equal or very nearly so to the density of the positive ions is called a plasma. We shall be referring, in what follows, to gaseous plasmas or to gaseous discharge plasmas. In the latter case, the plasma is produced in the gas by electric fields, dc or ac (high or low frequency).

The free charge densities in laboratory gaseous discharge plasmas, n_e and n_+, are, in general, very much smaller than the densities of the gas atoms N_g, $(n_e/N_g \leq 10^{-5})$.

A plasma can be considered as a mixture of gases. This mixture is composed of the gas of the free electrons, the gas of the positive ions, and that of the neutral atoms (a fraction of which can be partly in short or partly in long life excited states). For such a mixture we can write the classical laws of the gas mixtures and write, for instance, that the total pressure P_t is the sum of the partial pressures of the constituent gases: $P_t = p_g + p_e + p_+$, or in terms of the energy content in these gases we have

$$P_t = N_g k T_g + n_e k T_e + n_i k T_+$$

where T, with the appropriate subscripts, represents the "temperature" of these constituent gases respectively. This assumes that the particles in each of these gases have a Maxwellian distribution of velocity.

$$\left(\text{Then } \frac{Mv^2}{2} = \frac{3}{2} kT\right).$$

From a thermodynamic viewpoint, we have two essentially different cases of interest: an isothermal plasma where $T_e = T_+ = T_g = T$ or a nonisothermal plasma where $T_e \neq T_g$, and $T_e \neq T_+$.

The plasma constituents are in continuous interaction with each other. This interaction, with kinetic energy exchange, takes place through collisions which occur at a frequency generally designated by ν, with the appropriate subscript, ν_{e-m}, ν_{e-i}, ν_{e-e}.[2] There is a direct relation between the temperature of the constituent gases and the collision frequency of the interacting particles. The most important relations of immediate interest in gaseous discharge plasma in which electromagnetic wave propagation takes place are

$$\nu_{e-m} \cong Q \cdot N_g \cdot \bar{v}_e = Q \cdot N_g \left(\frac{3kT_e}{m}\right)^{1/2} \sim A \cdot T_e^{1/2} \tag{3}$$

if Q is independent of v_e, A is constant. The collision cross section Q is dependent on the nature of the gas.

$$\nu_{e-i} = 3.6 \frac{n_i}{T_e^{3/2}} \log_n \left\{\frac{3.7 \times 10^3}{n_i^{1/2}} T_e \left(\frac{2T_e \cdot T_i}{T_e + T_i}\right)^{1/2}\right\}$$

$$\sim B \cdot \frac{n_i}{T_e^{3/2}} \tag{4}$$

where B is a constant, since the log term is very slowly varying.

Thus

$$\nu = \nu_{e-n'} + \nu_{e-i} \cong A T_e^{1/2} + B \cdot \frac{n_i}{T_e^{3/2}} \cdot \tag{5}$$

The interaction between the constituent gases implies a tendency toward a (thermodynamic) temperature equilibrium which can be reached, unless one of the constituents is supplied, selectively, with some kinetic energy —either continuously or otherwise. For instance, if a plasma is produced and maintained by an electric field, then the charges gain energy from the electric field up to that steady-state value at which the energy gained from the field equals the energy transferred to the other constituents of the gas mixture. So in the steady state of "running" (dc or ac) gaseous discharges, the electron gas temperature is always higher than the temperatures of the other constituents and $T_e \gg T_+ \gtrsim T_g$.

If, however, we remove the electric field that maintains a gaseous discharge and thus abandon the plasma (to its fate), then the constituent gases can reach a temperature equilibrium. It is understood that since in

[2] The subscripts *e-m*, *e-i*, and *e-e* designate electron-molecule, electron-ion, and electron-electron, respectively.

such a plasma the free charges are being lost through various processes and are not being replaced, the abandoned plasma will decay.

In order to have a better understanding of a gaseous discharge plasma as a propagating medium of em waves, it is advisable to inquire into the nature of the electronic collisions with neutral gas atoms and with the other charged constituents. In the presence of electric or electromagnetic field, the electrons acquire kinetic energy between collisions, that is to say, during their free time (τ). This is the time the electrons spend on their free path (λ_e). The energy thus acquired is ordered kinetic energy. If and when this ordered motion is interfered with by a collision, the motion becomes disordered or thermalized, and a fraction of the electron kinetic energy is lost to the partner with which the collision took place. The fraction of the energy transferred to a gas molecule, in such a collision, depends upon whether the electron kinetic energy is adequate or inadequate to excite any of the possible quantized states of the colliding partner. If it is inadequate, the collision could only be elastic, and the fraction of the electron energy lost on the average is about $2m/M$ where M, m are the masses of the colliding partners, respectively. In the other case, the collision may result with a certain probability in the excitation of the atomic colliding partner. (Ionization is, of course, a particular state of excitation.) In that case, a large fraction of the electron kinetic energy is lost. It is then obvious that the nature of the gas (He, Ne, A, Kr, Xe) and the pressure etc., play essential roles in the behavior of such plasmatic media.

Behavior in Microwave Fields

Let us consider the high-frequency behavior of gaseous discharge plasmas. In order to describe the wave propagation properties of such a medium, we have to determine the polarizability, or dielectric coefficient, the conductivity, and the magnetic permeability of the plasma, and their behavior in high frequency em fields. As mentioned earlier, only the free electrons of the plasma which are capable of oscillating with full amplitude at high radio frequencies, affect microwave propagation.

The conductivity of a free electron gas in vacuum, in microwave fields of frequency ω, is imaginary $\sigma = j(ne^2/m\omega)$. The effective dielectric coefficient of free space containing a gas of free electrons is

$$\frac{\epsilon}{\epsilon_0} = 1 - \frac{n \cdot e^2}{\epsilon_0 m \cdot \omega^2}, \tag{6}$$

where ϵ_0 is the dielectric constant of free space.

In a plasma where the gas of free electrons interacts with the other plasma constituents, the conductivity is complex.

$$\sigma_c = \sigma_r + j\sigma_i \tag{7}$$

(the subscripts c, r, i designate complex, real, and imaginary, respectively).

The complex conductivity of a plasma in the absence of any magnetic field as calculated by Margenau[3] and Ginsburg,[3] is shown in Fig. 1.

$$\sigma_c = \frac{4}{3} \frac{e^2 \lambda_e n_e}{\sqrt{2\pi m K T}} \left[K_2(x_1) - j x_1^{1/2} K_{3/2}(x_1) \right] \tag{8}$$

where

$$x_1 = \frac{m(\omega\lambda)^2}{2kT}$$

n_e = electron density,
m = electron mass,
e = electron charge,
λ_e = electron mean free path,
k = Boltzmann's constant,
T = temperature (°K).

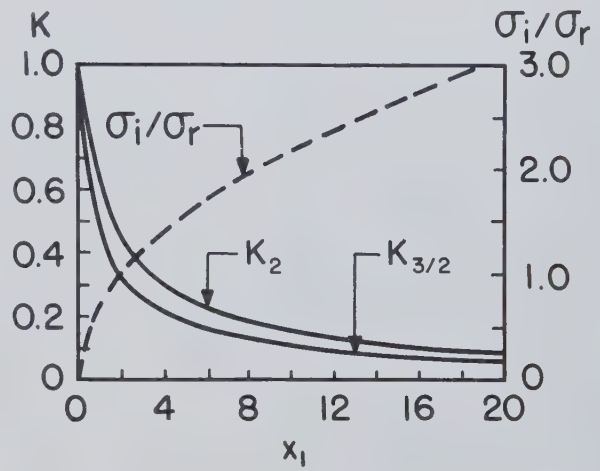

Fig. 1—Complex conductivity of a plasma (after Margenau[3]).

The functions $K_2(x_1)$ and $K_{3/2}(x_1)$ are plotted on Fig. 1. This formula of the complex conductivity of a gaseous plasma is approximated by the following simplified formula adequate for a general discussion:

$$\sigma_c = \frac{n_e e^2}{m} \left[\frac{\nu}{\nu^2 + \omega^2} - j \frac{\omega}{\nu^2 + \omega^2} \right] \tag{9}$$

where ν is the total collision frequency of the electrons. The magnetic permeability of a plasma of relatively low charge density is, essentially, that of free space in the absence of any magnetic field.

It is seen that both the real and imaginary parts of the complex conductivity are dependent on the electron density n_e and the electron collision frequency ν. The real part of the conductivity is maximum for $\nu = \omega$, in which case, $\sigma_r/\sigma_i = 1$.

At this point it is apparent that there are two plasma states of interest: 1) $\sigma_r/\sigma_i \ll 1$ and 2) $\sigma_r/\sigma_i \sim 1$. In the first case $\nu/\omega < 1$ and the plasma can be considered as a dielectric medium with a coefficient ϵ in the sense of electrostatics.

[3] H. Margenau, *Phys. Rev.*, vol. 69, p. 510; 1946.
V. Ginsburg, *J. Phys., U.S.S.R.*, vol. 8, p. 253; 1944. (In English.)

$$\frac{\epsilon}{\epsilon_0} = 1 - \frac{4\pi\sigma_i}{\omega} = 1 - \frac{4\pi n_e e^2}{m} \cdot \frac{1}{\nu + \omega^2} = 1 - \frac{\omega_p^2}{\nu^2 + \omega^2} \quad (10)$$

with

$$\frac{4\pi n_e e^2}{m} = \omega_p^2.$$

Whether in the absence of magnetic fields this dielectric plasma is transparent for em waves of frequency ω depends upon the sign of ϵ/ϵ_0. This is determined by the ratio of $\omega_p^2/\omega^2+\nu^2$.

The two extreme cases of interest mentioned from the viewpoint of ν and ω are 1) $\nu/\omega<1$ and 2) $\nu/\omega>1$. Case 1) indicates that the electrons are undergoing many oscillations per collision, which corresponds in general to low gas pressure and/or high frequencies, whereas case 2) indicates that the electrons undergo many collisions per oscillation. This case corresponds in general to high gas pressure and/or low-frequency oscillatory fields. In general, plasma conditions satisfying case 1) are selected for microwave frequency propagation in plasmas [although for certain cases; *e.g.*, case 2), could be more favorable]. In this case $\nu^2 \ll \omega^2$ and the real part of the conductivity is directly proportional to the electron density n_e and the electron collision frequency ν. The dielectric coefficient and, therefore, the wave propagation conditions, are controlled by the ratio of the plasma frequency to signal frequency. In particular, for frequencies lower than plasma frequency, no true propagation takes place since the phase velocity of the wave becomes imaginary.

$$V_{ph}^2 = \frac{c^2}{1 - \frac{\omega_p^2}{\omega^2}} \cdot \quad (11)$$

Under these conditions the plasma defines boundaries for wave propagation. This is the case of the ionosphere for the lower frequency ionospheric waves. However, these em waves still penetrate the plasma and progress in it with decreasing amplitude. The amplitude is decreased to $1/e$ of its value in a distance

$$d = \frac{c}{\omega_p}\left(1 - \frac{\omega^2}{\omega_p^2}\right)^{-1/2}$$

so that for $\omega \ll \omega_p$, d approaches $1/2\pi \times \lambda$ (free space) for radiation at the plasma frequency.

Since the plasma frequency is proportional to the square root of the electron density—a parameter essentially controllable—conditions for propagation of microwaves, or if desired, conditions for no propagation, can be adjusted at will. This control of wave propagation can be exercised on microsecond or shorter time scales, which makes this extremely flexible medium suitable for such wave propagation control.

Now for signal frequencies $\omega>\omega_p$ the wave propagates in the plasma. However, in view of the complex conductivity of a plasma in microwave (em) fields, its index of refraction is also a complex quantity.

$$\mathfrak{N} = N - jq,$$

where N is the ordinary index of refraction and q is the extinction index.

So that the amplitude of a wave of the form

$$E = a \cdot \exp\left[j\omega\left(t\frac{\mathfrak{N}}{c} z\right)\right]$$

propagating in the z direction, that can also be written as

$$E = a \cdot \exp\left(-\frac{\omega}{c} qz\right) \times \exp\left[j\omega\left(t - \frac{N}{c} z\right)\right],$$

decreases as the wave progresses in the medium.

This attenuation is due to dissipation of em energy in the medium through the agency of the electrons. Under the above conditions of $\nu^2 \ll \omega^2$, attenuation is controlled by both n_e and ν.

Gaseous Discharge Plasmas in DC or Slowly Varying Magnetic Fields

In the absence of a magnetic field an unbounded plasma is isotropic for em wave propagation. The dispersion relation for such a plasma is given in (11), for negligible collisional losses. If we now place the plasma in a finite dc or slowly varying magnetic field, such that the field direction is parallel or antiparallel to the direction of em wave propagation, then the propagating properties of such a medium are modified in two essential ways:

1) The medium is no longer isotropic. It behaves as a uniaxial crystal. Indeed, propagation in any material medium is dependent upon the electric and magnetic polarizability of the medium. In the plasma, the magnetic polarization can be disregarded since the spin contribution to the permeability is largely negligible. The contribution of the orbital diamagnetic electron current loops can also be neglected, since, for conditions outside of the cyclotron resonance, the total diamagnetic moment of the Maxwell distributed free electron gas is zero. Neglecting losses, which in a way implies low level microwaves in practice, the electric induction $\vec{D} = \epsilon\vec{E} + \vec{P}$ will largely control the wave propagation in the plasma. Now, since the magnetic field applied in the z direction causes the electrons to describe circular orbits around the dc magnetic field, the high-frequency electric field of the wave, here normal to the dc magnetic field, will develop a component of motion at right angles to itself and in time quadrature with it.

This can be expressed in the following matrix representation:

$$\begin{pmatrix} D_x \\ D_y \\ D_z \end{pmatrix} = \begin{pmatrix} \epsilon & -j\epsilon' & 0 \\ j\epsilon' & \epsilon & 0 \\ 0 & 0 & \epsilon'' \end{pmatrix} \begin{pmatrix} E_x \\ E_y \\ E_z \end{pmatrix} \tag{12}$$

where we have assumed:

$$\frac{\epsilon}{\epsilon_0} = 1 + \frac{\omega_p^2}{\omega_H^2 - \omega^2}, \quad \frac{\epsilon}{\epsilon'} = \frac{\omega_H \cdot \omega_p^2}{\omega(\omega_H^2 - \omega^2)}; \quad \frac{\epsilon''}{\epsilon_0} = 1 - \frac{\omega_p^2}{\omega^2}.$$

$\omega_H = \gamma H_{DC}$ and γ = gyromagnetic ratio of electron. It is seen that in the gas plasma it is the dielectric constant which is a tensor as compared to the permeability tensor in the ferromagnetic substances.

2) The plasma frequency has lost direct control of the propagation of plane polarized em waves. The gyrofrequency of the electrons ω_H, now contributes to this control.

If the wave is plane polarized and thus composed of two oppositely rotating circularly polarized waves, it is rotated in its progression in the medium; the circularly polarized waves having different phase velocities. The dispersion relation—again for $\nu/\omega < 1$—becomes

$$V_{ph}^2 = \frac{c^2}{1 - \frac{\omega_p^2}{\omega^2} \cdot \frac{1}{1 \mp \frac{\omega_H}{\omega}}}. \tag{13}$$

The minus sign before ω_H applies if the electric vector of the wave rotates in the same sense as the gyrating electrons. This circular wave is the equivalent in optics to the extraordinary wave, in opposition with the other (or plus) wave called the ordinary wave.

The above relation can also be written as:

$$V_{ph}^2 = \frac{c^2}{1 - \frac{\omega_p^2}{(\omega')^2}}, \tag{14}$$

where

$$(\omega')^2 = \omega^2\left(1 \mp \frac{\omega_H}{\omega}\right).$$

This now shows more clearly whether propagation can take place depending upon the value of $\omega_p^2/(\omega')^2$.

Eq. (13) invites the following remarks. 1) For zero magnetic field we have (11) (that is $\omega' = \omega$). For zero plasma frequency, the propagation is that in vacuum. For infinite magnetic field, whatever the plasma frequency, it is the same as in vacuum.

2) The angle of rotation of the linear wave, observed at a distance L inside the plasma for each value of the magnetic field, depends upon the electron density in the plasma; this angle is being determined by the difference in the refractive indices of the two oppositely rotating circular waves, that compose the linearly polarized wave.

3) The angle of rotation varies rapidly in the vicinity of the plasma frequency, which is one of the proper frequencies of the magnetic field permeated plasma. This is, of course, also the case for $\omega \sim \omega_H$.

4) It is also apparent that for certain values of ω_H/ω and ω_p^2/ω^2 resonance conditions prevail. In addition to the electron cyclotron resonance, a plasma resonance can also be observed. This resonance is called the magneto-plasma resonance, since for any value of the dimensionless parameter of ω_p^2/ω^2, it is a function of the magnetic field intensity.

The discussion of the case of a loss-less unbounded infinite plasma, even though unrealistic, is extremely useful in that it points out the basic wave propagation properties of such a medium when used in any practical form.

Guided Wave Propagation in Plasmas

Guided microwave propagation through gaseous discharge plasmas is, in several respects, different from plane wave propagation in unbounded plasmas. However, since the basic properties of such a medium in a waveguide even though bounded remain largely unaffected, the propagation phenomena do not differ in their essential features from the unbounded case.

Here, wave propagation is, of course, dependent upon waveguide geometries, the waveguide modes. Phase velocity of the em waves (guide wavelength) and waveguide cutoff condition are important parameters of the problem.

The detailed theoretical aspects of Faraday rotation of guided waves through gyromagnetic media and to some extent gyromagnetic (gaseous) plasmas—outside of the scope of this paper—have been discussed in particular by Suhl and Walker[4] in this country and also by a group of French workers.[5] It does not appear to be fruitful to elaborate on these in this paper.

However, before describing typical guided wave nonreciprocal propagation and resonance experiments in plasmas and discussing their possible applications, it seems worthwhile to point out that, in general, the experimental conditions, for which results are presented below, justify the approximations of the theory with regard to the use of "quasi" TE_{11} waves in a plasma filled circular waveguide on a length of the order of 1–2 free space wavelength, even though rigorously the circular waves are not true modes of propagation in the plasma filled guide that is immersed in a longitudinal magnetic field.

We also would like to draw attention to the action of an applied magnetic field (whose intensity is varied) on the plasma itself in the absence of any electromagnetic energy.

[4] H. Suhl and L. R. Walker, *Bell. Sys. Tech. J.*, vol. 33, pp. 579, 939, and 1133; 1954.
[5] M. Bonnet, M. Matricon, and R. Roubine, *Ann. Telecommun.*, vol. 10, p. 150; 1955.

Experiments on Guided Microwave Propagation Through Magnetic Field Produced Anisotropic Gaseous Discharge Plasmas

In what follows we shall describe and illustrate experiments of Faraday rotation and gyroresonance in circular or other waveguide geometries with two different types of plasmas: 1) isothermal at room temperature and 2) dc or ac maintained nonisothermal plasmas. Both are under widely varied conditions of plasma frequencies and electron collision frequencies (nature and pressure of the gases in which the plasmas were produced). These experiments were carried out with microwaves in the *C*-band (5000 mc) and *X*-band (9000 mc) frequencies.

The waveguide Faraday effect consists of the rotation of the whole field pattern of the linearly polarized TE_{11} waves. The plane of the maximum electric field in this angularly dependent mode, which is along a diametral line, is taken as its plane of polarization. By rotation of the wave by an angle θ is meant a rotation by that angle of the whole field pattern and consequently that of the plane of polarization (maximum E field).

For $\theta = 90°$, linearly polarized TE_{11} waves are in independent states of polarization—there being a twofold degeneracy. Any TE_{11} wave in any state of polarization may be regarded as composed of two such independent TE_{11} component modes of appropriate amplitudes and phases. Circular polarization of a TE_{11} wave as well as linear polarization is therefore possible. Consequently, polarization transformations also can be produced.

For magneto-rotation experiments, a cylindrical gaseous discharge tube is located coaxially in a cylindrical waveguide in which TE_{11} waves are propagated at a low power level. The rf waves were either cw or pulsed. The tube lengths were of the order of 1–2 free space wavelengths completely immersed in a longitudinal magnetic field. The magnetic field for the *C*-band experiments was produced by solenoids surrounding the gas discharge tube filled portion of a cylindrical waveguide. The notations $\sigma = \omega_H/\omega$ and $q = \omega_p/\omega$ are used in the figures. The typical results below on magneto-rotation are relative to isothermal gaseous plasmas at room temperature (~300°K). These plasmas are obtained in the afterglow period of a decaying gaseous discharge. Fig. 2, opposite, shows the Faraday rotation of guided waves through an isothermal helium plasma at 300°K in a longitudinal magnetic field as a function of electron density. Fig. 3 illustrates the magneto-rotation of TE_{11} linear polarized waves through a neon plasma as a function of magnetic field for various gas pressures. It is apparent that an increase in the electron collision frequency (corresponding to an increase in gas pressure) reduces the amount of rotation obtainable with a given value of magnetic field. Fig. 4 is a comparison of the measured angle of rotation of a linear TE_{11} wave with the calculated angles obtained from direct measurements of the phase velocities of the two circularly polarized TE_{11} waves. As one would expect, the agreement is quite good, Fig. 5 and Fig. 6 are plots of the rotation angle vs magnetic field for various electron densities and gas pressures. Fig. 7 indicates the insertion loss for the two waves and illustrates how such an effect could be used as an isolator. Fig. 8 shows the ellipticity of the linear incident wave after passing through a plasma for various values of electron density or time after the discharge occurred. Fig. 9 demonstrates the variation of the TE_{11} wave amplitude which is reflected after it has traversed the plasma as measured by an antenna perpendicular to the launching antenna, as a function of the angle of rotation of the TE_{11} wave. This indicates the nonreciprocal properties of an anisotropic plasma when used as a propagation medium.

Resonance Phenomena in Gyromagnetic Plasmas at Microwave Frequencies

Since large rotation angles are obtained in the vicinity of a proper frequency of the anisotropic medium, it is of multiple interest to study the medium behavior for signal frequencies in the vicinity of these proper frequencies. The plasma frequency corresponding to each value of the surrounding magnetic field and the gyrofrequency of the electrons are such proper frequencies. This leads us to investigate the corresponding magneto-plasma and pure cyclotron resonances in the anisotropic plasmas.

The resonances for *C*- and *X*-band microwaves were studied in dc and pulsed (decaying) gaseous discharge plasmas permeated by dc or ac magnetic fields.

While neglecting electron collisional effects in plasmas in pure Faraday rotation for low level, rf waves can be justified in many practical cases, this can no longer be justified, however, when resonance conditions prevail in the gyroplasma. The electron collision frequency then becomes a controlling parameter, hence in the region of resonance all propagation effects become increasingly nonlinear. This implies that wave propagation under these conditions becomes very power level dependent (in these experiments even on the milliwatt power levels).

Indeed the width of the cyclotron resonance of the electrons is determined by $2\nu/\omega$. It is, therefore, a function of the nature of the gas, the pressure, the temperature of the electron gas consequently of the power level of the rf wave.

All other conditions being equal, the cyclotron resonance width will be in general broader in dc discharges than in lower electron temperature plasmas. This is illustrated in Fig. 11. Considering for instance the x component of the real part of the magneto-plasma conductivity (tensor)

$$\sigma_{rx} = \frac{nev_x}{E_x} = \frac{ne^2}{m \cdot \nu}\left[\frac{1 + j\omega/\nu}{1 + (\omega_H{}^2 - \omega^2)\dfrac{1}{\nu^2} + 2\dfrac{\omega}{\nu}}\right] \tag{15}$$

Introducing the dimensionless quantities a, b, we have

Phase Constants ($\beta = \frac{2\pi}{\lambda_g}$) of the Circularly Polarized TE_{11} Waves in the Anisotropic Medium.

Plus Wave

$$\beta_+ \cong \beta_0 - \frac{\mu_0 e^3 B_0 N}{m^2 \omega \beta_0 (U_{11}^2 - 1)}$$

Minus Wave

$$\beta_- \cong \beta_0 + \frac{\mu_0 e^3 B_0 N}{m^2 \omega \beta_0 (U_{11}^2 - 1)}$$

$\beta_0 = \frac{2\pi}{\lambda_{g_0}}$

λ_{g_0} = Guide Wavelength in Isotropic Medium ($B_0 = 0$)

$U_{11} = 1.841$ for TE_{11} Waves

B_0 = Applied Magnetic Field

N = Electron Density

FARADAY ROTATION θ

$$\theta = V B_0 L = \frac{\beta_- - \beta_+}{2} L$$

L = Length of Medium

B_0 = Applied Magnetic Field

V = Verdet Constant

$$V = \sqrt{\frac{\mu_0}{\epsilon_0}} \frac{|e^3| N}{m^2} \frac{\lambda_{g_0}}{\lambda_0} \frac{1}{4\pi^2 (U_{11}^2 - 1)}$$

λ_0 = Free Space Wavelength

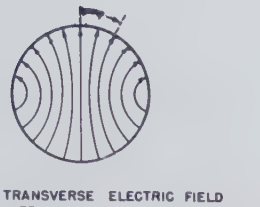

TRANSVERSE ELECTRIC FIELD PATTERN OF BASIC TE_{11} WAVE

Wave Polarization	Peripheral Field
Linear TE_{11}	Cos. φ
Plus Circular TE_{11}	Cos. $(\omega t + \varphi)$
Minus Circular TE_{11}	Cos. $(\omega t - \varphi)$

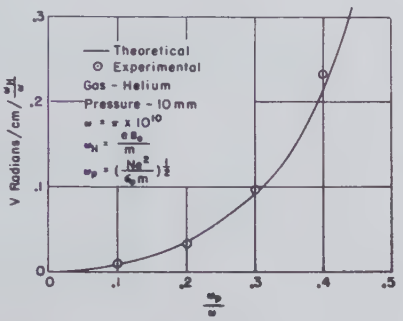

Fig. 2—Faraday rotation of guided waves.

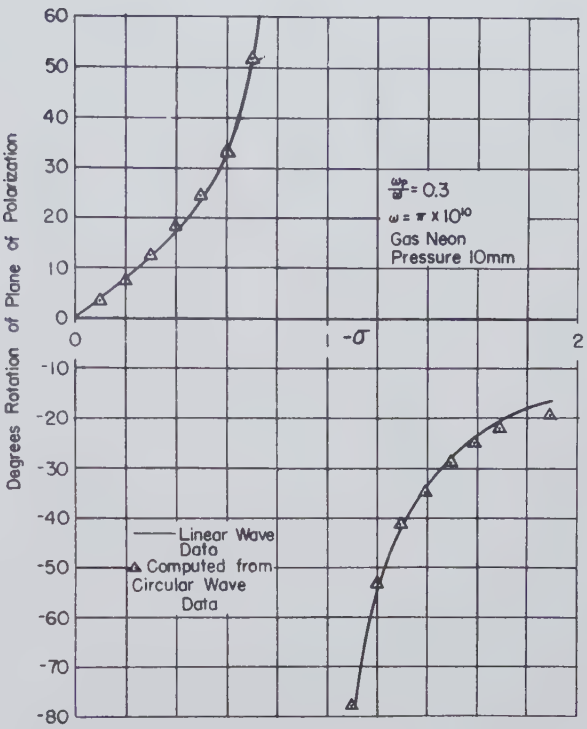

Fig. 4—Rotation of the polarization plane of the transmitted TE_{11} wave vs the magnetic field variable σ for a discharge 7.6-cm length.

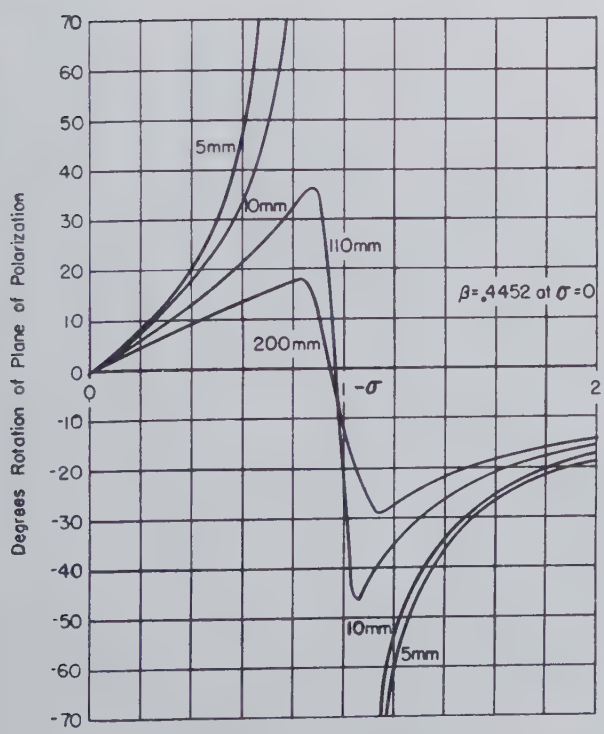

Fig. 3—Rotation of the polarization plane of the transmitted TE_{11} wave vs the magnetic field variable σ for several values of gas pressure. Gas-neon, frequency—5.10^9, discharge length—7.6 cm.

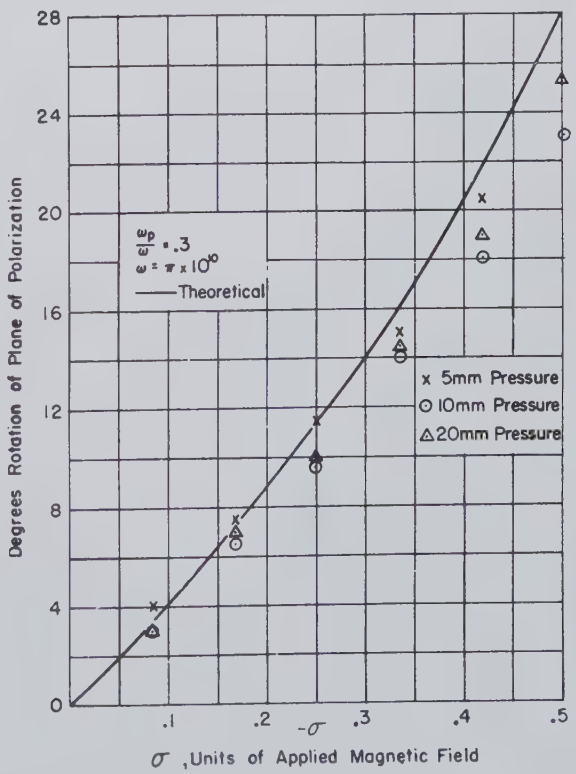

Fig. 5—Rotation of the plane of polarization of the transmitted TE_{11} wave for several values of pressure of a discharge in neon.

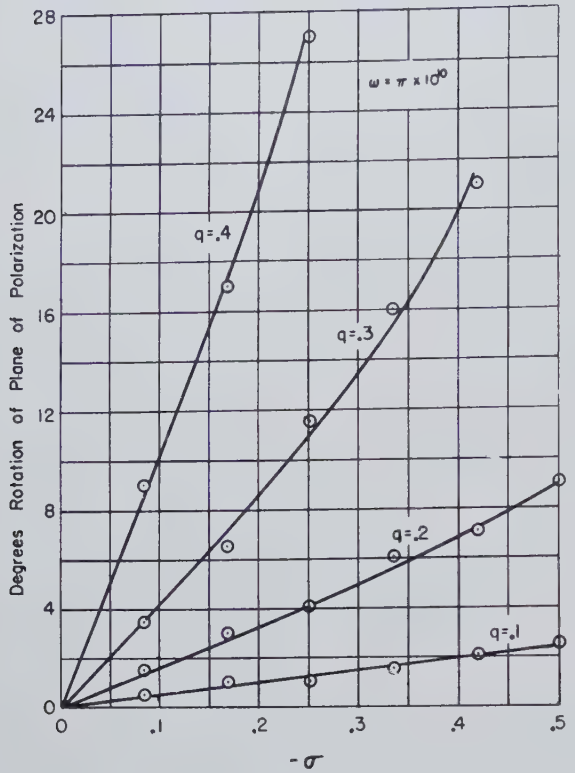

Fig. 6—Rotation of the plane of polarization of the transmitted TE_{11} wave for several values of the electron density variable q. Gas is helium at 10 mm Hg.

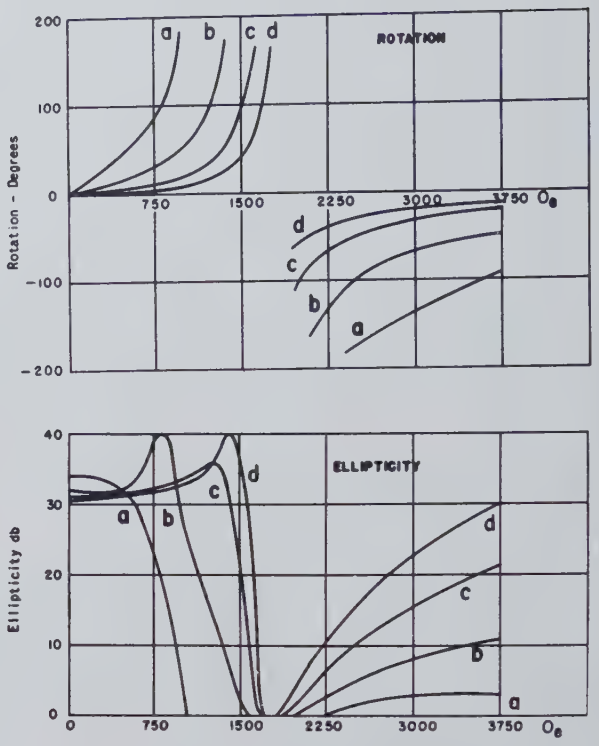

Fig. 8—Transmission of linearly polarized 5000-mc TE_{11} mode incident to decaying discharge. Neon gas, 8-mm Hg, delay (a) 200 μsec, (b) 400 μsec, (c) 700 μsec, (d) 1000 μsec.

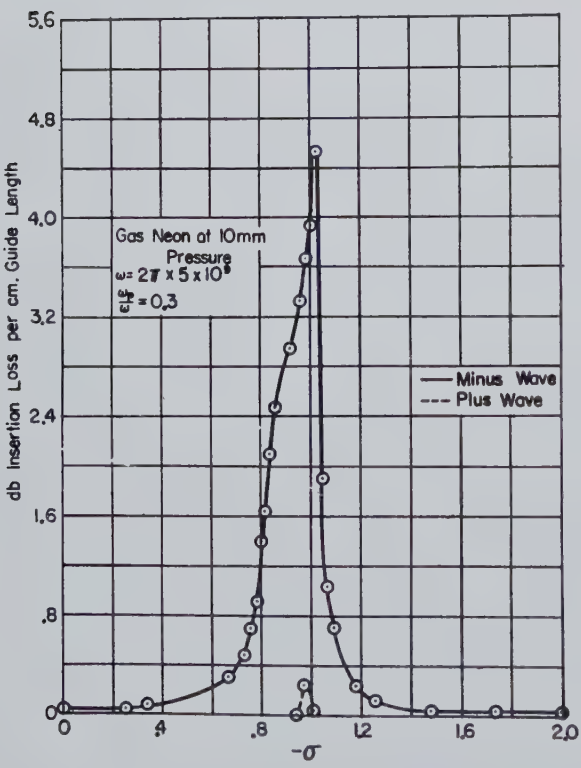

Fig. 7—Insertion loss of plus and minus waves as a function of applied magnetic field variable σ.

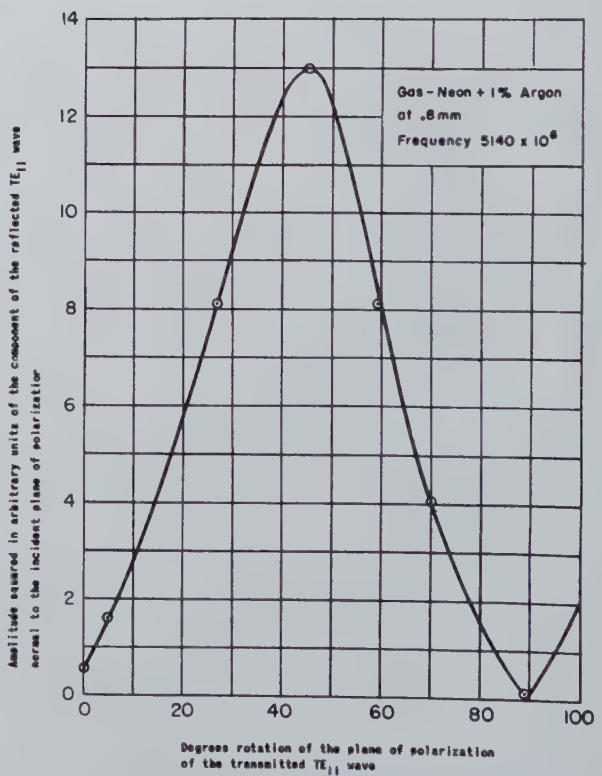

Fig. 9—Demonstration of the nonreciprocity of the anisotropic electron gas.

$$\frac{\sigma_{rx}}{\sigma_0} = \frac{1 + a^2 + b^2}{1 + b^2 - a^2 + 4a^2} \tag{16}$$

where $a = \omega/\nu$ and $b = \omega_H/\nu$, and $ne^2/m\nu = \sigma_0$, the dc conductivity of the plasma.

For the extraordinary wave undergoing resonance, this is reduced to $\sigma_r/\sigma_0 = \frac{1}{2}$. This formula simplifies for the case of $\nu = \nu_{e-m} + \nu_{e-i}$ and can be written as

$$\sigma_{rx} = \frac{ne^2}{m(\nu_{e-m} + \nu_{ei})}.$$

In a gas pressure range above 1 mm Hg, in general, $\nu_{e-m} > \nu_{e-i}$. The controlling factor is the collision frequency of the electrons with neutral gas molecules. For very low gas pressures, (<1/10 mm Hg) and low-level (*C*-band) rf signals but adequately large n, $\nu_{e-m} < \nu_{e-i}$. Then for the extraordinary wave $\sigma_r = ne^2/m \cdot \nu_{e-i}$.

$$\nu_{e-i} = A \frac{n_i}{T_e^{3/2}} \log_n \left\{ \frac{B}{n_i^{1/2}} T_e \left(2 \frac{T_e \cdot T_i}{T_e + T_i} \right)^{1/2} \right\} \tag{17}$$

neglecting the slowly varying logarithmic factor, $\nu_{e-i} \sim C(n_i/T_e^{3/2})$. Hence

$$\sigma_r = \frac{1}{C} \frac{e^2}{m} \cdot \frac{n}{n_i} \cdot T_e^{3/2} \cong C' \cdot T_e^{3/2}.$$

Here A, B, C, and C' are constants, so that the resonance absorption for the above case is essentially independent of the number density of the charges and increases with increasing electron temperature, consequently with rf power level.

Resonance experiments have been performed in cylindrical, rectangular, and square waveguides. The gaseous discharge tubes, generally of glass, in the rectangular and square waveguides were either coaxial with the waveguide or perpendicular to the axis of the waveguide. A slowly varying low-intensity ac magnetic field (also longitudinal) was superimposed on the dc magnetic field and this was used in the detailed exploration of the resonances produced by the main dc magnetic field. Resonance experiments at *X*-band (8–10 kmc) frequencies made use of pulsed magnetic fields. Fig. 10 and Fig. 11 show resonance curves for dc discharge plasmas in *X*-band rectangular waveguide. Fig. 12 illustrates the tube geometry used in these experiments. Fig. 13 indicates the time sequence of the pulsed operations. Fig. 14 illustrates the magneto plasma and cyclotron resonances as a function of electron density and incident rf power. Fig. 15 demonstrates the effect on the plasma of the rf input power level. As can be seen on the first trace of each set, at a power level of 6 mw, the plasma properties change through resonance absorption heating of the electron gas.

Applications

The anisotropic gaseous plasma lends itself to applications, in low-level rf wave propagation control, simi-

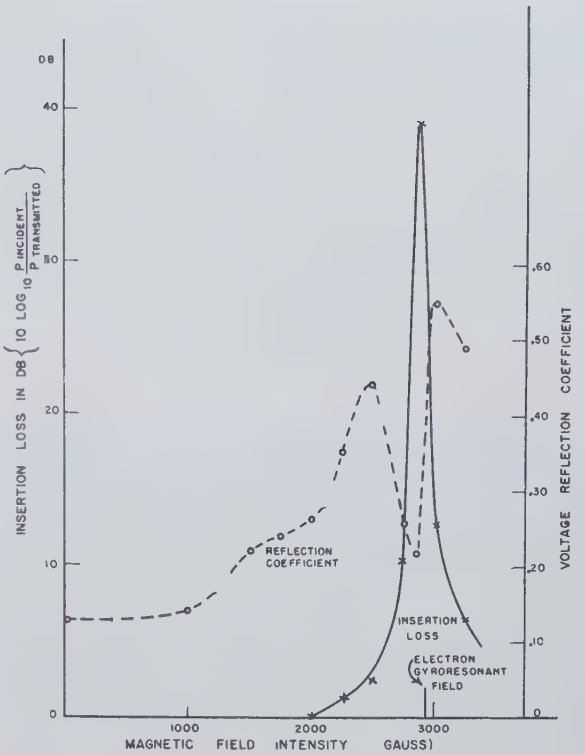

Frequency: 8200 mc
Gas: Ne+1 per cent A at 0.1-mm Hg pressure
Discharge Conditions: Steady dc plasma at 465 v and 30 ma (current limiting resistor of 10,000 Ω included)
Length: L of solenoid = 5 inches ≃ 2 guide wavelengths

Fig. 10—Transmission and reflection characteristics vs magnetic field intensity.

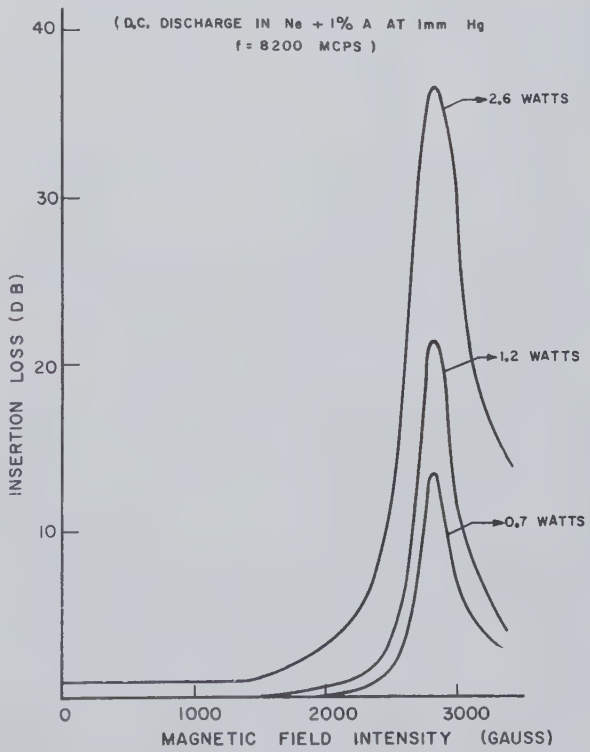

Fig. 11—Insertion loss vs magnetic field.

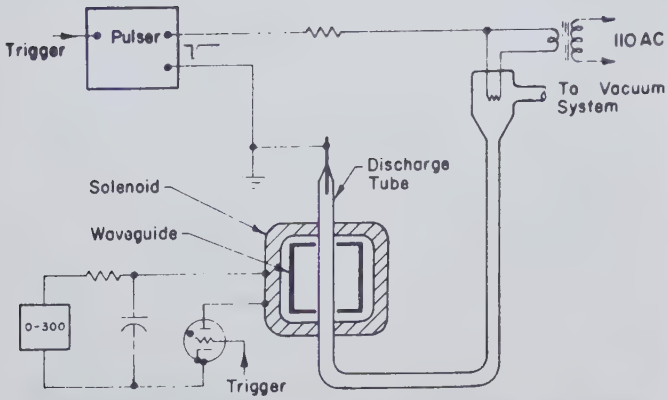

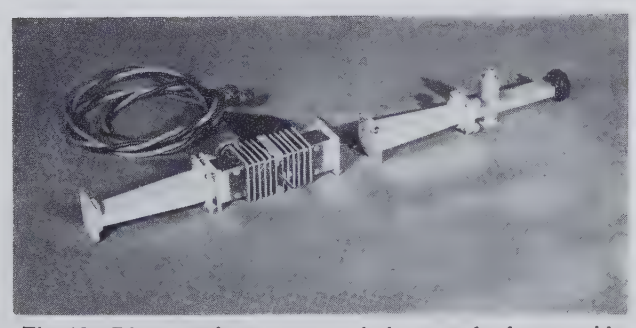

Fig. 12—Diagram of apparatus and photograph of waveguide and solenoid.

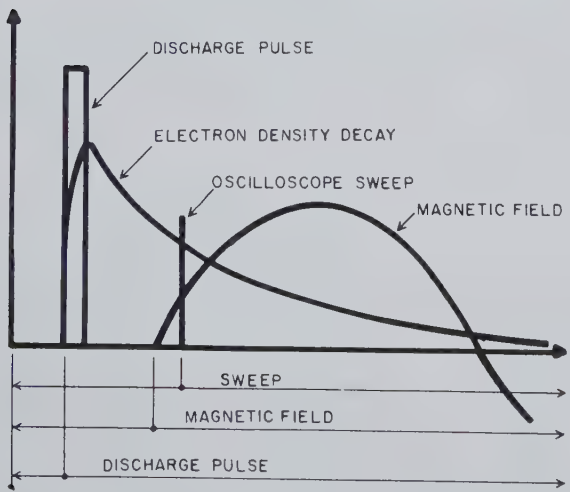

Fig. 13—Synchronization of apparatus.

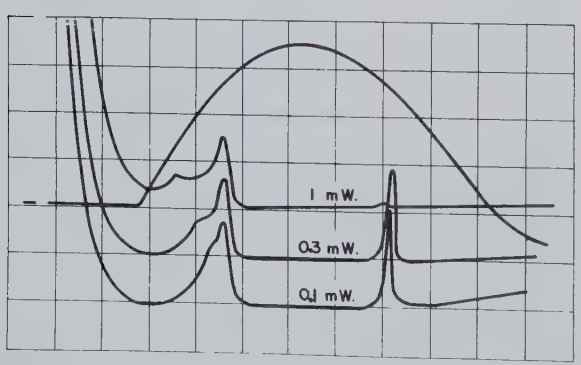

Fig. 14—Resonances—pulsed magnetic field.

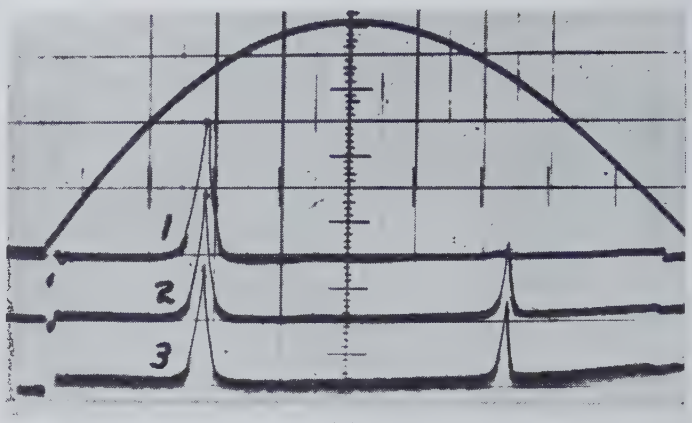

(a)

Power Level

1) 6 mw
2) 0.6 mw
3) 0.25 mw

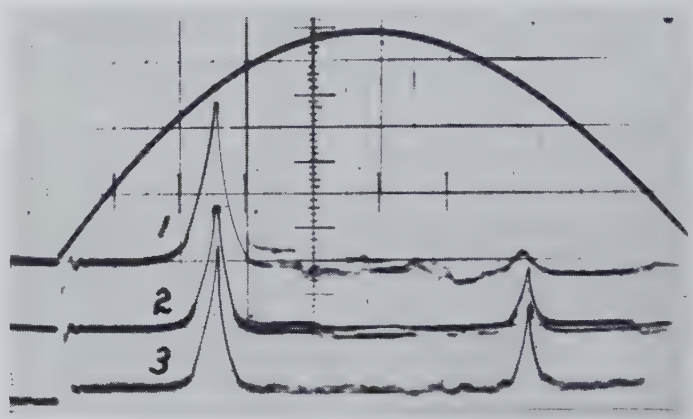

(b)

1) 6 mw
2) 1 mw
3) 0.25 mw

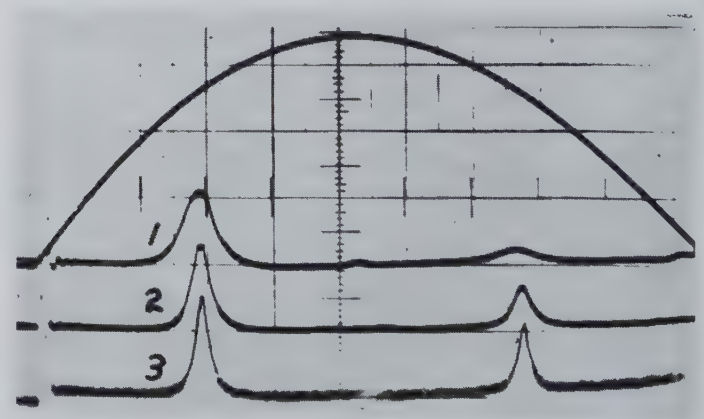

(c)

1) 8 mw
2) 1.5 mw
3) 0.25 mw

Fig. 15—Resonances—pulsed magnetic field.
(a) 4-mm Hg, 175 μsec delay. Sweep Speed 40 μsec/div.
(b) 10-mm Hg, 200 μsec delay. Sweep Speed 30 μsec/div.
(c) 20-mm Hg, 350 μsec delay. Sweep Speed 30 μsec/div.

lar to those in which ferrites are used, with no limitations of frequencies.

For pulsed rf waves decaying gyroplasmas may be more advantageous than stationary media. With pulsed magnetic fields, isothermal gyroplasmas may be used, in particular, for rapid broad-band spectrum analysis. The limitation on the bandwidth is determined by the waveguiding structure containing the magneto plasma. The fact that a gaseous discharge plasma can be established in any desired charge density state on microsecond or shorter time scale and be removed from that state on an equally short time scale makes the ionized gaseous medium a very flexible one whose potentialities have not been, as yet, explored to any great extent or even recognized by microwave engineers.

Acknowledgment

It is a pleasure to acknowledge here the contributions of M. A. Lampert, J. F. Heney, J. E. Etter, M. Gilden, L. P. McGrath, C. K. Chatterjee, and J. P. Monier who at one time or another have been associated with the author in the study of these problems.

The Three-Level Solid-State Maser*

H. E. D. SCOVIL†

Summary—**This article gives an introduction to amplification by solid-state maser techniques. Emphasis is placed on the three-level solid-state maser. The relevant physical properties of paramagnetic salts are discussed. The basis of the three-level excitation method is reviewed. Some design considerations are given. The design and performance characteristics of a particular device are mentioned.**

Introduction

MASERS (microwave amplifier by stimulated emission of radiation) offer the possibility of amplification with very low-noise figures. With suitable regeneration they may be converted into oscillators having a high degree of spectral purity.

The interaction medium consists of "uncharged" magnetic or electric dipoles. It is partially because of the lack of any charge fluctuations that these devices may exhibit low-noise characteristics. The medium is maintained in such a state that it presents negative loss or gain to incident radiation.

Beam-type masers,[1] because of their high stability, make excellent frequency standards. It is, however, just the properties that give them high stability, namely a high molecular Q and a fixed frequency, that limit their versatility as easily tunable broad-band amplifiers. In these respects solid-state masers offer advantages. The three-level maser now appears to be the most useful of the solid-state types since it amplifies in a continuous manner and its high permissible spin concentration leads to relatively large gain bandwidth products.

A review article on masers by Wittke has appeared.[2] It discusses the basic fundamentals as well as giving a brief description of each type. The purpose of the present article is to discuss in more detail the three-level solid-state maser.

The next section reviews some of the physical processes involved in the operation of the device. The following section discusses the three-level excitation method and the properties of suitable materials. Some remarks are then made about design considerations and the design and performance of a particular 6-kmc device is mentioned.

Properties and Processes of the Medium

General Remarks

The maser medium consists of an ensemble of atomic magnetic moments or "spins" in the solid state. The individual dipoles may take up only certain discrete or "allowed" energy states as a result of interaction with crystalline electric and applied magnetic fields.

Since the medium chosen is such that the mutual interaction between dipoles is weak, the entire ensemble may be treated statistically as though all of the particles are distributed over the allowed states of an individual particle.

This system is referred to as the spin system. Interactions occur within the spin system and between the spin and the remainder of the crystal lattice as well as with a radiation field. These interactions are now discussed.

* Manuscript received by the PGMTT, September 23, 1957.

† Bell Telephone Labs. Inc., Murray Hill, N. J.

[1] J. P. Gordon, H. J. Zeiger, and C. H. Townes, "The maser—new type of microwave amplifier, frequency standard, and spectrometer," *Phys. Rev.*, vol. 99, pp. 1264–1274; August, 1955.

[2] J. P. Wittke, "Molecular amplification and generation of microwaves," Proc. IRE, vol. 45, pp. 291–316; March, 1957.

Spin-Spin Relaxation or Dipolar Interaction

Interactions within the spin system have been examined by several authors.[3,4] A heuristic treatment is given here. Consider the case of a spin surrounded by neighboring spins and subject to a magnetic field H applied in the Z direction as depicted in Fig. 1 where only one neighbor is shown. Spin (a) will be subject not only to the applied magnetic field but also to the magnetic fields of its neighbors. The field of a neighbor may be resolved into two components, one parallel to H, the other perpendicular to H.

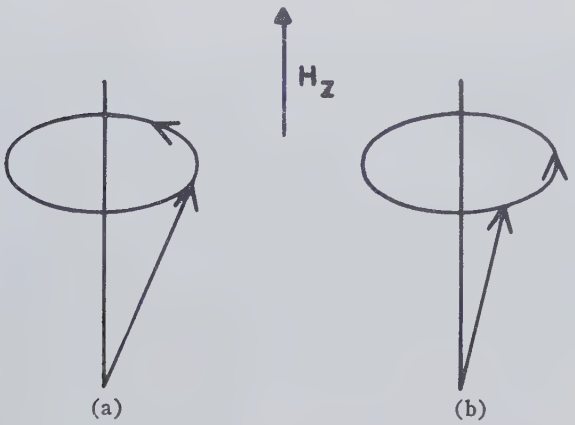

Fig. 1—Two neighboring spins (a) and (b) are depicted as precessing in an applied magnetic field. H.

The parallel component is added to H. Since the Z components of the neighbors are randomly distributed, this will cause a distribution of Larmor precession frequencies about that determined by H. This effect is known as "inhomogeneous spin-spin broadening" since its effect is closely related to the application of an inhomogeneous-magnetic field over the sample.

The transverse component of the precessing spin (b) will cause an rf magnetic field at spin (a) with a frequency equal to the Larmor frequency of (b). If spins (a) and (b) are equivalent, that is, if they have the same Larmor frequency, then this rf field is of the correct frequency to induce resonance in (a) and vice versa. Because this energy exchange reduces the lifetime of the spin states, it will broaden the resonance line. This "homogeneous spin-spin broadening" provides a mechanism whereby energy is transferred throughout the spin system. The interaction tends to keep the spin system in internal equilibrium and to destroy any coherence or phase relationships between spins in a characteristic "spin-spin relaxation time."

It is apparent that inhomogeneous broadening always occurs. Homogeneous broadening, however, is dominating only when nearby spins are equivalent. When all spins are equivalent the broadening of the resonance line by homogeneous broadening is the greater effect. The magnitude of the dipolar interaction depends upon the spin concentration. In practice it is controlled by "magnetic dilution" that is, mixed crystals are grown in which the magnetic atoms are partially replaced by isomorphous diamagnetic atoms.

Spin-Lattice Interaction

Thermal motion of the crystal lattice gives rise to time dependent crystalline electric fields. These fluctuating fields act on the orbital motion of the electron and then. via the mechanism of spin-orbit coupling on the spins. This provides a means whereby energy may be transferred between the spin system and the crystal lattice which is usually treated as a heat sink at the bath temperature. This thermalizing or spin-lattice relaxation process is temperature dependent, the relaxation time increasing as the temperature is lowered.

A simple but important relationship between relaxation times may be obtained as follows. Consider a simple two-state system as depicted in Fig. 2 with $N=n_i+n_j$ particles distributed over the states and with relaxation times T_{nm} as shown. The energies of the states are E_i and E_j with $E_j>E_i$. Then

$$\frac{dn_i}{dt} = n_j/T_{ji} - n_i/T_{ij} \tag{1}$$

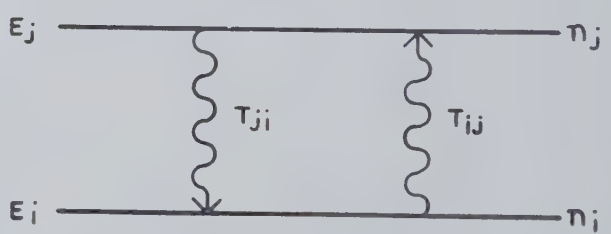

Fig. 2—Two states with energies E_j and E_i and spin populations n_j and n_i are shown. Spin-lattice relaxation times between states are indicated.

In Boltzmann equilibrium at temperature T, $dn_i/dt=0$ and n_i and n_j assume their equilibrium values N_i and N_j. Thus

$$T_{ij}/T_{ji} = N_i/N_j = e^{(E_j-E_i)/kT}. \tag{2}$$

Although (2) has been derived for only a two-state system, it may be shown to apply to a multistate system by solving simultaneously all of the rate equations.

Spin-lattice interaction shortens the lifetimes of the states and thus broadens the resonance line. A review of spin-lattice interaction is given by Cooke[5] and Gorter.[6]

Spin Temperature

It is frequently convenient to retain the form of the Boltzmann relation (2) even when the spin system is

[3] M. H. L. Pryce and K. W. H. Stevens, "The theory of magnetic resonance—line widths in crystals," *Proc. Phys. Soc. A*, vol. 63, pp. 36–51; January, 1950.

[4] J. H. Van Vleck, "The dipolar broadening of magnetic resonance lines in crystals," *Phys. Rev.*, vol. 74, pp. 1168–1183; November, 1945.

[5] A. H. Cooke, "Paramagnetic relaxation effects," *Rep. Prog. Phys.*, vol. 13, pp. 276–294; 1950.

[6] C. J. Gorter, "Paramagnetic Relaxation," Elsevier Press, Amsterdam, The Netherlands; 1947.

not in thermal equilibrium with the lattice. If the populations of two spin states (Fig. 2) are n_i and n_j then a spin-temperature T_s is defined by

$$n_i/n_j = e^{(E_j-E_i)/kT_s}. \tag{3}$$

That is, T_s is used as a measure of the ratio n_i/n_j even when thermal equilibrium is nonexistent. If

$$\begin{aligned} n_i > n_j \quad &\text{then} \quad T_s > 0, \\ n_i = n_j \quad &\text{then} \quad T_s = \pm\infty, \\ n_i < n_j \quad &\text{then} \quad T_s < 0. \end{aligned}$$

The last case that of negative spin temperatures may be caused by "population inversion." Negative spin temperatures are "hotter" than positive spin temperatures. From (3) one finds that

$$n_i - n_j = n_j[e^{(E_j-E_i)/kT_s} - 1]. \tag{4}$$

Since $(E_j-E_i)/kT_s$ is usually small when dealing with microwave frequencies

$$[e^{(E_j-E_i)/kT_s} - 1] \approx (E_j - E_i)/kT_s \text{ and } n_j \approx \frac{N}{2}$$

and (4) becomes

$$n_i - n_j \approx \frac{N}{2}(E_j - E_i)/kT_s. \tag{5}$$

Stimulated or Induced Emission and Absorption

A particle may exchange energy with an incident radiation field in accordance with the Bohr frequency condition

$$E_j - E_i = h\nu_j \tag{6}$$

emitting or absorbing a photon of frequency ν_{ji} depending on whether $E_j >$ or $< E_i$; $h = 6.6\times10^{-27}$ erg seconds is Planck's constant.

This energy exchange is governed by certain transition probabilities W_{ij} which are products of transition probability coefficients w_{ij} and the square of the field amplitude. Thus

$$W_{ij} = w_{ij}H_{rf}^2 \tag{7}$$

w_{ij} is a complicated function that depends on the nature of the states i and j as well as on the nature of the radiation field. The relevant field vector may be either E_{rf} or H_{rf}, H_{rf} is used in (7). Frequently $w_{ij}=0$ in which case the transition is said to be "forbidden." As a consequence of the fact that the coefficient w_{ij} contains the square of a matrix element connecting states i and j,

$$w_{ij} = w_{ji}. \tag{8}$$

That is, the probability for induced emission is equal to that for induced absorption. Consider the two-state system depicted in Fig. 3, radiation of frequency $\nu=(E_j-E_i)/h$ is incident.

The total power absorbed is $P_{ij} \propto n_i w_{ij} H_{rf}^2$, and the total power emitted, $P_{ij} \propto n_j w_{ij} H_{rf}^2$. Hence using (5), (6), and (8), the net power absorbed is

$$P_{abs} \propto \frac{N}{2}\frac{h_\nu}{kT_s} w_{12} H_{rf}^2. \tag{9}$$

So far it has been tacitly assumed that the energy levels are sharp, corresponding to zero width for the resonance line. In practice because of the broadening effects of the relaxation processes the resonance line will have some frequency spread $\Delta\nu$. As expected the broader the line the less the intensity of absorption. Thus (9) may be rewritten

$$P\,\text{abs} \propto \left(\frac{N}{T_s}\frac{1}{\Delta\nu} w_{12}\right) H_{rf}^2 \tag{10}$$

where the constants have been dropped. In this case the absorption is a magnetic one and macroscopically it would be represented as

$$P\,\text{abs} \propto \chi'' H_{rf}^2 \tag{11}$$

where χ'' is the imaginary component of the magnetic susceptibility of the material. Since the bracketed term in (10) depends only on the state of the material

$$\chi'' \propto \frac{N}{T_s}\frac{1}{\Delta\nu} w_{12}. \tag{12}$$

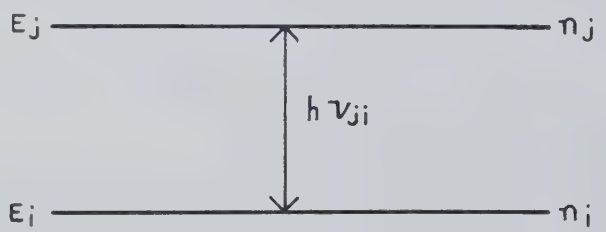

Fig. 3—Two states with energies E_j and E_i and spin populations n_j and n_i are shown. Radiation of frequency ν_{ji} is depicted as inducing transitions.

In thermal equilibrium, $T_s>0$ and both Pabs and χ'' are positive corresponding to positive losses. In a maser, population inversion corresponding to $T_s<0$ is produced and both Pabs and χ'' become negative corresponding to negative loss or gain. The stimulated emission may be shown in a more sophisticated treatment[7,8] to be coherent with respect to the incident radiation. Thus, in the case of a negative temperature material the amplified output signal is phase related to the input signal.

Spontaneous Emission

In addition to stimulated emission and absorption, there is the process of spontaneous emission which occurs in the absence of applied radiation. The mechanism may be considered to be that of stimulated emission induced by the zero point oscillations of the vacuum.

[7] L. I. Shiff, "Quantum Mechanics," McGraw-Hill Book Co., Inc., New York, N. Y.; 1955.
[8] W. Heitler, "The Quantum Theory of Radiation," Oxford University Press, New York, N. Y.; 1954.

Spontaneous emission tends to maintain thermal equilibrium between a particle system and the radiation field. This is in contradistinction to the nonradiative relaxation processes which tend to maintain equilibrium between particles.

The transition probability for spontaneous emission is $\propto \nu^3$. Although it is an important thermalizing process at optical frequencies, its effects are negligible compared with relaxation processes at microwave frequencies.

Spontaneous emission is, however, of great importance to a maser. Because it is radiative and independent of any incident radiation it is the ultimate source of noise in such a device.

Power Saturation

It is evident from (9) that resonance radiation tends to equalize populations. If $n_i > n_j$ there is a net absorption of energy and a net drift of particles from the lower to the higher state. Thus the population difference $n_i - n_j$ decreases. This process would continue until $n_i = n_j$ if it were not for the spin-lattice relaxation which tends to maintain Boltzmann equilibrium.

If the power level is low the relaxation process is predominant. At high-power levels, however, there will be appreciable departures from thermal equilibrium. In practice the populations may be essentially equalized. This is known as a condition of power saturation. A detailed discussion of this effect is given by Portis.[9]

The Three-Level Maser

The Three-Level Excitation Method

In a maser an emissive or negative temperature condition is produced. One way of achieving this continuously is the three-level method. This method was suggested by Basov and Prokhorov;[10] its application to the solid state was proposed by Bloembergen.[11]

Consider an ensemble of particles distributed over three energy levels as shown in Fig. 4.

Nonzero transition probability coefficients are assumed to exist between all states. Particles will tend to drift between states with the indicated spin-lattice relaxation times. In the absence of radiation-thermal equilibrium at the lattice temperature T will exist and the populations will be those of Boltzmann N_1, N_2, and N_3. Resonance radiation of frequency ν_{31} (henceforth called the "pump") will induce transitions between states 1 and 3 and disturb thermal equilibrium, and a new population distribution n_1, n_2, and n_3 will occur. If the pump is sufficiently powerful it will overcome relaxation processes; in practice populations n_1 and n_3 will be essentially equalized. The rate equation for n_2 becomes

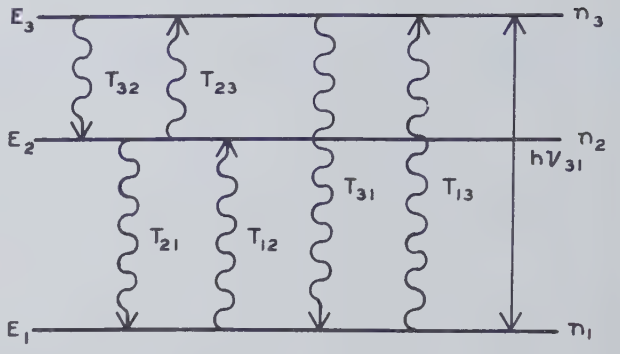

Fig. 4—Three states with associated energies, populations and spin-lattice relaxation times are depicted. Radiation induces transitions between states 1 and 3.

$$\frac{dn_2}{dt} = \frac{n_1}{T_{12}} + \frac{n_3}{T_{32}} - \frac{n_2}{T_{21}} - \frac{n_2}{T_{23}}. \tag{13}$$

In the steady state $dn_2/dt = 0$ and since $n_1 = n_3$

$$\frac{n_3}{n_2} = \frac{n_1}{n_2} = \frac{1/T_{21} + 1/T_{23}}{1/T_{12} + 1/T_{32}} \tag{14}$$

but $N_1/T_{12} = N_2/T_{21}$ and $N_2/T_{23} = N_3/T_{32}$ from (2), and (14) becomes

$$\frac{n_3}{n_2} = \frac{n_1}{n_2} = \frac{T_{32}/T_{21} + N_3/N_2}{\frac{T_{32}}{T_{21}}\frac{N_2}{N_1} + 1}. \tag{15}$$

It is seen that

$$n_3/n_2 > 1 \text{ or } n_2/n_1 > 1 \text{ as the right-hand side} > \text{or} < 1.$$

In either event gain will occur; in the first case for radiation of frequency ν_{32}, in the second case for radiation of frequency ν_{21}. It is possible theoretically for $n_3/n_2 = n_2/n_1 = 1$ but this requires a most unlikely combination of parameters in (15).

For high gain a large population inversion is required. Two extreme cases may be distinguished.

1) $T_{32}/T_{21} \approx 1$. Appreciable inversion will occur if N_3/N_2 differs greatly from N_2/N_1. Since these Boltzmann ratios are related to the frequencies ν_{32} and ν_{21} by equations of the form (2) and (6), it is seen that there must be a large ratio for the frequencies ν_{32} and ν_{21}. Further, the negative spin temperature will occur at the lowest frequency. This in turn requires a large ratio of pumping to signal frequencies. Although this approach is perhaps useful at low frequencies because of its simplicity, it has definite disadvantages in a high-signal frequency application.

2) $N_3/N_2 \approx N_2/N_1$ that is $\nu_{32} \approx \nu_{21}$. Appreciable inversion will occur only if T_{32} differs greatly from T_{21} and the negative temperature and gain will occur at that frequency with the longest associated relaxation time. Somewhat meager experimental data indicates that such relaxation times are usually about equal. One method

[9] A. M. Portis, "Electronic structure of F centers; saturation of the electron spin resonance," *Phys. Rev.*, vol. 91, pp. 1071–1078; September, 1953.

[10] N. G. Basov and A. M. Prokhorov, "Possible methods of obtaining active molecules for a molecular oscillator," *J. Exper. Theoret. Phys. USSR*, vol. 1, p. 184; July, 1955.

[11] N. Bloembergen, "Proposal for a new type solid state maser," *Phys. Rev.*, vol. 104, pp. 324–327; October, 1956.

for producing large relaxation time ratios has been demonstrated.[12] A small amount of paramagnetic impurity is introduced into the lattice in such a way that its resonance frequency is equal to one of the resonant frequencies of the active material. Resonant spin-spin interaction and energy exchange then occurs between the impurity and one pair of levels of the active material but not for the other pair. This mechanism effectively "short circuits" one relaxation time without affecting the other. This doping technique would appear to be of value in a high-frequency maser. Although it puts an additional restriction on the choice of material, this does not appear prohibitive.

In both of the above cases it is evident that if appreciable population inversion is to occur then both N_3/N_2 and N_2/N_1 should be small. This suggests the use of low-bath temperatures. It is evident that the two frequencies ν_{32} and ν_{21} should not be exactly equal. Otherwise a signal would simultaneously see gain and loss, a negative temperature at one transition being accompanied by a positive temperature at the other.

Some remarks are in order regarding the applicability of the simple theory of the three-level excitation method as outlined above. The populations n_1 and n_3 may never be exactly equal. The presence of a strong signal at either ν_{32} or ν_{21} will affect the population distribution. Both effects may be taken into account by solving simultaneously the three-rate equations for n_1, n_2, and n_3 including the radiation. For instance a strong signal at the amplifying frequency will reduce the population inversion and hence the gain—the device is self-limiting.

At first sight the frequency relationship $\nu_{21}+\nu_{32}=\nu_{31}$ may suggest that the device operates because of nonlinearities. If, however, the device operates as described here, this cannot be the case. For instance, it has not been necessary to take into account the phase of the radiation. Furthermore, if the device is in an amplifying condition then the pump may be turned off and amplification will persist for a time determined by the spin-lattice relaxation. However, it is possible to drive such a three-level system so that it behaves in a nonlinear fashion. This condition has been investigated by Javan,[13] Clogston,[14] and Prokhorov.[15] In order to achieve nonlinear operation, it is necessary for the radiation to be sufficiently powerful to overcome the disordering effects of spin-spin interaction and thereby create coherence in the spin system. Under these conditions, mixing and conversion gain are possible. Such a device would appear to be closely related to a parametric-type amplifier. In order for the linear theory given here to be applicable the pump must be sufficiently powerful to overcome the spin-lattice relaxation only and produce power saturation, but it must not be so powerful as to overcome spin-spin relaxation and produce a coherent ordering of the spin system. Essentially, this imposes a restriction on the material namely the spin-spin relaxation time must be much shorter than the spin-lattice relaxation time.

Some Remarks on Paramagnetic Salts

Ionically bound paramagnetic salts appear to be a particularly fruitful source of suitable materials for a three-level solid-state maser. The theory of such materials has been reviewed by Bleaney and Stevens[16] and experimental data on them has been reviewed by Bowers and Owen.[17]

When an atom enters into chemical combination the magnetic moments associated with its valence electrons are usually "paired off" resulting in a diamagnetic structure. Certain elements belonging to the "transition groups" have incomplete inner electron shells. When these atoms enter into a chemical compound the magnetic moments associated with the inner shells are not always "paired off" and a paramagnetic material results.

The relevant inner shells are those of the 3d, 4d, 5d, 4f, and 5f electron configurations. The corresponding groups are known as the iron, palladium, platinum, rare earth, and transuranic groups. In maser applications only the iron and rare earth groups would appear to be attractive. The palladium and platinum groups have a strong tendency to form diamagnetic covalent complexes and it is difficult to control the spin concentration by magnetic dilution methods in the few remaining paramagnetic materials. The transuranic group is for the most part strongly radioactive.

The number of useful ions is further reduced by the requirement of having at least three low-lying and therefore appreciably populated energy levels. Effectively this leaves Ni^{++}, Cr^{+++}, Fe^{+++}, Gd^{+++}, Mn^{++}, and V^{++}. The last two ions exhibit extensive hyperfine structures and except in extremely wide-band applications this has the effect of reducing the useful spin concentration.

The paramagnetic ion in the solid state is subject to strong crystalline electric field gradients. These fields produce strong perturbations of the electronic orbital motion. The electron spin is coupled to these orbits by spin-orbit coupling. The resulting states are complicated admixtures of orbital and spin-wave functions.

Fortunately, the magnetic behavior of the lowest lying group of states may be described by the use of a "Spin-Hamiltonian" which requires no detailed knowledge of these effects.

Essentially one may ignore the correct but complicated wave functions and simply characterize the lowest

[12] G. Feher and H. E. D. Scovil, "Electron spin relaxation times in gadolinium ethyl sulphate," *Phys. Rev.*, vol. 105, pp. 760–762; January, 1957.

[13] A. Javan, "Theory of a three level maser," *Phys. Rev.*, pp. 1579–1589; September, 1957.

[14] A. M. Clogston, "Susceptibility of the three level maser," *J. Phys. Chem. Solids*, in press.

[15] A. M. Prokhorov, "Theory of the Three Level Maser," paper presented at URSI Meeting, Boulder, Colo; September, 1957.

[16] B. Bleaney and K. W. H. Stevens, "Paramagnetic resonance," *Rep. Prog. Phys.*, vol. 16, pp. 108–159; 1953.

[17] K. D. Bowers and J. Owen, "Paramagnetic resonance II," *Rep. Prog. Phys.*, vol. 18, pp. 304–373; 1955.

lying group of states by a single quantum number S' known as the "effective spin." S' is defined by equating $2S'+1$ to the number of energy levels making up the ground state. In special cases S' is equal to the true-spin S but this is not necessarily so.

The ground state is now treated as a magnetic dipole which may assume $2S'+1$ orientations in an applied magnetic field. The effective magnetic moment of this dipole depends upon the correct wave functions but may easily be found by experiment. The effective spin is however not free since, unlike a real spin, it is affected by the crystalline electric field which produces a "Stark splitting" of the energy levels. This Stark energy must be taken into account along with the magnetic energy when describing the behavior of the states. The Hamiltonian $\mathcal{H}$ thus consists of a sum of magnetic and Stark energy operators which are to be applied to the effective spin states. The entire magnetic behavior of the material may then be described simply by specifying S' and a few constants.

The magnetic energy or Zeeman operator is simply $g\cdot\beta H\cdot S$ where β is the Bohr magneton $=9.21\times10^{-21}$ Gauss cm^3 and g is the "spectroscopic splitting factor" or "effective g." $g\beta S$ may be termed the effective magnetic moment. In most maser applications g will have a value near 2 and be almost isotropic.

Assuming that the crystalline potential is an electrostatic one it may be expanded in spherical harmonics as

$$V = \sum_{nm} A_n{}^m r^n Y_n{}^m(\theta, \phi).$$

To find the corresponding Stark energy operators one may follow a method given by Stevens.[18] A brief heuristic treatment is given here.

First of all one observes that the number of operators is finite. This is because the electron wavefunctions may also be expanded in spherical harmonics and d and f wavefunctions do not contain harmonics for which $n>4$ and 6, respectively. When forming the integral of the matrix elements of V all terms, for which $n>4$ and 6, respectively, vanish by the orthogonality relations for spherical harmonics. Similar arguments show that only terms for which n is even need be retained. The term $n=0$ may be dropped since it is just an additive constant. Further reduction occurs by taking into account the symmetry properties of the crystal. Finally, when looking for operators to be applied to states of the effective spin S' it is necessary to retain only those operators that have matrix elements spanning the manifold of S'. The remaining spin operators are now formed in such a manner that they transform under rotation as do the corresponding terms of the crystalline field expansion.

For most maser applications the following Hamiltonian provides an adequate description, where $S\pm = S_x \pm iS_y$. S, S_x, S_y, and S_z are the usual spin operators and may be considered to be the quantum equivalent of the corresponding classical spin mechanical momenta.

$$\mathcal{H} = g\cdot\beta H\cdot S + D[S_z{}^2 - 1/3S(S+1)] + 1/2E[S_+{}^2 + S_-{}^2] \tag{16}$$

where

S is the effective spin (the prime being dropped),
g and β have already been described,
D and E are constants determining the strength of the Stark interaction,
g, D, and E are conveniently found by experiment. Values for various materials are given by Bowers and Owen.[17]

The operator $[S_z{}^2-\frac{1}{3}S(S+1)]$ represents a term of axial symmetry and corresponds to the harmonic $Y_2{}^0$. The operator $[S_+{}^2+S_-{}^2]$ represents a term of rhombic symmetry and corresponds to the harmonic $Y_2{}^2$. Although additional terms may exist they are usually small.

The ions Ni^{++}, Cr^{+++}, Fe^{+++}, and Gd^{+++} have effective spins 1, 3/2, 5/2, and 7/2 respectively.

The material may be utilized in several ways. Some of these are now illustrated.

Case 1—H Applied Parallel to the Symmetry Axis Z, $S=3/2$: Consider initially only the first two terms in $\mathcal{H}$. The energy levels as a function of H are as shown in Fig. 5, opposite. For $H=0$ there is an initial splitting into two pairs of degenerate states by the Stark field—a positive sign is assumed for D. The usual type of magnetic dipole transitions corresponding to the selection rule $\Delta S_z=\pm1$ are permitted. These transitions require that the rf magnetic field be perpendicular to H as in the classical gyroscopic model. It is seen that three energy levels with the requisite transitions exist in the region near point A. At higher magnetic fields, above "crossover" maser operation may not occur since although the energy levels are available no "double jump" transitions are permitted for the pump.

Consider now the addition of the last term in $\mathcal{H}$. The term $\frac{1}{2}E[S_+{}^2+S_-{}^2]$ has only off diagonal matrix elements. It will have two effects. Depending on its magnitude it will shift the positions of the energy levels. However, it will also admix spin states differing by $\Delta S_z=\pm2$; *e.g.*, the original state $S_z=-3/2$ will now be an admixture of the states $S_z=-3/2$ and $S_z=+1/2$. As a result of this admixture transitions of the $\Delta S_z=0$ type are permitted when the rf magnetic field is parallel to H. These transitions correspond to double jumps and hence the requisite transitions for both signal and pump are now available in the region above crossover. In the high-field region the double jump transition probability is $\propto (E/g\beta H)^2$.

Case 2—H Applied Perpendicular to the Symmetry Axis, $S=3/2$: Consider again only the first two terms in $\mathcal{H}$. It is convenient to rewrite the Hamiltonian retaining H as the Z direction. The transformed Hamiltonian becomes

$$\mathcal{H} = g\beta HS_Z - 1/2D[S_z{}^2 - 1/3S(S+1)] + 1/4D[S_+{}^2 + S_-{}^2]. \tag{17}$$

[18] K. W. H. Stevens, "Matrix elements and operator equivalents connected with the magnetic properties of the rare earth ions," *Proc. Phys. Soc. A*, vol. 65, pp. 209–215; March, 1952.

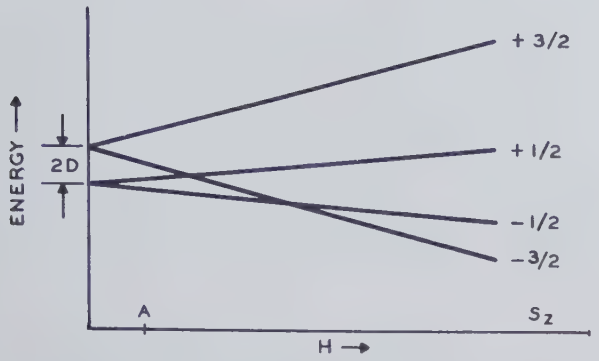

Fig. 5—Energy levels are shown as a function of magnetic field H when H is parallel to the crystalline symmetry axis. $S=\frac{3}{2}$.

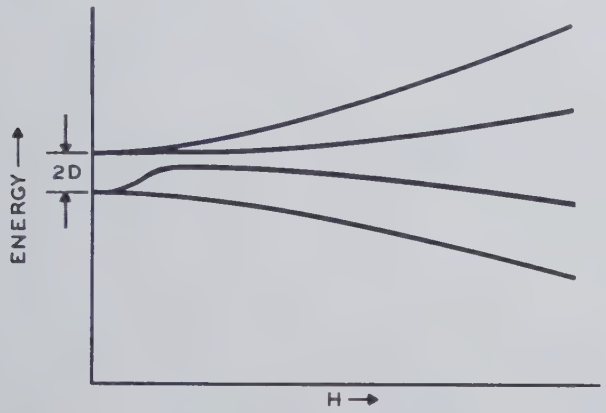

Fig. 6—Energy levels are shown as a function of magnetic field H when H is perpendicular to the crystalline symmetry axis. $S=\frac{3}{2}$.

The energy levels as a function of H are shown in Fig. 6. The requisite energy levels are available and so are the required transitions. It will be noted that the application of the magnetic field perpendicular to the symmetry axis has in effect created a term $[S_+^2+S_-^2]$ even though there is no term E of rhombic symmetry in the crystalline field. The resulting admixture again permits transitions of the $\Delta S_Z=0$ type. This transition probability is $\propto (D/g\beta H)^2$ in the high-field region.

Case 3—$H=0$, $S=1$: If all the terms in $\mathcal{H}$ are zero the ground state has a threefold degeneracy in spin. The term $[S_Z^2-\frac{1}{3}S(S+1)]$ partially removes the degeneracy leaving the states $S_Z=\pm 1$ still degenerate as shown in Fig. 7. The term $[S_+^2+S_-^2]$ removes the remaining degeneracy. All transitions are permitted. This particular mode of operation has been suggested by Bowers and Mims[19] and has the advantage that no applied magnetic fields are required to produce the requisite energy level scheme.

It is apparent that materials must be chosen for a particular mode and frequency of operation. In particular crystalline field parameters must be chosen such that the appropriate transition probabilities are sufficient. Materials with a wide range of D and E are available to make this possible.

Once the material, frequency and mode of operation

[19] K. D. Bowers and W. B. Mims, "Three Level Maser Without a Magnetic Field," paper presented at Conference on Electronic Tube Research, Berkeley, Calif.; June, 1957.

Fig. 7—Energy levels for $S=1$ are shown. (a) illustrates the effect of the axial terms $[S_z^2=\frac{1}{3}S(S+1)]$ only. (b) illustrates the combined effect of the axial term and a rhombic term $[S_+^2+S_-^2]$.

are fixed, the transition probability coefficients w_{ij} may be computed by standard techniques of Bleaney and Stevens[16] and the susceptibility evaluated.

In addition to having the requisite energy levels and transition probabilities the material must satisfy additional requirements. The spin-lattice relaxation time must be fairly long in order for the pump to produce power saturation with reasonable powers. The ions Ni^{++}, Cr^{+++}, Fe^{+++}, and Gd^{+++} normally have sufficiently long relaxation times at liquid helium temperatures.

In some materials crystalline field dislocations may produce appreciable inhomogeneous broadening of the resonance line. Inhomogeneous broadening from either crystal dislocations or nonresonant spin-spin interaction appears undersirable. Computations by Mims[20] show that under certain conditions of inhomogeneity a three-level maser will fail to exhibit gain. It appears desirable to increase the concentration of active spins to the point where homogeneous spin-spin broadening is the dominant line width determining mechanism. Further increase in concentration should be limited by bandwidth requirements since the pumping power is increased along with the concentration. In order to control the spin concentration, it is necessary to select a material such that it may be "magnetically diluted" with an isomorphous diamagnetic element; *e.g.*,diamagnetic Al^{+++} is frequently used to dilute paramagnetic Cr^{+++}.

Some Design Considerations

Design Considerations Relating to the Material

1) Gain—the intrinsic gain is proportional to χ''. Eq. (13) indicates that a high-spin concentration is desirable and that $\Delta\nu$ should be small. These two requirements are not independent. There is always some minimum $\Delta\nu$ arising from inhomogeneous broadening. Once the spin concentration is increased to the point where homogeneous broadening between active spins is the line width determining mechanism $\Delta\nu$ is approximately proportional to N and further increase of N has little effect on the gain. Relation (13) indicates that a small negative Ts is required—this infers a low bath temperature and appropriate relaxation time and frequency ratios.

[20] W. B. Mims, private communication.

2) Bandwidth—the intrinsic bandwidth is approximately proportional to $\Delta\nu$ if homogeneous broadening is predominant.
3) Pumping power—this increases as the spin-lattice relaxation time decreases and suggests the desirability of low bath temperatures. It increases with the spin concentration and consequently excessive concentrations should not be used. The pump transition probability shou'd be sufficiently high for the pump to be effectively matched to the material losses. If liquid helium is used as a refrigerant, pumping powers of a few milliwatts appear reasonable since liquid helium boils off at the rate of about 1 cc per hour for a power absorption of 1 mw.
4) Output Power—this is limited by saturation effects but will normally be quite sufficient if the device is used as a low-noise preamplifier.
5) Noise—several authors[21–23] have treated the subject of noise in masers. The noise of the device may be expressed in terms of kT_nB where T_n is the effective noise temperature. The computations indicate that the ultimate noise is that arising from spontaneous emission and that the ultimate noise temperature is just equal to the magnitude of the effective spin-temperature $|T_s|$. This again suggests the desirability of low-temperature operation since in a three-level maser large population inversions result only if the bath temperature is low. Additional noise may arise from resistive losses in the microwave circuit particularly from any parts which are at room temperature. With proper design it should be possible to keep this last source of noise small.
6) Refrigerant—the best results are obtained at helium temperatures since gain, bandwidth, noise, and pumping power requirements all deteriorate as the bath temperature increases. In some system applications it may be desirable to operate at higher temperatures. Liquid hydrogen because of its ease of handling and high-latent heat appears very attractive.
7) Linearity—as previously mentioned, linear operation imposes the restriction that spin-spin relaxation time be much shorter than spin-lattice relaxation time. Materials which satisfy normal bandwidth and reasonable pumping power requirements will automatically satisfy this condition.

Design Considerations Relating to the Microwave Circuit

First of all it is important, particularly from the noise aspect, to keep all losses in the microwave circuit to a minimum. The simple maser, like a negative resistance device, will amplify for both directions of propagation. It is important, therefore, to provide some type of nonreciprocal isolation between the interaction medium and the output load. Since the latter in most cases will be at room temperature its available noise power $kT_{290}B$ would otherwise enter and be amplified by the medium and return as amplified noise to the load, the result would be a minimum noise temperature of 290° for the entire device.

Conceptually, perhaps the simplest maser circuit is just a waveguide filled with active material. In this case, an input signal increases exponentially as it travels down the guide. For reasonable negative imaginary susceptibilities, however, such a system would have to be several tens of meters long in order to provide useful gain. Evidently a slow-wave structure is required so that the wave may interact for a longer time with a given amount of material.

The extreme case of a slow-wave structure is a simple cavity. Alternatively the cavity may be looked upon as a means of supplying regeneration or positive feedback, the amount of feedback being dependent on the cavity Q. The cavity provides a simple method of obtaining high gain in a relatively small volume. The bandwidth of such a device is initially limited by the cavity Q and then further reduced by the application of the positive feedback. A further disadvantage exists because the large amount of regeneration normally employed makes the device quite unstable at high gains. Frequently, a reflection type cavity is used, the input and output signals being separated by a circulator which also serves to decouple the noisy room temperature load from the interaction medium. In practice a cavity resonant at both the signal and pumping frequencies is employed, the resonant cavity for the pump serving to match the pumping power into the positive imaginary susceptibility associated with the pumping frequency.

A compromise between the waveguide and the cavity is an iterated structure. Such a maser may be made unidirectional and hence stable with the use of gyromagnetic material. The nonreciprocal material may be a ferrite or perhaps the active material itself since the classical gyroscopic model is derived from quantum mechanical transitions of the $\Delta S_Z = \pm 1$ type which have been shown to occur in paramagnetic salts. Perhaps the most elementary broad-band structure is simply an iterated linear array of low Q cavities and ferrite isolators. The most elegant type of structure appears to be a continuously loaded single periodic structure. The design of such a structure must be compatible with the requirement that the applied magnetic field must have specific orientations with respect to the signal and pumping rf fields. A further restriction is that it must exhibit nonreciprocal properties and the magnetic field applied to the active material should be the same field that is responsible for the nonreciprocity.

The interaction material and the corresponding

[21] K. Shimoda, H. Takahasi, and C. H. Townes, "Fluctuations in amplification of quanta with application to maser amplifiers," *J. Phys. Soc. Japan*, vol. 12, pp. 686–700; June, 1957.
[22] R. V. Pound, "Spontaneous emission and the noise figure of maser amplifiers," *Ann. Phys.*, vol. 1, pp. 24–32; April, 1957.
[23] M. W. P. Strandberg, "Inherent noise of quantum—mechanical amplifiers," *Phys. Rev.*, vol. 106, pp. 617–620; May, 1957.

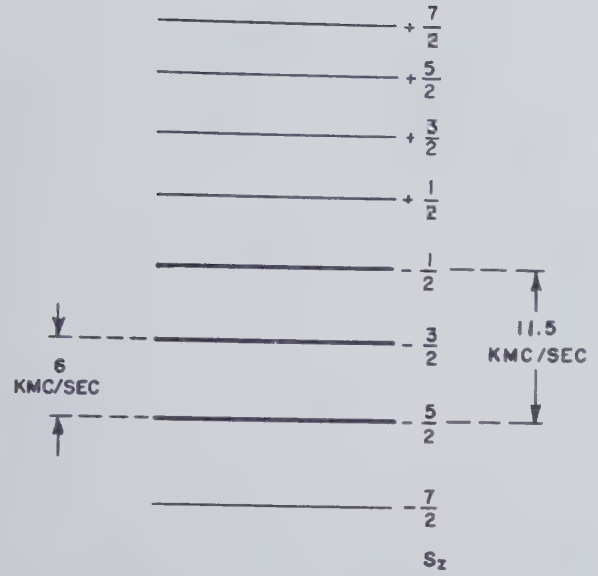

Fig. 8—The energy levels of Gd^{+++} in the ethyl sulfate for a large magnetic field applied perpendicular to the symmetry axis. The heavy lines identify the maser levels.

structure must be immersed in the refrigerant. Standard low temperature techniques are available for this.

Some Design and Performance Characteristics of a Particular Device

Design

A brief description of a 9-kmc three-level cavity maser developed at Bell Telephone Laboratories, has appeared in the literature.[24] The 6-kmc device described here is essentially a scaled version.

The material used is a lanthanum ethylsulphate crystal containing $\frac{1}{2}$ per cent gadolinium and $\frac{1}{5}$ per cent cerium. La^{+++} being diamagnetic acts as a magnetic diluting agent to reduce spin-spin interaction. Gd^{+++} acts as the active paramagnetic. Ce^{+++} acts as a spin-lattice relaxation time doping agent.

Gadolinium ethylsulphate was chosen because there was sufficient information available[25,26] to show that it possessed the requisite properties. In a practical application its slight chemical instability and its high room temperature dielectric loss are disadvantages.

Gd^{+++} being in a pure-spin state has an effective spin S' equal to the true-spin $S=7/2$. The magnetic behavior is described to a close approximation by the Hamiltonian (16) with $g\approx 2$, $D=0.02$ cm^{-1} and $E=0$. Although there are a total of eight low-lying energy levels only three adjacent energy levels are used as shown in Fig. 8. A field of $\sim$1800 ϕ is applied perpendicular to the symmetry axis and the mode of operation

[24] H. E. D. Scovil, G. Feher, and H. Seidel, "Operation of a solid state maser," *Phys. Rev.*, vol. 105, pp. 762–763; January, 1957.
[25] B. Bleaney, H. E. D. Scovil, and R. S. Trenam, "The paramagnetic resonance spectra of gadolinium and neodymium ethyl sulphates," *Proc. Roy. Soc. A*, vol. 223, pp. 15–29; April, 1954.
[26] H. A. Buckmaster, "$\Delta M=\pm 2$ transitions in dilute gadolinium ethyl sulphate," vol. 34, pp. 150–151; January, 1956.

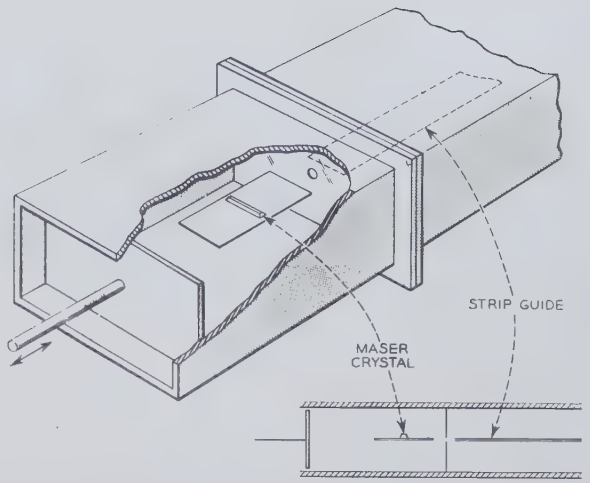

Fig. 9—The pump and signal cavity configuration is illustrated. The rectangular waveguide carrying the pump terminates in a $(\frac{3}{2})\lambda$ rectangular cavity. The signal propagates along the strip line. A $(\frac{1}{2})\lambda$ length of strip line placed inside the rectangular cavity acts as the signal cavity.

used is that described under Case 2) above.

The gadolinium ion experiences an inhomogeneous spin-spin broadening of $\sim$20 mc from the magnetic moments of the protons in the surrounding water molecules. Consequently the gadolinium spin concentration was increased to $\frac{1}{2}$ per cent so that the resulting homogeneous spin-spin relaxation time $\approx 10^{-8}$ seconds corresponding to a line width of $\approx$30 mc was predominant. The spin-lattice relaxation time of the unperturbed transitions is $\sim 10^{-4}$ seconds at the temperature of liquid helium and hence the material satisfies the requirements for linear operation. At 1800 ϕ the energy levels are fairly equally spaced and reliance must be placed on large spin-lattice relaxation time ratios to obtain appreciable population inversion. It has been found experimentally[12] that $\frac{1}{5}$ per cent cerium provides adequate preferential homogeneous spin-spin interaction for a sufficient ratio.

The interaction cavity was not sealed against liquid helium for experimental convenience. Liquid helium has an appreciable dielectric constant and when boiling at 4°K at atmospheric pressure the resulting bubbles modulate the cavity frequency. In order to prevent this the vapor pressure and hence the temperature was reduced by pumping, since bubble formation does not occur below the λ point. A temperature of 1.2°K was used.

A reflection-type cavity is used for the microwave circuit; the input and output signals being separated by a circulator at room temperature. The particular cavity geometry used is shown in Fig. 9. Pumping power at $\approx$11.5 kmc enters through an X-band waveguide which is terminated in a tunable rectangular cavity resonant in the $(3/2)\lambda$ mode. The signal propagates along the strip line. Inside the rectangular pumping cavity is a $(1/2)\lambda$ (at 6 kmc) length of a strip line which forms the signal cavity. The crystal is mounted at the rf magnetic field maximum in the center of the strip cavity. This in turn is so positioned that the crystal also sees an rf mag-

netic field maximum of the pump.

The signal, associated with a $\Delta S_z = \pm 1$ transition, requires that the signal rf magnetic vector be perpendicular to the large applied dc field. The pump, associated with a $\Delta S_z = 0$ transition, requires that its magnetic vector be parallel to the dc field. In the cavity geometry employed the signal, and pump rf magnetic fields are parallel to each other. The applied dc magnetic field is oriented at an angle of 45° to the plane of the strip in order to have rf field components satisfying the two transition probability requirements.

Performance

This device was constructed for some initial feasibility tests and its performance should not be taken to indicate the limits of performance which may be expected in a more practical device.

A pumping power of 38 mw was employed, probably less than 1 per cent of this being absorbed by the crystal. The discrepancy arises from the fact that a low pumping cavity Q provides a poor match. The pumping requirements may be materially decreased by better design.

With a gain of 20 db the bandwidth is $\approx$100 kc. Although the material has a line width of 30 mc this inherent bandwidth is not utilized because of the high $Q(\approx 6000)$ of the signal cavity and the associated positive feedback. The regeneration also results in a fairly small stability margin. Both bandwidth and stability would be improved if an appropriate unidirectional slow wave structure was employed.

The effective noise temperature of the entire device including circulator and monitoring equipment was $\sim$150°K. Most of this noise arose from the excessive, and easily reducible, room temperature losses of the circulator and monitoring equipment. The noise temperature of the actual maser was $<$35°K compared with the theoretical value of 4°K (obtained from a spin temperature of -4°K). The accuracy of the noise measuring apparatus was insufficient to allow identification of the true maser noise.

Nonmechanical Beam Steering by Scattering from Ferrites*

M. S. WHEELER†

Summary—**A small aperture radiating circularly polarized energy is loaded with a spherical ferrite to produce an electronic beam directing system. The ferrite is immersed in a static magnetic field which is in general at an oblique angle with the undeflected direction of radiation. It is shown that radiation is principally in the direction of the magnetic field when the polarization is in the negative sense. From symmetry this allows beam deflection with two degrees of freedom.**

To consider an application for such a device, it is proposed that this deflection system be used in conical scan. A mechanization is shown which solves the problem in principle, but it is not competitive with present mechanical scanners from the point of view of side lobes, etc.

Introduction

USE is continually being made of two ferrite properties, the Faraday rotation and resonant absorption, to produce the many microwave components used today in waveguides and antennas. When these principles are applied to beam steering in antennas, it would seem that the properties of the ferrite are used in an indirect manner. Alternately, it should be possible to use ferrites directly to produce a deflection as the energy is passed through and over the ferrite. Such an effect was reported by Angelakos and Korman.[1]

It would be required that the ferrite be immersed in a large fraction of the radiated energy, and yet the ferrite must be relatively free from boundaries in such a manner that the energy would be free to change direction. The asymmetry, which is controlled and used to change beam direction, would be the relatively static saturating magnetic field to which direction all of the anisotropic properties of the ferrite are referred.

The advantages of such a beam-steering device are obvious: no mechanically moving parts are necessary. Less control power would be required, low-temperature starting would cease to be troublesome, and higher operating speeds could be achieved with a ferrite as compared to a corresponding mechanical deflection system. However, to be practically useful, it would be required that a ferrite scatterer have low dissipative loss, that it be made relatively reflectionless, and that a sufficient degree of beam perfection be achieved considering cross polarization and extraneous side lobes.

* Manuscript received by the PGMTT, May 20, 1957; revised manuscript received, August 5, 1957.

† Westinghouse Electric Corp., Air Arm Div., Baltimore 3, Md.

[1] D. J. Angelakos and M. M. Korman, "Radiation from ferrite filled apertures," PROC. IRE, vol. 44, pp. 1463–1468; October, 1956.

Mechanization of Controllable Scattering by Ferrite

It is possible to visualize the mechanism for beam deflection from the previous discussion and from consideration of symmetry. Consider a waveguide radiating from an open end. The beam, formed along the waveguide center line, is to deflect symmetrically in azimuth and elevation. This symmetrical deflection, it would appear, could be most easily achieved with a circular waveguide and circular polarization of the incident energy. This condition is not a fundamental requirement, but it does produce a practical system and achieves the required symmetry automatically.

The ferrite would have to be near the end of the waveguide. When too far out of the guide, the ferrite intercepts only a small amount of the energy; when too deep in the guide, beam deflection is prevented by the guide walls. Considering now only uniform static magnetic fields, there would be, in general, two components—one axial which can produce no deflection because of its symmetry, and one transverse which is the only intentional asymmetry and the only source of the expected beam deflection.

The source of this static magnetic field may be a combination of permanent and electromagnets surrounding the ferrite. While it has been found possible to place the magnets internal to the ferrite resulting in very low control power, several practical considerations lead to the placing of the magnets external to the ferrite. In Fig. 1, a typical magnet-ferrite combination is shown from which considerable data have been taken.

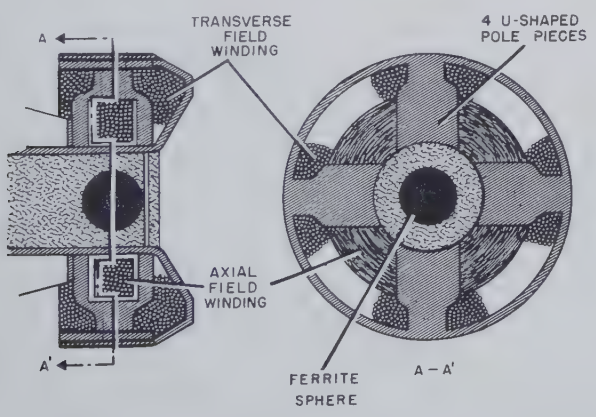

Fig. 1—Magnetic circuit for supplying oblique magnetic field.

An axial-field winding surrounds the end of the waveguide. Covering the axial-field winding in part, are four U-shaped pole pieces which complete the external magnetic circuit for the axial winding and at the same time provide a core upon which the transverse windings are placed. The U-shaped pole pieces thus provide both axial and transverse components of the static magnetic field. The transverse field magnetic circuits in both azimuth and elevation are closed around the periphery of the whole assembly by a soft iron ring. The transverse magnetic field path might be visualized in section A-A' of Fig. 1 as crossing the sphere, dividing in the U-shaped pole pieces, and proceeding to the outer ring where it again divides to return to the opposite pole piece around the outside diameter. The axial-field path might be visualized in the first cut of Fig. 1. As the axial field crosses the sphere, it splits four ways, returning to the opposite side of the sphere through the U-shaped pole pieces which also conduct the transverse field. The total static magnetic field in the ferrite is thus an oblique field which is the vector sum of three mutually perpendicular magnetic fields. The ferrite itself is shown imbedded in a teflon support which centers the ferrite and maintains propagation in the necked-down waveguide

Dipole Model for Small Sphere in a Plane Wave

Unfortunately, the deflection system as described above has not proved susceptible to analysis. It is instructive, however, to apply the work of Berk and Lengyel[2] for small spheres in plane waves. A coordinate system is shown in Fig. 2 where the static magnetic field is along the Z axis, and propagation is along the Z' axis which is tipped at an angle θ with respect to Z.

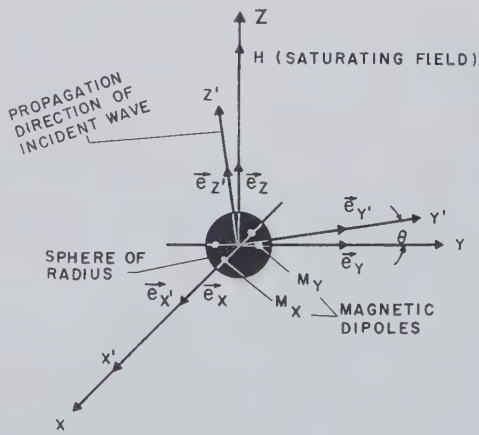

Fig. 2—Coordinate system for a small sphere of ferrite in a plane circularly polarized wave.

Here the $\vec{e}$ vectors are unitary along their respective axes. An elliptically polarized incident wave is assumed propagating in the Z' direction—$h=(h_{0x'}\vec{e}_{x'}+jh_{0y'}\vec{e}_{y'})$ exp $(j\omega t-\Gamma Z')$. Then in the notation of Berk and Lengyel, a field is found external to the sphere consisting of the original field plus a dipole field. The sphere will be assumed saturated in the Z direction:

$$H = \vec{e}_x h_{0x'} + \vec{e}_y j \cos\theta h_{0y'} + \vec{e}_z j \sin\theta h_{0y'}$$
$$+ (D_{1_{x'}} - D_{2_{y'}})\left[\vec{e}_x \frac{r^2-3x^2}{r^5} - \vec{e}_y \frac{3xy}{r^5} - \vec{e}_z \frac{3xz}{r^5}\right]$$
$$- (D_{1_{y'}} + D_{2_{x'}})\left[\vec{e}_x \frac{3xy}{r^5} - \vec{e}_y \frac{r^2-3y^2}{r^5} + \vec{e}_z \frac{3yz}{r^5}\right],$$

[2] A. D. Berk and B. A. Lengyel, "Magnetic field in small ferrite bodies with applications to microwave cavities containing such bodies," Proc. IRE, vol. 43, pp. 1587–1591; November, 1955.

where

$$D_{1_{x'}} = \left[\frac{3(\mu+2)}{(\mu+2)^2-\kappa^2} - 1\right] h_{0x'}a^3,$$

$$D_{2_{x'}} = \left[\frac{-3\kappa}{(\mu+2)^2-\kappa^2}\right] jh_{0x'}a^3$$

$$D_{1_{y'}} = \left[\frac{3(\mu+2)}{(\mu+2)^2-\kappa^2} - 1\right] jh_{0y'}a^3,$$

$$D_{2_{y'}} = \left[\frac{3\kappa}{(\mu+2)^2-\kappa^2}\right] h_{0y'}a^3.$$

If now three mutually perpendicular dipoles are assumed at the sphere on the xyz coordinates of magnitudes m_x, m_y, and m_z, it can be shown that the scattered portions of the field outside the ferrite can be reproduced by letting

$$m_x \frac{1}{4\pi\mu_0 h_{0x'}} = -\frac{(\mu^2-\kappa^2+\mu-2)+3\kappa\cos\theta\dfrac{h_{0y'}}{h_{0x'}}}{(\mu+2)^2-\kappa^2}$$

$$m_y \frac{1}{4\pi\mu_0 h_{0x'}} = -j\frac{(\mu^2-\kappa^2+\mu-2)\cos\theta\dfrac{h_{0y'}}{h_{0x'}}+3\kappa}{(\mu+2)^2-\kappa^2}$$

$$m_z = 0.$$

From this dipole orientation, it can be seen that the direction of maximum scattered energy is along the axis of the magnetic field. Then, if means were found to block the overriding plane incident wave, a beam would have been formed principally along the axis of the static magnetic field. There are three other significant observations that can be made regarding the scattered energy. First, with an incident circularly polarized wave ($h_{0y'} = \pm h_{0x'}$) and no deflection ($\theta = 0$), the scattered wave is circularly polarized. As deflection is produced, however, an increasing degree of depolarization must be expected. Second, as the functions are even in θ, the deflection left or right could be expected with equal amplitudes when the transverse field is reversed. Third, for typical X-band ferrites below magnetic saturation,[3] the dipole strengths, m_x and m_y, are greater for the negative sense of circular polarization ($h_{0y'} = h_{0x'}$). These three points are found generally in the measurements which will be described in the following section.

Measurements on a Spherical Ferrite Scatterer

The preceding analysis has shown that the field around a small sphere in a saturating magnetic field and a circularly polarized plane wave is made up of the incident wave plus a dipole field radiating principally along the magnetic field. In practice the incident wave must be blocked by a suitable boundary in order to achieve a useful deflection. Therefore, the sphere is no longer in a plane wave. Further, experiment finds that useful spheres are not small compared with the wavelength in the ferrite. For these reasons, the measurements which will be described here agree only qualitatively with the calculations.

Measurements have been made on cylindrical and spherical ferrite samples. The spherical ferrites, however, are definitely preferred for minimum depolarization for a given deflection. The transmitted power is measured at the peak of the beam in whatever direction it falls. It is referred to power transmitted with no ferrite at all in the system. Thus, power loss is made up of dissipation in the ferrite, reflection from the ferrite, and spreading of the transmitted beam. The incident and detected power are both circularly polarized. The beam deflection is measured by placing the detector at 45° with respect to the undeflected beam and measuring db change in transmitted power upon reversing the transverse field. This is found much more easily than measuring the angle of the broad peak involved. Although the normal input to the radiator is circularly polarized, standing wave ratios are measured with linear polarization along two axis—one with the magnetic rf field parallel to the transverse static field, and one with the rf field perpendicular to the transverse static field. The degree of depolarization (cross polarization) is measured to the same reference as the normal polarization by reversing the polarization sense of the detector.

The data in Fig. 3(a) were taken at 9200 mc with a 0.350-inch-diameter General Ceramics R-1 sphere supported in teflon at the end of a 0.582-inch-diameter waveguide as shown in Fig. 1. It should be mentioned that the extension of the dielectric beyond the sphere affects both the standing wave ratio and the beam deflection performance. In this case, the teflon is extended about 0.125 inch beyond the end of the sphere. In Fig. 3(a), the maximum db difference shown corresponds to about $\pm 15°$ of beam deflection. While this does not represent the maximum possible, the curves show typically a critical value of axial field giving maximum transmitted power, greater deflection with negative circular polarization than with positive, two symmetrical axial fields of minimum standing wave ratio, and an increasing depolarization of the fields of largest beam deflection.

Now the data in Fig. 3(a) were taken at constant transverse magnetic field. For a better comparison with the calculated dipole strengths m_x and m_y, the ratio of axial to transverse field was held constant to maintain the static field at 30° to the waveguide center line. In Fig. 3(b), measured deflections and cross polarization are compared with calculated pole strengths from ferrite characteristics given for R-1 by Spencer and Le Craw. From the previous equations, dipole strengths driving the rf fields along the 30° static magnetic field axis in the forward sense of polarization are $(m_x - jm_y)/2$. Similarly, $(m_x + jm_y)/2$ in Fig. 3(b) represents energy along this axis in the cross-polarized sense. It can be seen that

[3] See the characteristics of R. E. LeCraw and E. G. Spencer, "Tensor permeabilities of ferrites below magnetic saturation," 1956 IRE Convention Record, pt. 5, pp. 66–74.

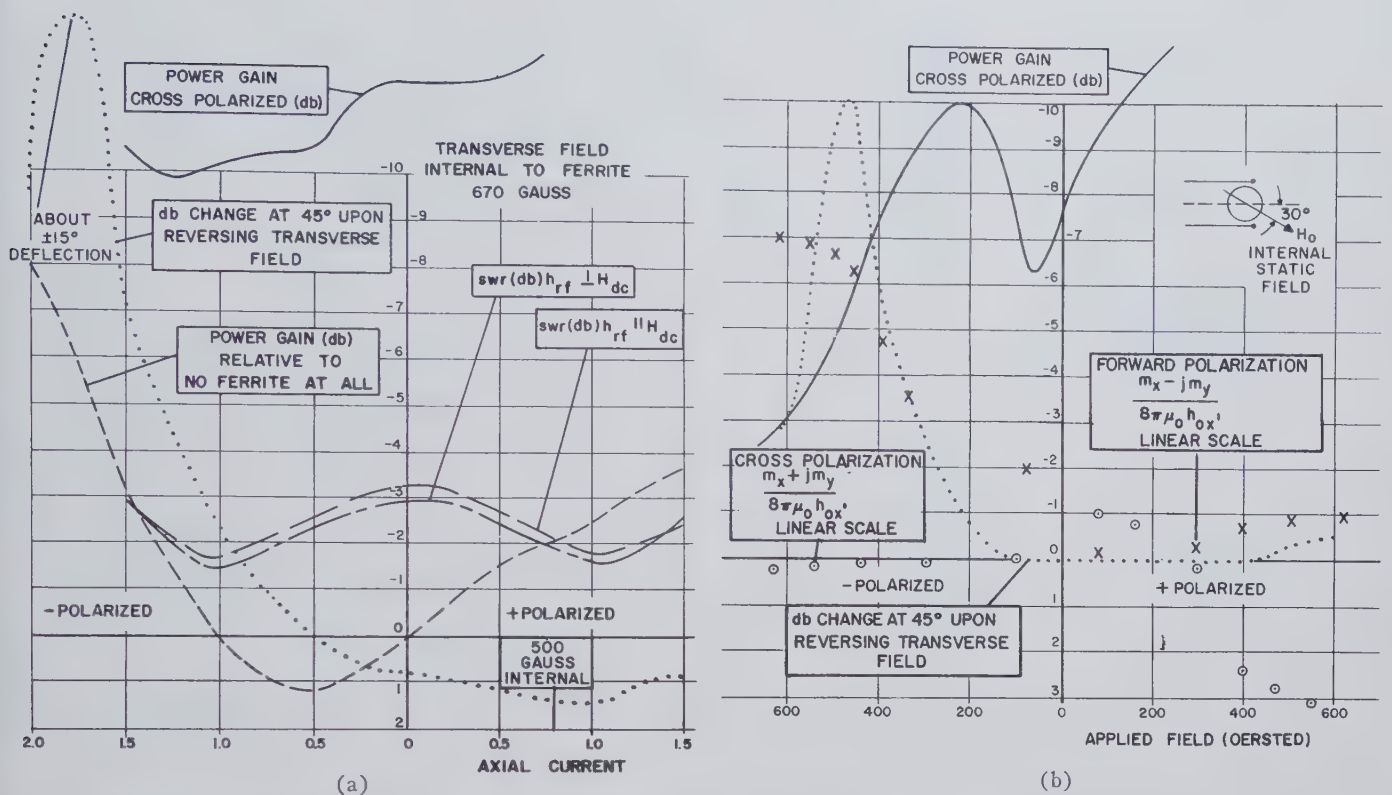

Fig. 3—(a) Deflection characteristic of 0.350-inch diameter sphere. (b) Beam deflection for static field at 30°. The X-data points indicate calculated dipole strengths driving circularly polarized energy in the direction of the static magnetic field with the same sense of polarization as the incident wave. The ⊙-data points are calculated dipole strengths in the reverse sense of polarization. The other curves are experimental.

the deflection is great where $(m_x - jm_y)/2$ is large and that the deflection is in the anticipated direction. Further, $(m_x + jm_y)/2$ predicts the cross-polarized component, except for the region of positive polarization where one would expect to measure severe depolarization. Thus the rf dipole representation of the problem gives a very nice qualitative picture of the beam deflection mechanism. Further, it is possible to judge the usefulness of any particular ferrite in this application if the microwave permeabilities are known.

Typical of most ferrite devices, the deflection direction is nonreciprocal. That is, a characteristic curve is preserved when the direction of propagation is reversed only if the sense of polarization is also reversed. This characteristic is, of course, no problem in a one-way antenna. In a two-way antenna, on the other hand, such as is used for radar, this may be an advantage or a disadvantage, depending upon the application. If this principle were applied to radar conical scanning, for example, the reciprocity problem could be solved with the transmitter and receiver coupled to a circular waveguide in space quadrature. The transmitted and received power would then have the opposite sense of circular polarization, and the transmitted and received beam would both lie in the same direction. Such a radar, though circularly polarized, would have the same rain rejection and target characteristics as if it were linearly polarized.

Application of a Ferrite Scatterer to Conical Scanning

While there are limited applications for the wide beam deflection system as it has been described, the original objective of this development was to produce conical scanning for radar by ferrite means. The required mechanical motion of conventional scanners is relatively rapid, and low-temperature operation is a recurrent problem. Further, conical scanning is a simplified problem as it is only a one-degree-of-freedom application.

The chief difficulty is this: in conical scanning from a parabolic reflector, an effective center of radiation is displaced from the axis of the parabola and rotated at a constant radius. The problem then becomes one of converting a deflected beam from the ferrite scatterer into a displaced center of radiation. Accordingly, various splash-plate and dielectric lens combinations have been tried in an effort to produce this effect.

Although this problem is far from being solved, one of the most effective combinations that has been found to the present is the feed shown in Fig. 4. Here power is deflected at the ferrite and reflected toward a parabolic antenna dish at the far left (not shown on the drawing). Relative sizes are preserved, and the ferrite diameter is 0.350 inch, which gives its approximate size. A complete physical description is not given, however, as the device is rather imperfect. For example, in order to achieve a 1-db conical scan crossover, the depolarized power is

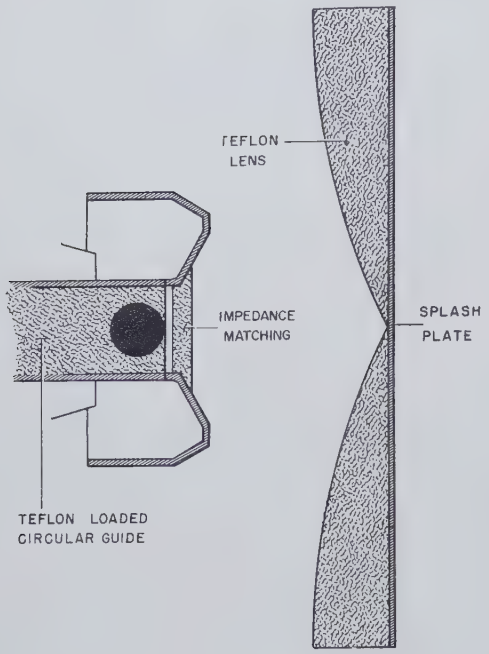

Fig. 4—Ferrite application to a feed for a conical scanning antenna.

only 10 db below the normal polarization. Further side lobes are up to 15 db below the peak of the beam, and antenna efficiency is low. Nevertheless, the device demonstrates an application which could produce a conical scanner in principle in all respects including the problem of reciprocity in the ferrite.

Conclusion

It has been shown that a small sphere immersed in an oblique uniform magnetic field and an rf circularly polarized plane wave will scatter electromagnetic energy principally along the magnetic field. It is demonstrated that this principle can be used to direct a wide radiated beam at the expense of some depolarization of the incident wave. Finally, it has been shown as an example that this could be applied to the problem of conical scanning although a scanner has not been made which could compete with present mechanical scanners.

Acknowledgment

Most of the measurements described were made by R. Cox of the Westinghouse Air Arm Division.

A Ferrite Boundary-Value Problem in a Rectangular Waveguide*

C. B. SHARPE† and D. S. HEIM†

Summary—**A solution is obtained for the electric field at the air-ferrite interface ($z=0$) in a rectangular waveguide filled with ferrite in the semi-infinite half ($z>0$) and magnetized in the direction of the electric field. The field is expressed in terms of a Neumann series obtained by iteration of a singular integral equation which satisfies the boundary conditions at the interface. The equivalent circuit for the junction is also presented.**

Introduction

THE mathematical difficulties which are encountered in the solution of many boundary value problems involving gyromagnetic media have been pointed out by several authors.[1–3] The formulation of these problems is usually straightforward but the imposition of the boundary conditions at the isotropic-to-anisotropic interface frequently makes them intractable. The one discussed here, in which the anisotropic media is a semi-infinite slab of ferrite filling a rectangular waveguide, appears to present some of the essential difficulties common to the solution of many such problems.

Referring to Fig. 1, we consider an infinite rectangular waveguide which is filled with a ferrite medium for $z>0$ and air for $z<0$. The ferrite region is magnetized in the y direction with an internal field H. A TE_{10} wave is incident from the left at the air-ferrite interface ($z=0$). The problem is to determine the electric and magnetic fields at the interface and the equivalent circuit for the junction. The ferrite medium is assumed to be lossless and characterized by a tensor permeability

$$(\mu) = \begin{bmatrix} \mu & 0 & j\kappa \\ 0 & \mu_0 & 0 \\ -j\kappa & 0 & \mu \end{bmatrix}$$

where

* Manuscript received by PGMTT, May 24, 1957; revised manuscript received, August 12, 1957. This work was sponsored by the Signal Corps Eng. Labs., Dept. of the Army, Contract No. DA-36-039 sc-63203.

† Electronic Defense Group, Dept. of Elec. Eng., Univ. of Michigan, Ann Arbor, Mich.

[1] P. S. Epstein, "Theory of wave propagation in a gyromagnetic medium," *Rev. Mod. Phys.*, vol. 28, pp. 3–17; January, 1956.

[2] A. A. Th. Van Trier, "Guided electromagnetic waves in anisotropic media," *Appl. Sci. Res.*, vol. 3, sec. B, pp. 305–370; 1953.

[3] H. Suhl and L. R. Walker, "Topics in guided wave propagation through gyromagnetic media," *Bell Sys. Tech. J.*, vol. 33, Part I, pp. 579–659; May, 1954, Part II, pp. 939–986; July, 1954, and Part III, pp. 1133–1194; September, 1954.

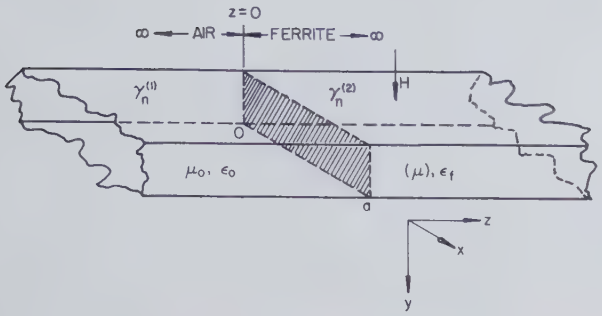

Fig. 1—Ferrite-filled waveguide.

$$\frac{\mu}{\mu_0} = 1 + \frac{\Gamma^2 M_s H}{\Gamma^2 H^2 - \omega^2},$$

$$\frac{\kappa}{\mu_0} = \frac{\omega \Gamma M_s}{\Gamma^2 H^2 - \omega^2}.$$

In rationalized mks units, which are used throughout, the gyromagnetic ratio is given by

$$\Gamma = -0.22 \times 10^6 \text{ m/ampere-second.}$$

M_s is defined as the magnetization at saturation using the convention

$$B = \mu_0(H + M).$$

All field quantities are taken proportional to $\exp(j\omega t)$.

The Equivalent Circuit

Assuming all field quantities are independent of the y coordinate, the transverse electric and magnetic fields in the ferrite [medium (2)] can be expressed by[4]

$$E_y^{(i)} = \sum_{n=1}^{\infty} T_n \sin n\pi x/a \, e^{-\gamma_n^{(2)} z}, \tag{1}$$

$$H_x^{(i)} = \sum_{n=1}^{\infty} T_n [nM \cos n\pi x/a - Y_n^{(2)} \sin n\pi x/a] e^{-\gamma_n^{(2)} z}, \tag{2}$$

where

$$\gamma_n^{(2)} = \sqrt{(n\pi/a)^2 - \omega^2 \mu_\perp \epsilon_f}, \qquad \mu_\perp = \frac{\mu^2 - \kappa^2}{\mu},$$

$$M = \frac{\pi}{a\omega} \frac{\kappa}{\mu^2 - \kappa^2}, \qquad Y_n^{(2)} = \frac{\gamma_n^{(2)}}{j\omega\mu_\perp}.$$

In the air-filled section [medium (1)] the incident TE_{10} wave is given by

$$E_y^{(i)} = \sin \pi x/a \, e^{-\gamma_1^{(1)} z} \tag{3}$$

$$H_x^{(i)} = -Y_1^{(1)} \sin \pi x/a \, e^{-\gamma_1^{(1)} z}, \tag{4}$$

and the reflected TE_{10} waves are given by

$$E_y^{(r)} = \sum_{n=1}^{\infty} R_n \sin n\pi x/a \, e^{\gamma_n^{(1)} z} \tag{5}$$

$$H_x^{(r)} = \sum_{n=1}^{\infty} Y_n^{(1)} R_n \sin n\pi x/a \, e^{\gamma_n^{(1)} z}, \tag{6}$$

[4] *Ibid.*, Part II.

where

$$Y_n^{(1)} = \frac{\gamma_n^{(1)}}{j\omega\mu_0}, \qquad \gamma_n^{(1)} = \sqrt{(n\pi/a)^2 - \omega^2 \mu_0 \epsilon_0}.$$

The necessity of (5) and (6) is discussed by Epstein.[5] Satisfying the boundary conditions at the interface $z=0$ and eliminating the R_n results in the following for the coefficients of the electric field:

$$[T_1(Y_1^{(1)} + Y_1^{(2)}) - 2Y_1^{(1)}] \sin \pi x/a = \sum_{n=1}^{\infty} nMT_n \cos n\pi x/a - \sum_{n=2}^{\infty} (Y_n^{(1)} + Y_n^{(2)}) T_n \sin n\pi x/a, \quad 0 \le x \le a. \tag{7}$$

Both Epstein[5] and Van Trier[6] have pointed out that (7) leads to an infinite system of simultaneous linear equations for which there is no practicable method of solution. Epstein has used a method of successive approximations to obtain a power-series expansion for R_1 in terms of $\kappa/(\mu^2-\kappa^2)$. However, as he points out, this leaves much to be desired, particularly since $\kappa/(\mu^2-\kappa^2)$ can be very large. In the solution which follows, (7) will be expressed as an integral equation in terms of the electric field E_y at the interface. The solution will yield the electric and magnetic fields directly for almost all values of $\kappa/(\mu^2-\kappa^2)$.

It will be convenient to normalize (7). Consider first the case where only the dominant mode propagates in the ferrite medium. That is,

$$(\pi/a)^2 < \omega^2 \mu_\perp \epsilon_f < (2\pi/a)^2.$$

It is assumed in all cases that only the dominant mode propagates in the air-filled section. The transmission line circuit illustrated in Fig. 2 will be equivalent to the waveguide junction if we can identify the voltage and current waves on the line with the fundamental components of the transverse electric and magnetic fields, respectively, in the waveguide. The analogy which we shall employ here makes the constant of proportionality between current and voltage equal to the wave admittance for the dominant mode in the corresponding waveguide. The quantity Re $[V^{(j)} I^{(j)*}]$, $j=i, r, t$, (Fig. 2) will be proportional to the power flow in the corresponding waveguide. Thus, in the air-filled section,

$$E_{y1}^{(i)} = V(z)^{(i)} \sin \pi x/a, \quad E_{y1}^{(r)} = V(z)^{(r)} \sin \pi x/a$$

$$H_{x1}^{(i)} = -Y_1^{(1)} E_{y1}^{(i)} = I(z)^{(i)} \sin \pi x/a,$$

$$H_{x1}^{(r)} = Y_1^{(1)} E_{y1}^{(r)} = I(z)^{(r)} \sin \pi x/a$$

where the subscript 1 denotes the first mode. In the ferrite-filled section a fundamental difficulty occurs since $H_{x1}^{(i)}$ is not simply proportional to $E_{y1}^{(i)}$. Nevertheless, a similar correspondence can be made:

[5] Epstein, *op. cit.*, p. 14.
[6] Van Trier, *op. cit.*, p. 335.

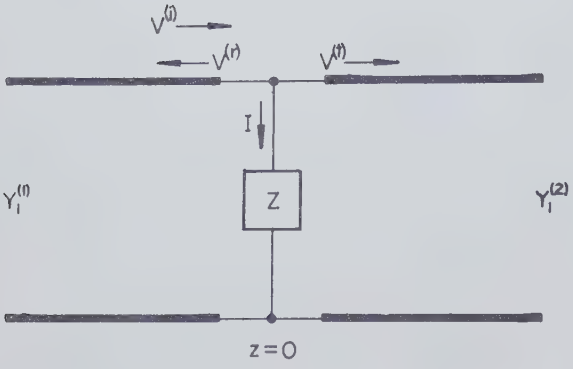

Fig. 2—Equivalent circuit for the air-ferrite junction.

$$E_{y1}^{(i)} = V(z)^{(i)} \sin \pi x/a$$
$$Y_1^{(2)} E_{y1}^{(i)} = I(z)^{(i)} \sin \pi x/a.$$

Power flow in the ferrite medium is still proportional to Re $[V^{(i)} I^{(i)*}]$ since the cosine term in (2) does not contribute to the integral of Poynting's vector over the cross section of the waveguide. Of course, the continuity of H_x at the junction no longer implies the continuity of current flow in the equivalent circuit. This discontinuity in current flow at the junction is accounted for by the current I flowing through the impedance Z.

Since, at $z=0$

$$V^{(i)} = 1, \qquad V^{(r)} = R_1, \qquad V^{(t)} = T_1,$$

it follows from Fig. 2 that

$$-I = T_1(Y_1^{(1)} + Y_1^{(2)}) - 2Y_1^{(1)}. \tag{8}$$

It will be useful to make the change of variable, $\phi = \pi x/a$. Then, at $z=0$

$$E_y^{(i)}(\phi) = \sum_{n=1}^{\infty} T_n \sin n\phi, \qquad 0 \leq \phi \leq \pi, \tag{9}$$

where

$$T_n = \frac{2}{\pi} \int_0^{\pi} E_y^{(i)}(\phi) \sin n\phi d\phi. \tag{10}$$

Following Miles,[7] we define a normalized field proportional to $E_y^{(i)}$,

$$E_y^{(i)}(\phi) = I\mathcal{E}(\phi). \tag{11}$$

Whence,

$$z = JX = \frac{V^{(i)}}{I} = \frac{2}{\pi} \int_0^{\pi} \mathcal{E}(\phi) \sin \phi d\phi.$$

It can be shown[8] that for a ferrite described by a Hermitian tensor the Re $[Z]=0$, which confirms the assumption of a lossless medium. Eq. (7) can now be written,

$$-\sin \phi = M\mathcal{E}'(\phi) - \frac{2}{\pi} \sum_{n=2}^{\infty} (Y_n^{(1)} + Y_n^{(2)}) \int_0^{\pi} \mathcal{E}(\phi') \sin n\phi' \sin n\phi d\phi', \quad 0 \leq \phi \leq \pi. \tag{13}$$

$\mathcal{E}'(\phi)$ denotes the derivative of $\mathcal{E}(\phi)$ with respect to ϕ.

When all modes are cut off in the ferrite,

$$\omega^2 \mu_\perp \epsilon_f < (\pi/a)^2,$$

and $Y_1^{(2)}$ is imaginary. The equivalent circuit of Fig. 2 will suffice for this case also with the understanding that no power is transmitted away from the junction to the right. We cannot neglect $I^{(i)}$ since it gives rise to an inductive susceptance in parallel with Z. The impedance Z accounts for the discontinuity in the sinusoidal component of H_x as before. The theory which follows will therefore be valid for both the case where only the dominant mode propagates in the ferrite and the case where all modes are cut off.

Theory

In order to solve (13) for $\mathcal{E}(\phi)$, it is necessary to make a commonly used assumption; namely,

$$\gamma_n^{(1)} = \gamma_n^{(2)} \cong n\pi/a, \qquad n > 1.$$

Then $Y_n^{(1)} + Y_n^{(2)}$ can be approximated by

$$Y_n^{(1)} + Y_n^{(2)} \cong -jKn, \qquad n > 1, \tag{14}$$

where

$$K = \frac{\pi}{a\omega} [1/\mu_0 + 1/\mu_\perp].$$

Eq. (14) is usually a reasonable assumption to make for problems where only the first mode propagates. However, we shall find in the present problem that this assumption appears to be of critical importance for the case where $M/K = 1$.

With this assumption, (13) can be written,

$$C \sin \phi = M\mathcal{E}'(\phi) + jK \frac{2}{\pi} \sum_{n=1}^{\infty} n \int_0^{\pi} \mathcal{E}(\phi') \sin n\phi' \sin n\phi d\phi', \tag{15}$$

where

$$-C = 1 + jK \frac{2}{\pi} \int_0^{\pi} \mathcal{E}(\phi) \sin \phi d\phi = 1 - KX. \tag{16}$$

Integrating the last term in (15) by parts and employing the identity[9]

$$\sin n\phi = \frac{1}{\pi} \int_0^{\pi} \frac{\sin \phi \cos n\psi}{\cos \psi - \cos \phi} d\psi, \quad (n = 0, 1, 2, \cdots),$$

[7] J. W. Miles, "The equivalent circuit for a plane discontinuity in a cylindrical wave guide," Proc. IRE, vol. 34, pp. 728–742; October, 1946.

[8] C. B. Sharpe and D. S. Heim, "Reflections in a Ferrite Filled Waveguide," Univ. of Michigan, Electronic Defense Group, Tech. Rep. No. 72; May, 1957.

[9] W. Magnus and F. Oberhettinger, "Formulas and Theorems for the Functions of Mathematical Physics," Chelsea Publishing Co., New York, N. Y., p. 141; 1954.

one obtains

$$C \sin \phi = M\mathcal{E}'(\phi) + jK \frac{2}{\pi^2} \sin \phi \sum_{n=1}^{\infty} \int_0^{\pi} \mathcal{E}'(\phi') \cos n\phi' d\phi' \cdot \int_0^{\pi} \frac{\cos n\psi}{\cos \psi - \cos \phi} d\psi. \quad (17)$$

Interchanging the order of integration and summation in (17) results in a singular integral equation of the second kind.

$$C \sin \phi = M\mathcal{E}'(\phi) + j \frac{K}{\pi} \int_0^{\pi} \frac{\mathcal{E}'(\psi) \sin \phi}{\cos \psi - \cos \phi} d\psi. \quad (18)$$

It is convenient to define

$$\mathcal{E}(\phi) = \mathcal{E}_r(\phi) + j\mathcal{E}_i(\phi).$$

Eq. (18) can then be expressed by the system,

$$C \sin \phi = M\mathcal{E}_r'(\phi) - \frac{K}{\pi} \int_0^{\pi} \frac{\mathcal{E}_i'(\psi) \sin \phi}{\cos \psi - \cos \phi} d\psi \quad (19)$$

$$0 = M\mathcal{E}_i'(\phi) + \frac{K}{\pi} \int_0^{\pi} \frac{\mathcal{E}_r'(\psi) \sin \phi}{\cos \psi - \cos \phi} d\psi. \quad (20)$$

Solution for Small M/K

Schmeidler[10] has shown how the system of integral (19) and (20) can be solved by a process of iteration when $|M/K| < 1$. We shall have need for the following integral equation and its solution:

$$f(s) = \frac{1}{\pi} \int_0^{\pi} \frac{\sin s}{\cos t - \cos s} g(t) dt \quad (21)$$

$$g(t) = \frac{1}{\pi} \int_0^{\pi} g(t) dt - \frac{1}{\pi} \int_0^{\pi} \frac{f(s) \sin s}{\cos s - \cos t} ds. \quad (22)$$

Recalling that $\mathcal{E}(\phi) = 0$ for $\phi = 0, \pi$, the application of (21) and (22) to (19) and (20) yields

$$\mathcal{E}_i'(\phi) = -\frac{C}{K} \cos \phi - (M/K)^2 \frac{1}{\pi^2} \int_0^{\pi} \frac{\sin \tau d\tau}{\cos \phi - \cos \tau} \cdot \int_0^{\pi} \frac{\mathcal{E}_i'(\psi) \sin \psi}{\cos \tau - \cos \psi} d\psi. \quad (23)$$

Eq. (23) can be identified as an integral equation of the form

$$\mathcal{E}_i'(\phi) = f(\phi) + \lambda \int_0^{\pi} K(\phi, \tau) d\tau \int_0^{\pi} \mathcal{E}_i'(\psi) K(\tau, \psi) d\psi \quad (24)$$

by making the correspondence,

$$K(\phi, \tau) = \frac{1}{\pi} \frac{\sin \tau}{\cos \phi - \cos \tau}$$

$$f(\phi) = -\frac{C}{K} \cos \phi$$

$$\lambda = -(M/K)^2. \quad (25)$$

[10] W. Schmeidler, "Integralgleichungen mit Anwendungen in Physik und Technik," Geest and Portig K.-G., Leipzig, Ger., 1955.

Iterating (24) yields,

$$\mathcal{E}_i'(\phi) = f(\phi) + \lambda \int_0^{\pi} K(\phi, \tau) d\tau \int_0^{\pi} f(\psi) K(\tau, \psi) d\psi + \lambda^2 \int_0^{\pi} K(\phi, \tau) d\tau \int_0^{\pi} K(\tau, \sigma) d\sigma \int_0^{\pi} K(\sigma, \rho) d\rho \cdot \mathcal{E}_i'(\psi) K(\rho\psi) d\psi.$$

Repeating the process leads to a Neumann series for $\mathcal{E}_i'(\phi)$. It can be shown[11] that for the kernel (25), the above series converges for $|\lambda| < 1$. Thus, the first order approximation to $\mathcal{E}'(\phi)$ can be taken as

$$\mathcal{E}_{i_1}'(\phi) = f(\phi)$$

and the second order approximation as

$$\mathcal{E}_{i_2}'(\phi) = f(\phi) + \lambda \int_0^{\pi} K(\phi, \tau) d\tau \int_0^{\pi} f(\psi) K(\tau, \psi) d\psi. \quad (26)$$

We shall obtain only the second order approximation, although the extension to higher order approximations is obvious. It follows that

$$\mathcal{E}_{i_2}'(\phi) = -\frac{C}{K}\left[1 + \frac{1}{2}\left(\frac{M}{K}\right)^2\right] \cos \phi - \frac{2C}{\pi^2 K}\left(\frac{M}{K}\right)^2 \ln \frac{1 + \cos \phi}{1 - \cos \phi} + \frac{C}{2\pi^2 K}\left(\frac{M}{K}\right)^2 \cos \phi \left(\ln \frac{1 + \cos \phi}{1 - \cos \phi}\right)^2, \quad \left|\frac{M}{K}\right| < 1. \quad (27)$$

The solution for $\mathcal{E}_r'(\phi)$ follows in the same manner. There results

$$\mathcal{E}_{r_2}'(\phi) = -\frac{C}{\pi K}\left[\frac{5}{3}\left(\frac{M}{K}\right)^3 + 2\left(\frac{M}{K}\right)\right] + \frac{C}{\pi K}\left[\left(\frac{M}{K}\right) + \frac{5}{6}\left(\frac{M}{K}\right)^3\right] \cos \phi \left(\ln \frac{1 + \cos \phi}{1 - \cos \phi}\right) + \frac{C}{\pi^3 K}\left(\frac{M}{K}\right)^3 \left[\left(\ln \frac{1 + \cos \phi}{1 - \cos \phi}\right)^2 - \frac{1}{6} \cos \phi \left(\ln \frac{1 + \cos \phi}{1 - \cos \phi}\right)^3\right], \quad \left|\frac{M}{K}\right| < 1. \quad (28)$$

It remains to determine C, which is a function of the unknown reactance X. From (12),

$$X = \frac{2}{\pi} \int_0^{\pi} \mathcal{E}_i'(\phi) \cos \phi d\phi. \quad (29)$$

[11] *Ibid.*, p. 429.

It follows that

$$C = \frac{\pi^2}{4}\left(\frac{K}{M}\right)^2,$$

$$X = -\frac{1}{K}\left[\frac{1+\frac{4}{\pi^2}\left(\frac{M}{K}\right)^2}{\frac{4}{\pi^2}\left(\frac{M}{K}\right)^2}\right], \qquad \left|\frac{M}{K}\right| < 1. \tag{30}$$

Solution for Large M/K

A Neumann series valid for $|M/K|>1$ can also be obtained from (19) and (20). By direct substitution,

$$\varepsilon_i'(\phi) = \frac{C}{\pi M}\left(\frac{K}{M}\right)\sin\phi\left(\ln\frac{1+\cos\phi}{1-\cos\phi}\right)$$

$$-\left(\frac{K}{M}\right)^2\frac{1}{\pi^2}\int_0^\pi \frac{\sin\phi\, d\tau}{\cos\phi-\cos\tau}\int_c^\pi \frac{\varepsilon_i'(\psi)\sin\tau}{\cos\tau-\cos\psi}\,d\psi \tag{31}$$

$$\varepsilon_r'(\phi) = \frac{C}{M}\sin\phi$$

$$-\left(\frac{K}{M}\right)^2\frac{1}{\pi^2}\int_0^\pi \frac{\sin\phi\, d\tau}{\cos\phi-\cos\tau}\int_0^\pi \frac{\varepsilon_r'(\psi)\sin\tau}{\cos\tau-\cos\psi}\,d\psi. \tag{32}$$

Both (31) and (32) reduce to an equation of the same form as (24) if we take

$$K(\phi,\tau) = \frac{1}{\pi}\,\frac{\sin\phi}{\cos\phi-\cos\tau}$$

$$\lambda = -\left(\frac{K}{M}\right)^2.$$

Iteration again yields a Neumann series in terms of λ. It can be shown that the series will converge for $|\lambda|<1$, that is, for $1<|M/K|$. The proof parallels that given by Schmeidler for the previous case. Second order approximations to $\varepsilon_i'(\phi)$ and $\varepsilon_r'(\phi)$ are found to be,

$$\varepsilon_{i_2}'(\phi) = \frac{C}{\pi K}\left[\left(\frac{K}{M}\right)^2+\frac{5}{6}\left(\frac{K}{M}\right)^4\right]\sin\phi\left(\ln\frac{1+\cos\phi}{1-\cos\phi}\right)$$

$$-\frac{1}{6\pi^3}\,\frac{C}{K}\left(\frac{K}{M}\right)^4\sin\phi\left(\ln\frac{1+\cos\phi}{1-\cos\phi}\right)^3 \tag{33}$$

$$\varepsilon_{r_2}'(\phi) = \frac{C}{K}\left[\left(\frac{K}{M}\right)+\frac{1}{2}\left(\frac{K}{M}\right)^3\right]\sin\phi$$

$$-\frac{C}{2\pi^2 K}\left(\frac{K}{M}\right)^3\sin\phi\left(\ln\frac{1+\cos\phi}{1-\cos\phi}\right)^2. \tag{34}$$

The constant C and the reactance X for this case are

$$C = \frac{-1}{1+\frac{4}{\pi^2}\left[\left(\frac{K}{M}\right)^2+\frac{2}{3}\left(\frac{K}{M}\right)^4\right]},$$

$$X = \frac{-1}{K}\left[\frac{\left(\frac{K}{M}\right)^2+\frac{2}{3}\left(\frac{K}{M}\right)^4}{\frac{\pi^2}{4}+\left(\frac{K}{M}\right)^2+\frac{2}{3}\left(\frac{K}{M}\right)^4}\right], \qquad \left|\frac{K}{M}\right| < 1. \tag{35}$$

Discussion

It is interesting to note that the example discussed by Schmeidler which gives rise to (19) and (20) is a problem in elasticity. The real and imaginary components of $\varepsilon'(\phi)$ are analogous to the horizontal and vertical components of pressure, respectively, at the base of a dam. The depth of water as a variable has the same significance as the magnitude of the magnetizing field H in the electromagnetic field problem.

The existence of both a real and imaginary part to the field at the interface is unique to boundary-value problems involving anisotropic media. Although the field strength at each position across the waveguide varies sinusoidally with time, the phase of this variation differs from one point to the next. Thus, the field exhibits a periodic "shimmy" in time.

The value of $|M/K|=1$ seems to be a critical point in the analysis. Not only do the fields display a marked difference in form for values of M/K on either side of unity but the series solution itself probably does not converge for this critical value. One would suspect the assumption of (14) to be the source of the difficulty.

The value of $|M/K|=0$ leads to an indeterminate solution for the normalized field $\varepsilon_i'(\phi)$ because the normalizing factor I is also zero at this point. This is of little consequence, however, since for $M=0$ the problem reduces to the case of an isotropic dielectric. It is interesting to note, again in contrast to isotropic problems that X may be either inductive or capacitive since K can be negative or positive.

Some Techniques of Microwave Generation and Amplification Using Electron Spin States in Solids*

D. I. BOLEF† AND P. F. CHESTER†

Summary—Possible modes of operation of two-level solid state masers utilizing the techniques of population inversion used in nuclear magnetic resonance are described. Methods of continuous operation of two-level masers and their usefulness as microwave generators are discussed.

Introduction

RECENTLY, several papers[1–7] have made clear the advantages to be expected of solid-state maser amplifiers with respect to noise figure, when compared with conventional microwave amplifiers, and with respect to tunability, bandwidth, power output, and simplicity, when compared with beam-type or gas cell masers.

The paper by Scovil[8] has described the first successful solid-state master oscillator, based on a three-level scheme and, therefore, inherently continuous in operation. The conditions under which such a scheme can be used, however, are somewhat circumscribed by the limited number of suitable paramagnetic materials and by considerations of "forbidden" transitions, relaxation times, and local oscillator power. Extension to operating temperatures appreciably above 1.2°K or to frequencies higher than X band is likely to depend on further investigation of paramagnetic materials. An upper frequency limit will eventually be set by the nonavailability of a source of saturating power. The inherent frequency-reducing characteristic of three-level masers precludes consideration of them as microwave generators.

Two-level solid-state masers, although basically intermittent in operation, should be realizable in practice with fewer restrictions on materials, operating temperature, frequency, and local oscillator power. The first attempted solid-state maser[1] was in fact based on a two-level scheme. It is the purpose of this paper to examine possible modes of operation and characteristics of two-level maser amplifiers, to suggest ways in which intermittency might be avoided, and to discuss the possibilities of two-level maser generators.

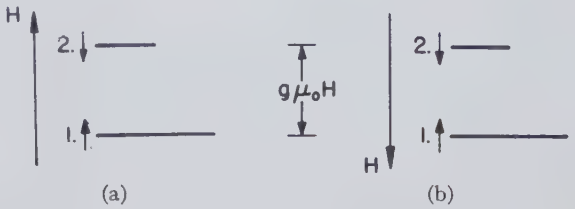

Fig. 1—(a) Energy levels of a free electron in a magnetic field. The population of a level is indicated schematically by the length of the horizontal line. (b) Situation after nonadiabetic field reversal.

Inversion in Two-Level Systems

Consider the two energy states for a free electron in a magnetic field H corresponding to magnetic moment parallel and antiparallel to the field, as shown in Fig. 1(a). The difference in energy is given by

$$E_2 - E_1 = h\nu = g\mu_0 H \tag{1}$$

where h is Planck's constant, ν the resonant frequency, μ_0 the Bohr magneton, and g has the value 2.0023 for a free electron. For a paramagnetic crystal in which the ions have an effective spin of $\frac{1}{2}$ and show no hyperfine interactions, it is a good approximation to use (1) with a suitably modified value of g. If the crystalline electric field is noncubic, g will be a function of the angle between the symmetry axis and the external magnetic field.

In a magnetic field the populations of the upper and lower states, N_2 and N_1 respectively, will in general not be equal and a spin magnetization M therefore will exist whose component along the field is given by

$$M_H = g\mu_0(N_2 - N_1)/2.$$

When the spin system is in equilibrium with the lattice at absolute temperature T,

$$\left[\frac{N_1}{N_2}\right]_{\text{equil.}} = \exp.\ h\nu/kT$$

where k is Boltzmann's constant. This corresponds to an equilibrium magnetization M_0. Under nonequilibrium conditions, M_H relaxes to the value M_0 with a time constant T_1, the spin-lattice relaxation time.

* Manuscript received by the PGMTT, June 14, 1957.
† Westinghouse Res. Labs., Pittsburgh 35, Pa.

[1] J. Combrisson, A. Honig, and C. H. Townes, "Utilisation de la resonance de spins électroniques pour réaliser un oscillateur ou un amplificateur en hyperfrequences," *Compt. Rend.*, vol. 242, pp. 2451–2453; May 14, 1956.

[2] N. Bloembergen, "Proposal for a new type solid state maser," *Phys. Rev.*, vol. 104, pp. 324–327; October 15, 1956.

[3] M. W. P. Strandberg, "Quantum mechanical amplifiers," PROC. IRE, vol. 45, pp. 92–93; January, 1957.

[4] J. P. Wittke, "Molecular amplification and generation of microwaves," PROC. IRE, vol. 45, pp. 291–316; March, 1957.

[5] M. W. Muller, "Noise in a molecular amplifier," *Phys. Rev.*, vol. 106, pp. 8–12; April 1, 1957.

[6] R. V. Pound, "Spontaneous emission and the noise figure of maser amplifiers," *Ann. Phys.*, vol. 1, pp. 24–33; April, 1957.

[7] K. Shimoda, H. Takahasi, and C. H. Townes, "Fluctuations in amplification of quanta," *J. Phys. Soc. Japan*, vol. 12, pp. 686–700; June, 1957.

[8] H. E. D. Scovil, "The three-level solid-state maser," this issue, p. 29.

Before maser action can be obtained, it is necessary for N_2 to be made greater than N_1, *i.e.*, for M_H to be made negative. When only two states exist this situation may be brought about in principle by exchanging populations between the states using one of the techniques familiar in transient nuclear resonance experiments.[9–12]

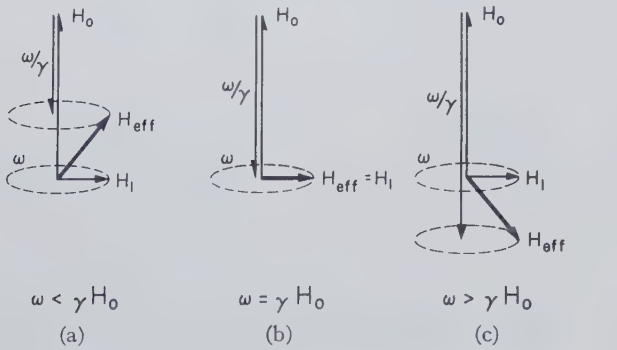

Fig. 2—The effective field in a frame of reference rotating about H_0 at frequency ω with the microwave field H_1, (a) ω below resonance, (b) at resonance, (c) ω above resonance.

An understanding of the two most common inversion techniques may be had by reference to the vector representation of Fig. 2. The paramagnetic sample is assumed to be in a steady magnetic field H_0 and subjected to a microwave field circularly polarized about the direction H_0, of amplitude H_1 and angular frequency ω. It will further be assumed that before the microwave field was switched on, the spin system was characterized by a magnetization M parallel to H_0. It is convenient to refer the subsequent motion of M to a coordinate system rotating about the H_0 axis with angular frequency ω. The effective field experienced in the rotating system is given by[13]

$$\vec{H}_{\text{eff}} = (\vec{H}_0 - \vec{\omega}/\gamma) + \vec{H}_1$$

where γ is the electron gyromagnetic ratio. Viewed in the rotating system, M will precess about H_{eff} with angular frequency Ω where

$$\Omega = \gamma H_{\text{eff}}.$$

Adiabatic Rapid Passage (ARP)

For a microwave field of frequency ω well below the value $\omega_0 (=\gamma H_0)$ required for resonance, the appropriate field relationship is shown schematically in Fig. 2(a). If $(H_0 - \omega/\gamma) \gg H_1$, H_{eff} is almost parallel to H_0. As ω is increased, H_{eff} diminishes in magnitude and inclination until at $\omega = \omega_0$ it becomes identical with H_1, Fig. 2(b). As ω is further increased well beyond ω_0, H_{eff} increases in magnitude and approaches an orientation antiparallel to H_0, Fig. 2(c).

If the change in H_{eff} is small during a precessional period of M, *i.e.*, in a time Ω^{-1}, M follows the changes in H_{eff} adiabatically. The orientation of M with respect to H_0 is, therefore, reversed as a result of the passage through resonance, *i.e.*, finally $N_2 > N_1$. The adiabatic condition may be written

$$(\gamma H_1)^{-1} \ll t$$

where t is the time to pass through the resonance half-width $\Delta\omega_0 (=\gamma \Delta H_0)$. Passage through resonance by sweeping H_0 is entirely equivalent to sweeping ω. In both cases, inversion of the initial magnetization results, whichever the direction of the sweep.

Another condition originally thought necessary[14] for ARP was that t be much shorter than both the spin-lattice relaxation time, T_1, and the spin-spin relaxation time, T_2. More recent work[15] indicates that the condition on t is in fact less stringent and that provided H_1 is well above the value required for saturation, it is sufficient merely for $t \ll T_1$. It follows that materials with narrow lines or long T_1s will be most amenable to ARP. Experiments[16–18] has shown inversion by ARP to be particularly easy in certain inhomogeneously broadened lines[19] where the unresolved sublines are exceedingly narrow. Such lines may not be the most suitable for maser action, however, unless all the sublines are able to give up energy to the microwave signal field. Such a situation might be assured by radio frequency mixing among the sublines when these are due to hyperfine interactions. No experimental report of inversion by ARP in dipolar-broadened or exchange-narrowed lines has yet appeared, but a number of such lines with widths less than one oersted are known[20–22] and ARP should be possible in some of these with reasonable microwave driving

[9] F. Bloch, W. W. Hansen, and M. Packard, "Nuclear induction experiment," *Phys. Rev.*, vol. 70, pp. 474–485; October 1, 1946.
[10] H. C. Torrey, "Transient notations in nuclear magnetic resonance," *Phys. Rev.*, vol. 76, pp. 1059–1067; October 15, 1949.
[11] E. L. Hahn, "Spin echoes," *Phys. Rev.*, vol. 80, pp. 580–594; November 15, 1950.
[12] E. M. Purcell and R. V. Pound, "A nuclear spin system at negative temperature," *Phys. Rev.*, vol. 81, pp. 279–280; January 15, 1951.
[13] I. Rabi, N. F. Ramsey, and J. Schwinger, "Use of rotating coordinates in magnetic resonance problems," *Rev. Mod. Phys.*, vol. 26, pp. 167–171; April, 1954.
[14] F. Bloch, "Nuclear induction," *Phys. Rev.*, Vol. 70, pp. 460–474; October 1, 1946.
[15] A. G. Redfield, "Nuclear magnetic resonance saturation and rotary saturation in solids," *Phys. Rev.*, vol. 98, pp. 1787–1809; June 15, 1955.
[16] A. M. Portis, "Rapid passage effects in electron spin resonance," *Phys. Rev.*, vol. 100, pp. 1219–1221; November 15, 1955.
[17] A. Honig, "Polarization of arsenic nuclei in a silicon semiconductor," *Phys. Rev.*, vol. 96, pp. 234–235; October 1, 1954.
A. Honig and J. Combrisson, "Paramagnetic resonance in As-doped silicon," *Phys. Rev.*, vol. 102, pp. 917–918; May 1, 1956.
[18] G. Feher and E. A. Gere, "Polarization of phosphorus nuclei in silicon," *Phys. Rev.*, vol. 103, pp. 501–503; July 15, 1956.
[19] An "inhomogeneously broadened" line is one in which the observed line width is an envelope of a number of narrower "sublines" due to a distribution of local magnetic fields at the paramagnetic centers. This distribution may arise from inhomogeneities in the applied magnetic field or from the presence of nuclear magnetic moments. By contrast a "homogeneously broadened" line is one in which the line width is due either to dipole-dipole interactions or to exchange interaction between the paramagnetic centers.
[20] R. A. Weeks, "Paramagnetic resonance of lattice defects in irradiated quartz," *J. Appl. Phys.*, vol. 27, pp. 1376–1381; November, 1956.
[21] B. Smaller, G. R. Hennig, and E. L. Yasaitis, "Paramagnetic resonance absorption in graphite compounds," *Phys. Rev.*, vol. 97, p. 239; January 1, 1955.
[22] J. E. Wertz and P. Auzins, "Crystal vacancy evidence from ESR," *Phys. Rev.*, vol. 106, p. 484; May 1, 1957.

power. Liquid helium temperatures are not expected to be necessary for successful ARP in some of the known materials.

180° Pulse

If the spin system in a magnetic field is subjected to a circularly polarized microwave field at the resonant frequency ω_0, the effective field is as shown in Fig. 2(b). The magnetization M, initially parallel to H_0, starts to precess about H_1 with angular velocity $\Omega=\gamma H_1$. Thus, after time t_π where

$$t_\pi = \frac{\pi}{\gamma H_1}, \tag{2}$$

M will be aligned antiparallel to H_0. If the microwave field is cut off at time t_π, the magnetization will be negative, *i.e.*, N_2 will be greater than N_1. Eq. (2) thus defines a "180° pulse." If H_1 does not exceed a few times ΔH_0 or if the microwave frequency deviates from resonance by as much as $(\Delta\omega_0)/2\pi$, or if (2) is not satisfied experimentally, the inversion will not be perfect. When a good 180° pulse can be produced, however, this technique has the advantage over ARP of requiring less time to accomplish and less average power from the microwave driving field. Pulse lengths between 10^{-8} and 10^{-6} seconds and amplitudes between 0.2 and 20 oersteds will be required for likely materials.

Nonadiabatic Field Reversal

Although this technique was used to invert Li^7 nuclear spin states in the classic negative temperature experiment of Purcell and Pound,[12] little or no attention has been paid to it in connection with solid-state masers. Consider the populations of the two energy levels for an electron in a magnetic field H as shown in Fig. 1(a). If the magnetic field is reversed in a time very much shorter than $(\gamma H)^{-1}$, the system suffers a sudden or nonadiabatic perturbation[23] with the result that the field is established in the reverse direction before the wave functions of the states have changed appreciably. The final situation, as shown in Fig. 1(b), is therefore that the more heavily populated state has become the state of higher energy and vice versa, the extra energy having been absorbed from the source of the changing magnetic field. Since the nonadiabatic condition is

$$\frac{dH}{dt} \gg \gamma H^2, \tag{3}$$

it will clearly be advantageous to reverse the smallest possible field, $H_{\min}$. The lower limit to $H_{\min}$ is set by the line width ΔH_0, or by field components normal to H_0. It should be sufficient to reduce the value of H adiabatically to a value several times larger than ΔH_0, reverse it nonadiabatically, and then increase it adiabatically to $-H_0$, all this taking place in a time much shorter than T_1. For a line of width 0.1 oersted, $H_{\min}$ might be 0.5 oersted and the reversal time for $H_{\min}\sim 5\times 10^{-8}$ seconds. Such a rate of change of field is possible with pulse techniques or with a combination of high static field gradients and high translational velocities. The conditions should be easier for inhomogeneously broadened lines having sublines narrower than 0.1 oersted provided that the "spin diffusion time"[24] between sublines at low fields is much longer than the field reversal time for a given subline.

This technique has the one advantage of requiring no microwave driving field. It may, therefore, find application in the generation of short microwaves.

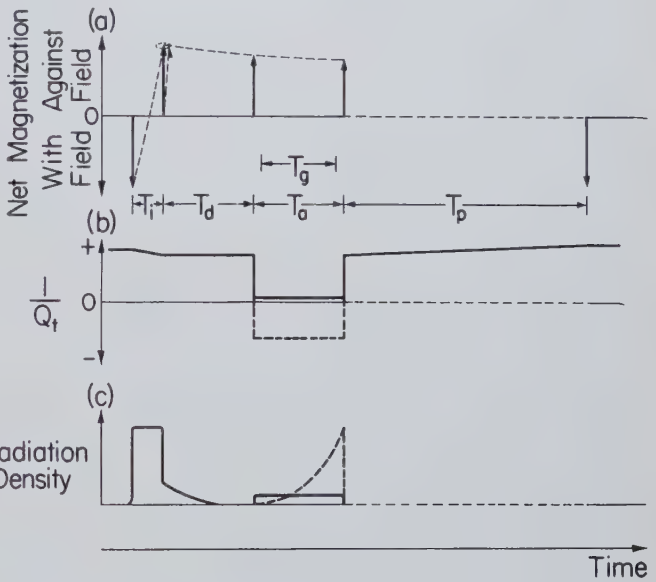

Fig. 3—Time sequence in a simple two-level maser (not to scale). (a) Magnetization vs time, (b) $(Q_t)^{-1}$ vs time, (c) radiation density in cavity vs time. In (b) and (c) the solid line refers to regenerative operation and the broken line to super-regenerative operation.

Intermittent Two-Level Masers

The interaction between the microwave signal which is to be amplified and the inverted spin system may be contrived with either a traveling-wave or a standing-wave (resonant cavity) structure. We shall consider only cavity-based structures.

It is apparent from the discussion of the previous section that, in a simple two-level maser, population inversion and amplification cannot proceed simultaneously and that some form of sequential operation is called for. The time cycle that is likely to be followed in such a maser may be divided into four main periods. Fig. 3 shows the behavior of spin magnetization, total Q, Q_t, and radiation density in the cavity during these periods. Inversion is effected during T_i by ARP or by a 180° pulse. The value of negative magnetization necessary for amplification is such as to make the magnetic Q, Q_m, close to (or smaller than) Q_a, the loaded Q of the cavity during

[23] D. Bohm, "Quantum Theory," Prentice-Hall, Inc., New York, N. Y., ch. 20; 1955.

[24] A. M. Portis, "Spectral diffusion in magnetic resonance," *Phys. Rev.*, vol. 104, pp. 584–588; November 1, 1956.

amplification. Q_m is given by the expression

$$Q_m = V_s/(4\pi M_H \gamma T_2 \eta)$$

where V_s is the volume of the sample, and η the filling factor. Q_m is, of course, negative after inversion.

Radiation damping of the transverse moment induced by the driving field H_1 gives rise to an opposing radiation field H_R whose magnitude is given by

$$H_R = 4\pi\eta Q M_T,$$

where M_T is the component of M transverse to H_0.[25] In order to achieve inversion, H_1 must exceed H_R.[4] This condition can always be satisfied by making H_1 large enough. Unless the inversion process is accomplished perfectly, afterwards there remains a finite transverse moment and the radiation damping field associated with it. The resulting radiative loss from the spin system is negligible when the loaded cavity Q is much less than $-Q_m$ but becomes catastrophic when the loaded cavity Q is equal to or greater than $-Q_m$. One method of avoiding such losses is to vary the cavity Q with time so that for the inversion period T_i and for a short period T_d after it the loaded cavity Q is kept at some low value $Q_i < -Q_m$. The required variation of Q may be realized either by periodically coupling a load to the cavity or by altering H_0 to take the inversion frequency away from the cavity resonant frequency. During T_d, H_R decreases exponentially because of the transverse relaxation of M_T. For $T_d \gg T_2$, H_R will fall to a value less than that of the signal to be amplified and thereupon the spin system can be used for amplification. The sum of the times T_i and T_d must of course be much shorter than T_1.

For regenerative amplification, the loaded Q of the cavity is restored at the start of T_a to a value Q_a, such that $-Q_m \geq Q_a$, *i.e.*, Q_l becomes large but remains positive in sign. T_a must, of course, be much shorter than T_1 for constancy of gain ($T_a \sim 10^{-3} T_1$ for a 10 per cent fall-off in gain at 30 db). For super regenerative amplification[26] the loaded Q is restored to a value such that $-Q_m < Q_a$, *i.e.*, Q_l becomes negative. Oscillation builds up with an amplitude proportional to the signal present at the start of T_a and the gain is determined by τ, the time constant for build-up and by the duration of T_a. The amplifying period may be terminated by reducing the loaded cavity Q to the value Q_i. In a super-regenerator, a self-quenching action due to spin-lattice relaxation is possible if T_a is made of the order T_1.

During T_p, the electrons are brought back to the same normal (though not necessarily equilibrium) distribution as they had prior to inversion. The simplest method of achieving this is to allow time for spin-lattice relaxation to act, but as this requires a time of the order of T_1, it normally results in $T_a \ll T_p$, *i.e.*, in a poor duty factor. There are various methods of shortening T_p which may depend on the particular paramagnetic material used. In semiconductors, radiative excitation into the conduction band followed by recombination,[4,27] is a convenient method if it does not cause excessive sample heating. Another method is to dope the working material with a paramagnetic ion having a very short T_1[28] and having a transition which can be made degenerate with that of the working substance by a suitable change in field. When the signal is small enough or when gain variations from cycle to cycle are not objectionable, a simple way to prepare a normal distribution is a second inversion at the start of T_p.

The transfer characteristic of a two level regenerative maser will approach that of a continuous amplifier as the duty factor is made to approach unity, *i.e.*, as the inactive time ($T_i + T_d + T_p$) is made much shorter than the active time T_a. This can only be brought about by "artificial" shortening of T_p. Since with presently known materials the minimum inactive time is likely to be of the order of microseconds, a high duty factor may involve values of T_a up to 10^{-4} seconds. For a gain fall-off of less than 10 per cent due to spin lattice relaxation over the active period a T, of the order 0.1 second, would then be required. While there is no difficulty in obtaining such long relaxation times in doped silicon below 4°K, when T_a is long the power output from the amplifier before saturation is low ($+10^{-9}$ watts in the above case). The linear power output may be increased at the expense of the duty factor by decreasing T_a. In certain applications, *e.g.*, in radio astronomy and microwave radiometry where the "signal" is just low-level noise power, a poor duty factor is quite acceptable. However, in such cases super-regenerative operation is to be preferred because of its greater linear power output and greater stability at high gains.[26]

The combination of the time cycling described above with intense transient magnetic fields should make possible the generation of submillimeter waves at a relatively high level of power, particularly if materials with high g values can be used. Such a technique, although intermittent, might well find application in fundamental research.

Continuous Two-Level Masers

If continuous operation is desired in a two-level maser, there must be some mechanical transport of material from one situation in which it is inverted to another situation in which it is used.

An obvious method of achieving continuous population inversion and transport of material is depicted in Fig. 4. The paramagnetic material is mounted on the periphery of a rotating disk so as to pass in sequence

[25] N. Bloembergen and R. V. Pound, "Radiation damping in magnetic resonance experiments," *Phys. Rev.*, vol. 95, pp. 8–12; July 1, 1954.

[26] P. F. Chester and D. I. Bolef, "Super-regenerative masers," Proc. IRE, vol. 45, pp. 1287–1289; September, 1957.

[27] G. Feher and R. C. Fletcher, "Relaxation effects in donor spin resonance experiments in silicon," *Bull. Amer. Phys. Soc.*, vol. 1, p. 125; March 15, 1956. (Pittsburgh Meeting.)

[28] G. Feher and H. E. D. Scovil, "Electron spin relaxation times in gadolinium ethyl sulphate," *Phys. Rev.*, vol. 105, pp. 760–762; January 15, 1957.

through a region of high field (b) which produces a positive magnetization, then into a cavity (c) excited by a suitable local oscillator and situated in a magnetic field gradient of form such that material in passing through the cavity (c) experiences ARP. The emerging material, now characterized by a negative magnetization, passes into a second cavity (d), situated in a uniform magnetic field, where amplification takes place at a frequency which may be considerably higher than the ARP frequency. The transit time from (c) to (d) must be much less than T_1 but long enough for the decay of any transverse magnetic moment. The transit time from (d) round to (c) must be long enough for the establishment of a positive magnetization. Thus, the rotational rates required depend on T_1 and on the conditions for ARP, and are entirely feasible for materials with T_1 greater than a few milliseconds. A field gradient over the first cavity of at least several times the line width is required for ARP.

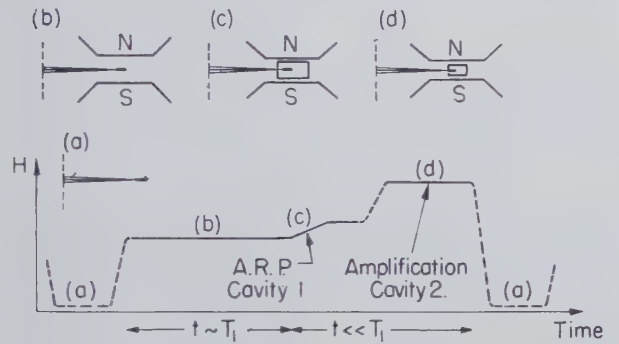

Fig. 4—Schematic representation of a continuous two-level maser using a rotating disk to achieve adiabatic rapid passage and transport of material. The magnetic field experienced by an electron is shown as a function of time. Also shown is the mechanical situation at four representative times.

A mechanically simpler device is conceivable if use can be made of a paramagnetic crystal in which the resonant frequency in fixed magnetic field is a strong function of the angle, Θ, which the crystalline field makes with the magnetic field. Such a material, situated in a cavity in a steady magnetic field, may be taken through resonance by altering Θ. Thus, ARP by crystal spinning is possible. The variation of the energy levels with Θ is in general somewhat complicated,[29] but takes on a particularly simple form for a paramagnetic ion of effective spin $\frac{1}{2}$ and no hyperfine structure. In this case, (1) holds with $g=(g_{\parallel}^2 \cos^2 \Theta+g_{\perp}^2 \sin^2 \Theta)^{1/2}$. Such a variation of g with Θ is shown in Fig. 5. If such a single crystal is situated in a doubly resonant cavity excited at its lower resonant frequency ν_1 by a local oscillator and is suitably rotated, it will undergo ARP at orientations marked (a) and (c) in Fig. 5.[30] If the spin system has a positive magnetization prior to passage through (a) and if the time taken to rotate from (a) to (b) is much shorter than T_1, amplification at the higher cavity frequency ν_2 is possible. A positive magnetization is reestablished after passage through (c). If ν_1 is made sufficiently close to ν_2 so that the time (a) to (c) is much shorter than the time (c) to (a), the cycle may be repeated indefinitely.

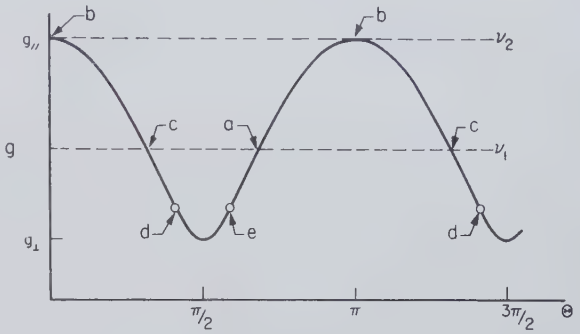

Fig. 5—The variation of g with angle between crystalline field axis and an external magnetic field for a simple case of anisotropy, $g=[g_{\parallel}^2 \cos^2 \Theta+g_{\perp}^2 \sin^2 \Theta]^{1/2}$.

If the specimen is made up of a number of crystallites oriented in the plane normal to the axis of rotation, there will always be some crystallites at the proper angle for amplification, which then proceeds continuously.

Possible materials (*e.g.*, sodium plutonyl acetate) for this maser do show hyperfine structure, however, which results in a mixing of energy levels near $\Theta=\pi/2$ and $3\pi/2$, and the magnetization is not expected to survive passage through these angles. The problem may be avoided if a positive magnetization can be achieved prior to (a) at some angle (e) greater than $\pi/2$ or $3\pi/2$. A possible means for this is to dope the crystal with a paramagnetic ion having a spin-lattice relaxation time much shorter than that of the crystal, and a g value equal to that of the crystal at the angle (e). At this point, a transition in the doping agent becomes degenerate with the transition in the crystal and thermalization is greatly assisted. Under such conditions, ν_1 does not have to be close to ν_2.

For reasonable rotational speeds, using likely materials, operation at liquid helium temperatures would be required. The size of sample required for maser action is larger in this type of maser than in the static sample type because only a fraction [=(angular width of resonance)/π] of the crystallites contribute to amplification at a given time. This fraction is of the order of 10^{-2} for sodium plutonyl acetate and ν_2 corresponding to maximum g.

In principle, the anisotropic-g maser has some advantages over a three-level continuous maser. The regenerative amplifying bandwidth, which is just the cavity bandwidth, can be made considerably larger than the resonance line width. The power required from the local oscillator for inversion is determined by the resonance line width and is therefore independent of the

[29] B. Bleaney, "Hyperfine structure in paramagnetic salts and nuclear alignment," *Phil. Mag.*, vol. 42, pp. 441–458; May, 1951.

[30] An alternative mechanism is to fix the crystal in the cavity and rotate a magnetic field of constant amplitude about it by means of suitably phased currents in a coil system.

bandwidth. The local oscillator frequency may be a factor of two or three lower than the signal frequency. Finally, the linear power output is higher because of the larger number of spins contributing to amplification in a given time.

A simple, continuous mechanical microwave generator should be possible using the principle of nonadiabatic field reversal. Paramagnetic material which has spent enough time in a magnetic field to acquire a positive magnetization is transported from that field into a reversed field through a magnet configuration of the general form shown in Fig. 6(a). The electrons experience a time-varying field of the form shown in Fig. 6(b) such as to produce state inversion. The material then passes into a microwave cavity situated in a uniform magnetic field of suitable strength where stimulated emission takes place and microwave oscillation is sustained. On emerging from the cavity the populations of the two states are equal and before the next inverting passage a normal distribution must be attained. One possible means of transport is a disk on the circumference of which the material is mounted so as to pass through the system of fields and the cavity just described. Although the time of transit between the inversion point and the cavity must be much shorter than T_1, the factor likely to determine the minimum rotational speed is the condition for nonadiabatic field reversal, (3). A rate of change of field of the order of 10^7 oersted/sec is required for a line of width 0.1 oersted. This would entail a 6-inch-diameter disk spinning at 4000 rpm through a field gradient, over the range $+1$ to -1 oersted, of 3000 oersted per cm.

Since the minimum rate of change of field is proportional to the square of the line width, materials having inhomogeneously broadened lines may prove most suitable in this application. An interesting property of this device is its ability so convert mechanical energy directly into microwave power with a theoretical efficiency of 50 per cent—the wasted energy going into the "cold" bath, via the lattice, during the preparation of the positive magnetization. The upper frequency limit is determined only by the magnetic field strength available at the cavity and might well extend into the one millimeter region, especially if high g-value materials can be used.

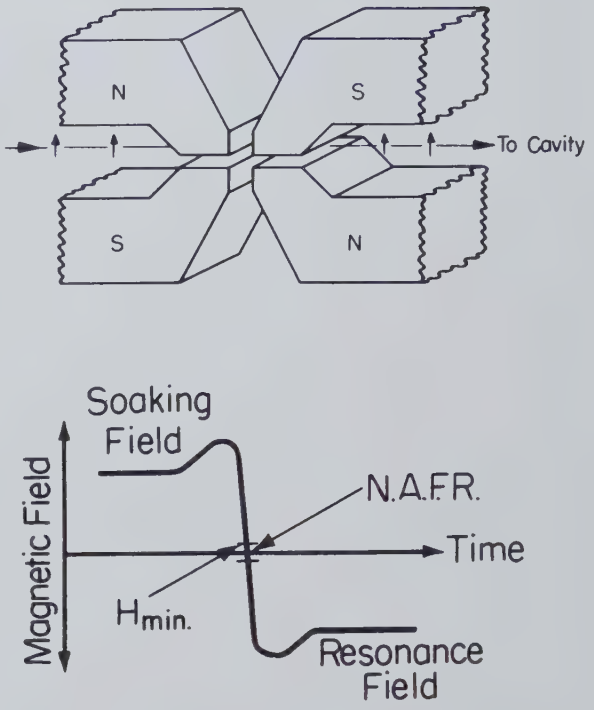

Fig. 6—Schematic magnet configuration (a) and variation of magnetic field as a function of time (b) for continuous state inversion by nonadiabatic field reversal.

Other things being equal, the power output from such a device increases with frequency, and for the disk mentioned above, with $N_2 - N_1 = 10^{17}$ per cm of circumference, would be about 20 milliwatts at a wavelength of 3 mm.

Conclusion

Several two-level, solid-state masers are feasible with presently available techniques and materials. A promising application appears to be as low noise amplifiers for radioastronomy and microwave radiometry in which case super-regenerative operation is to be preferred. In principle, a continuous two-level maser having some advantages over the three-level maser is possible using anisotropic materials. Masers are likely to be of use as generators in the millimeter region and even at shorter wavelengths where pulsed fields and intermittent operation are acceptable.

A Microwave Ferrite Frequency Separator*

HAROLD RAPAPORT†

Summary—When multiple filter groups are interconnected for operation out of a single source, interaction effects between filters can occur. Frequently, unless special precautions are taken, the filters may interact to such an extent that severe deterioration in performance may result. Introduction of the gyrator by Tellegen and the subsequent microwave realization of the circulator by Hogan, Rowen, and others provide new possibilities for design of channel-branching circuits and frequency-spectrum partition arrays.

The nature of the frequency separation problem is reviewed, and the application of the ferrite circulator to effect channel branching is considered in detail. Several specific multichannel systems comprising various circulator filter and one-way line filter arrays are presented and their relative merits examined.

A 4-port (3-channel) experimental prototype separator system consisting of a Faraday rotation type of circulator and maximally flat band-pass waveguide filters is described. A quantitative theory of operation of the prototype is developed. Experimental data and performance curves are given. These data show close agreement with results predicted by the theory.

General Considerations in Applying Frequency Partition Filters

Nature of The Frequency Separation Problem

IT is well known that when multiple filter groups are interconnected for operation out of a single source, interaction effects will occur between the individual filters.[1] In general, unless special precautions are taken, the filters may interfere with each other to such an extent that severe deterioration in performance throughout the entire frequency region of interest may result.

In the past, various techniques have been evolved in efforts to eliminate or at least minimize filter interaction. The general approach to the solution of the interaction problem lies in the design and synthesis of complementary pairs of filters, by techniques based on the methods developed by Zobel,[2] Norton,[3] and Bode.[4] In the low-frequency region, where line lengths are nonexistent and lumped elements are available, these techniques offer a reasonable solution to most "channel-branching" problems, provided the required number of channels is not too large. However, as the frequency is increased and the transmission-line nature of the problem must be considered, the utility of these techniques is substantially diminished.

* Manuscript received by the PGMTT, June 17, 1957. The work reported here was supported by the Electronic Warfare Laboratory, Rome Air Dev. Ctr. Contract No. AF-30(602)-981, and was carried out at the Microwave Research Institute, Polytechnic Institute of Brooklyn, when the author was a member of the staff.

† Defense Electronics Products, RCA, New York, N. Y.

[1] E. A. Guillemin, "Communication Networks," John Wiley & Sons, Inc., New York, N. Y., vol. 2, pp. 356–375; 1935.

[2] O. J. Zobel, "Distortion correction in electrical circuits with constant resistance recurrent networks," *Bell Sys. Tech. J.*, vol. 7, pp. 438–534; July, 1928.

[3] E. L. Norton, "Constant Resistance Networks with Applications to Filter Groups, Bell Sys. Monograph B-991; 1937.

[4] H. W. Bode, "A Method of Impedance Correction," *Bell Sys. Tech. J.*, vol. 9, pp. 794–835; October, 1930.

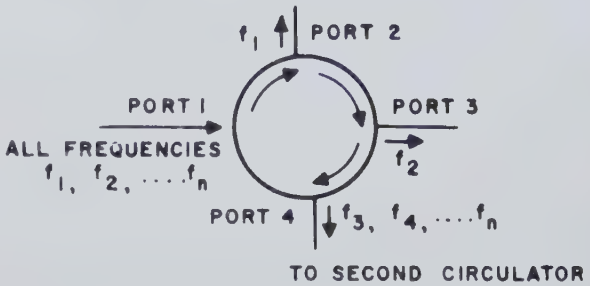

Fig. 1—Diagrammatic representation of frequency separation by means of a circulator

An investigation into the general properties of gyrator networks at the Microwave Research Institute by Rudner[5] and Carlin[6] indicated the potential application of the circulator principle to frequency separation problems. Consider the idealized 4-port circulator configuration as represented in Fig. 1.

Recalling the basic defining characteristic of the circulator; all energy incident on port 1 will be coupled to port 2, all energy incident on port 2 will couple to 3, energy into 3 will couple to 4, and energy into 4 will couple to 1—for the port designations used in the figure. In the ideal case, no reverse coupling or cross-coupling will exist. If, for the present, ideal behavior is assumed, the application of the circulator to the frequency separation problem is immediately apparent. As indicated in the figure, if a number of frequencies $f_1, f_2, \cdots, f_n$ are considered incident on port 1, they will all be transmitted to port 2 by virtue of the circulator action described above. Consider a filter located at port 2, with a frequency characteristic such that only f_1 (or a small band about f_1) will be passed.

It is clear that f_1 will be removed at port 2, but all other frequencies will be reflected and will proceed to port 3. If a second filter permitting passage only of f_2 is located at port 3, then only f_2 will be removed while $f_3, f_4, \cdots, f_n$ will be reflected to port 4. If provision is made at port 4 for the transmission of all of the remaining frequencies, they may be passed on to a second circulator in which further separation can be accomplished. Other arrangements of circulators and filters may be used, and several special cases will be considered later.

Quantitative Aspect

Some of the fundamental quantitative relationships concerning the operation of a 4-port circulator filter fre-

[5] B. Steinman, "Analysis of Some Microwave Ferrite Devices," Microwave Res. Inst., Polytech. Inst. of Brooklyn, Rep. R-367-53, PIB-301; February, 1954.

[6] H. J. Carlin, "Theory and Applications of Gyrator Networks," Microwave Res. Inst., Polytech. Inst. of Brooklyn, Final Rep. R-355-53, PIB-289; March, 1954.

quency separator will be developed. The scattering formulation of the network problem[7,8] will be used. Port 1 of the circulator is taken as input.

In terms of the voltage scattering parameters, the network equations for a 4-port are

$$\left.\begin{aligned} v_{r1} &= S_{11}v_{i1} + S_{12}v_{i2} + S_{13}v_{i3} + S_{14}v_{i4} \\ v_{r2} &= S_{21}v_{i1} + S_{22}v_{i2} + S_{23}v_{i3} + S_{24}v_{i4} \\ v_{r3} &= S_{31}v_{i1} + S_{32}v_{i2} + S_{33}v_{i3} + S_{34}v_{i4} \\ v_{r4} &= S_{41}v_{i1} + S_{42}v_{i2} + S_{43}v_{i3} + S_{44}v_{i4} \end{aligned}\right\}. \tag{1}$$

in which the v_{rm} represent the reflected voltages (energy flow polarized *out* of the network), the v_{in} represent the incident voltages (energy flow polarized *into* the network), and the S_{mn} are the complex voltage transfer coefficients of the scattering matrix (reflection coefficients if $m=n$). The S_{mn} have the form, $S_{mn}=|S_{mn}|e^{j\theta mn}$.

If structures defined by input reflection coefficients K_2, K_3, and K_4 terminate circulator ports 2, 3, and 4, respectively, then

$$\left.\begin{aligned} v_{i2} &= K_2 v_{r2} \\ v_{i3} &= K_3 v_{r3} \\ v_{i4} &= K_4 v_{r4} \end{aligned}\right\}. \tag{2}$$

Substituting the set of (2) into (1) and solving for the voltage ratios v_{rm}/v_{i1}

$$\frac{v_{r1}}{v_{i1}} = \frac{\begin{vmatrix} -S_{11} & S_{12}K_2 & S_{13}K_3 & S_{14}K_4 \\ -S_{21} & (S_{22}K_2-1) & S_{23}K_3 & S_{24}K_4 \\ -S_{31} & S_{32}K_2 & (S_{33}K_3-1) & S_{34}K_4 \\ -S_{41} & S_{42}K_2 & S_{43}K_3 & (S_{44}K_4-1) \end{vmatrix}}{|D|} \tag{3}$$

$$\frac{v_{r2}}{v_{i1}} = \frac{\begin{vmatrix} -1 & -S_{11} & S_{13}K_3 & S_{14}K_4 \\ 0 & -S_{21} & S_{23}K_3 & S_{24}K_4 \\ 0 & -S_{31} & (S_{33}K_3-1) & S_{34}K_4 \\ 0 & -S_{41} & S_{43}K_3 & (S_{44}K_4-1) \end{vmatrix}}{|D|}, \tag{4}$$

$$\frac{v_{r3}}{v_{i1}} = \frac{\begin{vmatrix} -1 & S_{12}K_2 & -S_{11} & S_{14}K_4 \\ 0 & (S_{22}K_2-1) & -S_{21} & S_{24}K_4 \\ 0 & S_{32}K_2 & -S_{31} & S_{34}K_4 \\ 0 & S_{42}K_2 & -S_{41} & (S_{44}K_4-1) \end{vmatrix}}{|D|}, \tag{5}$$

$$\frac{v_{r4}}{v_{i1}} = \frac{\begin{vmatrix} -1 & S_{12}K_2 & S_{13}K_3 & -S_{11} \\ 0 & (S_{22}K_2-1) & S_{23}K_3 & -S_{21} \\ 0 & S_{32}K_2 & (S_{33}K_3-1) & -S_{31} \\ 0 & S_{42}K_2 & S_{43}K_3 & -S_{41} \end{vmatrix}}{|D|}, \tag{6}$$

where

$$|D| = \begin{vmatrix} -1 & S_{12}K_2 & S_{13}K_3 & S_{14}K_4 \\ 0 & (S_{22}K_2-1) & S_{23}K_3 & S_{24}K_4 \\ 0 & S_{32}K_2 & (S_{33}K_3-1) & S_{34}K_4 \\ 0 & S_{42}K_2 & S_{43}K_3 & (S_{44}K_4-1) \end{vmatrix}. \tag{7}$$

The voltage ratios of (4)–(6) may be defined as circulator coefficients $C_{m1}=V_{rm}/v_{i1}$, associated with the loaded circulator and referred to the voltage incident on the input terminals of the terminating structures.

In the case under discussion, since terminations associated with the various ports are filters (2-port structures), the quantities of primary interest are the insertion loss from port 1 to the *output terminals* of the mth filter and, in certain instances, the input vswr measured at port 1. Since each filter is a 2-port structure, the scattering equations for the mth filter will have the form

$$\left.\begin{aligned} v_{r1}' &= [T_{11}]_m v_{i1}' + [T_{12}]_m v_{12}' \\ v_{r2}' &= [T_{21}]_m v_{i1}' + [T_{22}]_m v_{12}' \end{aligned}\right\} \tag{8}$$

in which the numerical subscripts 1 and 2 define the input and output terminals respectively of the *terminating structure*, and $[T]_m$'s are the scattering coefficients of the filter.

Filter performance is generally defined in terms of the insertion loss (or gain) of the filter when operating between matched terminations. Under these conditions, the value of v_{12}' is zero, so that

$$v_{r1}' = [T_{11}]_m v_{i1}' \tag{9a}$$

$$v_{r2}' = [T_{21}]_m v_{i1}' \tag{9b}$$

Now, from (9a) the coefficient T_{11} is seen to be the input reflection coefficient of the terminating structure associated with the mth circulator port. Further, the voltage *incident on* the input terminals of the mth filter is that *reflected out of* the circulator. Thus,

$$K_m = [T_{11}]_m \tag{10a}$$

$$v_{rm} = v_{i1}' \tag{10b}$$

where the v_{i1}' is understood to refer to the mth port terminating structure as implied by K and v_{rm}.

The voltage measured at the filter output terminals may now be expressed in terms of the input voltage at port 1 and the circulator filter coefficients. Using the C_{m1} of (4), (5), and (6), and combining (9b) and (10b)

$$v_{r2}' = [T_{21}]_m v_{rm} = [T_{21}]_m C_{m1} v_{i1}. \tag{11}$$

Assuming the same normalizing impedance for both port 1 and the termination of the mth filter, the insertion loss from port 1 to the mth output terminals may be written as

$$L_{m1} = 10 \log \left| \frac{v_{i1}}{v_{r2}'} \right|^2 \text{ db}. \tag{12}$$

[7] H. J. Carlin, "An Introduction to the Use of the Scattering Matrix in Network Theory," Microwave Res. Inst., Polytech. Inst. of Brooklyn, Rep. R-366-54, PIB-300; June, 1954.

[8] G. L. Ragan, "Microwave Transmission Circuit," Mass. Inst. Tech. Rad. Lab. Ser., McGraw-Hill Book Co., Inc., New York, N. Y., vol. 9, pp. 551–554; 1948.

Using (11) in (12)

$$L_{m1} = 10 \log \frac{1}{|T_{21}|_m^2 |C_{m1}|^2} \text{ db} \tag{13}$$

where the C_{m1} are obtained from (4)–(6) using the K_m as defined by (10a). Since the insertion loss of the mth filter alone, L_{Fm}, is by definition

$$L_{Fm} = 10 \log \frac{1}{|T_{21}|_m^2} \text{ db.} \tag{14}$$

Eq. (13) may be written as

$$\begin{aligned} L_{m1} &= 10 \log \frac{1}{|T_{21}|_m^2} + 10 \log \frac{1}{|C_{m1}|^2} \text{ db.} \\ &= L_{Fm} + L_{cm} \text{ db,} \end{aligned} \tag{15}$$

where the L_{cm} is understood to refer to port 1 as input.

Expressing the total loss in the form of (15) shows that the insertion loss for the interconnected circulator filter combination is a simple sum, and that the entire problem of interaction may be discussed in terms of the *variation* of the function L_{cm}.

The input vswr as measured at port 1 is quickly determined since by definition

$$\text{vswr} = \frac{1 + |K|}{1 - |K|}, \qquad K = \frac{v_{r1}}{v_{i1}}. \tag{16}$$

To illustrate the use of the equations developed above, the case of a 4-port circulator-filter combination will be discussed. The circulator is assumed to be matched but lossy, and to couple in a 1→2→3→4→1 pattern.

As may be shown,[5,6] the voltage scattering matrix for a perfect circulator of the Faraday rotation type with a 1→2→3→4→1 coupling pattern is

$$S^v = e^{j\theta} \begin{vmatrix} 0 & 0 & 0 & -1 \\ 1 & 0 & 0 & 0 \\ 0 & 1 & 0 & 0 \\ 0 & 0 & 1 & 0 \end{vmatrix}, \qquad \theta = \alpha + j\beta. \tag{17}$$

Using the S values as defined by (17) in (4)–(6) and taking the absolute values of the resulting voltage ratios

$$\left|\frac{v_{r1}}{v_{i1}}\right| = |K_2||K_3||K_4| e^{4\alpha}, \tag{18}$$

$$C_{21} = \left|\frac{v_{r2}}{v_{i1}}\right| = e^{\alpha} \tag{19}$$

$$C_{31} = \left|\frac{v_{r3}}{v_{i1}}\right| = |K_2| e^{2\alpha}, \tag{20}$$

$$C_{41} = \left|\frac{v_{r4}}{v_{i1}}\right| = |K_2||K_3| e^{3\alpha}. \tag{21}$$

These results show that the energy input into port 1 is not equally available to all terminations. Clearly, from (19) all energy except that dissipated in the ferrite is available to the structure terminating port 2. But (20) shows that energy at port 3 will depend on the input reflection factor of the port 2 structure. In the same way, (21) indicates energy available at port 4 will be a function of the reflections of both the port 2 and the port 3 structures. However, it should be stressed that the energy availability *does not* depend on the *relative phases* of the reflections. Only the *magnitudes* of the filter reflection factors enter into the interaction.

Using (19)–(21) in (15), the loss quantities, L_{cm}, are seen to be

$$L_{c2} = 10 \log e^{2\alpha}, \tag{22}$$

$$L_{c3} = 10 \log \frac{1}{|K_2|^2} = 10 \log \frac{1}{|T_{11}|_2^2} + \log e^{4\alpha}, \tag{23}$$

$$\begin{aligned} L_{c4} &= 10 \log \frac{1}{|K_2|^2 |K_3|^2} \\ &= 10 \log \frac{1}{[T_{11}]_2^2} + 10 \log \frac{1}{[T_{11}]_3^2} 10 \log e^{6\alpha}. \end{aligned} \tag{24}$$

These results demonstrate that in the case of the perfect circulator, the *variation* in insertion loss as measured at the output terminals of a given filter will depend *only* on the magnitudes of the reflection coefficients of the filters *preceding* it in the circulator coupling pattern. For example, (22) indicates that *regardless* of the terminations on all *succeeding* ports, the *variation* in insertion loss will be zero. Thus, the total insertion loss, L_{21}, will equal the original filter loss characteristic, L_{F2}, plus the circulator dissipative loss.

Eqs. (23) and (24) indicate that if the interaction effects are to be further evaluated, magnitudes of the input reflection factors of the various filters must be specified. For any lossless 2-port structure it may be shown[7,8] that

$$|T_{11}|^2 = 1 - |T_{21}|^2 \tag{25}$$

so that if the filters are lossless, (23) and (24) become

$$L_{c3} = 10 \log \frac{1}{1 - [T_{21}]_2^2} + 10 \log e^{4\alpha}, \tag{26}$$

$$\begin{aligned} L_{c4} &= 10 \log \frac{1}{1 - [T_{21}]_2^2} + 10 \log \frac{1}{1 - [T_{21}]_3^2} \\ &\quad + 10 \log e^{6\alpha}. \end{aligned} \tag{27}$$

These equations allow calculation of the interaction effects from knowledge of the insertion loss characteristics of the filters (if lossless), rather than knowledge of the input vswr as required in (23) and (24).

At this point it is necessary to define explicitly either the $|K|$'s of (23) and (24) or, if lossless, the $|T_{21}|$'s of (26) and (27). For purposes of further discussion, the $|K|$'s will be assumed to be related in the following sense. When the frequency is such that the filter located at port 2 is in the pass band ($|K_2| = 0$), then the filters at

ports 3 and 4 will be assumed to be completely rejecting ($|K_3| = |K_4| = 1$). Similarly when $|K_3| = 0$, then $|K_2| = |K_4| = 1$. Finally when $|K_4| = 0$, then $|K_2| = |K_3| = 1$. This situation is characteristic of the design of most channel branching systems in that a given branching filter will present a high rejection to frequencies which lie in the pass bands of neighboring filters. Thus, for the 4-port 3-filter system being considered, under these restrictions (23) and (24) show that

$$L_{c3} = 10 \log \frac{1}{|K_2|^2} = 10 \log e^{4\alpha},$$

$$L_{c4} = 10 \log \frac{1}{|K_2|^2 |K_3|^2} = 10 \log e^{6\alpha}. \qquad (28)$$

Thus, in the *pass bands* of the various filters, no interaction effects will occur, and the total insertion loss to the filter output terminals will be that produced by the filter alone plus circulator dissipation.

The reflections at port 1 will be zero since some $|K_k| = 0$. Thus, the vswr measured at port 1 will be unity and the system will appear matched. It should also be observed that if a matched load is placed at one of the ports, say port 4, rather than a filter, the system will appear matched at *all frequencies*—not only in the pass bands. This property may be quite desirable in certain systems applications in which the mismatch seen by the generator is of concern.

The interaction effects in those frequency regions in which the $|K|$ restrictions given above no longer apply cannot be summarized so simply. As (26) and (27) indicate, the extent of the interaction will depend on the explicit form and relationship of the filter functions considered. The interaction effects in these "crossover frequency" regions can be analytically treated but space does not permit further consideration of these effects here.

Experimental Prototype Frequency Separator

In order to experimentally verify the preceding analysis, an experimental prototype separator was designed and constructed in the 9.0 kmc frequency region. The separator was of the Faraday rotation type described by Hogan[9] and others.[10] The filters were bandpass with a maximally-flat characteristic and realized in rectangular waveguide. The filters were 100 mc wide at the 3 db points and had center frequencies of 8800, 8900, and 9000 mc. These elements of the prototype separator are shown in Fig. 2.

Briefly, the experimental characteristics pertinent to the present discussion are that the circulator exhibited a loss of 0.6 db and the filters a loss of 0.8 db in their pass bands.

[9] C. L. Hogan, "The ferromagnetic effect at microwave frequencies and its applications-the microwave gyrator," *Bell Sys. Tech. J.*, vol. 31; January, 1952.

[10] J. H. Rowen," "Ferrites in microwave applications," *Bell Sys. Tech. J.*, vol. 32; November, 1953.

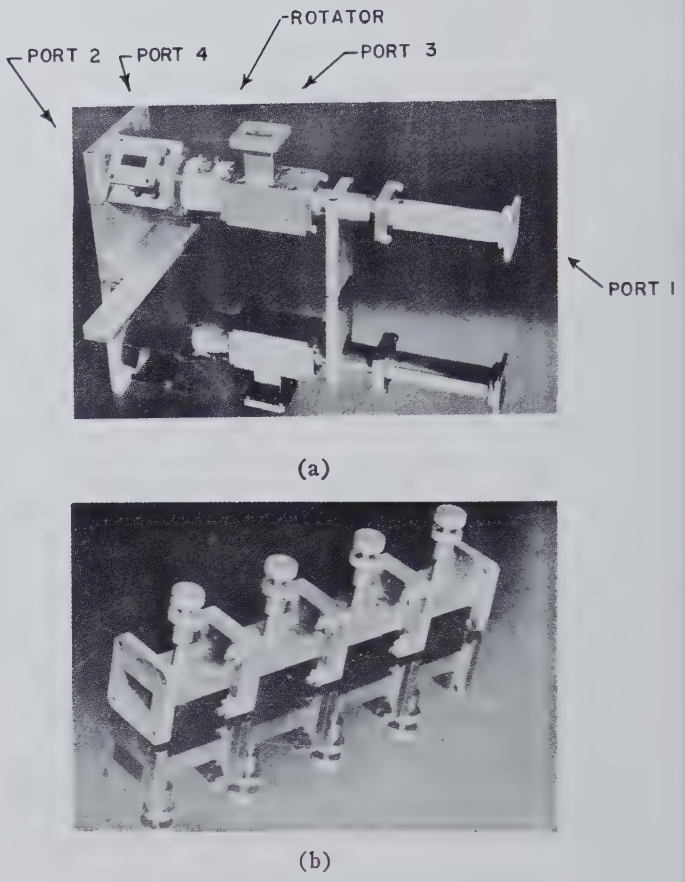

Fig. 2—Frequency separator components. (a) Circulator, (b) filter.

The characteristics of the associated filters alone are shown in Fig. 3. Here the experimentally measured insertion loss values have been superimposed on a frequency scale to show the crossover points. The midband losses are 0.8 db. It is seen that the filters are essentially identical.

In Fig. 4 the insertion losses to the outputs of these same filters, now located at circulator ports 2, 3, and 4 respectively, are shown again superimposed. This port-filter arrangement was chosen so that the increase in insertion-loss level produced by multiple transits of the ferrite would appear as "step-wise increasing" with increasing frequency in the data display. This increase in level was exhibited by the $e^{m\alpha}$ of the preceding analysis. Note that the leading edge of the insertion loss curves of the filters located at ports 3 and 4 are distorted.

This is an example of the interaction effect previously mentioned. The experimental results and analytical predictions agree fairly well for these distortions.

Shown in Table I is a tabulation of the pass band losses predicted by (15) and those measured experimentally. As the table shows, the agreement here is quite good.

Some General Frequency Partition Systems

The present model of the prototype frequency separator has been shown to function adequately in a 3-channel branching application, and the experimental results in-

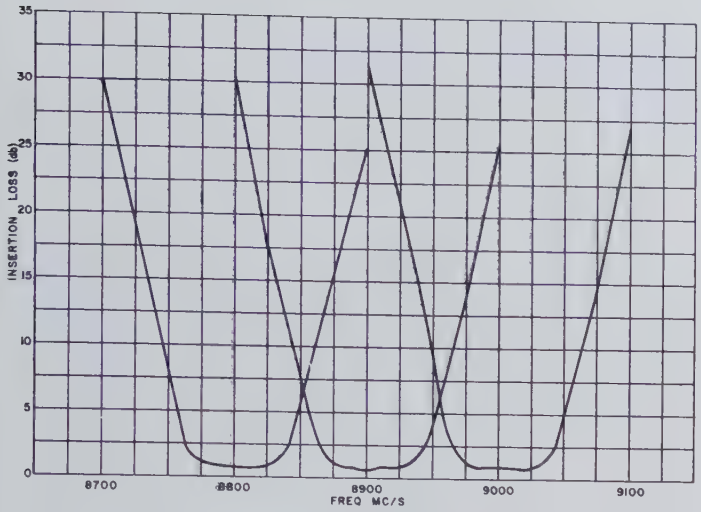

Fig. 3—Insertion loss of associated filters.

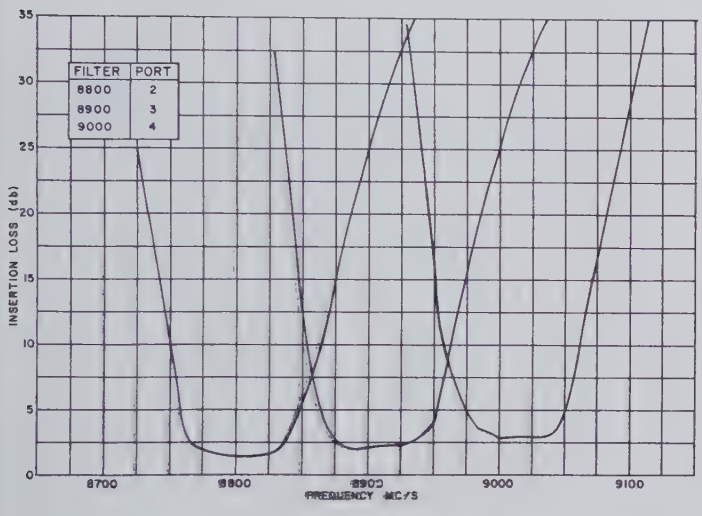

Fig. 4—Prototype frequency separator experimental results.

TABLE I

FREQUENCY SEPARATOR PASS BAND LOSSES

Port	L_{Fm}db	L_{cm}db	L_{m1}(pred.) db	L_{m1}(meas.) db
2	0.8	0.6	1.4	1.5–1.6
3	0.8	1.2	2.0	1.9–2.0
4	0.8	1.8	2.6	2.7–2.8
		$L_{m1}=L_{Fm}+L_{cm}$		

dicate the validity of the approximate theory developed However, it should not be construed that this *type* of circulator-filter arrangement is unique and must necessarily be used for channel-branching. The predictive aspects of the theory developed above should be capable of extension to other types of possible circulator-filter channel-branching arrays. As an illustration, the pass-band behavior of three possible arrays for a p-channel system will be considered. For simplicity any interconnecting lines or filters will be considered perfect, *i.e.* dissipationless and reflectionless in the pass band regions. The three systems are shown schematically in Fig. 5.

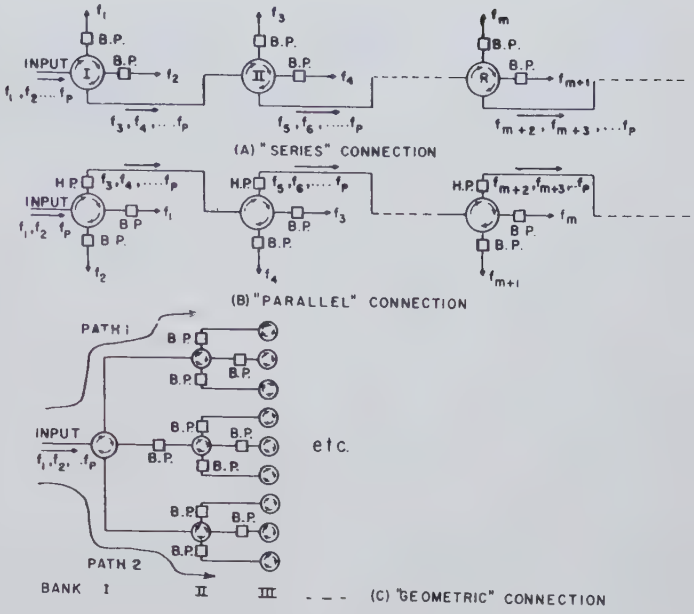

Fig. 5—Three possible branching arrays for frequency separation.

"Series" Connection

The first branching array, shown in Fig. 5(a), is similar to the system used in the prototype separator in that separation is realized by a set of sequentially arranged band-pass filters. Port 1 of circulator I is taken as input, and the arrows indicate the path of energy transmission between preferred ports. This array may be considered to be a "series" connection in the sense that prior to arrival at the proper filter, any energy input into the system must traverse *all* preceding circulators and be available to *all* preceding filters.

"Parallel" Connection

The branching array shown in Fig. 5(b) may be viewed as a "parallel" connection in that it is not necessary for input energy to traverse each circulator in its entirety before arrival at the proper filter.

It should be clear that the particular filter configuration used, *i.e.* high-pass and band-pass, is not the only possible arrangement for this type of service.

"Geometric" Connection

From its similarity to a geometric progression, the third branching array shown in Fig. 5(c) may be viewed as a "geometric" interconnection. The circulators may be considered to be grouped into a series of "banks".

Space does not permit a complete exposition of the performance of each of these systems. The pertinent characteristics are summarized in Table II. The performance can be compared in terms of the circulator loss function $U_{m1}A$; where A is the dissipative loss in the ferrite and U_{m1} is as shown in the table.

It is to be noted that while the required number of circulators is independent of the type of interconnection, the table shows that the ferrite loss function, U_{m1}, is *extremely sensitive* to the form of the array. From the

TABLE II

PASS BAND LOSSES OF THREE FREQUENCY SEPARATOR SYSTEMS

	Series	Parallel	Geometric
U_{m1}	$\frac{3m-2}{2}$ m even $\frac{3m-1}{2}$ m odd	$\frac{m+4}{2}$ m even $\frac{m+3}{2}$ m odd	b to $3b$ $b+1$ to $3(b+1)$
C_p	$\frac{p}{2}$ p even $\frac{p-1}{2}$ p odd	$\frac{p}{2}$ p even $\frac{p-1}{2}$ p odd	$\frac{p}{2}$ p even $\frac{p-1}{2}$ p odd
		$L_{m1}=L_{Fm}+L_{cm}$ where $L_{cm}=U_{m1}A$	

point of view of minimum ferrite loss (especially for large p), the geometric type of branching array is superior.

As may be seen from the table, for any given p the required number of circulators, C_p, is always the same, *i.e. independent* of the type of connection. This result may be viewed as a practical expression of the following gyrator network theorem recently established by H. J. Carlin of the Microwave Research Institute.

Theorem: The minimum number of gyrators necessary for the realization of an n-port (n-terminal-pair) circulator is given by

$$G_m = \begin{cases} \frac{1}{2}(n-1) & n \text{ odd}, \\ \frac{1}{2}(n-2) & n \text{ even}, \end{cases}$$

where G_m is the minimum number of necessary gyrators and n is the number of terminal pairs. It may be further stated that the minimum number realization can always be effected for any n by the interconnection of only 3-port and 4-port circulators, each type of which requires only one gyrator.

From the point of view of the theorem, each of the three systems previously described is equivalent to an n-port "minimum-number" type of interconnection in which $n=p+1$. Thus, since each circulator provides one gyrator, it immediately follows from the theorem that the minimum number of necessary circulators will be as shown below.

$$C_p = \begin{cases} \left(\frac{n-1}{2}\right) = \frac{p}{2} & n \text{ odd}, p \text{ even}, \\ \left(\frac{n-2}{2}\right) = \frac{p-1}{2} & n \text{ even}, p \text{ odd}. \end{cases}$$

The results for C_p tabulated in Table II represent special cases of this general result and there is no other possible connection which can use a smaller number of components.

ACKNOWLEDGMENT

The author wishes to acknowledge the helpful advice of Dr. H. J. Carlin of the Microwave Research Institute, and also the efforts of Carl Bollinger in making many of the measurements.

Ferrite-Loaded, Circularly Polarized Microwave Cavity Filters*

W. L. WHIRRY† AND C. E. NELSON†

Summary—**Circularly polarized cavities have made possible a group of compact, high-Q, microwave waveguide filters having useful directional properties. When these cavity filters are ferrite loaded, frequency sensitive circulators result and magnetic tuning becomes possible. This paper presents several new three- and four-port ferrite-loaded filters, some with 3-db waveguide couplers, which can be used as tunable band-pass filters, tunable band-rejection filters, or as passive, selective duplexers. As duplexers, they can be operated at a fixed frequency or can be magnetically tuned over a one to five per cent frequency range at X band depending upon the allowable loss. Experimental loss, bandwidth, isolation, and tuning data are presented. Temperature stability and power handling capacity are also discussed.**

Introduction

CAVITIES utilizing degenerate modes phased to produce circularly polarized microwave magnetic fields at some point in the cavity have been used extensively to measure ferrite permeability parameters. The circularly polarized cavity fields have been excited in several ways. A quarter-wave plate in a circular or square waveguide can be used to produce circularly polarized waveguide fields which are then coupled through a small aperture to the cavity.[1–3] Two apertures, which are 90 electrical degrees apart in the cavity have been used to excite orthogonal linear modes; by exciting them 90° apart in time phase circular polarization results. A single aperture has also been used to couple into a degenerate cavity with a ferrite placed in a region where a circularly polarized magnetic field can exist.[4–6] When a magnetic field is applied to the ferrite, the cavity degeneracy is removed in the sense that the resonant frequencies for positive and negative circular polarization separate. The single aperture thus sees two resonant frequencies, and at each of these resonances, couples primarily to only one sense of polarization. For some applications such as the tunable, band-pass filter, only one resonant frequency is desired, and a multiport filter which can distinguish between directions of field rotation is desirable.

In most of these experiments for the determination of ferrite properties, the desire has been to make the polarization at the ferrite as nearly circular as possible and to keep the ferrite samples as small as possible to increase the accuracy of the perturbation calculations. The coupling apertures used were generally much smaller than required for microwave filter applications.

Circularly polarized cavities have recently been incorporated as microwave circuit elements, and several compact, nearly reflectionless microwave filters have resulted.[7–9] The use of circular polarization in effect replaces two cavities and associated connecting plumbing with a single cavity. (Two previous filters requiring two cavities are described by Lewis and Tillotson[10] and Bowers and Curtis.[11] Another reflectionless filter requiring only one cavity is described by Klopfenstein and Epstein.[12]) In general, these filters have used coupling from two waveguide field components—for example, H_x and H_z—through a single aperture. This symmetrical type of coupling makes it possible to essentially eliminate reflections in the waveguide over a wide band of frequencies including the cavity resonant frequency. This property greatly simplifies cascading of the cavity filters. Band-pass and band-elimination filters have been built using these cavities, but perhaps the most interesting filter is a four-port device which can be used as a reflectionless, channel-separation filter.

Ferrite loading has been applied to these filters[13] with the object of producing tunable, nonreciprocal microwave elements while preserving the desirable features of the low-loss cavity. (Ferrite tuning of linear cavity

* Manuscript received by the PGMTT, June 24, 1957.

† Res. Labs., Hughes Aircraft Co., Culver City, Calif.

[1] J. O. Artman and P. E. Tannenwald, "Measurement of permeability tensor in ferrites," *Phys. Rev.*, vol. 91, pp. 1014–1015; August 15, 1952.
"Measurement of susceptibility tensor in ferrites," *J. Appl. Phys.*, vol. 26, pp. 1124–1132; September, 1955.

[2] E. G. Spencer, R. C. LeCraw, and F. Reggia, "Measurement of microwave dielectric constants and tensor permeabilities of ferrite spheres," PROC. IRE, vol. 44, pp. 790–800; June, 1956.

[3] M. Tinkham and M. W. P. Strandberg, "The excitation of circular polarization in microwave cavities," PROC. IRE, vol. 43, pp. 734–738; June, 1955.

[4] A. D. Berk and B. Lax, "Cavities with complex media," 1953 IRE CONVENTION RECORD, pt. 10, pp. 65–69.

[5] B. Lax and A. D. Berk, "Resonance in cavities with complex media," 1953 IRE CONVENTION RECORD, pt. 10, pp. 70–74.

[6] R. C. LeCraw and E. G. Spencer, "Tensor permeabilities of ferrites below magnetic saturation," 1956 IRE CONVENTION RECORD, pt. 5, pp. 66–74.

[7] S. B. Cohn and F. S. Coale, "Directional channel-separation filters," PROC. IRE, vol. 44, pp. 1018–1024; August, 1956; also, 1956 IRE CONVENTION RECORD, pt. 5, pp. 106–112.

[8] C. E. Nelson, "Circularly polarized microwave cavity filters," IRE TRANS., vol. MTT-5, pp. 136–147; April, 1957.

[9] C. E. Nelson and W. L. Whirry, "Development of circularly polarized microwave cavity fiters," 1957 NATIONAL IRE CONVENTION RECORD, pt. 1, pp. 191–196.

[10] W. D. Lewis and L. C. Tillotson, "A nonreflecting branching filter for microwaves," *Bell Sys. Tech. J.*, vol. 27, pp. 83–95; January, 1948.

[11] E. O. Bowers and C. W. Curtis, "A resonant cavity frequency duplexer," 1956 IRE CONVENTION RECORD, pt. 5, pp. 113–118.

[12] R. W. Klopfenstein and J. Epstein, "The polarguide—a constant resistance waveguide filter," PROC. IRE, vol. 44, pp. 210–218; February, 1956.

[13] C. E. Nelson, "Ferrite-Tunable microwave cavities and the introduction of a new reflectionless, tunable microwave filter," PROC. IRE, vol. 44, pp. 1449–1455; October, 1956.

mode filters is described.[14–16] One can show from perturbation theory that for a given mode, a symmetric ferrite placed at a point where the rf magnetic field is circularly polarized should give a greater total magnetic tuning range for a given allowable loss than a ferrite placed at a point of linearly polarized rf magnetic field. The above presumes a ferrite with small zero field magnetic loss which will allow the total tuning range to include zero field.

Ferrite-loaded band-elimination filters have been constructed using the TE_{111} and the TM_{110} circular cylindrical modes. Ferrite-loaded four-port filters have been described using the TE_{112} and TM_{110} modes with coupling to the end of the cylindrical cavity. These devices can be used as magnetically-tunable band-pass filters or as selective, passive duplexers.

The TE_{112} mode, with coupling apertures at each end of the circular cylinder, requires that the ferrite be supported in the center of the cavity, making the application of the dc magnetic field from a permanent magnet difficult. The TM_{110} mode is desirable for use with ferrites because a long rod can be located in the circularly polarized magnetic field and yet remain magnetically small in a perturbation sense.[6] For ease of ferrite support and to allow the magnetic air gap to be as small as possible, it is convenient to have both ends of the cylindrical cavity free. This paper describes several four-port filters which meet these requirements. Three-port variations are then described; these, when ferrite loaded, will perform many of the useful functions of the four-port filters.

Four-Port Filters Using Directional Couplers

By using two 3-db directional waveguide couplers to satisfy the power splitting and 90° phase shift requirements for exciting circular polarization with two apertures, a group of compact, four-port, single-cavity, reflectionless filters has been developed which are well suited to ferrite loading. One version is shown in Fig. 1(a): a degenerate TM_{110} circular cavity is coupled magnetically by four apertures to four rectangular waveguides. One 3-db side-wall coupler is used on each side, as shown. Apertures 1 and 3 couple to one TM_{110} cavity mode and apertures 2 and 4 couple to the orthogonal TM_{110} mode. The frequency sensitivity of the quarter-wave aperture-short distance could be eliminated by coupling to the end of the waveguides. Energy entering port A will be divided by the 3-db coupler. One half of the incident input energy reaches aperture 1 and the other half arrives at aperture 2, lagging that at aperture 1 by 90° in time. Thus, a counterclockwise rotating cavity mode tends to be excited. At or near resonance,

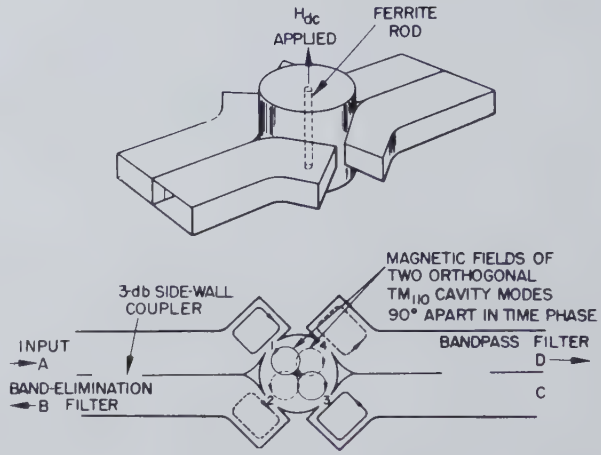

Fig. 1(a)—Four-port, circularly polarized filter using two 3-db couplers.

energy will be coupled out of apertures 3 and 4 and will be 90° out of time phase so that addition occurs in arm D and cancellation in arm C.

Consider the behavior of the cavity without the ferrite, or with the ferrite demagnetized. In terms of linear modes; two orthogonal cavity modes which have equal amplitudes but are 90° out of time phase are excited by apertures 1 and 2. There are band-pass filters between apertures 1 and 3 and between 2 and 4. At the cavity resonant frequency (each mode will be resonant at the same frequency), energy will be coupled out apertures 3 and 4 and will be of the proper phase so that addition occurs in arm D and cancellation occurs in arm C. Ideally, energy reflected at apertures 1 and 2 and at the short circuits, both on and off resonance, will add in arm B and cancel in arm A. Therefore, there is a reflectionless, band-pass filter between ports A and D, and a band-elimination filter between ports A and B. The characteristics are, of course, reciprocal and symmetrical with respect to any port, in this case.

When a longitudinally magnetized ferrite rod is placed in the center of the cavity, the normal modes of the cavity become rotating field patterns with different resonant frequencies for positive and negative senses of rotation.[4] Energy entering port A will tend to couple into a clockwise rotating mode, which corresponds to positive circular polarization with resonant frequency f_+ for the direction of dc magnetic field shown. Energy entering port B will tend to excite negative circular polarization, resonant at f_-. At f_+, the filter is essentially a four-port circulator with energy circulating between ports in a clockwise direction. At f_-, energy circulates in a counterclockwise direction. A magnetically tunable band-pass cavity acts in series with legs A–D and B–C. Far from resonance, the device is no longer a circulator, and a waveguide path which will take high power exists between ports A and B and between ports C and D.

For an experimental model of this filter, curves of frequency shift due to the ferrite vs applied dc field are shown in Fig. 1(b) for three Ferramic R-1 rods of different sizes. The rods are slightly shorter than the length

[14] J. C. Cacheris and G. Jones, "Magnetic tuning of klystron cavities," Proc. IRE, vol. 43, p. 1017; August, 1955.
[15] G. R. Jones, J. C. Cacheris, and C. A. Morrison, "Magnetic tuning of resonant cavities and wide band frequency modulation of klystrons," Proc. IRE, vol. 44, pp. 1431–1438; October, 1956.
[16] C. E. Fay, "Ferrite-tuned resonant cavities," Proc. IRE, vol. 44, pp. 1446–1449; October, 1956.

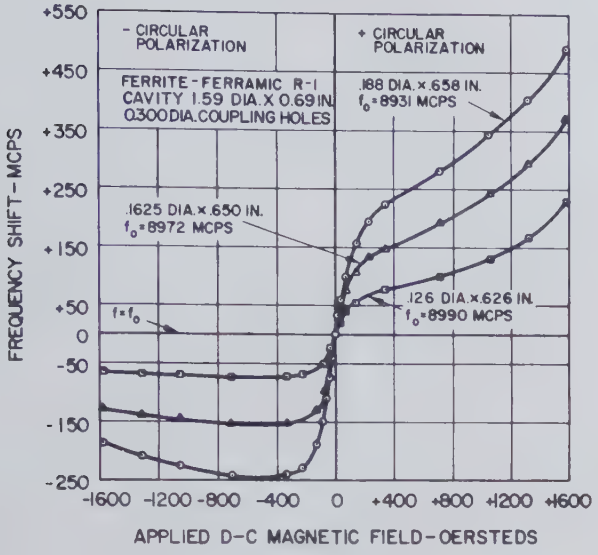

Fig. 1(b)—Resonant frequency, port A to port D, vs dc magnetic field.

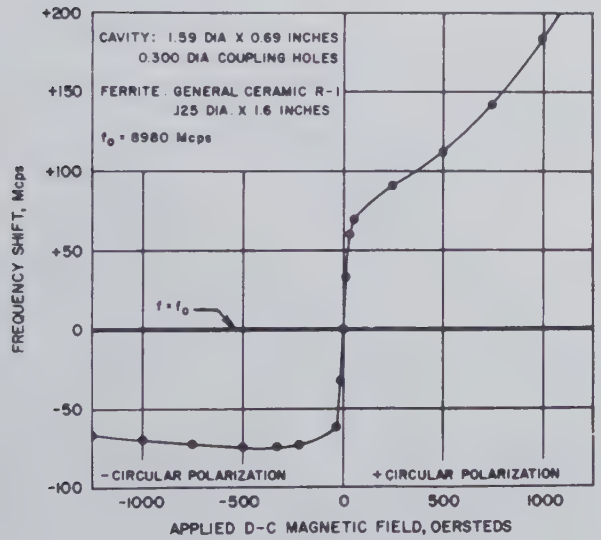

Fig. 1(c)—Resonant frequency, port A to port D, vs dc magnetic field.

of the cavity in each case. The curves have the general shape of the effective permeability curves for circular polarization. The way in which the frequency shift for the larger diameter rod is departing from a simple perturbation might be roughly seen by comparing the ratio of the frequency shifts due to the large and small ferrites at a given magnetic field, to the ratio of their volumes. At a field of -500 oersteds, the 0.188-inch-diameter rod gives nearly 50 per cent more frequency shift than would be predicted from the shift for the 0.126-inch-diameter rod and the increase in volume. At $+500$ oersteds, it gives approximately 30 per cent more. For positive fields greater than about 1300 oersteds, the larger rods give less frequency shift than would be expected. The different value of f_0 for each rod is due primarily to the zero field permeability of the ferrite. Because of the severe effect of ferromagnetic resonance

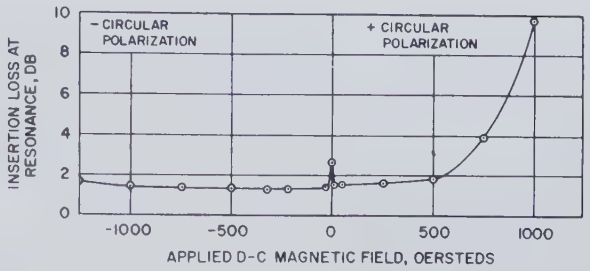

Fig. 1(d)—Insertion loss, port A to port D, vs dc magnetic field.

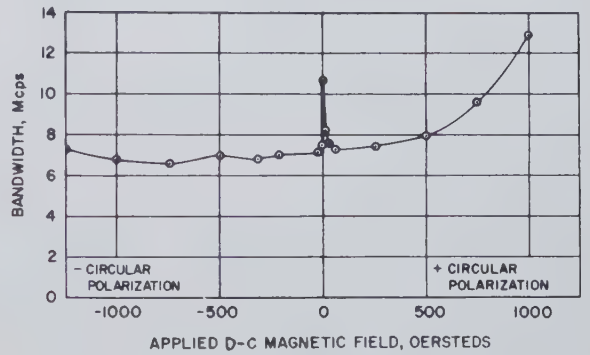

Fig. 1(e)—Bandwidth, port A to port D, vs dc magnetic field.

losses on the total cavity loss, it will be seen that the useful operating region of these cavities as tunable, band-pass filters is the region near and below saturation for both positive and negative circular polarization. Above saturation for negative circular polarization, the frequency shift moves back toward zero.

A ferrite rod which is longer than the cavity would be expected to give a more uniform dc field in the ferrite and more uniform circularly polarized rf fields. Fig. 1(c) shows the frequency shift curve for a $\frac{1}{8}$-inch diameter Ferramic R-1 rod which extends beyond each end of the cavity. The frequency shift at a given dc field is seen to be slightly larger than for the shorter R-1 rod, as expected.

Figs. 1(d) and 1(e) illustrate the insertion loss at resonance and bandwidth of the tunable band-pass filter between ports A and D for the long ferrite rod. The higher loss and larger bandwidth at zero field are due to stray coupling and consequent loss in the unwanted sense of circular polarization, since both senses are resonant at the same frequency with the ferrite unmagnetized. The loss and bandwidth could undoubtedly be reduced by closer mechanical tolerances. When magnetized, the ferrite actually improves the performance of this filter. For larger negative fields than are shown in the curves, the insertion loss and bandwidth for negative circular polarization rise rapidly. This is presumably due to the component of positive circular polarization present off the cavity axis. For most applications, this effect is unimportant.

The insertion loss of the band-pass filter and the unloaded cavity Q, including ferrite losses, for a given fre-

quency shift are plotted in Fig. 1(f) for the three shorter ferrites. The empty cavity, without ferrite, has an unloaded Q of approximately 9000. Each window has a window-coupling factor, Q_w, of 3000 for coupling to a linear cavity mode or a Q_w of 6000 for coupling to a single rotating mode using a magnetized ferrite. When coupling to a rotating mode, the two windows on one side of the filter give a combined window Q of 3000. It can be seen that a tuning range of 175 mc can be obtained with an unloaded Q near 6000 using the smallest diameter ferrite, while a tuning range of 550 mc can be obtained with an unloaded Q of 3000 to 4000 using the largest diameter rod. This behavior is the result of the ferrite permeability and loss characteristics considered as perturbations, but the broadening and flattening of the central portion of the curve for the larger rods is aided by the way in which the operation is departing from a simple perturbation.

As this filter is a circulator at resonance, it might also be used as a selective, passive duplexer. The transmitter is connected to port A and operates at f_-. The antenna is connected to port B and the receiver to port C. Energy from the transmitter encounters a cavity off resonance and is reflected to the antenna. Incoming energy from the antenna at f_- sees a resonant cavity and is coupled out port C. Since reflections from the antenna reach the receiver directly, this system requires a very well matched antenna to operate without some additional protective tr device for the receiver. There is some remote possibility of using the cavity itself as the tr switch. The duplexer can be operated at a fixed frequency or it can be tuned over a limited range by varying the dc field. Zero field must be avoided. To minimize antenna-receiver losses, the 0.125-inch-diameter×1.69-inch ferrite was used in the experimental cavity. From Figs. 1(c)–1(e), it is seen that for fixed-frequency operation with minimum loss and bandwidth, transmission through the cavity should be via negative circular polarization with magnetic fields between about 100 and 1000 oersteds. Over this range, stray variations in magnetic field have little effect on the resonant frequency. A small Alnico 5 permanent magnet ($\frac{1}{2}$ by $\frac{1}{2}$ by $2\frac{1}{2}$ inches) was chosen which gave an effective field of approximately 175 oersteds. At this field strength the nonuniformity of the field was found to have little effect on loss. The separation between the resonant frequencies for positive and negative polarization was about 150 mc, and the loss between transmitter and antenna was 0.2 db. The loss between antenna and receiver was 1.36 db and the bandwidth was 7.0 mc. The theoretical cavity-wall losses for silver would produce a loss of 0.85 db. Normally, the cavity-wall losses are from 25 to 40 per cent higher than this value. Therefore, in this case the added loss due to the ferrite is small. Fig. 1(g) shows the isolation between transmitter and receiver for a perfectly matched antenna, as a function of frequency. At the operating frequency the isolation, before any attempts at maximizing

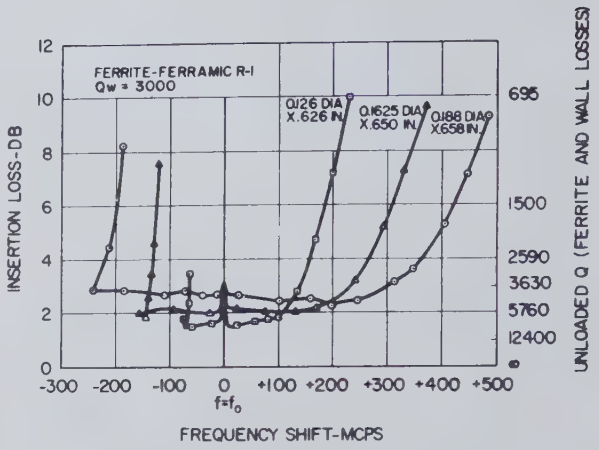

Fig. 1(f)—Insertion loss and unloaded Q, port A to port D, vs frequency shift.

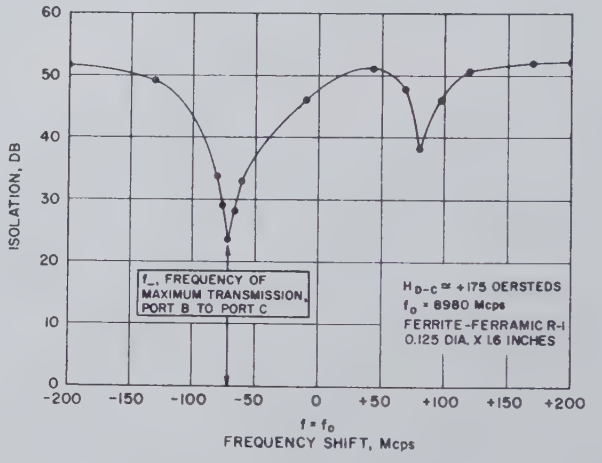

Fig. 1(g)—Isolation, port A to port C, vs frequency.

it, was only 23 db. Fig. 1(g) is included because it gives a good indication of the way in which stray coupling is occurring between transmitter and receiver. The large dip near the operating frequency f_- is mainly due to energy transmitted through the cavity via negative circular polarization. This energy can reach the cavity because of imperfect power division and phase errors in the left-hand 3-db coupler, unequal coupling-hole sizes in apertures 1 and 2, and phase errors due to unequal line lengths or coupling holes not spatially at 90°. By correcting the phase and equalizing the power division on the transmitter side, the isolation was raised above 40 db at the operating frequency. The smaller dip in Fig. 1(g) near $\Delta f = +80$ mc, is a measure of the energy coupled through the cavity by positive circular polarization. This energy is directly coupled into the cavity which is off resonance to this frequency and can reach the receiver only through phase and power-splitting errors occurring on the right-hand side of the filter.

The input vswr of the filter is less than 1.25 over the range of the couplers. At resonance it drops to 1.1. In tentative tests, the device operated at a transmitter-pulsed peak power of 250 kw without breakdown into a load vswr in arm B of 1.1.

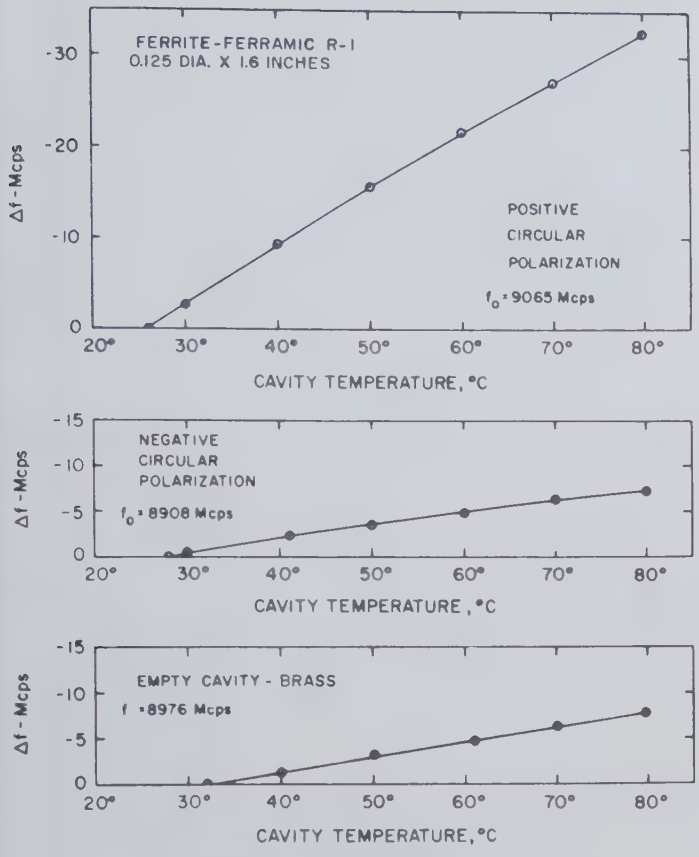

Fig. 1(h)—Frequency drift vs temperature.

Fig. 1(h) shows the variation in cavity resonant frequency vs temperature with the small Alnico 5 permanent magnet in place. As would be expected, for transmission on negative circular polarization, the frequency drift was slightly less than that for the brass cavity without ferrite. For positive circular polarization at this field the drift for the ferrite-loaded cavity was approximately four times larger. By proper choice of cavity mode and magnet configuration, low-expansion ferromagnetic alloys, such as invar, can be used to reduce this drift as in normal cavity design. Electrical temperature compensation is also possible.

Many variations of this filter are possible by using top- or side-wall couplers and other cavity modes. For example, Fig. 2 shows one version using only two apertures. In this arrangement, energy is reflected from the cavity near resonance and emerges from port B. Off resonance, the rf energy does not see the cavity and adds at port C.

Three-Port Ferrite-Loaded Filters

For duplexer operation, the previous four-port filters have an unused arm which must be terminated in a load. In lossless nonreciprocal devices it is possible to have three- as well as four-port networks which are theoretically matched looking into all ports, and the resulting three-port circulators have the proper characteristics for passive duplexer operation, again assuming a very well matched antenna. It does not appear possible to

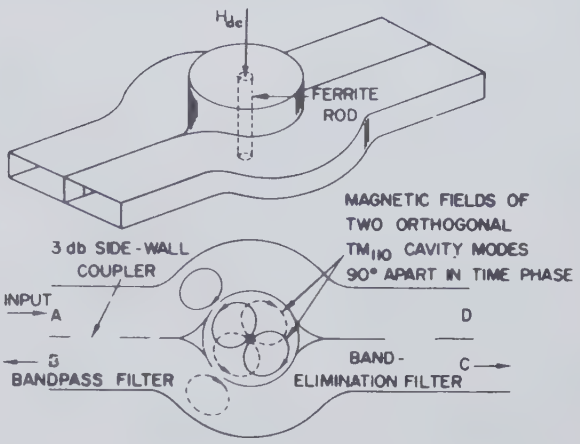

Fig. 2—Ferrite loaded, circularly polarized filter using two 3-db couplers, and two coupling apertures.

build a two-port, tunable, band-pass filter using a circularly polarized cavity which will have only one resonant, transmission frequency, unless nonreciprocal or nonlossless elements in the cavity-waveguide coupling system are allowed. A three-port filter should thus be the simplest configuration for this purpose. As will be seen, however, difficulty arises in trying to tune through the zero dc field condition. With these characteristics in mind, several three-port filters were investigated.

Fig. 3(a) illustrates a three-port filter which uses ferrite-loaded, degenerate, circular, TM_{110} cavity modes. The coupling aperture in waveguide A–B is placed at the point of circularly polarized magnetic field in the waveguide. Waveguide C is magnetically coupled to the TM_{110} cavity mode. Energy entering port A tends to excite a positive circularly polarized TM_{110} cavity mode and energy entering B, a negative circularly polarized mode for the dc magnetic field shown. Port C couples energy out of the linearly polarized component of these fields shown by the solid lines in the top view in Fig. 3(a). Port C thus has equal coupling to either positive or negative sense of cavity field rotation. The magnetic field at the wall of the cavity is, of course, linearly polarized in either case. The position of arm C around the cavity does not alter the operation of the filter.

The filter has nonreciprocal directional properties similar to those of the four-port filter previously described. The filter is band-pass at one frequency from A to C or from C to B and band elimination from A to B. The filter is band-pass at another frequency from B to C or from C to A and band elimination from B to A. These are the directional properties of a three-port circulator which circulates the energy between ports in one direction at or near f_+ and in the opposite direction at or near f_-. Far from resonance, ports A and B are directly connected and port C is decoupled.

For an experimental, X-band model, the resonant frequency for maximum transmission through the band-pass filter from port A to port C as a function of dc magnetic field is shown in Fig. 3(b). It is seen in Figs. 3(c) and 3(d) that losses are a minimum for transmis-

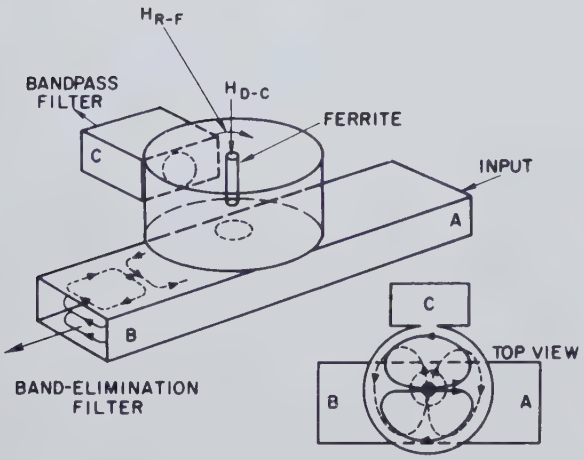

Fig. 3(a)—Ferrite loaded, three-port, circularly polarized filter using two TM_{110} cavity nodes.

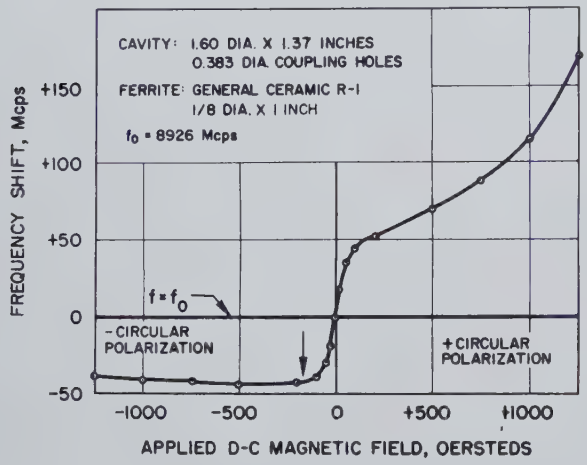

Fig. 3(b)—Resonant frequency, port A to port C, vs dc magnetic field.

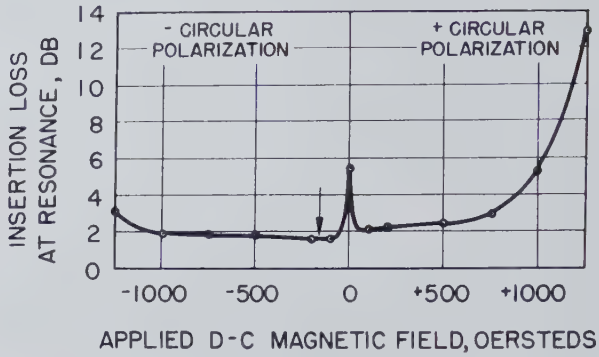

Fig. 3(c)—Insertion loss, port A to port C, vs dc magnetic field.

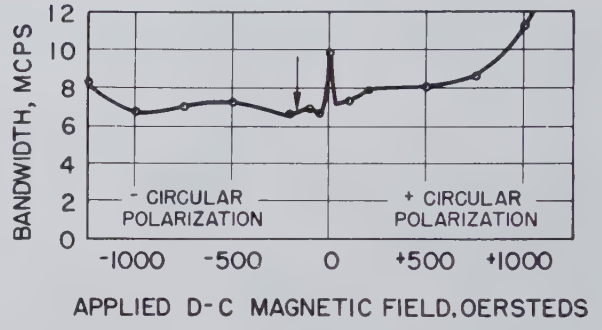

Fig. 3(d)—Bandwidth, port A to port C, vs dc magnetic field.

sion via negative circular polarization and rise rapidly with appreciable positive dc fields. As before, for transmission via negative circular polarization the resonant frequency is nearly independent of applied field below about -100 oersteds, while the insertion loss remains low between -100 and -1000 oersteds. With transmission by positive circular polarization a limited tuning range is possible before the insertion loss begins to rise because of ferrite resonance losses.

This filter might also be used as a selective duplexer. The transmitter would be connected to port B, the antenna to port A, and the receiver to port C. The frequency curve in Fig. 3(b) gives the operating frequency for a given dc field from a permanent magnet. The insertion loss and bandwidth curves in Figs. 3(c) and (d) are then the loss and bandwidth between the antenna and receiver. Energy from the transmitter sees a cavity off resonance and passes to the antenna with negligible loss. Energy from the antenna sees the cavity on resonance and is passed to the receiver.

It can be seen from Figs. 3(c)–3(d) that an effective magnetic field of -175 oersteds again gives nearly minimum losses and a reasonable frequency separation between f_+ and f_-.

When a small permanent magnet is used, energy entering arm B from the transmitter sees a cavity that is 100 mc off resonance, and any energy reaching the receiver in arm C by this path is attenuated over 30 db. This isolation of receiver from transmitter is shown as a function of frequency in Fig. 3(e). The curve closely follows the calculated coupling through a cavity off resonance except for the peak near the frequency of maximum A to C transmission. This cancellation is probably caused by stray coupling due to asymmetries in the cavity and coupling holes.

The vswr looking into arm B is less than 1.10 over a 10 per cent bandwidth at X band, including both resonances.

A theoretical analysis of the filter shows that there is a definite relation between coupling-hole diameters for minimum insertion loss, as would be expected. The holes in the filter just presented were near to the optimum size. A small adjustment in hole diameter did reduce the insertion loss from 1.6 to 1.2 db, but it raised the bandwidth from 6.7 to 8.6 mc.

It is interesting to consider the characteristics of the filter looking from the receiver into arm C. Energy entering this port can couple into the cavity at either of the two resonant frequencies of the circularly polarized cavity modes. The side-coupling hole has the proper symmetry for coupling into the linearly polarized TM_{110} mode shown by the solid lines in Fig. 3(a). The ferrite then couples energy from this mode into the orthogonal mode which lags or leads by 90° in time. Consequently,

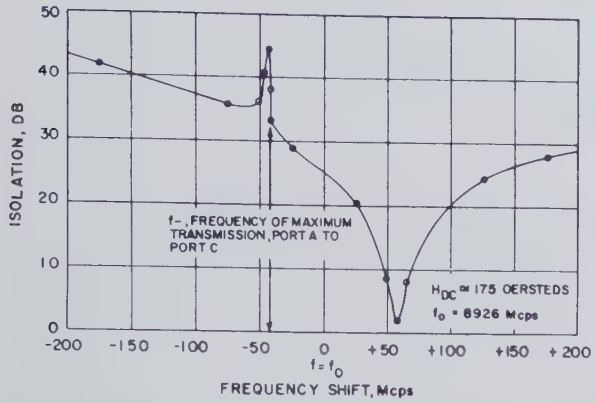

Fig. 3(e)—Isolation, port B to port C, vs frequency.

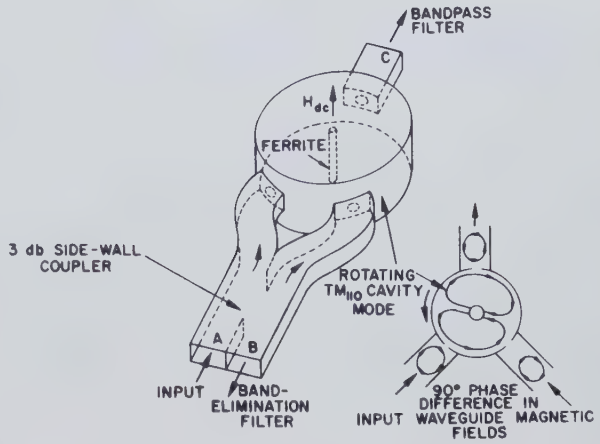

Fig. 4—Ferrite loaded, three-port filter using one 3-db coupler.

a nearly pure circularly polarized cavity field results at each resonant frequency when they are well separated. Off resonance, the excited cavity field is small, and essentially all energy entering C is reflected. With zero dc field, there is no coupling through the ferrite; hence, only the single linearly polarized mode is excited which couples equally out ports A and B. This single mode could also be decomposed into oppositely rotating fields which would then couple equally out of ports A and B. This division accounts for the increased loss and bandwidth seen in Fig. 3(c) at zero field. It should also be noted that the vswr looking into ports A and B rises at zero field because the two linear cavity modes are not loaded equally and consequently their reflections do not cancel in the main guide.

The input vswr looking into port C at resonance for the negative circularly polarized fields is 1.3. This value could theoretically be made 1.0 with only a negligible increase in loss with the same bandwidth by a slight increase in coupling-hole size at port C and a slight reduction in the other coupling-hole size.

Fig. 4 shows a three-port filter using one 3-db side-wall coupler. The over-all characteristics with respect to ports A, B, and C are similar to those of the previous three-port filter. The power-handling capacity is probably slightly higher, and a closed magnetic circuit can be more easily used. As with the other three-port filter, the isolation is dependent upon the off-resonance characteristic of the cavity and is not aided by the added directivity of a second 3-db coupler.

Conclusion

By exciting circularly polarized modes in microwave cavities, a new group of compact filters is made available. By ferrite-loading cavities, these filters become tunable and nonreciprocal. This paper has presented preliminary experimental data on these ferrite-loaded filters to indicate some of their general properties. For the ferrite sizes used, the ferrite losses in the filters are less than the cavity-wall losses when operating away from ferromagnetic resonance; therefore, these losses should not restrict the use of ferrites in microwave cavity filters.

Resonant Properties of Nonreciprocal Ring Circuits*

F. J. TISCHER†

Summary—**The ring circuit investigated consists of a resonant ring guide coupled to a main guide. The properties can be described by the equations for the waves in the ring guide resulting from excitation in the main guide. The influence of nonreciprocity on the properties is investigated under conditions of varying coupling. The representation of the ring waves by the poles and zeros is chosen to permit interpretation of the results under the large variety of operational conditions with respect to coupling and nonreciprocity. The application for measuring the material constants of ferrites is discussed.**

Introduction

THE properties of ring circuits under different coupling conditions were described in a previous paper.[1] Applications and special cases have been considered in the literature.[2–5] The general properties of nonreciprocal ring circuits are the subject of this investigation.

The properties of nonreciprocal ring circuits are interesting from the viewpoint of different applications, one of which is the possibility to measure the properties of ferrite materials in a directionally coupled resonant ring guide.[6] In properly conducted experiments, the intrinsic tensor permeability can be determined.

Nonreciprocal conditions in ring circuits can be obtained by filling a part of the cross section of the ring guide along a section or along the total circumference with premagnetized ferrite material. As a consequence, the propagation constants have different values for waves progressing in the ring guide in both directions. Two cases are of primary significance. One occurs when the phase velocity is different in the two directions. The other case results from excessive attenuation in one direction.

Since the properties of ring circuits depend on the coupling conditions, it is convenient to study the waves in the ring guide under interaction with a waveguide to which it is coupled and from which the energy is fed into the ring. One can distinguish between different coupling conditions as directional, nondirectional, and semidirectional coupling. A fourth significant condition occurs if an additional discontinuity is introduced into the ring guide. This additional discontinuity takes into account the case where energy is coupled out of the ring guide into a second waveguide by a second coupling element.

The great number of significant operational conditions complicates the description of the properties. This description should show primarily the influence of the nonreciprocity on the resonant frequency or resonant frequencies and on the Q value. A valuable tool for describing the properties was found in the representation of the ring-wave amplitudes as rational functions by their poles and zeros. The method is derived in Appendix II for the case of the reciprocal ring guide. The interpretation of the results is further simplified if the coupling conditions are described by the wave-coupling factors. The derivations of the corresponding relations are shown in Appendix I.

The System Under Investigation

The system under investigation consists of a waveguide to which a ring guide is coupled as shown schematically in Fig. 1. The coupling element, shown in Fig. 2, is a four port of which arms 3 and 4 are connected by a section of waveguide or transmission line forming the annular ring. Arms 1 and 2 form the waveguide to which the ring guide is coupled.

The scattering properties of the junction will be described by the reflection coefficients ρ_{nn}, transmission coefficients τ_{nm}, and by the coupling factors k_r and k_h for the waves passing from one waveguide into the other. The simplifying assumption is made that port 2 is terminated with a matched termination and that the circuit is fed by port 1. The general case, which includes a reflected wave h_2 incident into port 2, can be considered as a superposition of the waves in the two cases when the circuit is fed alternately by port 1 and 2.

The reflected wave r and the incident wave h in the region of the junction are related by a scattering matrix S:

$$r = Sh. \tag{1}$$

Because of symmetry of the junction, reciprocity, and matched termination, the scattering matrix has the form

$$S = \begin{pmatrix} \rho_0 & \tau & k_h & k_r \\ \tau & \rho_0 & k_r & k_h \\ k_h & k_r & \rho_0 & \tau \\ k_r & k_h & \tau & \rho_0 \end{pmatrix}, \tag{2}$$

where k_h and k_r are the coupling factors between the

* Manuscript received by the PGMTT, July 5, 1957.
† Dept. of Elec. Eng., Ohio State University, Columbus, Ohio.

[1] F. J. Tischer, Swedish Patent No. 152,491, August 26, 1952.
——, "Resonance properties of ring circuits," IRE Trans., vol. MTT-5, pp. 51–56; January, 1957.
[2] L. Young, "A hybrid-ring method of simulating higher powers than are available in waveguides," *Proc. IEE*, pt. 3, pp. 189–190; May, 1954.
[3] P. S. Sferrazza, "Traveling-wave resonator," *Tele-Tech*, vol. 74, pp. 84, 85, 142, and 143; November, 1955.
[4] Lj. Miloševič and R. Vautey, "Resonator a ondes progressives," *Revue tech. Comp. franc. Thomson-Houston*, pp. 65–78; November 21, December, 1955.
[5] K. Tomiyasu, "Effect of a mismatched ring in a traveling-wave resonant circuit," IRE Trans., vol. MTT-5, p. 267; October, 1957.
[6] L. A. Ault, E. C. Spencer, and R. C. Le Craw, "Traveling-wave cavity for ferrite tensor permeability measurements," 1957 IRE National Convention Record, pt. 1, pp. 282–287.

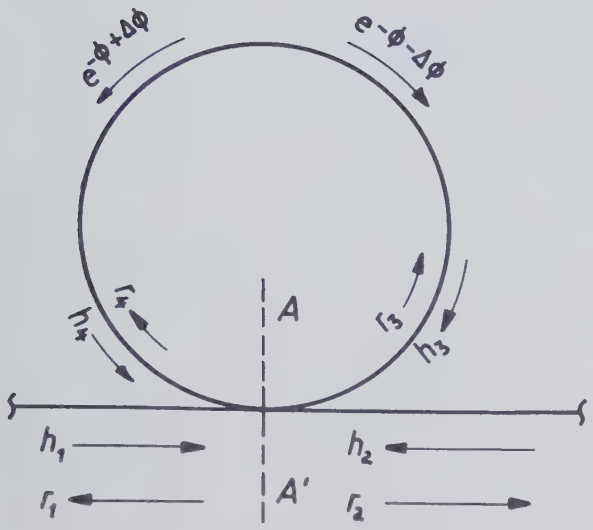

Fig. 1—Nonreciprocal ring circuit.

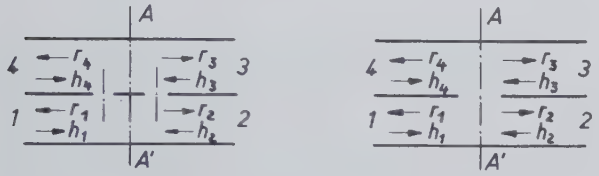

Fig. 2—Coupling conditions: (a) directional coupling, (b) nondirectional coupling.

coupled waveguides in the forward and reverse directions;

$$k_h = \tau_{13} = \tau_{31} = \tau_{24} = \tau_{42}, \tag{3}$$

$$k_r = \tau_{12} = \tau_{21} = \tau_{34} = \tau_{43}. \tag{4}$$

The scattering matrix yields a system of equations from which the different waves can be determined. The waves progressing in the ring guide in both directions to the junction are denoted by h_3 and h_4. With the magnitudes of h_3 and h_4 known, the total input reflection coefficient ρ_{in} and transmission coefficient in the main guide τ_{12} can be calculated,

$$\rho_{in} = \frac{r_1}{h_1} = \rho_0 + \frac{h_3 k_h + h_4 k_r}{h_1} \tag{5}$$

and

$$\tau_{12} = \frac{r_2}{h_1} = \tau + \frac{h_3 k_r + h_4 k_h}{h_1}. \tag{6}$$

The properties of the ring circuit as a filter are completely defined by the waves in the ring h_3 and h_4. The superposition of h_3 and h_4 yields ρ_{in} and τ_{12} which describe the reaction of the ring circuit on the main guide. A similar relation can be obtained for the case in which energy is coupled out of the ring guide by a second coupling element into a second waveguide. Under this condition, the circuit operates as a transmission type filter. Also in this case h_3 and h_4 define completely the properties of the circuit. Therefore, the investigation will concentrate on the ringwaves h_3 and h_4.

Coupling Conditions

It is possible to distinguish between three distinct coupling conditions: 1) directional ($q=0$), 2) nondirectional ($q=1$), and 3) semidirectional ($0<q<1$) coupling, where $q=k_r/k_h$. The coupling depends on the properties of the coupling element.

The results of an investigation of the coupling problem are shown in Appendix I. Capacitive coupling between the waveguides is considered. According to the derivations, the junction data can be described in a general manner by approximate expressions for ρ_0 and τ;

$$\rho_0 \approx -iq\,|k_h| \approx -k_r \tag{7}$$

and

$$\tau \approx 1 - |k_h|^2(1+q^2) - i\,|k_h|. \tag{8}$$

Eqs. (7) and (8) will permit a better interpretation of the results.

Description of Nonreciprocal Ring Waves by Poles and Zeros

The representation of ring waves h_4 and h_3 by poles and zeros is used to show the influence of nonreciprocity on the properties of the ring circuit. The equations are similar to those of Appendix II for the reciprocal case.

The wave propagation within the ring guide is characterized by (9) and (10)

$$h_3 = r_4 e^{-\phi} e^{-\Delta\phi}, \tag{9}$$

$$h_4 = r_3 e^{-\phi} e^{+\Delta\phi}, \tag{10}$$

where $e^{\Delta\phi}$ takes into account the nonreciprocity in both directions (Fig. 1). The introduction of (9) and (10) into the system of equations derived from (2), yields

$$r_3 = h_1 k_h \frac{1 - \tau e^{-\phi} e^{-\Delta\phi} + q\rho_0 e^{-\phi} e^{-\Delta\phi}}{(1 - \tau e^{-\phi} e^{-\Delta\phi})(1 - \tau e^{-\phi} e^{+\Delta\phi}) - \rho_0^2 e^{-2\phi}} \tag{11}$$

and

$$r_4 = h_1 k_h q \frac{1 - \tau e^{-\phi} e^{+\Delta\phi} + \frac{1}{q}\rho_0 e^{-\phi} e^{+\Delta\phi}}{(1 - \tau e^{-\phi} e^{-\Delta\phi})(1 - \tau e^{-\phi} e^{+\Delta\phi}) - \rho_0^2 e^{-2\phi}}. \tag{12}$$

It follows that

$$h_4 = h_1 k_h e^{+\Delta\phi} \frac{e^{\phi} - e^{\phi_3}}{(e^{\phi} - e^{\phi_1})(e^{\phi} - e^{\phi_2})}, \tag{13}$$

$$h_3 = h_1 k_h q e^{-\Delta\phi} \frac{e^{\phi} - e^{\phi_4}}{(e^{\phi} - e^{\phi_1})(e^{\phi} - e^{\phi_2})}, \tag{14}$$

in which

$$e^{\phi_{1,2}} = \tau \cosh \Delta\phi \pm \rho_0 \sqrt{\frac{\tau^2}{\rho_0^2}(\sinh^2 \Delta\phi + 1)}, \tag{15}$$

$$e^{\phi_3} = e^{-\Delta\phi}(\tau - q\rho_0), \tag{16}$$

$$e^{\phi_4} = e^{+\Delta\phi}\left(\tau - \frac{1}{q}\rho_0\right). \tag{17}$$

The poles $e^{\phi_{1,2}}$ are obtained as solutions of quadratic a equation when the denominators of (11) and (12), which are equal, are multiplied by $e^{2\phi}$ and equated to zero. Expressions for e^{ϕ_3} and e^{ϕ_4} are derived from the numerators.

Difference of Wave Velocity in Both Directions

As a significant case of nonreciprocity, the value of $\Delta\phi$ is assumed purely imaginary:

$$\Delta\phi = i\Delta\beta L.$$

This case results from differences of the wave velocities in both directions in the ring guide. Low dc magnetization of ferrites yields this condition.

If the variation $\Delta\beta L$ of the total phase shift due to nonreciprocity is small, the trigonometric functions derived from (15) may be replaced by the corresponding series and higher order terms may be neglected. Introduction of the approximate coupling data [(17) and (18)] gives

$$e^{\phi_{1,2}} \approx 1 - |k_h|^2(1 + q^2 + \tfrac{1}{2}m^2) - i|k_h|(1 \mp \sqrt{q^2 + m^2}), \quad (18)$$

$$e^{\phi_3} \approx 1 - |k_h|^2(1 + q^2 + \tfrac{1}{2}m^2) - i|k_h|(1 - q^2 + m), \quad (19)$$

and

$$e^{\phi_4} \approx 1 - |k_h|^2(1 + q^2 + \tfrac{1}{2}m^2) + i|k_h|m, \quad (20)$$

where $m = \Delta\beta L/|k_h|$ is the ratio of the phase shift difference to $|k_h|$ which is the coupling coefficient for the waves passing in the forward direction from the main guide into the ring guide. The coupling conditions (directional, nondirectional, and semidirectional) are defined by q.

According to (13) and (14), the poles e^{ϕ_1}, e^{ϕ_2} and the zeros e^{ϕ_3} and e^{ϕ_4} describe the frequency dependence of the ring waves h_4 and h_3, based on the same concept as used in Appendix II in connection with Fig. 7. The real parts $|k_h|^2(1+q^2+\frac{1}{2}m^2)$ show the influence of coupling and nonreciprocity on the Q value, and the imaginary parts of the poles show the influence on the resonant frequencies. Caution must be exercised if a zero coincides with a pole thus yielding a single-peak resonance curve.

The imaginary parts $Y_n = \mathrm{Im}\,(e^{\phi_n})$ which show the influence of coupling and nonreciprocity on the resonant frequencies are plotted in Fig. 3 as a function of the coupling (q) for different values of $m = \Delta\beta L/|k_h|$. The magnitude of m is a measure of the nonreciprocity. The poles are shown in the diagram a, the zeros for the waves in both directions in diagram b. The diagrams show for which value of q and m the poles and zeros coincide, such as Y_1, Y_2, and Y_3 for $q=0$ and $m=0$ and Y_1 and Y_3 for $m=0$ and $q=1$. It is interesting to note that only in the case of purely directional coupling ($q=0$) the nonreciprocity does not dislocate coinciding poles and zeros. In all other cases, nonreciprocity leads to a splitting of

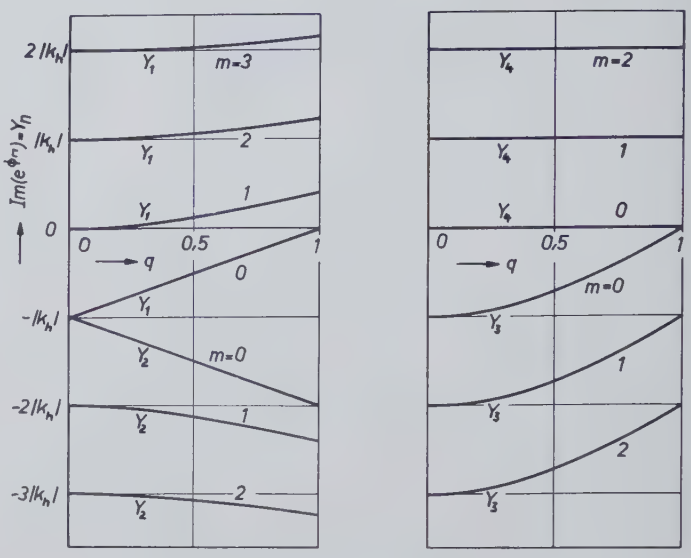

Fig. 3—Influence of nonreciprocity on the resonant frequencies. Imaginary parts of poles and zeros. ($q = k_r/k_h$; $m = \Delta\phi/|k_h|$.)

poles and zeros. This is important in the case of nondirectional coupling ($q=1$) where the single-peak resonance curve changes into a double-peak curve due to nonreciprocity. Effects of this type are important in the case of the measurement of ferrite properties in a ring guide.

Excessive Attenuation in One Direction

Other interesting conditions result from excessive attenuation in one direction and negligible attenuation in the other direction in the ring guide. Under these conditions the ring waves are related by

$$h_3 = r_4 e^{-\phi} e^{-\Delta\phi} \quad (21)$$

and

$$h_4 = r_3 e^{-\phi}, \quad (22)$$

where

$$\Delta\phi = \Delta\alpha L. \quad (23)$$

The excessive attenuation in one direction can be produced by ferrite material magnetized near gyromagnetic resonance. An isolator as a section of the ring circuit has the same effect.

Calculation of the poles and zeros yields:

$$e^{\phi_{1,2}} \approx 1 - 2|k_h|^2 - i|k_h| - \frac{\Delta\phi}{2} \pm \sqrt{\frac{\Delta\phi^2}{4} - |k_h|^2}, \quad (24)$$

$$e^{\phi_3} \approx 1 - 2|k_h|^2 - \Delta\phi \quad (25)$$

and

$$e^{\phi_4} \approx 1 - 2|k_h|^2, \quad (26)$$

for nondirectional coupling which is the most interesting case ($k_r = k_h$). Fig. 4 shows the locus of the poles for varying excessive attenuation in one direction.

The quotient r_3/r_4 is another quantity which is of particular interest in the case of differing attenuation. It

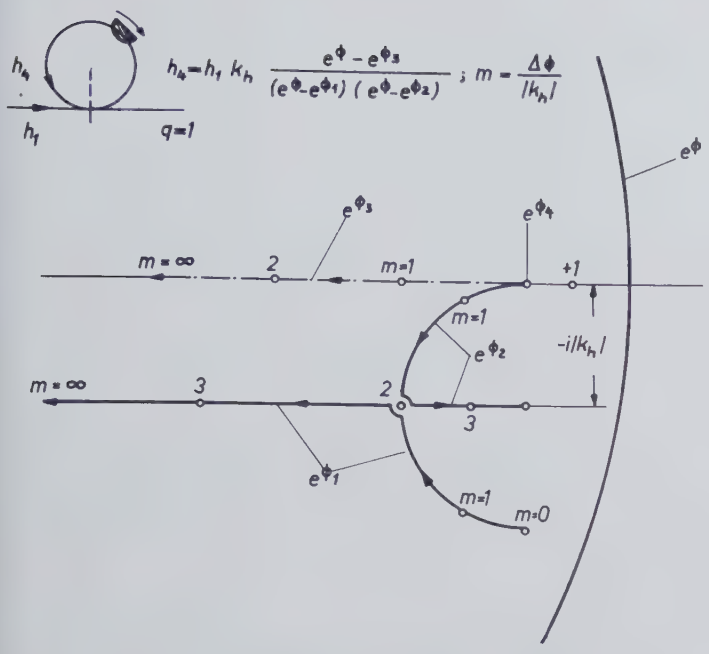

Fig. 4—Loci of poles and zeros of the ring waves for varying excessive attenuation. Nondirectional coupling.

may be shown from (11) and (12) that

$$\frac{r_3}{r_4} = \frac{e^{\phi} - e^{\phi_3}}{e^{\phi} - e^{\phi_4}}. \tag{27}$$

Eq. (27) can be treated in the same manner as one of the wave functions.

Additional Discontinuity in the Ring Guide

The ring guide has similar properties to those of a cavity with different wave modes which resonate at the same or at different frequencies. The latter case corresponds to a nonreciprocal ring guide. A single-peak resonance curve is obtained if no coupling exists between the waves in both directions in the ring guide. This occurs for purely directional coupling where the discontinuity of the coupling element is negligible ($\rho_0 = 0$). Consequently, the question of what happens if a discontinuity is introduced into a nonreciprocal, directionally coupled ring guide arises. This problem occurs in practice when a ferrite material probe is introduced into a ring circuit for determination of its material properties.

The ring waves are expressed by

$$h_3 = r_3\rho_1 e^{-\phi} + r_4(1 + \rho_1)e^{-\phi}e^{-\Delta i\beta L}, \tag{28}$$

$$h_4 = r_4\rho_1 e^{-\phi} + r_3(1 + \rho_1)e^{-\phi}e^{+\Delta i\beta L}, \tag{29}$$

where reflections result from a symmetrical discontinuity located diametrically opposite to the coupling element in the ring guide. The reflection coefficient of the discontinuity is ρ_1, and for the nonreciprocity, a difference of total phase shift in both directions $2\Delta\beta L$ is introduced.

The ring waves are described by

$$r_3 = h_1 k_h \frac{e^{\phi} - e^{\phi_3}}{e^{-\phi}(e^{\phi} - e^{\phi_1})(e^{\phi} - e^{\phi_2})} \tag{30}$$

and

$$r_4 = h_1 k_h 9 \frac{e^{\phi} - e^{\phi_4}}{e^{-\phi}(e^{\phi} - e^{\phi_1})(e^{\phi} - e^{\phi_2})}, \tag{31}$$

where the poles and zeros are defined by

$$e^{\phi_{1,2}} \approx \tau\left[1 - i\frac{\Delta p}{2} - \frac{(\Delta\beta L)^2}{2} \pm i\sqrt{(\Delta\beta L)^2 + \frac{\Delta p^2}{4}}\right], \tag{32}$$

$$e^{\phi_3} \approx \tau\left(1 - i\frac{\Delta p}{2}\right)e^{-i\Delta\beta L} \tag{33}$$

and

$$e^{\phi} - e^{\phi_4} \approx -i\tau\frac{\Delta p}{2}e^{-\phi}, \tag{34}$$

for small values of the discontinuity ($\rho_1 = -i\Delta p/2$) and of the nonreciprocity.

Evaluation of (30) through (34) shows that the ring waves in the reversed direction result directly from the discontinuity, (34), and that the discontinuity splits a coinciding pole and zero. Instead of a single-peak resonance curve without discontinuity, a double-peak curve is obtained.

Conclusion

It is desirable to treat the ring circuit under a variety of conditions which take into account coupling to an input and output waveguide. The representation of the waves in the ring guide by the poles and zeros of a rational function gives a satisfactory description of the ring circuit properties and shows clearly the influence of nonreciprocity under the different coupling conditions. Consideration of practical coupling conditions and the introduction of the corresponding relations (Appendix I) further improves the representation. The poles and zero representation permits calculation of the resonant frequencies, a simple graphical determination of resonance curves and a calculation of the loaded and unloaded Q values.

With respect to the nonreciprocity, two particular cases have been treated separately. One is characterized by a difference of wave velocity in both directions, the other by excessive attenuation in one direction. Both can be superimposed to show the influence of nonreciprocity in the general case.

The results obtained for a difference of the wave velocity show clearly the influence of the nonreciprocity on the resonance frequencies (Fig. 3) for the different coupling conditions described by $q = k_r/k_h$. Presence of an additional discontinuity in the ring guide in the case of directional coupling ($q = 0$) adds one more interesting operational condition. The additional discontinuity may

result from a second coupling element by which energy is coupled out from the ring guide.

The case of an additional discontinuity is of particular interest when it is desired to determine the properties of ferrite materials in a directionally coupled ring guide. It is assumed that for directional coupling only waves in one direction progress in the ring guide. However, since the ferrite material probe represents a discontinuity, reflected waves occur in the opposite direction. These reflected waves contribute to a variation of the resonant frequency. This variation must be taken into account if the material properties are to be determined from the shift of the resonance frequency by perturbation methods.

The influence of the additional discontinuity can be visualized clearly in the poles and zero presentation. The discontinuity results in a split of a coinciding pole and zero which changes the zero-peak resonance curve into a double-peaked curve. The split of the pole and the zero must be taken into account in the determination of the Q value. The discontinuity can be avoided if two thin cylindrical ferrite material probes are inserted $\lambda_g/4$ apart, if the probe has the form of a rectangular disk of a length $\lambda_g/2$ or, if the probe extends over the total circumference.

The nonreciprocal ring circuit has interesting properties which differ from those of other circuits. Besides the application for determination of the ferrite material properties, especially for high field strengths, one can anticipate applications in other fields of microwaves.

Appendix I

Coupling Relations

Two waveguides are coupled together by a nondirectional coupling element in the cross-sectional plane AA'. In Fig. 5(a), a capacity C is shown as the coupling element. Derivation of the junction data yields

$$\rho_0 = -\frac{i\Delta p}{1 + 2i\Delta p}, \tag{35}$$

$$\tau = -\frac{1 + i\Delta p}{1 - i\Delta p} \tag{36}$$

and

$$k_h = k_r = k = \frac{i\Delta p}{1 + 2i\Delta p},$$

where

$$\Delta p = \omega C Z_0/2.$$

If high order terms are neglected, approximate expressions are obtained;

$$\rho_0 \approx -i\,|\,k_h\,|\,, \tag{37}$$

$$\tau \approx 1 - 2\,|\,k_h\,|^2 - i\,|\,k_h\,|\,. \tag{38}$$

Eqs. (37) and (38) also are valid for inductive coupling where $k_r = -k_h$.

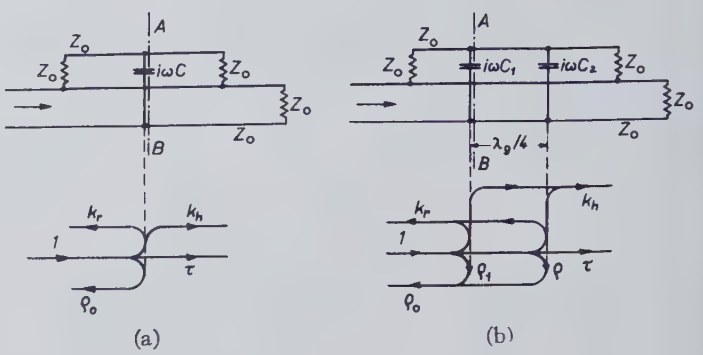

Fig. 5—Capacitive coupling. (Nondirectional and semidirectional coupling.)

The corresponding equivalent circuit for directional and semidirectional coupling is shown in Fig. 5(b). Coupling is performed by two capacitances $\lambda_g/4$ apart. Consequently,

$$\Delta p_1 = \omega C_1 Z_0/2, \qquad \rho_1 = -\frac{i\Delta p_1}{1 + 2i\Delta p_1},$$

$$\Delta p_2 = \omega C_2 Z_0/2, \qquad \rho_2 = -\frac{i\Delta p_2}{1 + 2i\Delta p_2}.$$

If all junction data are reduced with respect to the cross sectional plane AA', the following equations are obtained:

$$[\rho_0]_{AA'} = \frac{\rho_1 - \rho_2 - 2\rho_1\rho_2}{1 + \rho_1\rho_2},$$

$$[\tau]_{AA'} = \frac{1 + \rho_1 + \rho_2 + \rho_1\rho_2}{1 + \rho_1\rho_2},$$

$$k_h + k_r = -2\rho_1,$$

$$k_h - k_r = -2\rho_2,$$

$$q = k_r/k_h.$$

The dropping of higher order terms and the disregarding of reflections between the coupling capacitances yields

$$\rho_0 \approx -iq\,|\,k_h\,| \approx -k_r \tag{39}$$

and

$$\tau \approx 1 - |\,k_h\,|^2(1 + q^2) - i\,|\,k_h\,|\,. \tag{40}$$

Appendix II

Poles and Zeros of the Ring Waves

The properties of the ring circuit can be described by the waves h_4, h_3 progressing in the ring guide in both directions. These waves are characterized in the case of the reciprocal ring guide by

$$h_3 = r_4 e^{-\phi},$$

$$h_4 = r_3 e^{-\phi},$$

$$\phi = (\alpha + i\beta)L,$$

where L is the circumference and α and β are the attenuation and phase constants, respectively, of the ring guide. Combination with the system of equations corresponding to the matrix (2) gives

$$h_4 = h_1 e^{-\phi} \frac{k_h(1 - \tau e^{-\phi}) + k_r \rho_0 e^{-\phi}}{(1 - \tau e^{-\phi})^2 - \rho_0^2 e^{-2\phi}},$$

$$h_3 = h_1 e^{-\phi} \frac{k_r(1 - \tau e^{-\phi}) + k_h \rho_0 e^{-\phi}}{(1 - \tau e^{-\phi})^2 - \rho_0^2 e^{-2\phi}}.$$

Transformation and introduction of $q = k_r/k_h$ yields

$$h_4 = h_1 k_h \frac{e^{\phi} - (\tau - q\rho_0)}{[e^{\phi} - (\tau + \rho_0)][e^{\phi} - (\tau - \rho_0)]}$$

$$= h_1 k_h \frac{e^{\phi} - e^{\phi_3}}{(e^{\phi} - e^{\phi_1})(e^{\phi} - e^{\phi_2})} \tag{41}$$

and

$$h_3 = h_1 k_h q \frac{e^{\phi} - (\tau - \rho_0/q)}{[e^{\phi} - (\tau + \rho_0)][e^{\phi} - (\tau - \rho_0)]}$$

$$= h_1 k_h q \frac{e^{\phi} - e^{\phi_4}}{(e^{\phi} - e^{\phi_1})(e^{\phi} - e^{\phi_2})}. \tag{42}$$

Eqs. (41) and (42) describe the waves h_4 and h_3 by poles (e^{ϕ_1}, e^{ϕ_2}) and zeros (e^{ϕ_3}, e^{ϕ_4}) which correspond to the "resonances" and "antiresonances" in the language of network theory.

The representation by poles and zeros is advantageous because it aids the analysis of the frequency dependence of the wave functions. It permits simple graphical determination of $|h_4|$ and $|h_3|$ as a function of frequency.

The locus of e^{ϕ} as a function of frequency is a circle with the radius $e^{\alpha L}$ where $e^{-\alpha L}$ expresses the attenuation of the waves along the circumference of the ring guide. The attenuation is assumed to be constant in a small frequency range near resonance. The poles and zeros e^{ϕ_n} are complex quantities which also are approximately constant near resonance. Fig. 6 shows these magnitudes in the complex plane. The point T which corresponds to $e^{\phi} = e^{\alpha L} e^{i(2\pi/\lambda g)L}$ travels with increasing frequency along the circle in the direction of the arrow. With P_1, P_2 for the poles and Z for the zero, the absolute value $|h_4|$ is proportional to $\overline{TZ}$ divided by the product of $\overline{TP}_1 \times \overline{TP}_2$. Plotting $|h_4|$ as a function of frequency yields the resonance curve. When T passes near a pole the resonance curve has a peak. Near a zero the resonance curve has a minimum.

Eqs. (41) and (42) show that the locations of the poles and zeros are dependent on ρ_0, τ, and q. Introduction of the approximate values derived in Appendix I yields

$$e^{\phi_1} = 1 - |k_h|^2(1 + q^2) - i|k_h|(1 + q),$$
$$e^{\phi_2} = 1 - |k_h|^2(1 + q^2) - i|k_h|(1 - q),$$
$$e^{\phi_3} = 1 - |k_h|^2(1 + q^2) - i|k_h|(1 - q^2)$$

and

$$e^{\phi_4} = 1 - |k_h|^2(1 + q^2).$$

If the poles and zeros are plotted in the complex plane as a function of q, the curves of Fig. 7(b) are obtained. The coupling is defined by q, where directional, semidirectional, and nondirectional coupling are signified by $q=0$, $0<q<1$, and $q=1$, respectively. For three values,

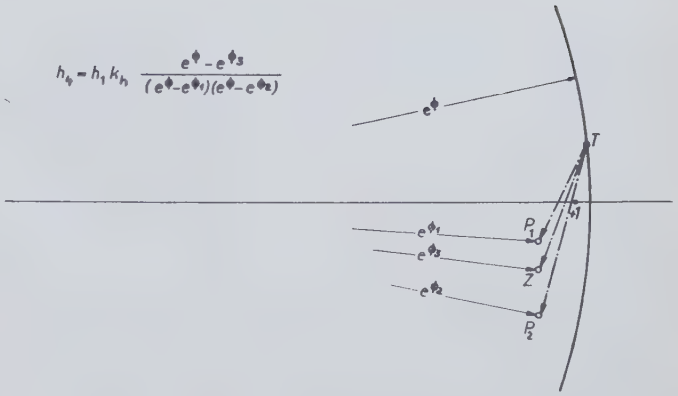

Fig. 6—Complex poles and zeros of the ring wave h_4.

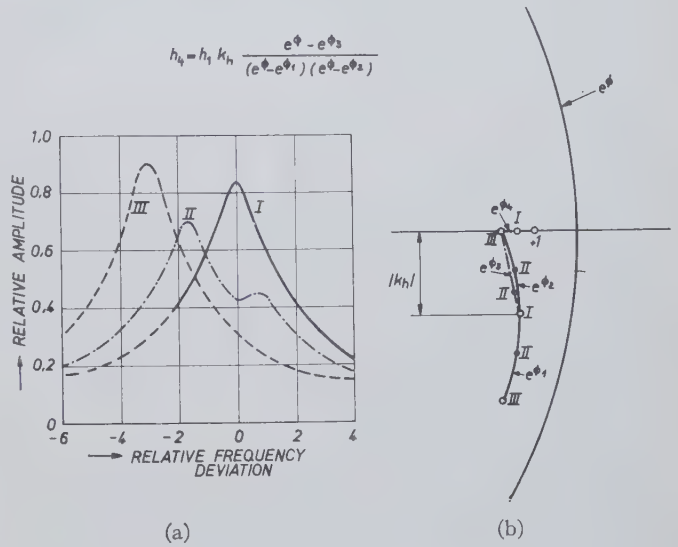

(a) (b)

Fig. 7—Loci of poles and zeros for varying coupling and corresponding resonance curves.

$q=0$, 0.5, 1, the resonance curves are shown in Fig. 7(a).

For $q=0$ (I), the two poles and the zero coincide. Consequently, a single-peak resonance curve is obtained. The same result is obtained for nondirectional coupling ($q=1$), (III). For values $0<q<1$ the poles and the zeros have different locations (II) and a double peak is obtained as shown in Fig. 7(a).

The poles and zeros representation permits a simple approximate calculation of the Q value. The Q value may be derived for a circuit with a single-peak resonance curve from the half-power bandwith. The half-power bandwith corresponds to travel on the e^{ϕ} circle over an arc which equals twice the distance of the pole e^{ϕ_0} from the circle.

Use of this concept yields

$$Q = \frac{\beta L}{2(\alpha L + 1 - e^{\phi_0})} \left(\frac{\lambda g}{\lambda_0}\right)^2$$

for the loaded Q value, and

$$Q = \frac{\beta}{2\alpha} \left(\frac{\lambda g}{\lambda_0}\right)^2$$

for the unloaded value where the coupling approaches zero ($|k_h| \to 0$).

Exact Solution for a Gyromagnetic Sample and Measurements on a Ferrite*

H. E. BUSSEY† AND L. A. STEINERT†

Summary—An outline of an exact solution for a gyromagnetic rod centered in a right circular cylindrical cavity resonator is given. This solution is applied in evaluating dielectric and tensor-magnetic measurements on a well-known ferrite. Complex frequencies and constitutive parameters are introduced and the solution is expanded in series to obtain a convenient calculational scheme. Comparisons are made of exact and perturbation calculations of results from a small and a large sample. The effect of insufficient symmetry of the cavity is discussed and the condition for sufficient symmetry is given. The g value of electrons was 2.02.

I. Introduction

A METHOD for the measurement of tensor permeability, based on an exact mathematical solution rather than the perturbation solution for a circular cylindrical resonator with a sample, is given. Results obtained using the two-dimensional TM_{nm0} modes of a circular cylindrical resonator are shown. In this case the sample can protrude through holes in the cavity walls, thus permitting very uniform magnetization of the ferrite samples.

An advantage of this exact method is the convenience of measuring the comparatively large frequency and Q changes produced by the samples. Samples were used having diameters of 0.025 and 0.075 inch for measurements at 9200 mc.

It is pertinent to mention that the exact calculations yield directly the constitutive electrical parameters of the sample; *i.e.*, the dielectric constant and the permeability. On the other hand, perturbation calculations yield directly a "demagnetized susceptibility," $(\mu-\mu_0)F(\mu)$, where $F(\mu)$ is a demagnetizing factor and μ is obtained with an additional step. The demagnetized susceptibility and the permeability should not be confused.

II. Solution for Gyromagnetic Sample

An exact solution for a circular cylindrical cavity resonator containing as a sample a centered rod of gyromagnetic material has been given previously.[1] A brief outline is included here, along with several details previously omitted.

The properties of the gyromagnetic material are described first. With the rf magnetic field h and the induction b in right circular cylindrical coordinates, the material is a substance with constitutive parameters which may be expressed as

$$\begin{pmatrix} b_r \\ b_\phi \\ b_z \end{pmatrix} = \begin{pmatrix} \mu & i\alpha & 0 \\ -i\alpha & \mu & 0 \\ 0 & 0 & \mu_z \end{pmatrix} \begin{pmatrix} h_r \\ h_\phi \\ h_z \end{pmatrix}. \tag{1}$$

The dielectric constant ϵ is assumed to be a scalar. The signs of the off-diagonal terms specify that the time dependence is exp $(-i\omega t)$. The antisymmetric matrix (μ) in (1) is identical with the matrix which represents the tensor permeability in the usual Cartesian coordinates. This may be shown by applying rotation operators to the matrix equation $b=(\mu)h$ in Cartesian space and obtaining (1) as a result. The matrix (μ) has an inverse which is written as

$$(\mu)^{-1} = \begin{pmatrix} M & iK & 0 \\ -iK & M & 0 \\ 0 & 0 & M_z \end{pmatrix}. \tag{2}$$

It is introduced because its elements occur most naturally in the wave solutions to be obtained.

To obtain a solution for the cavity with a gyromagnetic rod, the wave equation in the sample must be solved and the waves in it matched to those in the remaining space of the cavity.

The wave equation for a gyromagnetic medium is of the fourth order,[2] for a general three-dimensional wave, or of the second order[3] for two-dimensional waves; *i.e.*, for waves that are independent of one coordinate, here chosen to be the z coordinate. The advantage of working with the two-dimensional waves lies in the simplicity of solution, and they are selected for the remaining work, with the foreknowledge that there exist two-dimensional modes of oscillation for cavity resonators. The two-dimensional wave equation that has solutions which may fit boundary conditions[1] in a closed resonator is

$$(\nabla_p^2 + \omega^2\epsilon/M)E_z = 0, \tag{3}$$

where

$$\nabla_p^2 = \frac{1}{r}\frac{\partial}{\partial r}r\frac{\partial}{\partial r} + \frac{1}{r^2}\frac{\partial^2}{\partial\phi^2}$$

is the Laplacian in transverse (r, ϕ) space; ω is the angular frequency. Eq. (3) is valid in free space after replacing M by $M_0 \equiv 1/\mu_0$ and ϵ by ϵ_0, where μ_0 and ϵ_0 are the constitutive parameters of free space.

* Manuscript received by the PGMTT, July 8, 1957; revised manuscript received, September 23, 1957. Supported by Order No. BuShips/1700R-564.

† National Bureau of Standards, Boulder Labs., Boulder, Colo.

[1] H. E. Bussey and L. A. Steinert, "Exact solution for a cylindrical cavity containing a gyromagnetic material," PROC. IRE, vol. 45, pp. 693–694; May, 1957.

[2] P. S. Epstein, "Theory of wave propagation in a gyromagnetic medium," *Rev. Mod. Phys.*, vol. 28, pp. 3–17; January, 1956.

[3] M. L. Kales, "Modes in waveguides containing ferrites," *J. Appl. Phys.*, vol. 24, pp. 604–608; May, 1953.

The solutions of (3) are of the form

$$E_z = (Ae^{in\phi} + Be^{-in\phi})[FJ_n(\beta r) + GY_n(\beta r)], \quad (4)$$

where $\beta = \omega(\epsilon/M)^{1/2}$, J_n and Y_n are Bessel functions of the first and second kinds, respectively, of inetgral order n, and A, B, F, and G are coefficients to be determined by the boundary conditions. The solutions of (3) in free space are the same as in (4), provided that the cylinder functions have the argument kr where $k = \omega(\epsilon_0/M_0)^{1/2}$. [The time factor exp $(-i\omega t)$ is understood with (4) and other field quantities below.]

Now we consider the boundary value problem of fitting the waves (4) into a right circular cylindrical resonator with a centered gyromagnetic rod (Bussey and Steinert,[1] Fig. 1). The rod has radius a and the cylindrical wall of the cavity is at $r = b$, $b > a$. Since the fields do not vary with z, the height of the assembly is arbitrary.

It is known that in this problem the $e^{+in\phi}$ and $e^{-in\phi}$ solutions have, in general, different resonant frequencies, thus either frequency can be selected for excitation. A choice of signs indicates this selection. The physical or boundary conditions at $r = 0$ and $r = b$ are satisfied with (4) expressed as:

$$E_z = De^{\pm in\phi}J_n(\beta r), \qquad r < a, \quad (5)$$

$$E_z = Ee^{\pm in\phi}C_n(kr), \qquad r > a, \quad (6)$$

where $C_n(kr) = J_n(kr) - Y_n(kr)\,[J_n(kb)/Y_n(kb)]$ is always zero at $r = b$.

The magnetic fields are obtained from (5) and (6) by applying Maxwell's curl equation, $(\mu)^{-1}$ curl $E = i\omega H$. A convenient matrix form for this equation is

$$\begin{pmatrix} M & iK & 0 \\ -iK & M & 0 \\ 0 & 0 & M_z \end{pmatrix} \begin{pmatrix} 0 & -D_z & r^{-1}D_\phi \\ D_z & 0 & -D_r \\ -r^{-1}D_\phi & r^{-1}D_r r & 0 \end{pmatrix} \begin{pmatrix} E_r \\ E_\phi \\ E_z \end{pmatrix} = i\omega \begin{pmatrix} h_r \\ h_\phi \\ h_z \end{pmatrix}, \quad (7)$$

where the D's are derivative operators.

It remains to make E_z and h_ϕ continuous across the boundary at $r = a$. This fixes the ratio of the amplitudes D/E and the value of ω and gives the equation of resonance for the system as:

$$\frac{M\beta a J_n'(\beta a)}{J_n(\beta a)} \pm nK = \frac{M_0 ka C_n'(ka)}{C_n(ka)}, \quad (8)$$

where the primes indicate derivatives with respect to the arguments. Eq. (8) represents two resonances for $n > 0$. The upper sign $(+nK)$ is used with the Larmor[4] rotating pattern and the lower sign with the anti-Larmor case. When $n = 0$, we have a nondegenerate TM_{0m0} mode and in this mode a small ferrite rod furnishes mostly a dielectric effect on the resonator. In order to evaluate the three unknowns, ϵ, M, and K, three measurements on a ferrite in three different cavity modes are required. It is convenient to make one measurement in a TM_{0m0} resonator and two in a TM_{110} resonator (Larmor and anti-Larmor). A fourth experiment in a TE_{011} cavity can furnish M_z exactly.

[4] Larmor refers to the case where the rf magnetic field pattern rotates in the same sense as the precessing magnetization, and anti-Larmor refers to the opposite sense of rotation.

III. Losses and Complex Arguments

It is apparent that the above equation of resonance (8) does not directly indicate what happens when the frequency of the excitation is not at the resonant frequency. In our experiments, however, excitation away from resonance was carried out to find the Q which indicates the losses; *i.e.*, Q was measured by noting the change in the transmitted power as the frequency departed from resonance. Alternatively, the Q of a resonator may also be measured in the time domain by viewing the exponential decay of the energy, and this, of course, is a resonant oscillation with what appears to be a complex frequency,[5] $\omega^* = \omega' - i\omega''$. In this case, the important feature is that the frequency does not depart from resonance and the equation of resonance is satisfied during the Q measurement.

We will assume that the Q obtained from the variation of transmission with frequency (as it actually was measured) is the same Q obtained from a transient measurement; that the resonant frequency was complex with $\omega^* = \omega' - i\omega'/2Q_F$, where Q_F is the *contributed* Q of the ferrite sample to the resonator, found from $1/Q_F = 1/Q_s - 1/Q_e'$, where Q_s is the resonator Q with the lossy sample, and Q_e' is the Q with the same sample assumed to be lossless. For the present work we will employ the additional widely used assumption that, for a small sample, $Q_e' \doteq Q_e$, the Q of the empty resonator. (Exact expressions for Q_e' of the resonator with a lossless gyromagnetic sample have been developed, but they are rather cumbersome and were not used in the present work.)

IV. Calculation of Results

Eq. (8) may be expressed using relative dielectric and magnetic constants $\epsilon^* = \epsilon/\epsilon_0$, $M^* = \mu_0 M$, and $K^* = \mu_0 K$, where the asterisks also specifically indicate that these quantities are taken to be complex. In addition, we will expand the functions on the left side of (8) in series assuming that a, the sample radius, is small so that to a good approximation, for $n = 1$,

$$M^* \pm K^* = T_\pm(k^*a) + \epsilon^*(k^*a)^2/4 + \epsilon^{*2}(k^*a)^4/96M^*, \quad (9)$$

[5] This may be seen as follows. Consider an electromagnetic field with the time dependence $e^{-i\omega^* t} = e^{-i(\omega' - i\omega'')t} = e^{-\omega'' t}e^{-i\omega' t}$. There is exponential decay for $\omega'' > 0$. Now consider the general definition of $Q = \omega' W/(-dW/dt)$, the stored energy W is divided by the power dissipation per radian. This may be rearranged into the logarithmic differential equation $dW/W = -\omega' dt/Q$. The solution is $W(t) = W(t = 0)e^{-\omega' t/Q}$. The field strength, obtained from the square root of the energy, then decays as $e^{-\omega' t/2Q}$. Comparing the two exponential decays, we have a possible physical representation by using the complex $\omega^* = \omega' - i\omega'/2Q$.

where T is the right-hand side of (8) multiplied by μ_0. In (9) we specifically indicate that $k^*=\omega^*(\mu_0\epsilon_0)^{1/2}$ is complex. M^* is first estimated without the last term on the right, then is used in the last term to improve the estimation. A term in $(ka)^6$ can easily be carried in the series.

The benefits of the above expansion especially are apparent during practical calculations, because from (9) we then obtain simple pairs of algebraic equations instead of the difficult four simultaneous transcendental equations that would arise if (8) were solved directly.

Assuming (temporarily) that ϵ^* is known directly from a TM_{0m0} experiment, then it is only necessary to evaluate the TM_{110} data using (9) separated into its real and imaginary parts with $M^*=M'+iM''$, $\epsilon^*=\epsilon'+i\epsilon''$, etc., for exp $(-i\omega t)$ time dependence,

$$M' \pm K' = T_\pm' + a^2[\epsilon'(\omega'^2-\omega''^2)+2\epsilon''\omega'\omega'']_\pm/4c^2 \quad (10)$$

$$M'' \pm K'' = T_\pm'' + a^2[\epsilon''(\omega'^2-\omega''^2)-2\epsilon'\omega'\omega'']_\pm/4c^2, \quad (11)$$

where now we have exhibited only the first term of the expansion; c is the velocity of light. The $\pm$ sign choice indicates, as before, that Larmor and anti-Larmor frequencies enter separately and that each equation represents two equations. T separates into real and imaginary parts as indicated because of the complex frequency in k. The assumption that ϵ^* was known was introduced here for a convenient discussion. In practice, one may iterate the above calculations and use the first estimates of ϵ, M, and K to obtain improved self-consistent results. After calculating the values from (10) and (11), we find μ^* and α^* [the relative constants of the tensor (1)] from

$$\mu^* \pm \alpha^* = (M^* \pm K^*)^{-1}. \quad (12)$$

V. Equipment

A photograph (Fig. 1) shows the microwave source, a Pound stabilized unit, and the magnet. Galvanometers were used as power indicators. An accurate wavemeter was used to measure frequency changes, including Q widths. It has an accurate micrometer movement which seems to repeat its settings to 10^{-5} inches. A table of frequencies for each 10^{-4}-inch change in setting was constructed (using an automatic computer) which made the wave meter convenient to use. Its Q_L (loaded Q) was 16,000 and its transmission was -11 db. Invar was used to give some temperature compensation, although temperature effects are not a major problem when, as here, frequency differences are the main interest.

VI. Dielectric Measurement

Measurements were made of the dielectric and magnetic constants of the ferrite R-1 of General Ceramics. The samples were ground with a diamond wheel from pressed bars (1955 manufacture, dimensions $0.4\times0.9\times6$ inches) that were cut up.

The TM_{020} resonator for dielectric measurements had an empty frequency f_e of 9860 mc and a Q_L of 8000. The

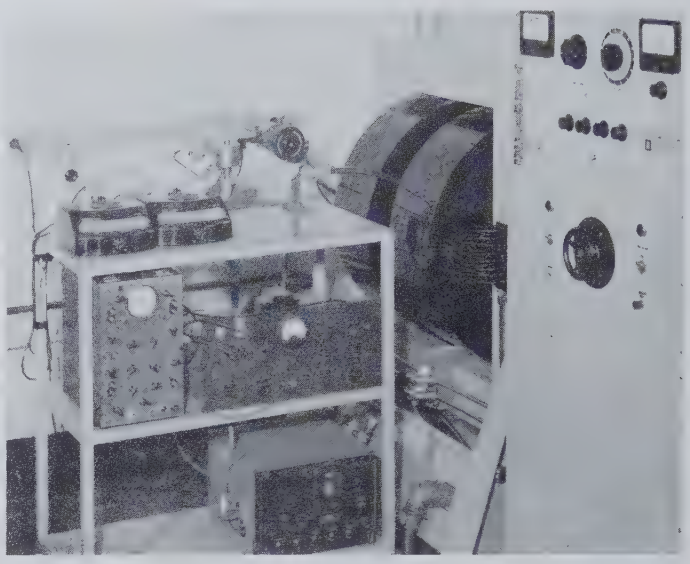

Fig. 1—The experimental assembly.

R-1 sample was 0.075 inch in diameter and 2 inches long. The sample shifted the frequency to 9090 mc which leads to an ϵ' of about 17 by perturbation theory and 11.4 when evaluated by formula (8) with $n=0$ and $\mu'=0.76$, the unmagnetized value. The value obtained for ϵ'' was 0.013. In this present work, it is assumed that ϵ is independent of the applied dc magnetic field. This, of course, needs to be checked and with the advent of exact calculations a check may be feasible. A convenient expansion of (8) for $n=0$ is $\epsilon^*(k^*a)^2=2T/(1-\epsilon^*(k^*a)^2/8M^*)$. For unmagnetized material M^{*-1} is replaced by μ^*.

Since the perturbation method[6] using a rectangular waveguide cavity is widely used for dielectric measurements of ferrites, we will indicate the results from this method. With 0.080-inch holes in each face for inserting the sample, the value of ϵ' is about 12.5. If the holes are eliminated and the sample enclosed, a value near 13.5 is obtained. The holes weaken the electric field, thus compensating some of the error of perturbation theory.[7]

VII. Magnetic Measurement

In this section, tensor permeability measurements on a small (0.025-inch diameter) and a large (0.075-inch diameter) sample rod are compared. In addition, perturbation and exact theory methods of calculating the results are compared. Two different resonators were used for the two sizes of rods. Both resonators had four irises as shown in Fig. 2, but differed in that, for the large sample, excitation of the resonator was through only one iris, whereas the resonator shown in Fig. 2 and used for the small sample was excited through two adjacent irises by waves of equal magnitude (within 2 per

[6] G. Birnbaum and J. Franeau, "Measurements of dielectric constant and loss of solids and liquids by a cavity perturbation method," *J. Appl. Phys.*, vol. 20, pp. 817–818; August, 1949.

[7] An investigation of these matters has been completed and a report will be written. Corrections for the perturbation approximation and hole error were developed.

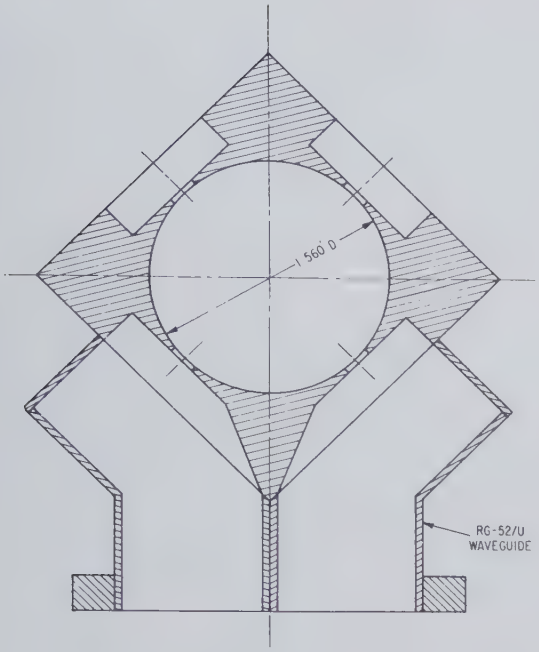

Fig. 2—Cross section of TM_{110} resonator with 4 irises and guides permitting excitation of a rotating field pattern.

cent) and 90° out of phase. This allowed either Larmor or anti-Larmor excitation to be impressed, as was necessary because with a small sample the two modes "overlapped." With the 0.075-inch sample, the two modes were separated sufficiently so that results were obtained with a single input iris. The four irises in this case were used to maintain symmetry.

Both cavities had a length (along the z axis) of 0.9 inch. The small sample was 1.25 inch long and the large sample was 2.0 inch long. This allowed the sample ends to protrude outside the resonator, thus the dc magnetization of the measured part was essentially uniform,[8] except near zero dc field.

The results for the small rod are shown in Fig. 3 and Fig. 4 as evaluated both by the exact solution and by perturbation theory. The results for the large rod are shown in Fig. 5 and Fig. 6. The curves in Fig. 3 and the Larmor curve in Fig. 4 very closely fitted the experimental points, which were omitted for clarity. The anti-Larmor loss data were rather erratic and these points are shown in Fig. 4. [*Note added in proof:* The anti-Larmor loss curve (Fig. 4) is incorrect. The curve probably starts at about 0.0015 unmagnetized and comes down to 0.0002 at 1000 oersteds, remaining at about this value to 8000 oersteds.]

The indications of the rotating-coil Gauss meter were found to be 2.2 per cent too high and, therefore, the abscissa H_{dc} needs to be lowered everywhere by 2.2 per cent.

Comparing the "exactly" calculated small and large rod data, it is seen that the excursions of the curve at resonance are all slightly greater for the large sample. The perturbation approximation introduces relatively little error for the small rod, but considerable error for the large rod. It also artificially displaces the resonance.

From the frequencies of gyromagnetic resonance, 9216 mc and 9114 mc, for the small and large rods, respectively, and with H_{dc} corrected as above, it was found that the g factor of the electrons was 2.013 for the small rod and 2.023 for the large rod, found from $f = geH_{dc}/4\pi$ mc.

The above measurements may be compared with published[9] perturbation results on the same ferrite. The results for the real parts, $\mu' \pm \alpha'$, differ in detail, especially at low values of H_{dc}. The peak absorptions agree to within the inconsistency of the small and large rod data. The g factor obtained from the perturbation rod data[9] would be approximately 1.9; our perturbation results also tend to give g's that are too low.

The missing data in Fig. 3–Fig. 6 were missed due to a resonant absorption and resulting weak signal. It will be observed that the loss factor, $\mu'' + \alpha''$ is not particularly great in the missed region. There are, however, geometrical effects that create a resonant absorption there. These effects may be seen by examining the behavior of the perturbation quantity, $(\mu - \mu_0)F(\mu)$, (see Introduction) where $F(\mu)$ allows for demagnetization, or alternatively, by examining Kittel's resonance formula[10] that allows for demagnetization. It may be shown that these two viewpoints are in agreement.

VIII. Symmetry of the Resonator

Symmetry in the mechanical structure of the resonator is important in tensor permeability measurements. The mathematical solution in Section II assumed that the resonator was perfectly circular. To avoid gross errors, due to initial splitting of the degeneracy by geometrical perturbations, it is sufficient that the symmetry group of the perturbed TM_{110} resonator be C_3 or higher. This means that with irises, loops, or probes around the periphery of the cylinder, there must be three or more identical irises, etc., spaced at equal angles. A circular iris on the axis would be desirable, as it leaves the symmetry C_∞, but is not always practicable.

The deleterious effect of insufficient symmetry was observed with a 9200-mc TM_{110} resonator in which the sine and cosine modes were already split by 5 mc with no sample inserted. Results for the small rod were in general wrong, except that the unmagnetized scalar value was correct and the gyromagnetic resonance was fairly well indicated. However, all of the results for the large rod were very nearly correct.

The resonator with four irises shown in Fig. 2 was annealed and carefully machined and, when empty, the independent sine and cosine modes differed in frequency by only a few hundredths of a megacycle. Furthermore,

[8] R. C. LeCraw and E. G. Spencer, "Tensor permeabilities of ferrites below magnetic saturation," 1956 IRE Convention Record, pt. 5, pp. 66–74.

[9] E. G. Spencer, L. A. Ault, and R. C. LeCraw, "Intrinsic tensor permeabilities on ferrite rods, spheres, and disks," Proc. IRE, vol. 44, pp. 1311–1317; October, 1956.

[10] C. Kittel, "On the theory of ferromagnetic resonance absorption," *Phys. Rev.*, vol. 73, pp. 155–161; January 15, 1948.

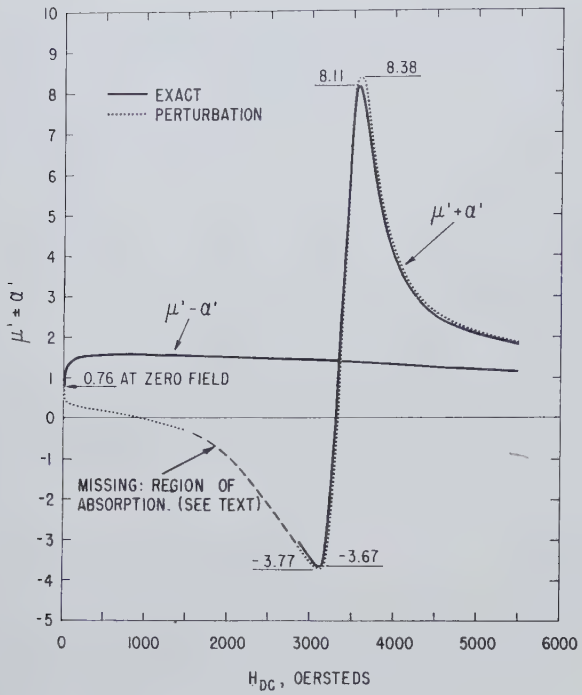

Fig. 3—Circularly polarized relative permeabilities for 0.025-inch-diameter sample.

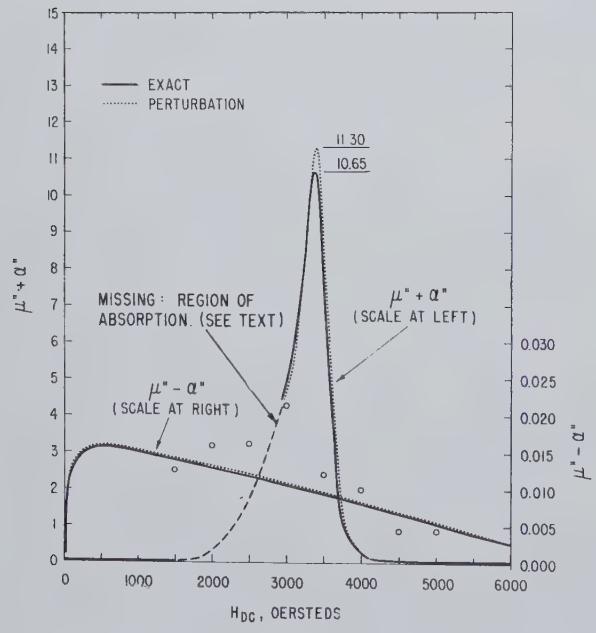

Fig. 4—Circularly polarized relative loss factors for 0.025-inch-diameter sample.

the loaded Q values (about 8000) differed by less than three per cent.

IX. Acknowledgment

The authors are indebted to A. J. Estin for the great help on equipment and measurements, to Drs. D. M. Kerns and P. F. Wacker for valuable advice, especially on group theory, to J. L. Dalke for support, and to R. C. LeCraw for discussions of experimental techniques and the loan of some R-1 ferrite. A. Koran, A. Himle, and C. Malone helped with data taking and analysis. Thanks are due to W. W. Longley, Jr. for programming subroutines of the Bessel functions with complex arguments that were used in evaluating the data on the automatic computer. Dr. J. R. Wait made valuable suggestions about the mathematical section.

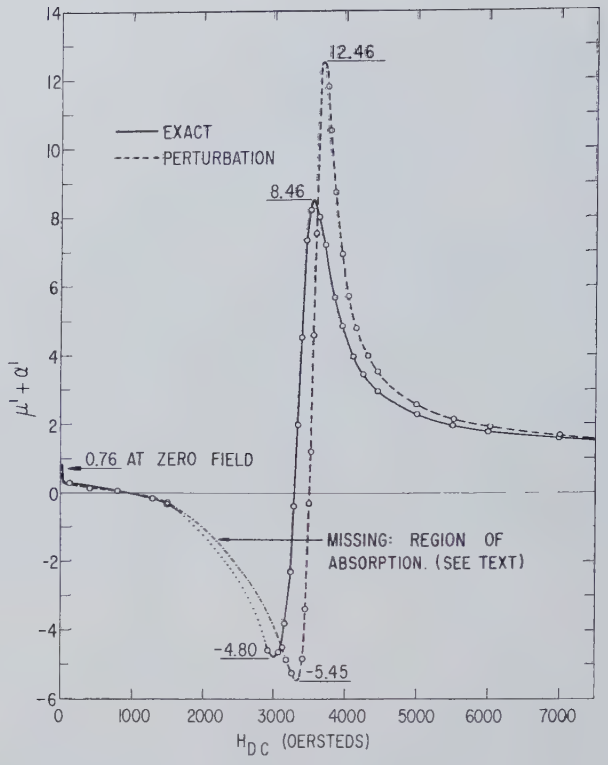

Fig. 5—Circularly polarized relative permeability for 0.075-inch-diameter sample.

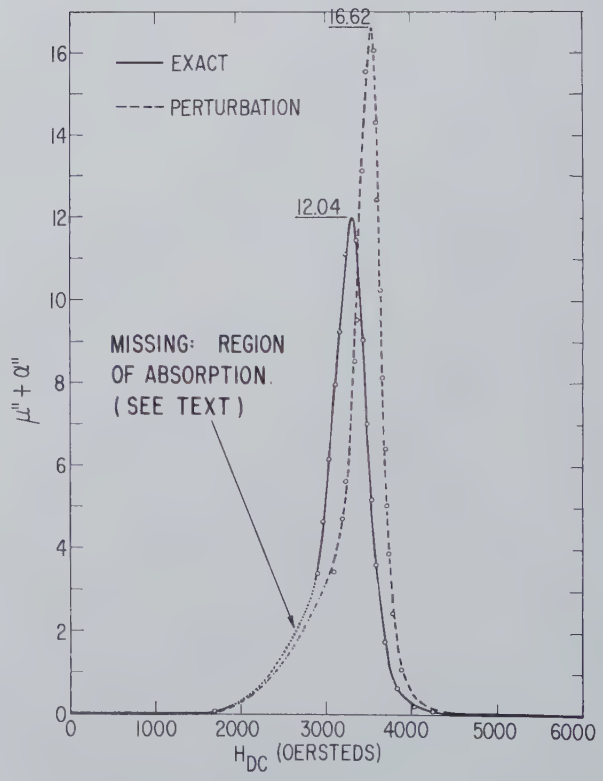

Fig. 6—Circularly polarized relative loss factor for 0.075-inch-diameter sample.

Resonance Measurements on Nickel-Cobalt Ferrites as a Function of Temperature and on Nickel Ferrite-Aluminates*

J. E. PIPPIN† AND C. L. HOGAN†

Summary—The variation of line width (ΔH) and effective g factor (g_{eff}) with cobalt content and with temperature is studied in a series of ferrites of composition $Ni_{1-\alpha}Co_{\alpha}Mn_{0.02}Fe_{1.9}O_{4\pm}$. Here α lies between 0 and 0.09; temperatures range from 20°C to 340°C. A minimum in ΔH is observed at $\alpha=0.027$; g_{eff} decreases with increasing α. The temperature dependence of each is qualitatively that which would be expected on the basis of the temperature dependence of the anisotropy of the mixed ferrite. Above room temperature ΔH and g_{eff} increase or decrease, depending on the cobalt content. It is also shown that the shape of the resonance line is determined by the sign of the anisotropy constant. For negative K_1 the line is steeper on the low-field side of resonance—for positive K_1 it is steeper on the high-field side.

Resonance data are presented on several nickel-cobalt ferrite-aluminates, of composition $Ni_{1-\alpha}Co_{\alpha}Mn_{0.02}Fe_{2-t}Al_tO_{4\pm}$, with α varying from 0 to 0.025 for $t=0.3$, 0.4, 0.5, and 0.6. The reduction of ΔH and g_{eff} expected from anisotropy considerations is observed.

Introduction

NICKEL ferrite has a negative first-order anisotropy constant K_1 whose magnitude decreases with temperature above room temperature. Cobalt ferrite has a positive anisotropy constant of much greater magnitude, and it also decreases with temperature above room temperature. It might be expected, and it is indeed true, that a solid solution of the proper (small) amount of cobalt ferrite in nickel ferrite would reduce the anisotropy of the mixed ferrite. By varying α in the formula $Ni_{1-\alpha}Co_{\alpha}Fe_2O_4$, ferrites with varying K_1 can be made; K_1 can be caused to vary from the negative value for nickel ferrite through zero to high-positive values. This has been demonstrated by Sirvetz and Saunders[1] in polycrystalline nickel-cobalt ferrite.[2] More direct measurements on single crystals[3] have substantiated this statement. The work of Sirvetz and Saunders suggests that the anisotropy constant of the mixed ferrite is equal to the weighted algebraic sum of the values for the individual ferrites. This would be expected theoretically, also, if it is assumed that the anisotropy is a property of the individual ions arising from crystalline field effects from the surrounding lattice. In such a case it would be true only for small cobalt additions for which the exchange (*i.e.*, Curie temperature) does not change significantly.[4] The temperature variation of K_1 for the mixed ferrite would then be determined by the variation of the *difference* of the K_1 curves for the constituent ferrites. In Fig. 1 $|K_1|$ vs temperature for nickel ferrite is shown (Healy's values[5]). To determine the K_1 for $Ni_{1-\alpha}Co_{\alpha}Fe_2O_4$, K_1 for cobalt ferrite[6] is multiplied by α and plotted, as for the case $\alpha=0.02$ shown in Fig. 1. The net K_1 is then the difference of the two curves (shaded area, for example), and is positive when the cobalt K_1 predominates and negative when the nickel $|K_1|$ is larger. (Actually, the nickel ferrite values should be multiplied by $1-\alpha$, but this is unimportant here). Where the two curves intersect the net K_1 is zero. This intersection moves to higher temperatures as the cobalt content is increased.

Our resonance measurements from room temperature to 340°C on several of these mixed polycrystalline ferrites are reported here. The variation of K_1 is reflected in the effective g factor, line shape, and line width. The smaller K_1, the narrower the line in reasonably high-density materials; for this reason cobalt-doped nickel ferrite, with small K_1, has been used recently in devices where a sharper resonance line was desired. It is well to emphasize that all the ferrites under discussion are high-density, low-loss ferrites (except where noted), suitable for microwave applications.

* Manuscript received by the PGMTT, July 22, 1957. This paper was presented in part at the Annual PGMTT Meeting, New York, N. Y., May 9–10, 1957. The research reported in this paper was supported by the Air Force under Contract AF 19(604)-1084 with Air Force Cambridge Research Center.

† Gordon McKay Lab., Harvard Univ., Cambridge, Mass.

[1] M. H. Sirvetz and J. H. Saunders, "Resonance widths in polycrystalline nickel-cobalt ferrites," *Phys. Rev.*, vol. 102, pp. 366–367; April 15, 1956.

[2] L. R. Bickford, Jr., J. Pappis, and J. L. Stull, "Magnetostriction and permeability of magnetite and cobalt-substituted magnetite," *Phys. Rev.*, vol. 99, pp. 1210–1214; August 15, 1955.

C. M. Van der Burgt, "Controlled Crystal Anistropy and Various Mixed Ferrites," presented at Conference on Magnetism and Magnetic Materials, Boston, Mass.; October 16–18, 1956.

[3] P. E. Tannenwald and M. H. Seavey, "Anisotropy of cobalt-substituted Mn ferrite single crystals," PROC. IRE, vol. 44, pp. 1343–1344; October, 1956.

[4] W. P. Wolf, "Origin and temperature dependence of magnetic anisotropy in nonconducting ferromagnetics," *Bull. Amer. Phys. Soc.*, ser. II, vol. 2, p. 117; March 21, 1957.

[5] D. W. Healy, Jr., "Ferromagnetic resonance in nickel ferrite as a function of temperature," *Phys. Rev.*, vol. 86, pp. 1009–1013; June 15, 1952.

[6] The cobalt values are from H. Shenker, "The Magnetic Anisotropy of Cobalt Ferrite and Nickel Ferrite," U. S. Naval Ordnance Lab., Navord Rep. 3858; February 8, 1955. Shenker's values were obtained on a crystal of composition $Co_{1.01}Fe_{2.00}O_{3.62}$. The room temperature value is two times larger than that obtained elsewhere (Bozorth, Tilden, and Williams, "Anisotropy and magnetostriction of some ferrites," *Phys. Rev.*, vol. 99, pp. 1788–1798; September 15, 1955) on crystals of slightly different compositions. A simple sum of anisotropies would indicate a minimum anisotropy at room temperature for $\alpha=0.015$, using Shenker's values, whereas our experiments show a minimum for $\alpha=0.027$, as reflected in the line width; this gives a factor of 2 also. Furthermore, K_1 for cobalt ferrite is affected strongly by heat treatment. In any event, the quantitative details of Fig. 1 should not be taken too seriously—the qualitative aspects are of interest here.

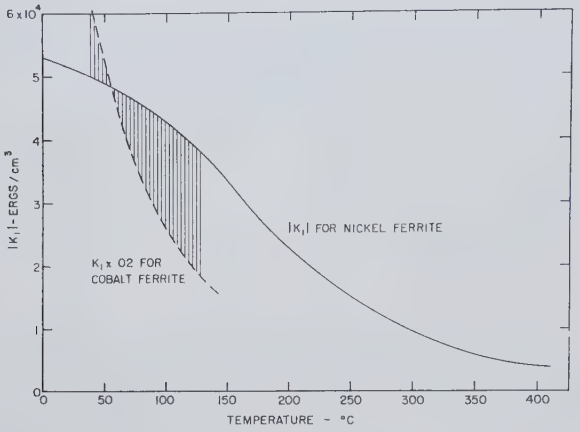

Fig. 1—First order anisotropy constant $|K_1|$ as a function of temperature for nickel ferrite (after Healy), and 0.02 K_1 for cobalt ferrite (after Shenker).

Many of the effects would not be observable were it not for the high density, and the variations with temperature would be different in very porous samples.

Materials

All the ferrites studied were prepared in our laboratory, using ceramic techniques which have been described in detail elsewhere.[7] With the exception of the ferrite-aluminates, all samples were iron-deficient and were of starting composition $Ni_{1-\alpha}Co_{\alpha}Mn_{0.02}Fe_{1.9}O_{4\pm}$, with α varying from zero to 0.09. The ferrite-aluminates had the starting formula $Ni_{1-\alpha}Co_{\alpha}Mn_{0.02}Fe_{2-t}Al_tO_{4\pm}$. Density, magnetic moment, and dielectric loss tangent at 20 mc were measured on all samples as a kind of quality-control. Densities of the nickel-cobalt ferrites varied between 95 per cent and 96 per cent of the theoretical maximum value for stoichiometric nickel ferrite, which is 5.38 gm/cm³; dielectric loss tangents were 0.001 to 0.003. The magnetic moments of samples in this series increased slightly with the small additions of cobalt in the expected way, starting from about 3230 Gauss for the nickel ferrite, corrected to X-ray density. The densities of the ferrite-aluminates were high; they will be given later.

Experimental Procedure

The resonance measurements were made at X band on ferrite spheres, using a reflection-type apparatus similar to that described by Artman and Tannenwald[8] and by Spencer, LeCraw, and Reggia.[9] The small spheres (0.015 inch to 0.040 inch) were mounted about $1\frac{1}{2}$ diameters off the center of the end wall of a rectangular TE_{101} mode cavity, which operated at 9208 mc at room temperature. Brass and copper cavities were used interchangeably at room temperature. For higher temperatures the copper cavity was used, and was flushed continuously with dry nitrogen gas to prevent corrosion. A small furnace surrounding the cavity gave temperatures up to 350°C. The temperatures were measured by means of an iron-constantan thermocouple attached to the cavity wall.

Line widths are estimated to be accurate to 8 per cent. The magnetic field was measured with extreme accuracy by means of nuclear magnetic resonance, so errors in g factor are due primarily to uncertainty in adjusting the magnetic field for maximum absorption and to imperfect spheres. The possible error is about 0.5 per cent in the nickel-cobalt series, and somewhat higher in some of the ferrite-aluminates.

Results and Discussion

The Nickel-Cobalt Ferrites

That crystalline anisotropy broadens the resonance line of a polycrystalline ferrite has been known for some time; Sirvetz and Saunders[1] observed this broadening experimentally in the nickel-cobalt ferrites. Porosity also broadens the line[10] due to the presence of localized demagnetizing fields set up by the pores. These effects have been treated theoretically by Schlömann,[11] who finds for the line broadening due to anisotropy and porosity, respectively,

$$\Delta H_{\text{anis}} = \left| \frac{K_1}{M_s} \right| \tag{1}$$

and

$$\Delta H_{\text{pores}} = 1.5(4\pi M_s)\frac{v}{V} \cdot \tag{2}$$

Here M_s is the saturation moment, V is the total volume of the sample, and v is the volume of the pores alone.

The effective g factor defined by the familiar equation for a sphere

$$\omega_0 = \gamma H_0 \tag{3}$$

(with H_0 being the applied resonance field and $\gamma = g\ e/2$ mc) varies with porosity and anisotropy. The true polycrystalline g factor should be calculated from[12]

$$\omega_0 = \gamma(H_0 + H_i), \tag{4}$$

where H_i is an "internal field" which depends on anisot-

[7] J. E. Pippin and C. L. Hogan, "The Preparation of Polycrystalline Ferrites," Harvard Univ. Gordon McKay Lab., Cambridge, Mass., Sci. Rep. No. 8, Contract AF 19(604)-1084; July, 1957.

[8] J. O. Artman and P. E. Tannenwald, "Measurement of susceptibility tensor in ferrites," *J. Appl. Phys.*, vol. 26, pp. 1124–1132; 1955.

[9] E. G. Spencer, R. C. LeCraw, and F. Reggia, "Measurement of microwave dielectric constants and tensor permeabilities of ferrite spheres," 1955 IRE Convention Record, pt. 8, pp. 113–121.

[10] S. Blum, J. Zneimer, and H. Zlotnick, "The effects of ceramic parameters on the microwave properties of a nickel ferrite," *J. Amer. Ceram. Soc.*, vol. 4, p. 143; May, 1957.

[11] E. Schlömann, "The Microwave Susceptibility of Polycrystalline Ferrites in Strong DC Fields and the Influence of Nonmagnetic Inclusions of the Microwave Susceptibility," presented at Conference on Magnetism and Magnetic Materials, Boston, Mass.; October, 1956.

[12] This equation was suggested by T. Okamura, Y. Torizuka, and Y. Kojima, "The g factor of ferrites," *Phys. Rev.*, vol. 88, pp. 1425–1426; December 15, 1952.

ropy and porosity.[13–15] Schlömann's theoretical work gives for the internal field

$$H_i = \frac{-K_1}{2M_s} + \frac{4\pi M_s}{2} \frac{1}{\frac{V}{v} + 1}, \qquad (5)$$

the anisotropy and porosity contributions being given by the two terms, respectively. The effective g factor defined by (3) is the one of greatest engineering interest, and is the one reported here. Thus it will be expected to vary with cobalt content.

One other effect should be mentioned before the data are presented. It is well known that most ferrites exhibit a resonance line that is steeper on the low-field side of resonance than on the high-field side. Several causes for this have been suggested. Spencer, Ault, and LeCraw[16] have attributed this to anisotropy. Artman[17] has shown that propagation effects (size effects) tend to make the line steeper on the low-field side. Schlömann's[11] theory predicts that the line will be steeper on the low-field side for ferrites with negative anisotropy (the usual case), and steeper on the high-field side for those with positive anisotropy.[18] Furthermore, he shows that porosity effects lead to a line steeper on the low-field side. The present series of ferrites with varying anisotropy can be used to check these ideas.

It is seen that porosity influences these three parameters—line width, effective g factor, and line shape—in much the same way as anisotropy. Since the densities in our nickel-cobalt ferrites are about the same throughout, however, any change in these parameters with cobalt content can be presumed to be due to the change in anisotropy.

Fig. 2 shows measured values of line width and effective g factor as a function of cobalt content. ΔH decreases to a minimum near $\alpha = 0.027$ and then increases with more cobalt addition, in the manner observed by Sirvetz and Saunders. The narrowest line width obtained was 175 oersteds. The scatter near the minimum is probably due to nonuniform distribution of cobalt throughout the ferrite, and therefore incomplete cancellation of K_1. It is assumed that K_1 starts at about -5×10^4 ergs/cm^3 at $\alpha = 0$, becomes less negative and passes through zero at $\alpha \doteq 0.027$, and then increases positively. The results are in fairly good agreement with

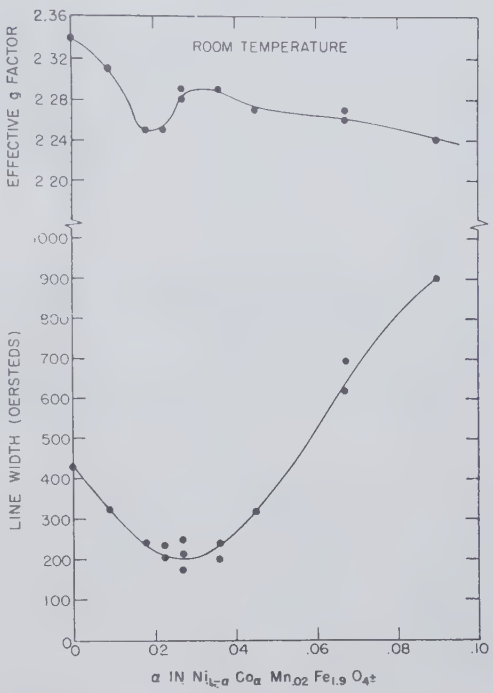

Fig. 2—Line width and effective g factor as a function of α in $Ni_{1-\alpha}Co_\alpha Mn_{0.02}Fe_{1.9}O_{4\pm}$.

(1) and (2). The line width at the minimum should be about 200 oersteds for 96 per cent density, according to (2); this is the case experimentally. Also (1) predicts that the anisotropy contribution to ΔH for nickel ferrite is about 200 oersteds, so that the line width for $\alpha = 0$ should be about 400 oersteds, adding in the effect of porosity. The observed value is 430. The *exact* amount by which anisotropy broadens a line is probably open to question, and may, in general, be a function of the density.[19]

Eqs. (3)–(5) predict a continuous decrease in effective g factor with cobalt content, in view of the uniform density of the samples. Eq. (3) gives

$$g_{\text{eff}} = \frac{f_0}{1.4H_0}. \qquad (6)$$

Let it be assumed that $H_{i_{anis}} = -AK_1/M_s$ rather than $0.5(K_1/M_s)$, as indicated in (5). Then assuming density and M_s do not change significantly for small α, and that $K_1(\alpha)$ is a simple sum of the constituent K_1's, (4) and (6) combine to give

$$g_{\text{eff}}(\alpha) = g_{\text{eff}}(\alpha = 0) - 6.4A\alpha = 2.34 - 6.4A\alpha \qquad (7)$$

for small α. Here we have used $K_1 = -5\times10^4$ for nickel ferrite and $K_1 = +2\times10^6$ for cobalt ferrite (see Bozorth, *et al.*[6]). Fig. 2 shows the decrease in g_{eff} with cobalt content. The dip near minimum anisotropy is not explained —perhaps it is due to inhomogeneities also. Except for the dip, the curve is more nearly fitted for $A = 0.2$ in

[13] Y. Kojima, "The g factor of ferromagnetic spinels," *Sci. Rep. Res. Inst., Tohoku University*, vol. A-6, pp. 614–622; December, 1954.
[14] P. A. Miles, "Ferromagnetic resonance in ferrites," *Nature*, vol. 174, pp. 177–178; July 24, 1954.
[15] T. R. McGuire, "The frequency dependence of g values in ferrites," *Proc. AIEE Conf. on Magnetism and Magnetic Material*, pp. 43–46; 1955.
[16] E. G. Spencer, L. A. Ault, and R. C. LeCraw, "Intrinsic-tensor permeabilities on ferrite rods, spheres, and disks," Diamond Ordnance Fuze Labs. Rep. No. TR-343; April 20, 1956.
[17] J. O. Artman, "Effects of size on the microwave properties of ferrite rods, disks, and spheres," *J. Appl. Phys.*, vol. 28, pp. 92–98; January, 1957.
[18] C. A. Morrison and N. Karayianis of Diamond Ordnance Fuze Labs. independently obtained a similar result, using a somewhat different model; private communication.
[19] See, *e.g.*, S. Geschwind and A. M. Clogston, "Narrowing effect of dipole forces on inhomogeneously broadened lines," *Phys. Rev.*, vol. 108, pp. 49–53; October 1, 1957.

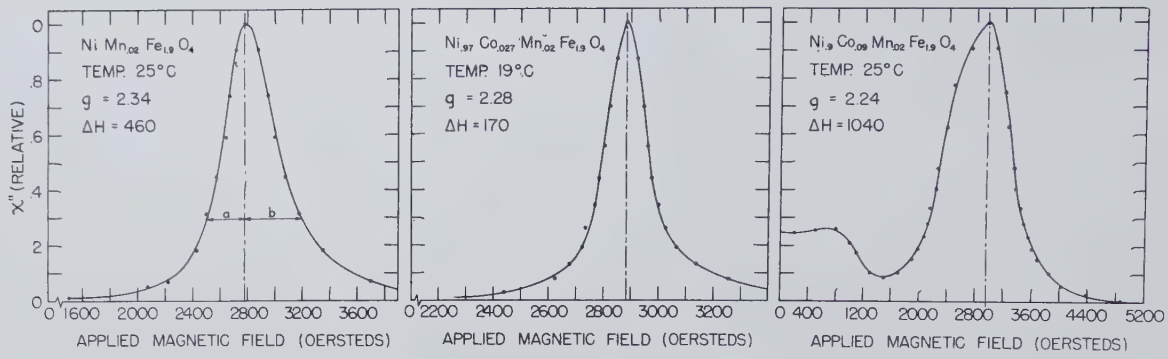

Fig. 3—Normalized resonance lines, illustrating dependence of asymmetry on the sign of K_1. For the line at left K_1 is negative; for that in the center K_1 is presumed zero; for the line at right, K_1 is positive.

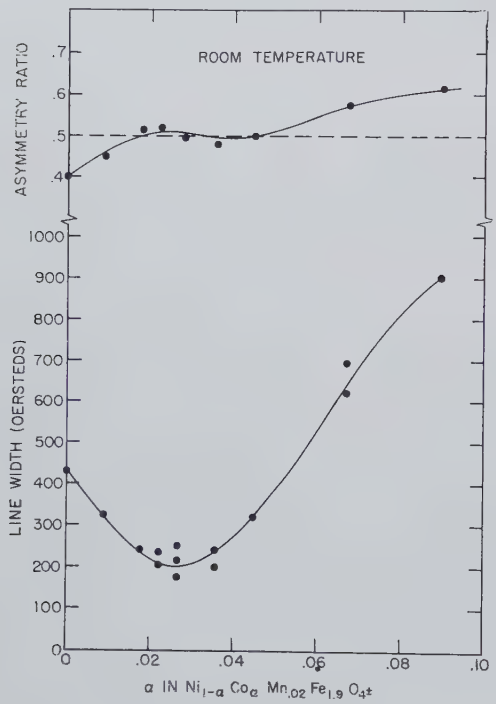

Fig. 4—Asymmetry ratio and line width vs α in $Ni_{1-\alpha}Co_{\alpha}Mn_{0.02}Fe_{1.9}O_{4\pm}$.

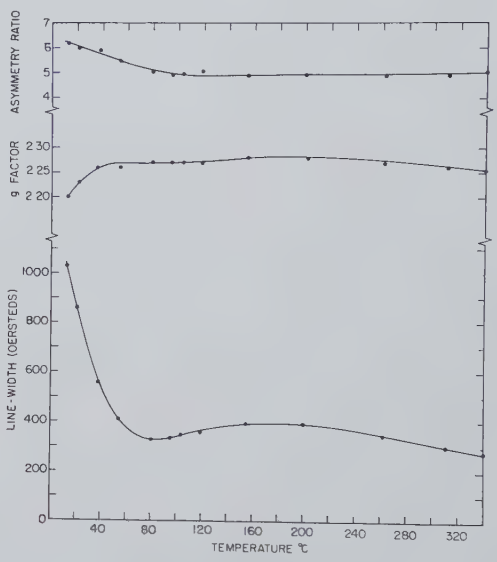

Fig. 5—Line width, effective g factor, and asymmetry ratio vs temperature for $Ni_{0.9}Co_{0.09}Mn_{0.02}Fe_{1.9}O_{4\pm}$.

(7), as suggested by Miles,[14] rather than for Schlömann's value of 0.5.

Fig. 3 shows normalized resonance lines for three values of α, and illustrates the asymmetry dependence on the sign of the anisotropy constant. For the first curve α is zero and K_1 is negative; the line is steeper on the low-field side of resonance. The second curve, for $\alpha=0.027$ and K_1 presumably zero, is almost symmetrical. The third curve, steeper on the high side, is for $\alpha=0.09$ and K_1 positive. The very slight asymmetry in the center curve may be due to porosity or inhomogeneity—sphere sizes were such that the size effect probably does not occur. In order to see how this asymmetry varies continuously with α, we may define an "asymmetry ratio" with reference to Fig. 3, first curve, as

$$\text{A.R.} = \frac{a}{a+b}. \tag{8}$$

The distances a and b are taken at a height which is 0.3 of maximum on the curve, where the asymmetry is fairly pronounced. Negative anisotropy should give a value less than 0.5 for A.R., zero anisotropy should give 0.5, and positive anisotropy a value greater than 0.5. This asymmetry ratio is plotted in Fig. 4 vs α, with ΔH on the same graph for emphasis. A.R. is 0.4 for nickel ferrite, increases to 0.5 in the region where ΔH is a minimum corresponding to zero anisotropy, and increases above 0.5 to the right of the ΔH minimum where K_1 is positive. It seems, then, that the line asymmetry in this case, where the anisotropy field is small compared to the resonance field and appreciably greater than the single-crystal line width, is caused primarily by anisotropy.

Since K_1 changes with temperature, ΔH, g_{eff}, and A.R. change with temperature. In Fig. 5 these quantities are shown for $\alpha=0.09$ for temperatures up to 340°C. The variations can be explained, qualitatively at least, purely in terms of anisotropy. Near room temperature K_1 is positive and decreasing towards zero. From the data it would appear that $K_1=0$ near 100°C; then it becomes negative with further increase in temperature and ultimately, of course, starts to drop to-

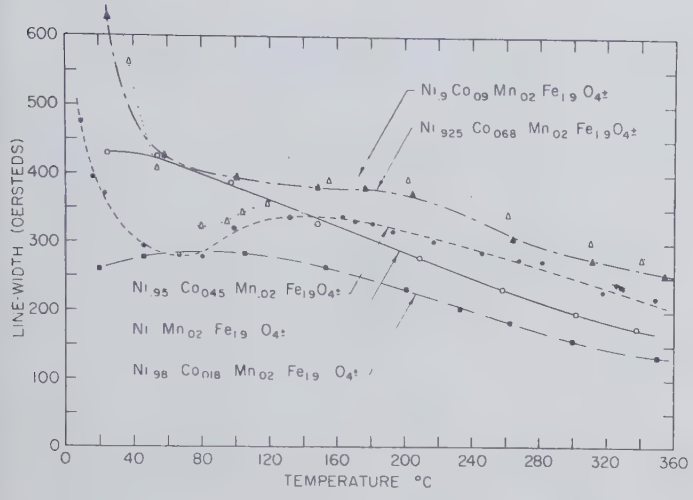

Fig. 6—Line width vs temperature for five nickel-cobalt ferrites.

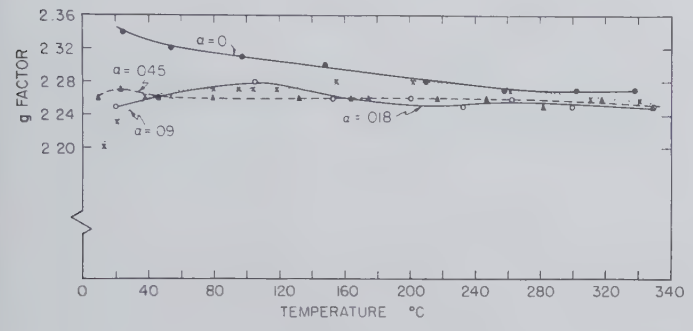

Fig. 7—Effective g factor vs temperature for four nickel-cobalt ferrites.

ward zero at still higher temperatures, as the Curie temperature is approached. The line width varies in this way, decreasing to a minimum, then increasing to a maximum, and decreasing at higher temperatures. The g factor increases as K_1 becomes less positive, reaches a plateau where ΔH is a minimum, and increases slightly as K_1 becomes negative. The asymmetry ratio behaves in the expected way, except that at higher temperatures it remains at 0.5. This is because the asymmetry ratio plotted in Fig. 5 was measured at the half-point of the line rather than at the 0.3 point, and here the asymmetry is not so sensitive to K_1.

The temperature variation of ΔH for five of the nickel-cobalt ferrites is shown in Fig. 6, while Fig. 7 shows the g factor vs temperature for four of the materials. All these curves can be explained qualitatively by considering anisotropy.

The Nickel-Cobalt Ferrite-Aluminates

In ferrites for microwave devices it would be desirable to be able to control the saturation moment, line width, and g factor independently. It was shown sometime ago[20] that the magnetization of nickel ferrite can be reduced by the substitution of aluminum for part of the iron, with some decrease in the Curie temperature.

[20] L. R. Maxwell and S. J. Pickart, "Magnetization in nickel ferrite-aluminates and nickel ferrite-gallates," *Phys. Rev.*, vol. 92, pp. 1120–1126; December 1, 1953.

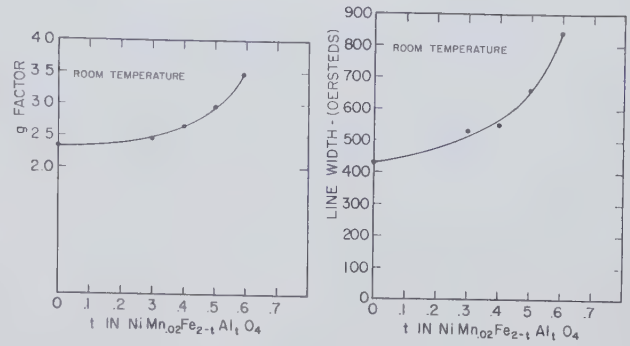

Fig. 8—Line width and effective g factor vs t in nickel ferrite-aluminate of composition Ni $Mn_{0.02}Fe_{2-t}Al_tO_{4\pm}$. Note that the point for $t=0$ was taken on composition Ni $Mn_{0.02}Fe_{1.9}O_{4\pm}$.

However, the line width and g factor increase rapidly when this is done,[21] and for some applications (*e.g.*, most low-frequency applications) this is undesirable. Fig. 8 shows these parameters at room temperature as a function of t in Ni $Mn_{0.02}Fe_{2-t}Al_tO_{4\pm}$. (Note that the point for $t=0$ was taken on a ferrite of starting composition Ni $Mn_{0.02}Fe_{1.9}O_{4\pm}$ rather than Ni $Mn_{0.02}Fe_2O_{4\pm}$.) The trend is the same as that shown by McGuire, but the numbers are different, due probably to the higher densities of our samples.

The possibility of adding cobalt to nickel ferrite-aluminate to reduce the line width and, to some extent, the effective g factor immediately arises, and it should be possible to do this without changing the saturation moment appreciably. The results for our samples of starting composition $Ni_{1-\alpha}Co_\alpha Mn_{0.02}Fe_{2-t}Al_tO_{4\pm}$ are shown in Fig. 9 and Fig. 10, with α between 0 and 0.025 and t between 0 and 0.6. The expected decrease in line width is observed although the magnitude of the decrease is not great for the higher aluminum contents. This could be a practical consequence of the ceramic techniques employed in making the materials; the saturation moment is lower for higher t, so that $|K_1|/M_s$ is large. Then slight inhomogeneities in the K_1 of the mixed ferrite would be more serious than for higher magnetizations. On the other hand, single-crystal measurements of line widths for nickel ferrite-aluminates are not available—it may be that the natural line width is larger for higher t.

The peculiar behavior of the $t=0.4$ and $t=0.5$ curves is not explained. However, Schlömann[22] has shown that these low magnetization ferrites may have shoulders on the resonance curve. In this event the line width is not very meaningful and the entire curve should be studied. Shoulders were observed on some of our samples, but complete lines were not plotted for all of them.

The g factor decreases as expected when cobalt is added. Of course, even in the absence of anisotropy, the

[21] T. R. McGuire, "Microwave resonance absorption in nickel ferrite-aluminate," *Phys. Rev.*, vol. 93, pp. 682–686; February 15, 1954.

[22] E. Schlömann, "Shape of the ferromagnetic resonance line in polycrystalline ferrites," *Bull. Amer. Phys. Soc.*, ser. II, p. 238; April 25, 1957.

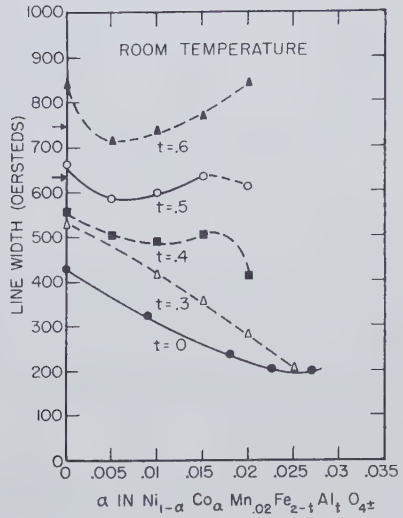

Fig. 9—Line width vs α in $Ni_{1-\alpha}Co_{\alpha}Mn_{0.02}Fe_{2-t}Al_tO_{4\pm}$. See text for comment on $\alpha=0$ values.

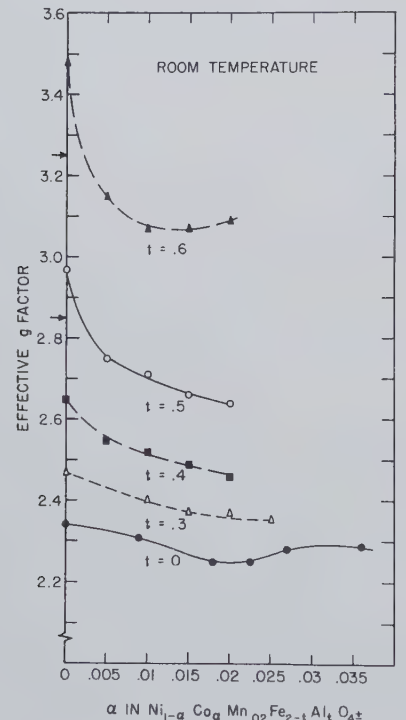

Fig. 10—Effective g factor vs α in $Ni_{1-\alpha}Co_{\alpha}Mn_{0.02}Fe_{2-t}Al_tO_{4\pm}$. See text for comment on $\alpha=0$ values.

g factor would be expected to increase with t, as the compensation point in the magnetization is approached.

The saturation moment and other properties of nickel ferrite-aluminates are very sensitive to the firing cycle. The ferrite-aluminates for $\alpha=0$ were prepared earlier and in a slightly different manner from those for $\alpha\neq0$. As a result their moments are somewhat different from those for corresponding t with $\alpha\neq0$. The properties of the samples are presented for comparison in Table I. If the differences in magnetization are taken into account, it is estimated that the intercepts (for $\alpha=0$) of the $t=0.6$ and $t=0.5$ curves of Fig. 9 and Fig. 10 should occur at the small arrows along the vertical scales.

TABLE I

Properties of the Ferrite-Aluminates of Composition $Ni_{1-\alpha}Co_{\alpha}Mn_{0.02}Fe_{2-t}Al_tO_{4\pm}$. The Values for $\alpha\neq0$ are Average Values.

Composition α	t	X-Ray Density[20]	Per Cent of X-Ray Density	Measured $4\pi M_s$ Corrected to X-Ray Density
0	0.3	5.27 gms/cm³	94.4%	1970
≠0	0.3		97.4	1980
0	0.4	5.23	97.0	1490
≠0	0.4		97.0	1570
0	0.5	5.19	95.7	1040
≠0	0.5		96.6	1190
0	0.6	5.15	93.8	710
≠0	0.6		96.6	840

Conclusion

The performance of microwave ferrite devices with large average power variations or in fluctuating ambient temperatures depends strongly on the temperature dependence of the properties of the ferrite. Here, this dependence of g and ΔH for several nickel-cobalt ferrites has been presented. It is perhaps worth while remarking that the resonance field for an isolator operating at high temperatures will be shifted not only because of the variation of M_s, as reflected through the demagnetizing fields, but also because of a change in the g factor itself. For certain cobalt contents it is also true that g and ΔH show little temperature dependence.

The reduction of ΔH and g_{eff} by addition of cobalt to nickel ferrite-aluminates has been demonstrated; another advantage that should result from this addition is a significant reduction of the maximum frequency at which low-field losses occur, in view of the reduction of $|2K_1|/M_s$—which is comparable to $4\pi M_s$ in some of the ferrite-aluminates. These examples again point up the fact that it is possible to tailor ferrite materials for a particular application, sometimes within wide limits. Thus, by adding cobalt and aluminum to nickel ferrite, $4\pi M_s$, g_{eff}, ΔH, and low-field losses can be varied; an additional control of ΔH, almost independent of the other parameters, can be realized by controlling firing temperature to obtain the desired density. The ferrite-aluminates above were fired at 1400°C in oxygen, and had relatively high dielectric losses. By using a deficiency of iron, adding some copper, and firing at 1250°C in oxygen, excellent dielectric loss tangents can be obtained with 96 per cent density.

Acknowledgment

The authors are indebted to Mrs. L. Lin and R. W. Stephens for assistance in preparing the samples, to T. Ricketts for helping to carry out the resonance measurements, to C. H. Nowlin for making the magnetization measurements, and to Dr. W. P. Wolf and G. P. Rodrigue for constructive criticism of the paper.

Ferrimagnetic Resonance in Some Polycrystalline Rare Earth Garnets*

G. P. RODRIGUE†, J. E. PIPPIN†, W. P. WOLF†, AND C. L. HOGAN†

Summary—Ferrimagnetic resonance measurements have been carried out on a series of polycrystalline garnets of composition $5Fe_2O_3 \cdot 3M_2O_3$ with M = Y, Sm, Gd, Dy, Ho, Er, and Yb. These measurements were made over a temperature range from 20°C to the Curie points (approximately 280°C). The variations of line widths and effective g values over this temperature range are reported. Y, Yb, and Sm garnets have g values of approximately 2.0 at room temperature while those of Dy, Ho, and Er are appreciably less than 2.0. High-density yttrium garnet has a line width of approximately 50 oersteds at room temperature; line widths of other members of this series were found to vary from 400 to greater than 3000 oersteds. The effective g value and line width of the gadolinium garnet tend to very high values as its compensation point (17°C) is approached. The narrow line width of the yttrium garnet is found to depend strongly on the density of the sample. When the density decreases from 96 per cent to approximately 92 per cent of the theoretical value, the line width increases from 50 to about 150 oersteds. Several technical applications in which these materials might be particularly advantageous are discussed briefly.

Introduction

THE CLASS of ferrimagnetic oxides containing iron and rare earths and having the garnet crystal structure comprise a new series of compounds similar to ferrites but different in several important respects. They were discovered by Bertaut and Forrat[1] in the course of their work on ferrites containing rare earths, and they were also identified independently by Gilleo and Geller.[2] These compounds first aroused interest because of their rather unusual saturation magnetization vs temperature curves, which were first reported by Pauthenet[3] and are shown in Fig. 1. It will be seen that several of them have a "compensation point" at which the magnetization is zero, and that all of them have rather low absolute values of M_s above room temperature. This latter fact, coupled with their moderately high Curie temperature of approximately 280°C, immediately suggests the importance of these compounds in low-frequency microwave applications. However, for a material to be useful in this connection it is also necessary that it have a reasonably low resonance g value and, more important still, a narrow line width.

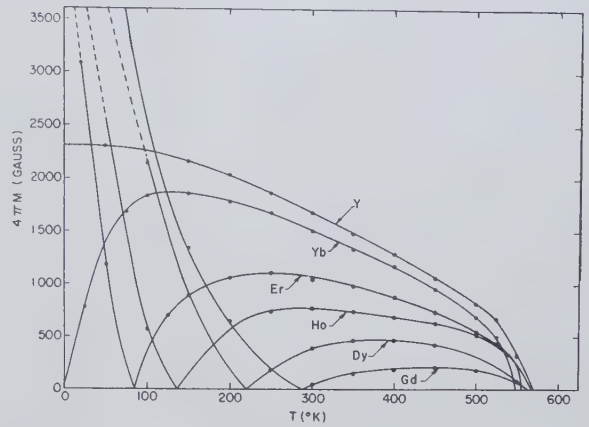

Fig. 1—Saturation magnetization vs temperature curves for $5Fe_2O_3 \cdot 3M_2O_3$ with M = Y, Yb, Er, Ho, Dy, and Gd (after Pauthenet).

In this paper we describe experiments carried out on seven different polycrystalline garnet materials to measure these two quantities from room temperature up to the Curie point.

The only previous resonance measurements reported in the literature are those of Dillon[4] on yttrium iron garnet single crystals, and Paulevé[5] on the polycrystalline gadolinium compounds. Dillon's measurements excited a great deal of interest since he reported resonance lines only a few oersteds wide, far narrower than for any ferrites previously examined. Furthermore, he found a rather low value for the anisotropy at room temperature and above, K_1/M ranging from 45 to 2 oersteds. One might expect therefore that even in the polycrystalline material line widths considerably narrower than those of ferrites might be obtained, especially if high-density materials could be made. This we have found to be the case, the line width for a sample of 96 per cent of theoretical density ranging from 50 oersteds at room temperature to 13 oersteds at 270°C. On other garnets nothing has been published concerning either the anisotropy or the natural line width. Our measurements show that none of the six other compounds we have examined are as promising as that containing yttrium, although they may prove to be useful as minor additions to the yttrium garnet.

There are several basic differences between the garnet crystal structure and the spinel structure of the ferrites. In the garnet there are three types of lattice sites for the metal ions; two of them, the 16*a* and the 24*d* are oc-

* Manuscript received by the PGMTT, July 22, 1957. This work was carried out under Contract AF 19(604)-1084 with the AF Cambridge Res. Ctr., while one of the authors, G. P. Rodrigue, was a Union Carbide and Carbon Corp. Fellow in Applied Physics.

† Div. of Eng. and Appl. Phys., Harvard University, Cambridge, Mass.

[1] F. Bertaut and F. Forrat, "The structure of ferrimagnetic ferrites of the rare earths," *Compt. Rend.*, vol. 242, pp. 382–384; January, 1956.

[2] S. Geller and M. A. Gilleo, "The crystal structure and ferrimagnetism of yttrium-iron garnet," *Acta Crystall.*, vol. 10, p. 239; March, 1957, and private communications to be published.

[3] R. Pauthenet, "Magnetic properties of rare earth ferrites $5Fe_2O_3 \cdot 3M_2O_3$ with M = Tb, Dy, Ho, Er, Tm, Yb, Lu—experimental results," *Compt. Rend.*, vol. 243, pp. 1499–1502; November, 1956.

[4] J. F. Dillon, Jr., "Ferrimagnetic resonance in yttrium iron garnet," *Phys. Rev.*, vol. 105, pp. 759–760; January, 1957.

[5] J. Paulevé, "Ferrimagnetic resonance in Gd garnet at 9300mc," *Compt. Rend.*, vol. 244, pp. 1908–1910; April, 1957.

cupied by Fe^{3+} ions and the other, the 24*c*, by the rare earth or yttrium ions. The magnetization curves shown in Fig. 1 can be explained[6,7] on the basis of Néel's theory, by postulating a strong antiparallel interaction between the ions on the 16*a* and 24*d* sites, and a weaker, also antiferromagnetic, coupling between the 24*c* and 24*d* sites. The resultant magnetization of the iron ions on the *a* and *d* sites is thus antiparallel to that of the rare earth ions on the *c* sites, and compensation points occur at temperatures where the magnitudes of the two magnetizations become equal. In the yttrium compound this complication does not arise since the trivalent yttrium ion has no magnetic moment so that the magnetization arises from the iron ions alone. A detailed description of the structure and magnetostatic properties of the garnets has been given in a series of articles by the workers at Grenoble[1,3,6–9] and also at the Bell Telephone Laboratories.[2,10] The fact that all the metallic ions in the garnet are trivalent suggests another important difference between garnets and ferrites. In ferrites the simultaneous presence of ions of the same element in different valence states greatly facilitates electrical conduction and hence leads to losses in high-frequency applications. Since ferrites invariably contain metal ions of different valencies, usually 2 and 3, it is often necessary to strike a compromise in the preparation process between keeping the one type of ion oxidized and the other reduced. This is sometimes difficult although a great deal can be done by the inclusion of certain additives (*e.g.*, manganese). In garnets, on the other hand, all metal ions present are trivalent (which is normally their state of highest oxidation). Thus no compromise need be made in the firing conditions, and one would expect extremely low electrical losses. The loss tangents for our various samples shown in Table I, opposite, indicate that this is indeed the case, when it is remembered that these were "pure" stoichiometric samples, free from any beneficial additives.

The other remarkable feature of the garnet structure is that all of the *a*, *c*, and *d* sites allowed for metal ions are filled, as compared with ferrites in which only half the *A* and *B* sites are randomly filled. This fact is important in connection with the mechanisms giving rise to the "natural" ferrimagnetic resonance line width,[11] as well as in aiding the interpretation of the other basic physical properties.

[6] R. Pauthenet, "Interpretation of the magnetic properties of ferrites $5Fe_2O_3 \cdot 3M_2O_3$ with M = Y, Gd, Tb, Dy, Ho, Er, Tm, Yb, Lu," *Compt. Rend.*, vol. 243, pp. 1737–1740; November, 1956.

[7] L. Néel, "On the interpretation of the magnetic properties of rare earth ferrites," *Compt. Rend.*, vol. 239, pp. 8–11; July, 1954.

[8] R. Aléonard, J. Barbier, and R. Pauthenet, "Magnetic properties of yttrium ferrite $5Fe_2O_3 \cdot 3Y_2O_3$ of the garnet type," *Compt. Rend.*, vol. 242, pp. 2531–2533; May, 1956.

[9] R. Pauthenet, "Magnetic properties of gadolinium ferrites," *Compt. Rend.*, vol. 242, pp. 1859–1862; April, 1956.

[10] S. Geller and M. A. Gilleo, private communication to be published.

[11] A. M. Clogston, H. Suhl, L. R. Walker, and P. W. Anderson, "Ferromagnetic resonance line width in insulating material," *J. Phys. Chem. Solids*, vol. 1, no. 3, pp. 129–136; 1956.

Materials

The chemical formula for the ferrimagnetic garnets is $5Fe_2O_3 \cdot 3M_2O_3$ where M denotes a trivalent rare earth ion from samarium to lutecium, or yttrium. For the present investigation samples were prepared with M = Sm, Gd, Dy, Ho, Er, Yb, and Y, using the coprecipitation technique described elsewhere.[12] This method has the advantage of producing high-density, low-loss materials whose chemical composition can be accurately controlled even on a small scale preparation. X-ray powder diffraction patterns were taken on all the samples using a General Electric XRD5 spectrometer. No lines other than those characteristic of the garnet structure were found. The lattice constants determined from the patterns are in good agreement with those found by Bertaut, *et al.*, and by Gilleo and Geller, as seen in Table I. Measurements of magnetic moment at room temperature, kindly made for us by C. H. Nowlin using a pendulum magnetometer, yielded values of $4\pi M_s$ given in column 8. The values are given in Gauss adjusted to the theoretical X-ray density. Values of $4\pi M_s$ calculated from Pauthenet's published magnetization curves in Bohr magnetons/molecule are shown in column 9. It will be seen that there is some systematic discrepancy. This may be due in part to difficulty in reading values off Pauthenet's curves.

Experimental Procedure

Resonance measurements were made on small (0.015-inch to 0.035-inch) spherical samples at *X* band, using a reflection-type apparatus similar to that described by Artman and Tannenwald[13] and by Spencer, LeCraw, and Reggia.[14] To minimize wall effects the spheres were placed about $1\frac{1}{2}$ diameters off the center of the end wall of the rectangular cavity. The cavity was operated in the TE_{101} mode at a resonant frequency of 9208 mc at room temperature, decreasing by 40 mc as the temperature was raised to 300°C. The cavity was made of copper and continuously flushed with dry nitrogen gas to prevent corrosion at high temperatures. Temperatures up to 300°C were obtained by a small furnace completely surrounding the cavity. The temperatures were measured, with an accuracy of ± 3°C, by means of an iron-constantan thermocouple attached to the cavity wall.

The reflection coefficient of the cavity (and therefore the standing wave ratio in front of the cavity) was measured by sampling the direct and reflected signals and comparing them after detection, using two crystal detectors calibrated to agree within ± 0.05 db over the range of signal variations. A HP X382A precision cali-

[12] W. P. Wolf and G. P. Rodrigue, "The Preparation of Polycrystalline Ferrimagnetic Garnet Materials for Microwave Applications," Harvard Univ. Gordon McKay Lab., Cambridge, Mass., Contract AF 19(604)-1084 Sci. Rep. No. 9; also to be published.

[13] J. O. Artman and P. E. Tannenwald, "Measurement of susceptibility tensor in ferrites," *J. Appl. Phys.*, vol. 26, pp. 1124–1132; September, 1955.

[14] E. G. Spencer, R. C. LeCraw, and F. Reggia, "Measurement of microwave dielectric constant and tensor permeabilities of ferrite spheres," 1955 IRE Convention Record, pt. 8, pp. 113–121.

TABLE I

$3M_2O_3 \cdot 5Fe_2O_3$

M	Lattice Constant (in A°)		Density (exp.) in gm/cc	Theoretical X-Ray Density in gm/cc	Per Cent Density	Dielectric Loss tan (at 20 mc)	$4\pi M_s$ (Gauss ±Per Cent)	$4\pi M_s$ (Gauss) (Pauthenet)	ΔH Oersteds at Room Temp.
		(Bertaut *et al.*)							
Y	12.360±0.007	12.36	4.95	5.190	95.5	~0.003	1740±3.6	1680	50
Sm	12.505±0.005	12.52	5.11	6.265	82	~0.002	1695±5.4		2500
Gd	12.445±0.005	12.44	6.22	6.490	96	~0.0015	169±4.2	50	
Dy	12.385±0.005	12.38	6.08	6.701	91	~0.004	537±3.2	400	
Ho	12.350±0.005	—	6.05	6.811	89	~0.0015	976±3.6	780	
Er	12.330±0.005	12.33	6.33	6.892	92	~0.004	1308±3.6	1100	1400
Yb	12.283±0.005	—	6.08	7.097	86	~0.0025	1640±6	1500	530

brated attenuator in the direct arm was used to measure the change in reflected power with magnetic field. Its absolute accuracy, guaranteed by the manufacturer to be within 2 per cent, was found to agree well with a second attenuator of the same type. From the measured reflection coefficients it is possible to calculate the imaginary part (χ_{xx}'') of the diagonal component of the "external" susceptibility tensor, using standard Bethe-Schwinger perturbation theory. In mks units χ_{xx}'' is given by

$$\chi_{xx}'' = \frac{V}{4\Delta v}\left(\frac{\lambda_g}{\lambda_0}\right)^2 \frac{1}{Q_e}(\rho - \rho_0),$$

where

V = volume of the cavity,
Δv = volume of the sample,
λ_g = wavelength in the empty cavity,
λ_0 = free space wavelength,
Q_e = "external" or radiation Q of the cavity,
ρ = vswr in front of the loaded cavity at some applied H field,
ρ_0 = vswr in front of the empty cavity.

The estimated accuracy in the absolute values of χ_{xx}'' is approximately 20 per cent. Relative measurements, from which line width and effective g values are determined, are more accurate. Line widths are estimated to be accurate to 5 per cent except for the samples having extremely wide lines (Sm and Ho), for which the error may be as large as 10 per cent.

Because the magnetic field was measured with extreme accuracy by means of nuclear magnetic resonance, errors in g factor are due primarily to uncertainty in adjusting the magnetic field for maximum absorption, and thus they depend strongly on the line width of the particular sample. For yttrium garnet, with a line width of 50 oersteds, the error is about 0.2 per cent while the g factors of samarium and holmium garnets are accurate to about 2 per cent.

Results

Room Temperature Measurements

At room temperature, four of the seven samples gave a ferrimagnetic resonance absorption for magnetic fields in the range zero to 6100 oersteds. The absorption

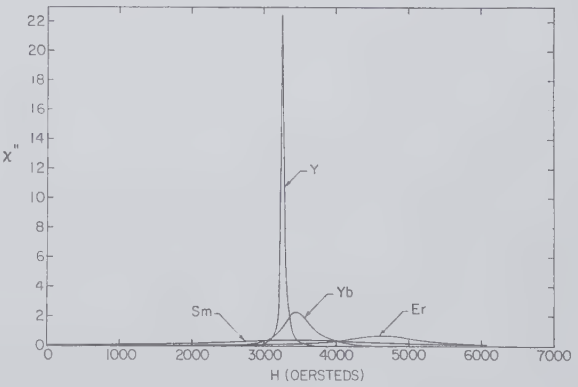

Fig. 2—Room temperature curves of χ_{xx}'' (mks values) vs H.

curves, expressed in absolute mks units of χ'' are shown in Fig. 2. It will be seen that the yttrium garnet has by far the narrowest line width (~50 oersteds) and correspondingly the largest value of χ''. For greater ease of comparing the line widths and resonance field values, these absorption curves were normalized to the same peak height; the results are shown in Fig. 3 where each line is compared to that of yttrium. The absence of resonance in the cases of the holmium and dysprosium garnets was explained by measurements made at higher temperatures (see below) which indicated that the resonance field at room temperature is greater than 6100 oersteds, our highest available field. Resonance in the gadolinium garnet was also observed at higher temperatures, and here the results indicated a trend towards broader and weaker lines as the magnetic compensation point at about 17°C was approached.

In order to detect the possible effect of sphere size on observed g factor and line width, spheres of at least two different diameters were tried for all samples. When the diameter was doubled from 15 to 30 mils, no appreciable effect on the g factor was observed beyond the limits of experimental error mentioned previously. This doubling of the sphere diameter increased the observed line width in all samples by roughly 10 per cent. The values quoted below refer to the smallest sphere in each case.

The effective g factors reported here were calculated from the well-known equation

$$\omega_0 = \gamma H_0 \qquad (1)$$

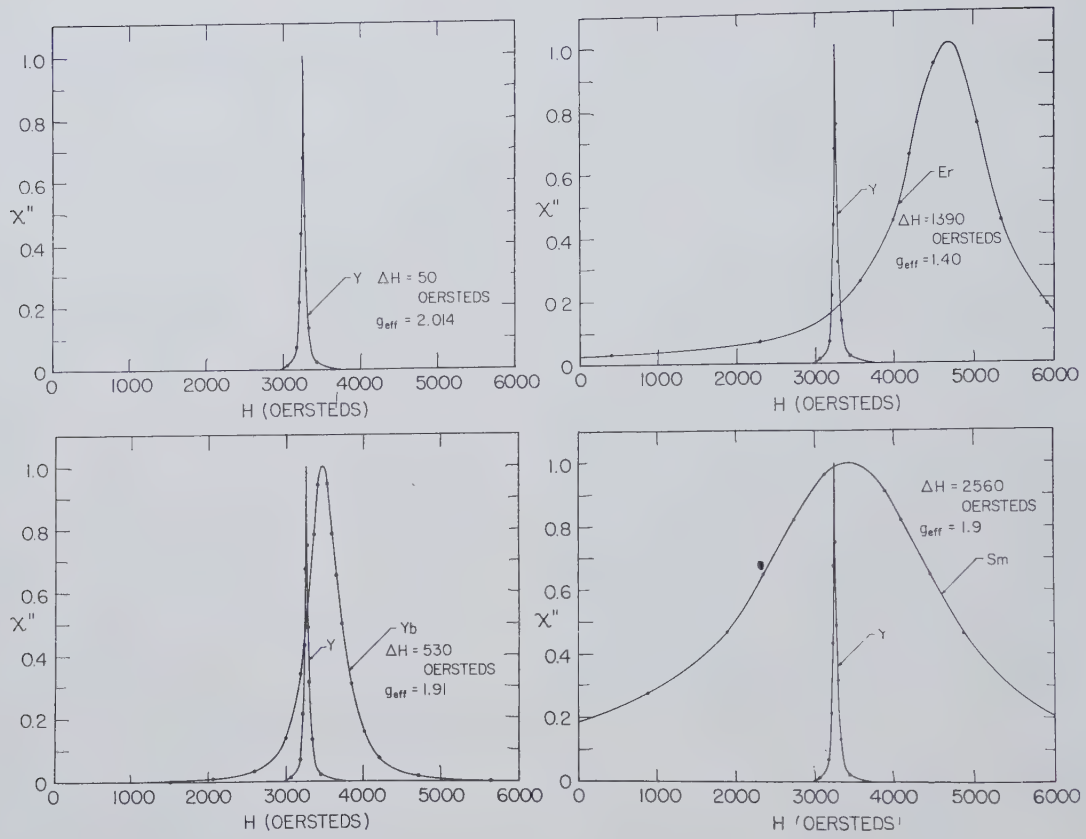

Fig. 3—Normalized room temperature curves of χ_{xx}'' vs H.

where $\gamma = g_{eff}(e/2mc)$, and H_0 is the resonance field. However, Okamura *et al.*[15] have observed that the effective g factor is frequency dependent, and they attributed this to the existence of an apparent internal field H_i. Thus the true g factor should be determined from

$$\omega_0 = g_{true}\frac{e}{2mc}(H_0 + H_i). \tag{2}$$

Kojima[16] and McGuire,[17] noting the effect of porosity on g factor, have suggested that this internal field must, in part at least, be dependent upon the density of the sample. This density effect and the shift in resonant field due to anistropy have been treated theoretically by Schlömann,[18] who has obtained for the internal field of (2) the expression

$$H_i = \frac{4\pi M_s}{3}\frac{v}{V} + \frac{1}{4}H_a, \tag{3}$$

where V is the total volume of the sample, v the volume of all pores, and $H_a = 2K_1/M$, K_1 being the first order anisotropy constant. As the density effect is directly proportional to the magnetization, it should for our samples be most important in the yttrium compound. Samples of yttrium garnets with densities varying from 81 to 96 per cent of the theoretical X-ray density were tested. Fig. 4 shows the agreement with Schlömann's theory. The experimental points for the internal field were calculated by combining (1) and (2) to give

$$H_i = \left(\frac{1}{g_{true}} - \frac{1}{g_{eff}}\right)\frac{f_0}{1.400}.$$

The true g factor was taken from Dillon's single crystal measurements at room temperature, and g_{eff} is that observed in samples of the various densities; f_0 is the frequency in mc. The large uncertainty at the lower densities is due to difficulties in obtaining true spheres from the lower density materials. The slope of the theoretical line was determined by the saturation magnetization, and the line was then drawn so as to obtain the best agreement with the experimental values. The intercept corresponding to 100 per cent density indicates a value for $\frac{1}{4}H_a$ of the order of 15 to 20 oersteds, in satisfactory agreement with Dillon's value. The densities are those measured on the gross sample and represent a minimum density of the sample. They may be in error by 3 per cent.

Schlömann[18] has also treated the effect of density on

[15] T. Okamura, Y. Torizuka, and Y. Kojima, "The g factor of ferrites," *Phys. Rev.*, vol. 88, pp. 1425–1426; December 15, 1952.
[16] Y. Kojima, "The g factor of ferromagnetic spinels," *Sci. Rep. Res. Inst., Tohoku University*, vol. A-6, pp. 614–622; December, 1954.
[17] T. R. McGuire, "The frequency dependence of g values in ferrites," *Proc. AIEE Conf. on Magnetism and Magnetic Materials*, pp. 43–46; 1955.
[18] E. Schlömann, "The Microwave Susceptibility of Polycrystalline Ferrites in Strong DC Fields and the Influence of Nonmagnetic Inclusions on the Microwave Susceptibility," presented at Conference on Magnetism and Magnetic Materials, Boston, Mass.; October, 1956.

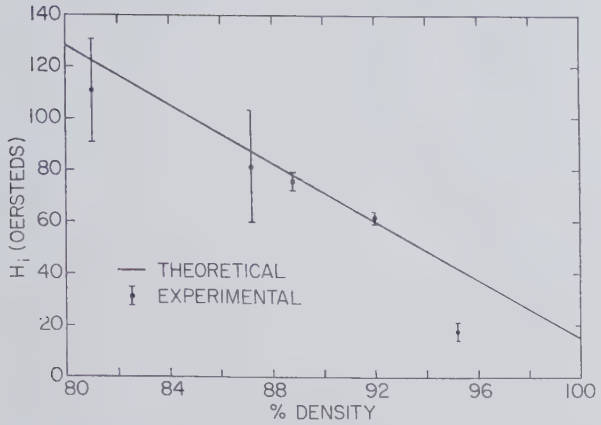

Fig. 4—Internal field of (3) as a function of density. Slope of theoretical line determined by $4\pi M_s = 1680$ Gauss. Best fit with experimental points obtained with $H_a \doteq 15$ oersteds.

line width. He suggests that the line broadening due to pores alone would be given by

$$\Delta H_{\text{pores}} = 1.5(4\pi M_s) \frac{1}{\frac{V}{v} + 1} \cdot \qquad (4)$$

This effect is observed to be of great importance in the yttrium garnet because of its extremely small intrinsic line width and low anisotropy field. Fig. 5 shows the experimentally observed line widths and the theoretical curve representing the line broadening due to pores *alone*, as calculated from (4). Again the densities may be in error by 3 per cent.

The close agreement suggests that in this material, in which K_1/M is known to be small compared with $4\pi M$, anisotropy contributes very little to the line width, in agreement with the recent theory of Geschwind and Clogston[19] on dipolar narrowing. It appears that the intrinsic line width of a 100 per cent dense polycrystalline yttrium garnet sphere at room temperature would be considerably narrower than the 50 oersteds reported here. It is obvious that to take full advantage of the narrow line widths in polycrystalline yttrium garnets extremely high densities must be obtained. In even a 93 per cent dense sample most of the line broadening is due to pores.

A close examination of the shape of the resonance curves shows that all of them are slightly asymmetric, particularly on the lower parts of the χ'' curves, as can be seen in Fig. 3 and Fig. 6. For Y, Gd, and Yb, the wings of the resonance curves are steeper on the low field side, while those of Er, Ho, and Sm are steeper on the high field side. If the polycrystalline line width were entirely due to anisotropy broadening this would indicate, according to Schlömann's theory,[18] that Y, Gd, and Yb have negative anisotropies while those of Ho, Er, and Sm are positive. However, if the line widths were entirely due to anisotropy, we would expect very

[19] S. Geshwind and A. M. Clogston, private communication.

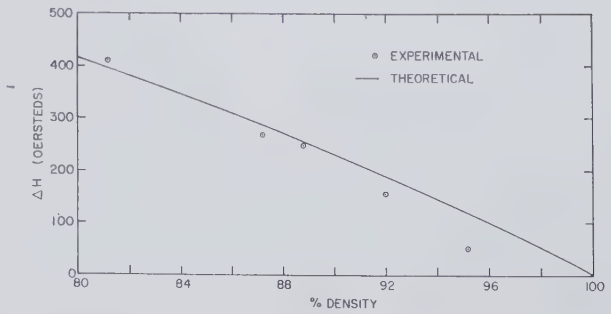

Fig. 5—Line width of yttrium garnet as a function of density. Theoretical curve calculated from (4).

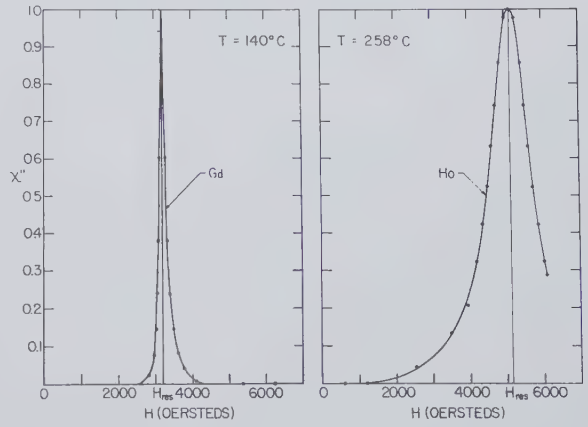

Fig. 6—Resonance lines in polycrystalline holmium and gadolinium garnets.

much larger asymmetries than those observed, and we must suspect therefore that there are other important contributing factors. In the yttrium garnet we know that porosity plays an important role in determining the line width while preliminary measurements on single crystals of the gadolinium and samarium garnets have shown that even single crystals have line widths very close to those reported here for the polycrystalline materials. It must be concluded, therefore, that there is no simple relationship between the asymmetry and the sign of the anisotropy in these materials, and in fact some recent measurements have shown that the samarium garnet has a negative anisotropy, with K_1/M of only about 120 oersteds. The line width of the samarium garnet single crystal was found to be about 2000 oersteds at room temperature, approximately independent of crystal orientation. Measurements on single crystals of gadolinium garnet by R. L. White (private communication) have shown that the line width depends markedly on crystalline orientation and varies from about 1000 oersteds at 20°C to about 140 oersteds at 90°C. K_1 was found to be negative.

High-Temperature Measurements

Ferromagnetic resonance measurements were made as a function of temperature on all samples from room temperature to the Curie points, which for all the seven materials are in the range of 265° to 280°C.

The variation of effective g factor with temperature

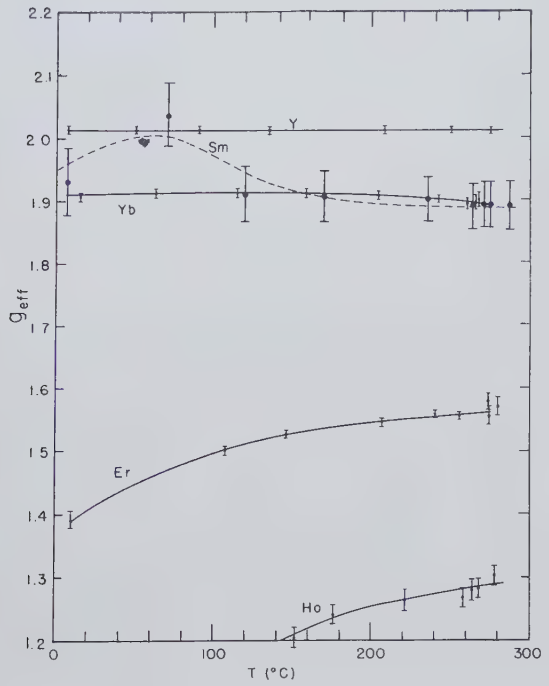

Fig. 7—Temperature variations of the effective g value in polycrystalline garnets.

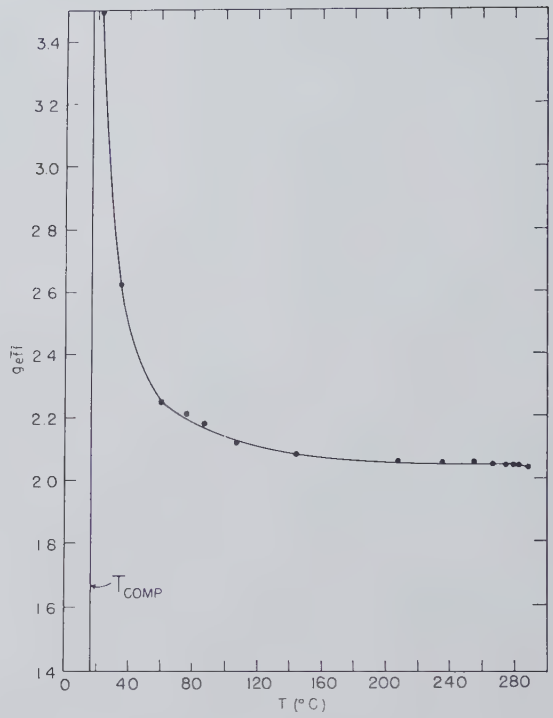

Fig. 8—Effective g value of gadolinium garnet as a function of temperature. ($T_{comp}=17$°C.)

for Y, Yb, Er, Ho, and Sm garnets is shown in Fig. 7, and for Gd garnet in Fig. 8. It will be seen that all of them with the exception of the yttrium compound have g factors which are temperature dependent and appreciably different from 2. There may be several factors contributing to this. As the temperature changes both the anisotropy and the magnetization change and hence the internal field H_i, given by (3), changes. Moreover, in all but the yttrium and gadolinium garnets there are ions having orbital angular momentum which will be partially quenched in the solid. The effect of the quenching may be expected to change with temperature and this will be reflected by a change in g factor. For the gadolinium garnet g moves towards extremely large values as the compensation point T_c, is approached. This has also been reported by Paulevé.[5] It is probably due to the combined effects of anisotropy shift and of the existence of slightly different compensation points for the total magnetization and the total angular momentum.

At high temperatures where the shift in g due to anisotropy and porosity is negligible, the g factor observed on the yttrium garnet ($g_{eff}=2.011\pm0.002$) agrees very well with that reported by Dillon[4] on a single crystal at the same temperature ($g=2.009\pm0.002$).

The peak of the holmium resonance curve was first observed below 6100 oersteds at about 140°C. The peak in the resonance line of the dysprosium garnet was not found below 6100 oersteds at any temperature, though the lower wing of the line was plainly observable at the highest obtainable fields at temperatures above 240°C. Thus its effective g factor remained less than 1.2.

The results of measurements of line width vs temperature for Yb, Er, Sm, and Ho garnets is shown in Fig. 9 and for yttrium and gadolinium in Fig. 10. The minimum line width on all curves occurs at temperatures slightly below the Curie point reported by Pauthenet.[3] The sudden increase in the vicinity of 270° to 280°C was observed in all samples. It is probably due to the combined effect of several causes: near the Curie point M tends to small values very rapidly while K_1 tends to zero more slowly.[20] Thus K_1/M would increase as M decreases. This would cause an increase in the line width both by increasing the usual anisotropy broadening and also by reducing the effect of dipolar narrowing as suggested by Geschwind and Clogston. Near the Curie point, even in single crystals, the effect of exchange interaction also becomes small and thus the usual exchange narrowing, which leads to lines considerably narrower than would otherwise be expected on the basis of magnetic dipole—dipole interaction—ceases to operate. A sharp increase in the line width of a single crystal has been observed by Dillon[21] in yttrium garnet near the Curie point. The narrowest line observed below the Curie point in the polycrystalline material was 13 oersteds for the yttrium compound at 272°C. It should be noted that a substantial part of this decrease from the value at room temperature is due to the lessening of porosity broadening as the magnetization decreases.

It can be seen from Fig. 9 and Fig. 10 that the curves of line width vs temperature for all the garnet materials studied have the same general shape, with the obvious

[20] W. P. Wolf, to be published.
[21] J. F. Dillon, Jr., private communication.

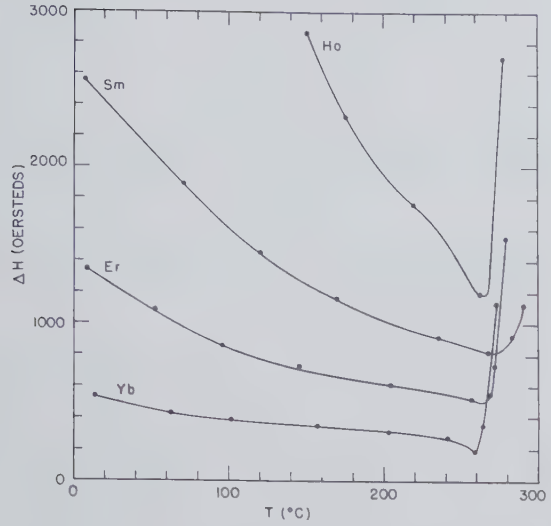

Fig. 9—Line width vs temperature in polycrystalline garnet materials.

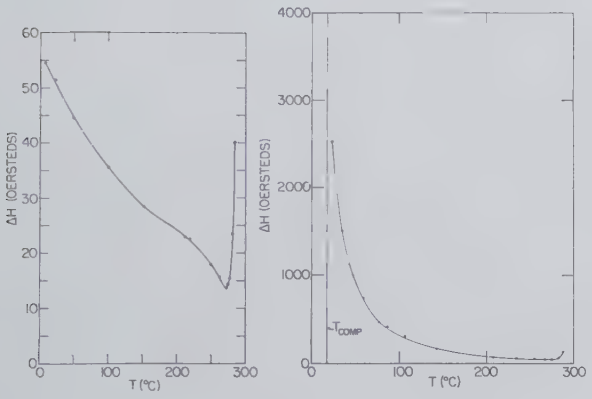

(a) (b)

Fig. 10—(a) Line width of yttrium garnet as a function of temperature. (b) Line width of gadolinium garnet as a function of temperature.

exception of that of the gadolinium garnet, which has a compensation point near room temperature. The anomalous behavior of the gadolinium garnet in this range of temperature is of course to be expected, since the effective anisotropy field, $2K_1/M$, grows rapidly as M tends to zero at the compensation point. The recent experiments on single crystals quoted above have shown, however, that this is not the only cause for the increase in line width and that there is also a considerable contribution from the intrinsic line width of the individual crystallites.

A Discussion of Technical Applications

Because of their unusual properties the garnets offer unusual possibilities in low frequency microwave applications. Hogan[22] and Lax[23] have discussed the low-frequency problem in some detail.

[22] C. L. Hogan, "The low-frequency problem in the design of microwave gyrators and related elements," IRE Trans., vol. AP-4, pp. 495–501; July, 1956.

[23] B. Lax, "Frequency and loss characteristics of microwave ferrite devices," Proc. IRE, vol. 44, pp. 1368–1386; October, 1956.

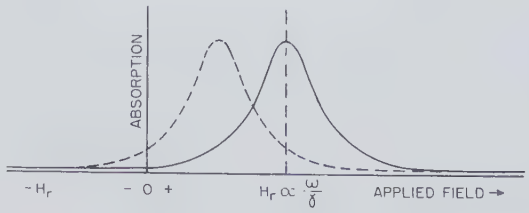

Fig. 11—Depicting absorption curve in an isolator neglecting all phenomena except ferromagnetic resonance. The dotted curve is for a lower frequency or higher γ.

We will discuss here the very important materials aspect of the low-frequency problem with the realization that certain design techniques can significantly modify any numerical results which are obtained. For simplicity the infinite medium theory as discussed by Hogan will be used. It does not apply quantitatively in waveguides, of course, but it is useful for comparison purposes and for helping to make the physical picture more concrete.

Consider the resonance absorption isolator. Fig. 11 depicts the absorption curve, neglecting all phenomena except ordinary ferromagnetic resonance. For positive circular polarization the absorption peak occurs at a field H_r which is proportional in some way (depending on the geometry) to ω/γ. For negative circular polarization the insertion loss is determined in part by the tail of the absorption line at $-H_r$. The narrower the line, the lower the absorption on the tail for a given H_r, and the higher the peak for a given magnetic moment. For lower frequency or higher γ the line moves toward lower fields and the back-to-front ratio decreases, *i.e.*, the isolator deteriorates. This simple physical picture demonstrates the desirability of low g values and narrow line widths at low frequencies. The g value of polycrystalline yttrium garnet is for practical purposes 2.0,[24] and the line width 50 oersteds at room temperature. These numbers show a striking advantage over ordinary ferrites with equivalent Curie temperature (~300°C), where one might expect line widths no smaller than about 200 oersteds. In even denser yttrium garnet the line width might be reduced to around 30 oersteds, as previously discussed, with the attendant improvement in low-frequency operation. Furthermore, some of the garnets have very low g values (Er, 1.4; Ho and Dy, 1.2).

The physical picture discussed here is informative, but the problem is more correctly treated by solving mathematically for the attenuation in terms of the intrinsic properties of the material. Hogan[22] has done this in terms of circularly polarized waves in an infinite medium, and he finds for the back-to-front ratio,

$$R = \sqrt{128\left(\frac{\omega}{\gamma\Delta H}\right)^3}, \qquad (5)$$

[24] In the nickel ferrite-aluminates which have been developed for low-frequency applications (see Pippin and Hogan, this issue, p. 77) the g value is significantly greater than 2.

where ΔH is the line width. This can be rearranged to give

$$\omega_{\min} = \frac{\gamma \Delta H R^{2/3}}{5.0} . \tag{6}$$

This is the minimum frequency for a given back-to-front ratio. If a ratio of 10 is desired, this gives

$$\frac{\omega_{\min}}{\gamma} = 0.92 \Delta H. \tag{7}$$

Inserting $\gamma = 2.8$ mc/oersted and $\Delta H = 50$ oersteds,[25] the values for the yttrium garnet, one gets

$$f_{\min} \doteq 130 \text{ mc.}$$

By comparison a ferrite with $\Delta H = 200$ oersteds would give $f_{\min} = 520$ mc.

The narrow line width has been made to look attractive in this discussion; however, the more narrow line width materials tend to deteriorate more rapidly at high powers, and this can be a serious limitation. On the other hand, the narrow line yttrium garnet should prove extremely effective in all microwave devices designed to exploit nonlinear behavior, such as passive limiters. Others such as frequency doublers, mixers,[26] and detectors[27] depend on the ability of the magnetization vector to "fan out" in large precessional motion, and this motion is accentuated in narrow line width materials. With respect to the detector, magnetostrictive properties of the material are important; little, if anything, is known about magnetostriction in the garnets at this time.

While dealing fancifully with 130-mc isolators, we have neglected some important considerations at low frequencies. The material must be magnetized for the theory to apply, and to gain the most from the ferromagnetic absorption phenomenon. The resonance field for extremely low frequencies may be insufficient to magnetize the material unless care is taken in choosing the geometry. A field necessary for saturation is approximately equal to the demagnetizing field plus the anisotropy field and in this respect the yttrium garnet is favorable, having an anisotropy field of only 90 oersteds at room temperature. As an example, a long thin slab magnetized perpendicular to the plane of the slab has a resonance field given roughly by

$$H_r = \frac{\omega}{\gamma} + 4\pi M.$$

The field necessary to magnetize it is

$$H_{\text{mag}} = 4\pi M + H_{\text{anis}},$$

and so if the resonance field is to magnetize the slab, then

$$\frac{\omega}{\gamma} \geq H_{\text{anis}} = \frac{2K_1}{M} .$$

For yttrium garnet, with $2K_1/M = 90$, this requires that

$$f \geq 250 \text{ mc.}$$

For comparison, nickel ferrite with $H_{\text{anis}} = 400$ and $g = 2.34$ would require

$$f \geq 1300 \text{ mc.}$$

Up to now the low field losses have been neglected. These losses occur because of domain structure in incompletely magnetized materials, and have been studied in the ferrites by Rado and others.[28] There is insufficient information to describe these losses quantitatively at present, and such losses have not yet been measured at all in the garnets. Nevertheless, it has been shown[29] that in general, zero field losses extend up to a frequency of

$$\omega_{\max} = \gamma(H_{\text{anis}} + 4\pi M_s)$$

and for yttrium garnet this gives $\omega_{\max} = 4900$ mc.

One way of lowering this limit which has been used in the past for ferrites is to reduce M_s by replacing some of the magnetic ions by aluminum. However, this also reduces the Curie point and there is a limit beyond which one cannot go in practice. Such considerations would not arise if one were to use instead an yttrium garnet with some of the yttrium ions replaced by rare earth ions with large magnetic moments (*e.g.*, Gd or Tb), since the Curie point is almost the same for all the rare earth garnets. With such a mixed garnet any value of M_s between zero and the value for the pure yttrium compound could be obtained.

Another way in which mixed garnets might become technically useful is as materials whose magnetization is almost constant over a certain range of temperatures. It can be seen from Fig. 1 that M increases with T over a considerable range of temperatures for all compounds having compensation points, while for the yttrium (and lutecium) garnets it decreases steadily with T. Thus it is easy to envisage a mixed compound whose M vs T curve would have a stationary point at any desired temperature below the Curie point and relatively little variation on either side.

The low field losses, occurring in unmagnetized media, are completely reciprocal with respect to wave propagation. This is another strong reason for having the ferrite saturated by the resonance field in an isolator; else the low field losses will produce attenuation in the forward direction and decrease the isolation ratio. This is illustrated in Fig. 12 in which the low field losses and ferromagnetic resonance losses are shown separately. Gen-

[25] This assumes the line width does not change with frequency.

[26] W. P. Ayres, P. H. Vartanian, and J. L. Melchor, "Frequency doubling in ferrites," *J. Appl. Phys.*, vol. 27, pp. 188–189; February, 1956. Also, J. E. Pippin, "Frequency doubling and mixing in ferrites," PROC. IRE, vol. 44, pp. 1054–1055; August, 1956.

[27] D. Jaffe J. C. Cacheris, and N. Karayianis, "Ferrite microwave detector," 1957 NATIONAL IRE CONVENTION RECORD, pt. 1, pp. 242–249.

[28] G. T. Rado, R. W. Wright, and W. H. Emerson, "Ferromagnetism at very high frequencies. III. Two mechanisms of dispersion in a ferrite," *Phys. Rev.*, vol. 80, p. 273; October 15, 1950.

[29] L. G. Van Uitert, J. P. Shafer, and C. L. Hogan, "Low-loss ferrites for applications at 4000 mc/sec," *J. Appl. Phys.*, vol. 25, pp. 925–926; July, 1954.

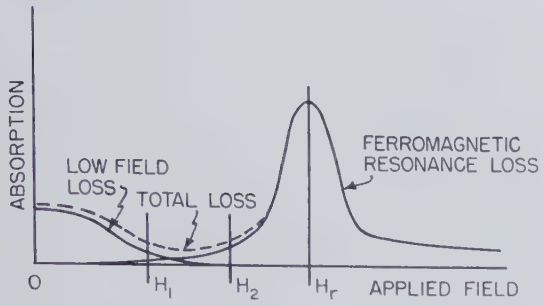

Fig. 12—The effect of low field loss on total loss in an isolator. A phase shifter would operate between H_1 and H_2.

erally the low field loss is reduced in magnitude when the saturation moment is decreased;[30] for this reason it is often desirable to have a low saturation moment even in an isolator. The moments of the garnets are relatively low.

For nonreciprocal phase shifters operating below the field required for resonance, the low frequency problem is even more difficult. Generally such phase shifters operate in the region of minimum attenuation, where the low field losses have nearly disappeared and the resonance losses have not yet become large (for example, between H_1 and H_2 of Fig. 12). For low frequencies the minimum may be very narrow or even nonexistent, as the absorption line gets closer to zero field. Then it becomes necessary to reduce the saturation moment until the low field losses do not occur. Fig. 12 also demonstrates the desirability of a narrow line width and low g factor for phase shifters.

[30] This is true for sufficiently high frequencies. For lower microwave frequencies (~1000 mc) the problem is more complicated.

Using infinite medium theory, Hogan has calculated the differential phase shift per db loss for such a phase shifter, neglecting the low field loss and including only the ferromagnetic resonance loss due to the tail of the absorption line. He finds

$$\theta/L_+ = \frac{\omega}{2.2\gamma\Delta H},$$

where θ is differential phase shift and L_+ is the attenuation of the positive circularly polarized wave. If a differential phase shift of $\pi/2$ radians with 0.5 db loss is desired, then for the yttrium garnet

$$\frac{\omega}{\gamma} \geq 380$$

or

$$f \geq 1050 \text{ mc}.$$

For a ferrite with $\Delta H = 200$, this would give $f \geq 4200$ mc. Actually both numbers are pessimistic since, for polycrystals, the absorption on the tail of the curve is usually smaller than that predicted by the Lorentzian line with the given half-width. For the numbers to be meaningful at all, the low field loss must be eliminated by making sure that the material is completely magnetized, or by reducing the saturation moment so that they do not occur.

ACKNOWLEDGMENT

The authors wish to thank Mrs. L. Lin for help in preparing samples and T. Ricketts for assistance in obtaining the resonance measurements.

Reciprocal Ferrite Devices in TEM Mode Transmission Lines*

D. FLERI† AND B. J. DUNCAN†

Summary—**Several new reciprocal ferrite devices have been designed in TEM mode transmission lines to operate over both narrow and extremely broad bandwidths in the low-microwave frequency region. These include variable attenuators, an amplitude modulator, and a traveling-wave tube equalizer. Each component utilizes the attenuation associated with gyromagnetic resonance in low saturation magnetization ferrites. The techniques used to overcome the matching problems inherent in TEM mode transmission lines when ferrite loaded, and the design considerations pertinent to each component, are treated in detail. The parameters affecting the characteristics of each device are discussed and both final design and operating characteristics of the components are presented.**

* Manuscript received by the PGMTT, August 9, 1957. This work was partially supported by the U. S. Air Force, Wright Air Development Center, Contract No. AF 33(038)-14524.

† Sperry Gyroscope Co., Div. Sperry Rand Corp., Great Neck, N. Y.

INTRODUCTION

IN recent years, considerable effort has been devoted to the design of a wide assortment of ferrite devices in various types of microwave transmission lines. Included among these are nonreciprocal ferrite

components designed in circular waveguide,[1,2] rectangular waveguide,[3–5] coaxial line,[6,7] strip transmission line,[8] and a helical transmission line.[9] However, only a limited amount of information has appeared in the literature on useful reciprocal ferrite devices designed in TEM mode transmission lines.[10,11]

It is the purpose of this paper to describe a series of reciprocal ferrite devices designed for both narrow and broad-band applications. These devices are designed in coaxial line and strip transmission line structures with particular emphasis on maintaining size and weight as small as practical. Included in this series of components are variable attenuators, an amplitude modulator, and a traveling-wave tube equalizer. The design considerations leading to the development of these components are given, as are the parameters affecting their operation. Also included are the physical design of each of these component types. Finally, the pertinent features and operating characteristics of each component are presented.

General Discussion

Gyromagnetic resonance effects are the result of a coupling between a microwave magnetic field and the electrons within a ferromagnetic medium. The greater the concentration of the microwave magnetic field, the greater is the degree of coupling. In coaxial line propagating the TEM mode, the microwave magnetic field concentration is greatest in the boundary of the center conductor and decreases inversely with radial distance. Maximum interaction between the microwave energy and a ferromagnetic material will occur at the boundary of the inner conductor and, therefore, the ferrite configuration used in the coaxial structures discussed in this paper consists of thin cylindrical tubes fitting about the center conductor. Each of the coaxial components utilizes a longitudinal biasing field and since the microwave magnetic field is linearly polarized, each of these components is reciprocal.

For purposes of analysis, the thin cylindrical ferrite tubes may be considered to exhibit the same demagnetizing factors as a thin ferrite slab when longitudinally biased. The expression relating the resonant frequency, ν_{res}, and the magnetic biasing field, H_{DC}, for a thin ferrite slab, infinite in extent, biased and saturated perpendicular to its narrow dimension is:

$$\nu_{res} = \gamma[H_{DC}(H_{DC} + 4\pi M_S)]^{1/2} \tag{1}$$

where:

γ = gyromagnetic ratio for the electron = 2.8 mc/oersted

$4\pi M_S$ = saturation magnetization of the ferrite in Gauss.

Even though the ferrites may not be completely saturated in the cases considered herein, (1) can be used as an approximate expression relating ν_{res} and H_{DC}. The approximation becomes more accurate as the wall thickness of the ferrite tube is made smaller and/or as the ferrite becomes more nearly saturated.

At a given frequency, and for a particular material, resonance attenuation is a function of ferrite length. As should be expected, the attenuation increases linearly with ferrite length and for a given length, the resonance attenuation increases with increasing frequency.

Fig. 1 demonstrates the variation of resonance attenuation with ferrite wall thickness. In the region of the curve corresponding to small wall thickness, the variation is linear. As the wall thickness becomes larger, the rate of increase of attenuation falls off. This is due in part to the decrease of the microwave field concentration with radial distance. Also, the ferrite loading gives rise to the generation of higher order modes, which causes the field pattern to be somewhat different from the pure TEM mode configuration.

The linear variation of vswr with ferrite wall thickness is also shown in Fig. 1. For a twenty-five thousandths wall, the vswr is very high, approximately 4. Even for a five thousandths wall, the vswr is appreciable, approximately 1.5. At first glance, this appears to be too high a vswr to be caused by such a thin tube. However, the incident microwave energy encounters a discontinuity greater than the actual physical discontinuity, this is, greater than the ferrite wall thickness, by a factor equal to the square root of $\mu\epsilon$, where μ is the effective permeability of the ferrite and ϵ is the dielectric constant. Since μ is about 10 or 15 at resonance, and since ϵ is of the same order of magnitude, the electrical discontinuity exceeds the physical discontinuity by a factor of 10 or greater. The discontinuity susceptance plus the change in characteristic impedance in the region of ferrite loading both contribute to the high vswr's.

The first step in reducing the vswr is to use the

[1] P. H. Vartanian, J. L. Melchor, and W. P. Ayres, "Broad-band ferrite microwave isolator," IRE Trans., vol. MTT-3, pp. 8–13; January, 1956.

[2] C. L. Hogan, "The ferromagnetic Faraday effect at microwave frequencies, and its applications: The microwave gyrator," *Bell Sys. Tech. J.*, vol. 31, pp. 1–31; January, 1952.

[3] S. Weisbaum and H. Boyet, "A double slab ferrite field displacement isolator at 11 kmc," Proc. IRE, vol. 44, pp. 554–555; April, 1956.

[4] A. G. Fox, S. E. Miller, and M. I. Weiss, "Behavior and applications of ferrites in the microwave region," *Bell Sys. Tech. J.*, vol. 34, pp. 5–103; January, 1955.

[5] P. H. Vartanian, J. L. Melchor, and W. P. Ayres, "Broad-banding ferrite microwave isolators," 1956 IRE Convention Record, pt. 5, pp. 79–83.

[6] B. J. Duncan, L. Swern, K. Tomiyasu, and J. Hannwacker, "Design considerations for broad-band ferrite coaxial line isolators," Proc. IRE, vol. 45, pp. 483–490; April, 1957.

[7] H. Seidel, "Ferrite slabs in transverse electric mode waveguide," *J. Appl. Phys.*, vol. 28, pp. 218–226; February, 1957.

[8] O. W. Fix, "A balanced stripline isolator," 1956 IRE Convention Record, p. 5, pp. 99–105.

[9] B. N. Enander, "A new ferrite isolator," Proc. IRE, vol. 44, pp. 1421–1430; October, 1956.

[10] J. H. Burgess, "Ferrite-tunable filter for use in *S*-band," Proc. IRE, vol. 44, pp. 1460–1462; October, 1956.

[11] B. Vafiades and B. J. Duncan, "An *L* band ferrite coaxial line modulator," 1957 IRE National Convention Record, pt. 1, pp. 235–241.

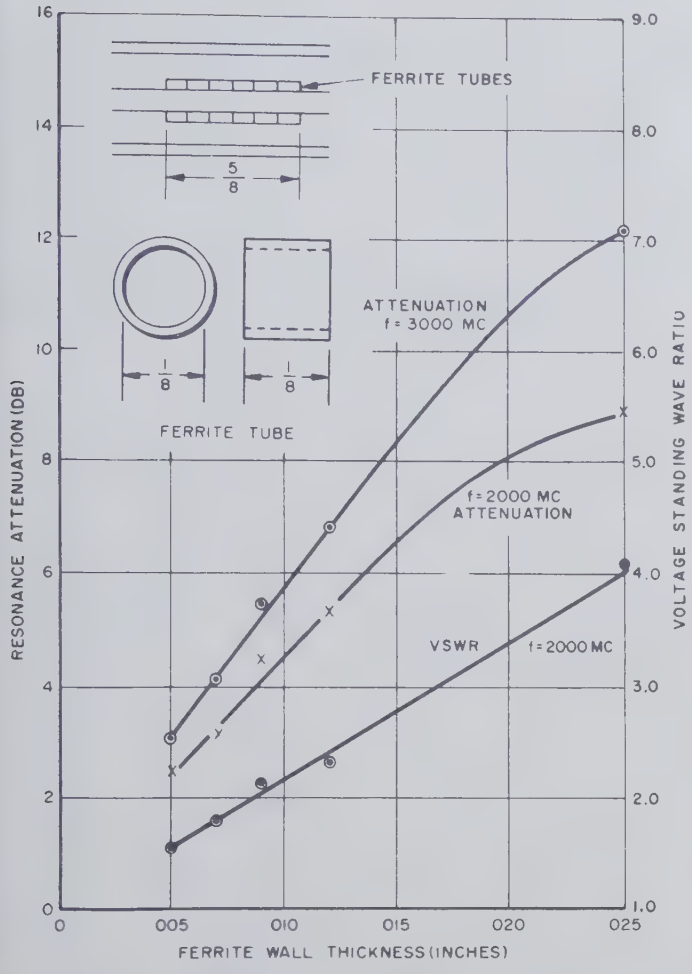

Fig. 1—Variation of gyromagnetic resonance attenuation and vswr with ferrite wall thickness.

thinnest tubes practicable. A Smith chart analysis of this structure showed that the impedance varied with frequency in an abrupt and erratic manner, both in phase and magnitude. Thus the conventional matching techniques were not effective over any appreciable bandwidth. It was found that the most effective matching technique was to space the ferrite tubes in groups of two or three along the transmission line. An optimum spacing was determined empirically such that the reflections from each of the several distributed discontinuities interfered destructively. In this way a satisfactory match was attained over very broad bandwidths.

Another TEM mode structure useful in the design of reciprocal ferrite devices is strip transmission line. The field configuration of the dominant mode is as shown in Fig. 2(a). The microwave magnetic field is most intense in plane a–b and is linearly polarized at all points in this plane. The field intensity decreases rapidly with lateral displacement and at a point, a distance w from the end of the center strip, it is 27 db below the maximum value. If a thin ferrite slab is positioned on the center strip at plane a–b, gyromagnetic resonance effects are obtained. The bias may be either longitudinal or transverse to the broad dimension of the transmission line.

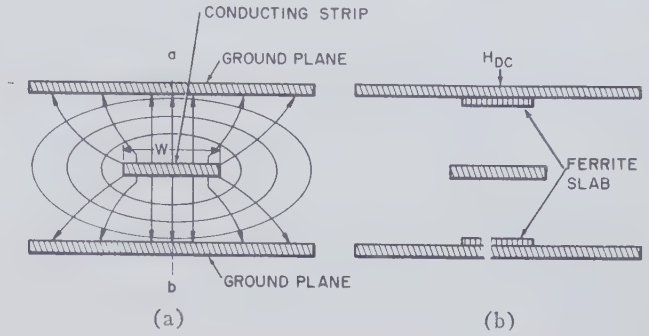

Fig. 2—(a) TEM mode field configuration of balanced strip transmission line. (b) End view of ferrite-loaded strip-transmission-line structure.

Two ferrite slabs were used: one centrally positioned on the upper ground plane, the other positioned directly below it on the lower ground plane [Fig. 2(b)]. This ferrite configuration was chosen since it preserves the symmetry of the transmission line and gives a reasonable match. The dc magnetic bias was applied transverse to the broad dimension of the transmission line.

Securing a good match is less difficult in strip transmission line than in coaxial line. In the latter case, the ferrite is situated in the region of maximum magnetic field. Also, the microwave magnetic field encounters the ferrite medium throughout its closed loop. Neither of these conditions exist in the balanced stripline configuration of Fig. 2(b). Therefore, the discontinuity created by the ferrite is less in this structure and the match is correspondingly better.

Devices

Variable Attenuator

A direct application of the ferrite-loaded TEM mode transmission line structure is the variable attenuator. For a fixed microwave frequency, there is but one value of magnetic bias corresponding to the resonant condition. If the bias field is varied from its resonant value, the attenuation will decrease from its maximum value. The value of minimum attenuation is determined by the low field characteristics of the particular ferrite employed. At a fixed frequency, the upper and lower limits of attenuation and the swing in bias required to span these limits, are solely a function of ferrite type.

The ideal ferrite for this application saturates at low bias fields, has a small imaginary component of the dielectric constant, a large imaginary component of the effective permeability at resonance, a high saturation magnetization, and a high Curie temperature. As a consequence of the first two characteristics, the insertion loss and the lower limit of attenuation will be small. The condition on the imaginary component of the effective permeability ensures a high resonance loss, and hence a large upper limit of attenuation. Eq. (1) demonstrates that at a particular frequency a ferrite of high saturation magnetization requires a low value of bias for resonance. This permits use of a small electromagnet both in terms of size and driving power. If the power

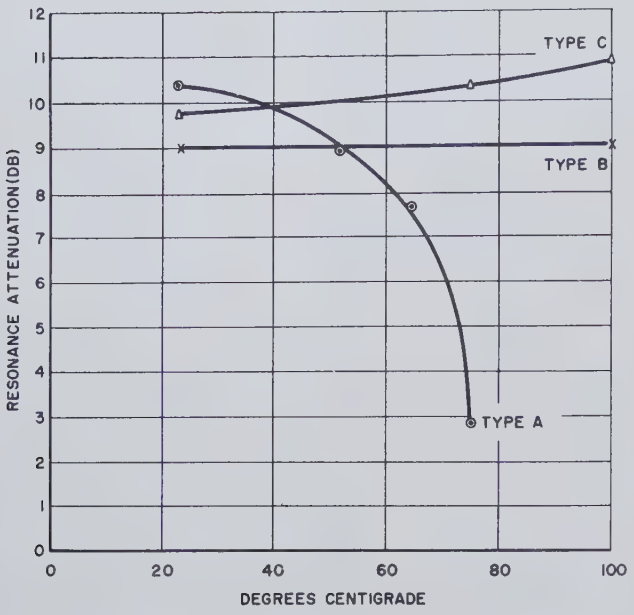

Fig. 3—Temperature dependence of resonance attenuation for several ferrite aluminates.

ferrite chosen for this application met all the criteria except that of high saturation magnetization. The material used was a ferrite aluminate having a saturation magnetization of 650 Gauss.

The variable attenuator was designed in $\frac{3}{8}$ coaxial line to operate from 2 kmc to 4 kmc. A continuous change in attenuation from 0.5 to 6 db was attained at the low end of the band and from 0.2 to 10 db at the high end. The maximum vswr was less than 1.5. Whereas this component is suitable for the particular application for which it was designed, improved results are attainable in strip transmission line.

The strip transmission line variable attenuator utilized two slabs of low loss ferrite aluminate centrally positioned on the upper and lower ground planes [Fig. 2(b)]. The attenuation was variable from a minimum of 0.3 db to a maximum of 10 db. Maximum vswr was equal to 1.22 (Fig. 4). While no attempt has been to optimize these results, they are significant in that they illustrate the feasibility of strip-transmission line in reciprocal ferrite applications.

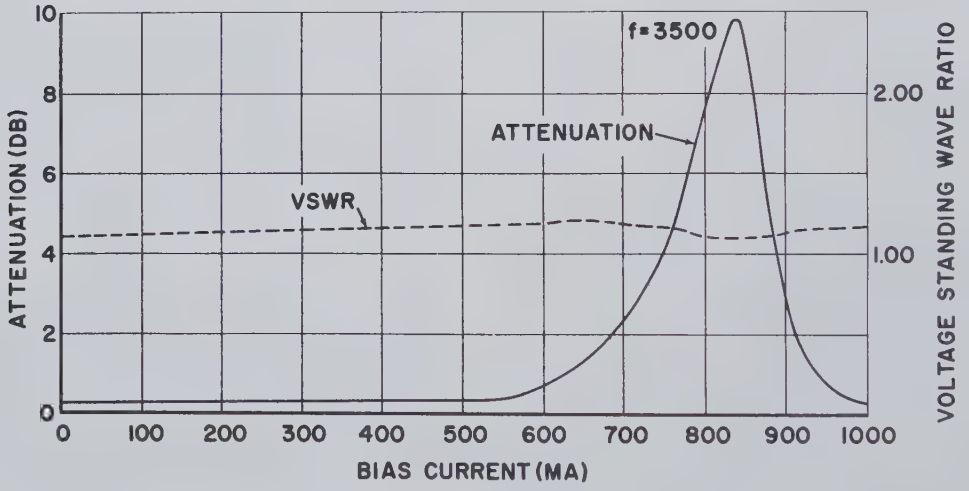

Fig. 4—Variation of attenuation and vswr with magnetic biasing at a single frequency for the strip-transmission-line variable attenuator.

dissipation of the magnet becomes too great, the temperature in the vicinity of the ferrite may approach or exceed the Curie temperature of the ferrite with a resultant deterioration or complete collapse of the attenuation characteristic.

Fig. 3 shows the temperature dependence of resonance attenuation for three ferrite aluminates at 3 kmc. Type A has a low Curie temperature and hence exhibits a rapid deterioration of ferromagnetic effects even with small increase in temperature. Types B and C have high Curie temperatures and suffer no appreciable decrease in their ferromagnetic properties over the desired temperature operating range. The resonance attenuation of type C increases with temperature because the material is not fully saturated at 3 kmc.

The criteria established with respect to ferrite characteristics were not all achievable in a single ferrite. The

Equalizer

An equalizer is used at the output of a traveling-wave tube amplifier, to correct the variation of gain with frequency. For example, if the amplification of the traveling wave tube varies with frequency as shown in Fig. 5(a), the equalizer should possess an attenuation characteristic [Fig. 5(b)] such that the output of the tube is made independent of frequency. [Fig. 5(c)].

A stagger tuning method is employed to achieve the equalizer characteristic. Several ferrites, each of different saturation magnetization, were used. At a fixed magnetic bias, each ferrite will resonate at a different frequency. Kittel's formula for this configuration (1) indicates that a ferromagnetic material characterized by a high $4\pi M_s$ will introduce attenuation at the high end of the frequency band. Similarly, low $4\pi M_s$ ferrites will introduce attenuation at the low end of the band. By

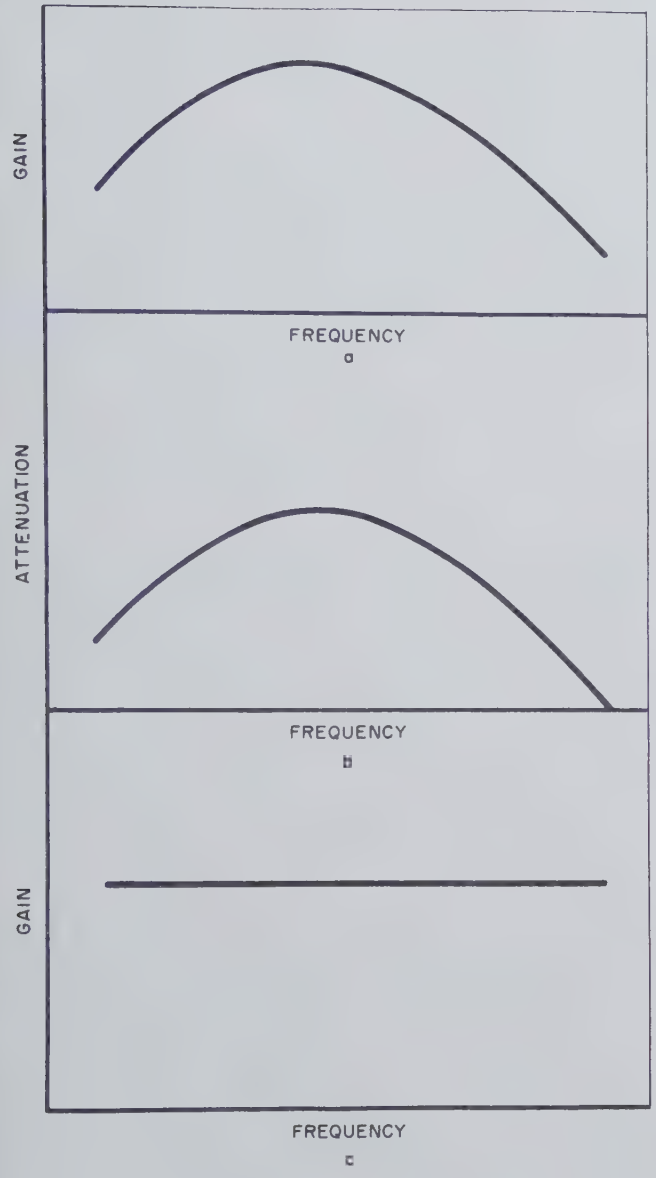

Fig. 5—(a) Typical gain-frequency characteristic of a twt amplifier. (b) Attenuation characteristic required to equalize twt output. (c) Equalized twt output.

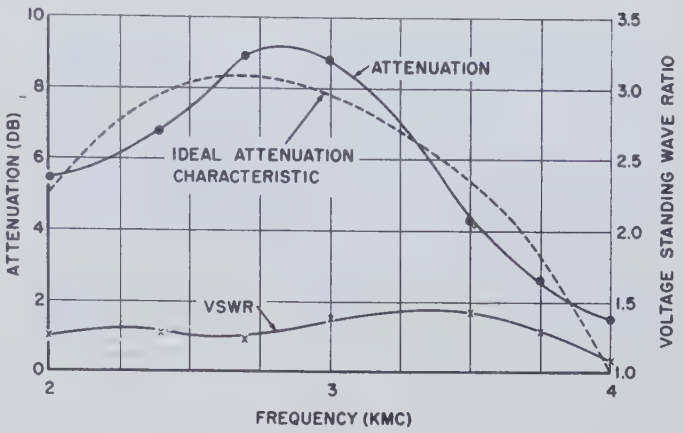

Fig. 6—Final attenuation and vswr characteristics of the coaxial traveling-wave-tube equalizer.

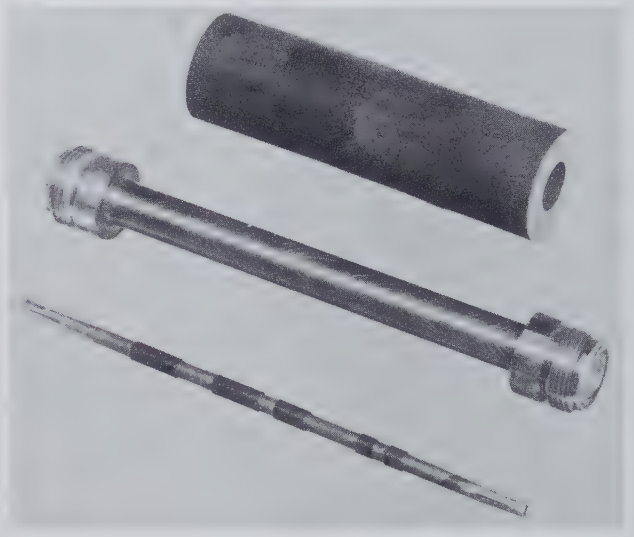

Fig. 7—Component parts of traveling-wave-tube equalizer.

suitable choice of $4\pi M_s$ values, and proper adjustment of ferrite length, the desired attenuation characteristic is achievable.

Fig. 6 shows both the ideal and actual attenuation curves. They match within approximately ± 1 db over the band. Three ferrite aluminates having saturation magnetizations of 800, 1800, and 2000 Gauss were used. Since vswr's of 1.5 could be tolerated in this application and since the over-all length of this component was to be kept at a minimum, ferrite tubes with a 12 thousandths wall were used.

The vswr varied from a maximum of 1.45 to a minimum of 1.10. A photograph of this component appears in Fig. 7. The total length is $4\frac{1}{2}$ inches.

If an electromagnet is used to provide a portion of the magnetic bias field, the attenuation characteristic may be varied. Thus the equalizer may be adapted for use with traveling-wave tubes differing in their gain-frequency dependence.

Modulator

The last component to be discussed is a $\frac{3}{8}$ coaxial line *S*-band amplitude modulator operating from 2 kmc to 4 kmc (Fig. 8). The ferrite-loaded transmission line structure is used in conjunction with both an electromagnet and a permanent magnet (the former fitting within the latter). The permanent magnetic field is of the proper value to bias the ferrite to resonance at the center of the frequency band. When the electromagnet is energized, the axial field produced contributes to the field of the permanent magnet, thereby, changing the bias. This in turn causes the resonant frequency to shift in accordance with (1). Thus the resonance attenuation peak may be shifted throughout the frequency range by appropriately varying the bias. The further removed a frequency is from resonance, the less is the attenuation, until at frequencies in excess of several hundred megacycles from resonance, the attenuation is negligible. If an alternating current is applied to the electro-

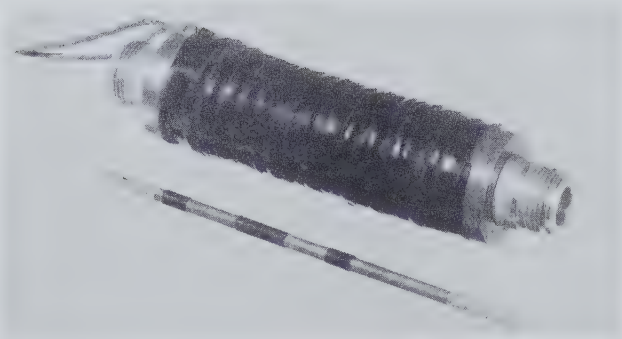

Fig. 8—Component parts of *S*-band coaxial amplitude modulator (permanent bias magnet not shown).

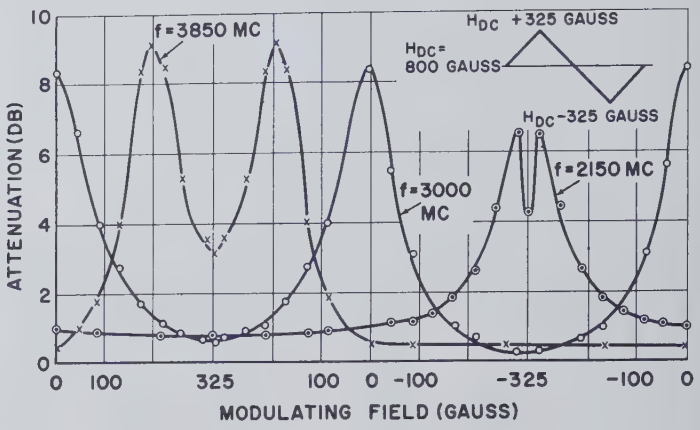

Fig. 9—Modulation characteristic at several frequencies of the *S*-band amplitude modulator.

magnet, the frequencies on either side of the center frequency will undergo cyclic variation in attenuation; maximum attenuation occurring at that frequency determined by the vector sum of H_{DC} and the instantaneous value of H_{AC} in (1). If the modulation current produces fields of sufficient strength, even the frequencies at the extremities of the band will undergo this cyclic variation; *i.e.*, amplitude modulation. Fig. 9 shows the modulation characteristic at several frequencies within the band. The modulating current waveshape was triangular and of sufficient amplitude to shift the resonance to within 150 mc of both ends of the frequency range.

A narrow linewidth ferrite aluminate was used in this application. Ten ferrite tubes, each $\frac{1}{8}$ inch long and 0.007 inch thick were spaced on the inner conductor. The average vswr was 1.35. The total length of this component is $4\frac{1}{2}$ inches.

Conclusion

A presentation has been made of the basic principles underlying the design of several reciprocal ferrite devices in TEM mode transmission line structures. Each component operated at gyromagnetic resonance and utilized either coaxial line or strip transmission line. An analysis of the mismatch ferrite loading creates in coaxial line was given and the technique used to improve the match described. A comparison was made between results in coaxial and strip transmission lines. The effect of ferrite size, shape, linewidth, saturation magnetization, temperature, and frequency on component performance was discussed and final operating data presented on each of the components.

Acknowledgment

The authors express their gratitude to L. Swern for his helpful advice during the course of this work. They also thank R. Mangiaracina for his temperature data and E. Grimes for his strip transmission line information. In addition, the authors wish to extend their appreciation to V. Lanzisera for his significant contribution in obtaining the experimental data reported herein.

Measurement of Ferrite Isolation at 1300 MC*

G. S. HELLER† AND G. W. CATUNA†

Summary—Optimum geometry for ferrite isolators at low microwave frequencies in rectangular waveguide is discussed and measurements are presented which show the feasibility of constructing a practical isolator at 1300 mc using commercially available ferrites.

Further data for a narrower line-width ferrite are presented. The high-reverse to forward-loss ratios obtained are in accord with predictions from perturbation theory.

Introduction

MOST of the effort of the Ferrite Application Section of the Solid State Group at Lincoln Laboratory, has been directed toward an investigation of the feasibility of constructing nonreciprocal devices at lower microwave frequencies. The device which probably can be most easily extended to operate at lower frequencies is the resonance isolator. The reason for this has been pointed out by Lax[1] who has shown that the optimum reverse-to-forward loss for a resonance isolator is inversely proportional to the square of the resonance line width, whereas corresponding figure of merit for a nonreciprocal phase-shift device, measured by the differential phase shift per unit average attenuation, is inversely proportional to the first power of the line width. This is in accord with the fact that at the present time the lowest frequency of commercially available resonance isolators is about 3000 mc, while the lowest frequency at which commercially available nonreciprocal phase-shift type devices operate, is approximately 6000 mc. In addition to line width, the other important limitation at low frequency is the low-field loss. However, by using geometries which require higher external fields for resonance, this loss sometimes may be reduced enough so that a practical device is possible. The measurements reported in this paper were performed for the purpose of testing the theoretical predictions expressed above and evaluating the performance of lower frequency resonance isolators.

Optimum Geometry at Low Frequencies in Rectangular Waveguide

The Kittel formula for the resonant frequency of a magnetically-saturated ellipsoidal sample shows that a thin slab magnetized perpendicular to its plane raises the magnetic field required for ferromagnetic resonance while magnetization parallel to its plane, lowers it. In order to avoid as much as possible low-field loss in the forward direction, one should use a high external dc field. Another reason for the use of a thin slab, magnetized perpendicularly, has been pointed out by Lax[1] who showed that the rf magnetic field inside the ferrite is most nearly circularly polarized for this geometry. Furthermore, at high powers, a thin slab attached to the guide wall will dissipate heat more efficiently. This geometry is also in accord with the skin depth considerations which show that if the ferrite is made too thick the electromagnetic wave will not penetrate the entire thickness and the additional material is not only ineffective, but also it inhibits heat conduction to the guide wall at high powers.

The distance between the ferrite slab and the side wall of the waveguide can be predicted approximately from perturbation theory. The criterion used is either minimum forward loss as used by Heller[2] or the maximum reverse-to-forward ratio used by Lax.[1] These two criteria give approximately the same results and are in accord with experimental evidence.

The waveguide used was the standard *L*-band waveguide (RG-69/U) with the height cut down to 1-inch O.D. This was done to reduce the gap dimensions of the magnet required and to increase the percentage of waveguide cross section filled with ferrite.

Measurements Using Ferramic R1

Measurements were made at 1300 mc, of forward and reverse attenuation as a function of applied magnetic field using a slab of Ferramic R1 (0.125 inch×0.801 inch×4.00 inches) placed 1.90 inches from the side wall of the guide. The reverse loss was 2.2 db and the forward loss was approximately 0.40 db giving a ratio of 5.5. The data are plotted in Fig. 1.

In order to improve the reverse-to-forward ratio, dielectric loading was used. When the dielectric, Stycast K-12, was placed between the guide center and the ferrite as described by Weiss[3] (Fig. 2), the forward attenuation was reduced to 0.29 db and the reverse attenuation was increased to 2.40 db resulting in a reverse-to-forward ratio of 8.3. These results are shown in Fig. 3.

The ratio was increased further by enclosing the ferrite in dielectric material as shown in Fig. 4. In this case the Stycast was longer than the ferrite and tapered to reduce reflections. For this arrangement the forward loss was 0.40 db, the reverse loss 4.60 db, and the ratio 11.5 (Fig. 5). Thus, it is possible, using this geometry and Ferramic R1, to achieve 10 db isolation with a forward loss of less than 1 db (Fig. 5).

* Manuscript received by the PGMTT, August 16, 1957. The research in this paper was supported jointly by the U. S. Army, Navy, and Air Force under contract with Mass. Inst. Tech.

† Lincoln Lab., Mass. Inst. Tech., Lexington, Mass.

[1] B. Lax, "Loss characteristics of microwave ferrite devices," PROC. IRE, vol. 44, pp. 1368–1386; October, 1956.

[2] G. S. Heller, Quart. Prog. Rep. on Solid State Res., M.I.T. Lincoln Lab., Lexington, Mass., p. 55; November 1, 1955.

[3] M. T. Weiss, "Improved rectangular waveguide resonance isolators," IRE TRANS., vol. MTT-4, pp. 240–243; October, 1956.

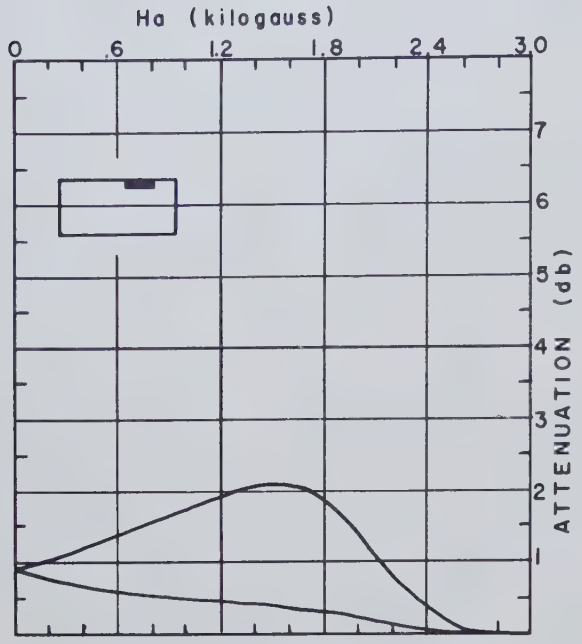

Fig. 1—Reverse and forward attenuation as a function of applied magnetic field for Ferramic R1 (0.125 inch×0.801 inch×4.00 inches) at 1300 mc.

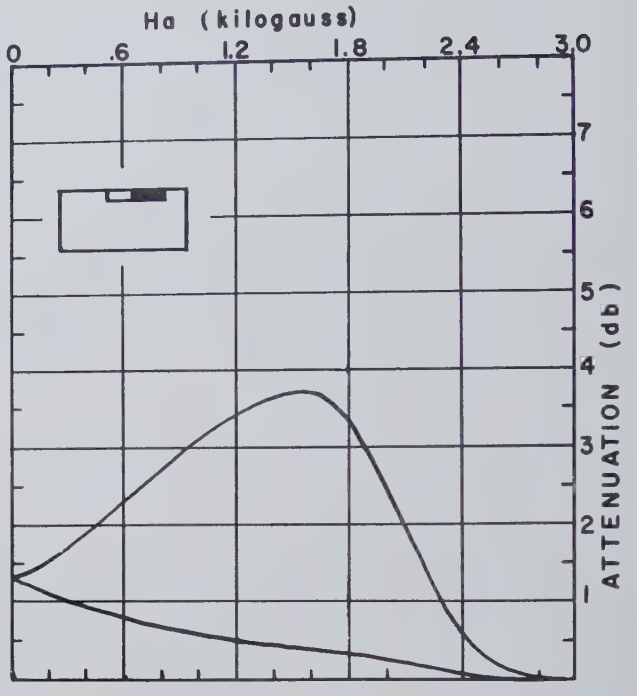

Fig. 3—Reverse and forward attenuation as a function of applied magnetic field for Ferramic R1 (0.125 inch×0.801 inch×4.00 inches) at 1300 mc in waveguide dielectrically loaded with Stycast K-12 (0.125 inch×0.801 inch×4.00 inches).

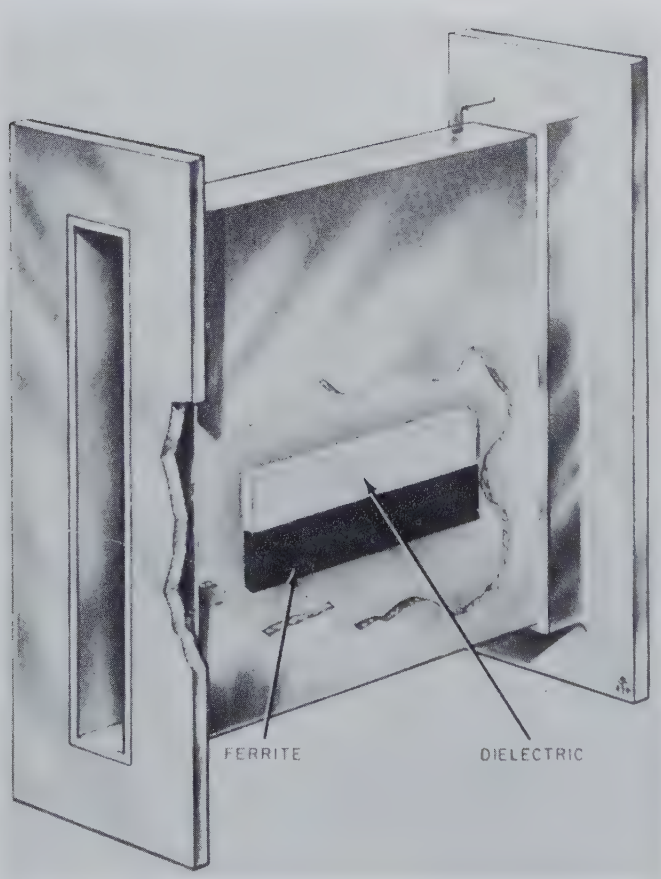

Fig. 2—Sample section showing ferrite sample and dielectric load.

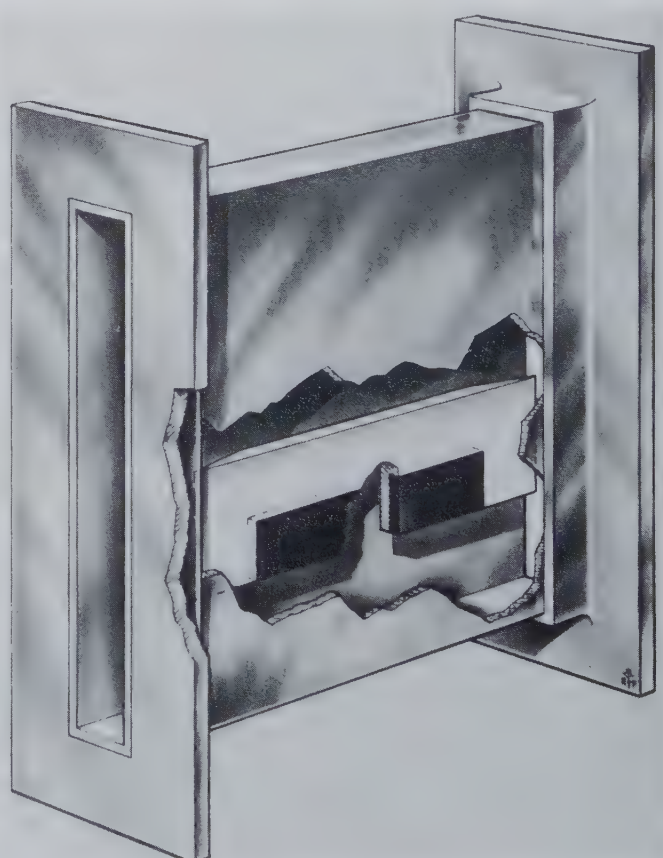

Fig. 4—Sample section showing ferrite sample and Stycast envelope.

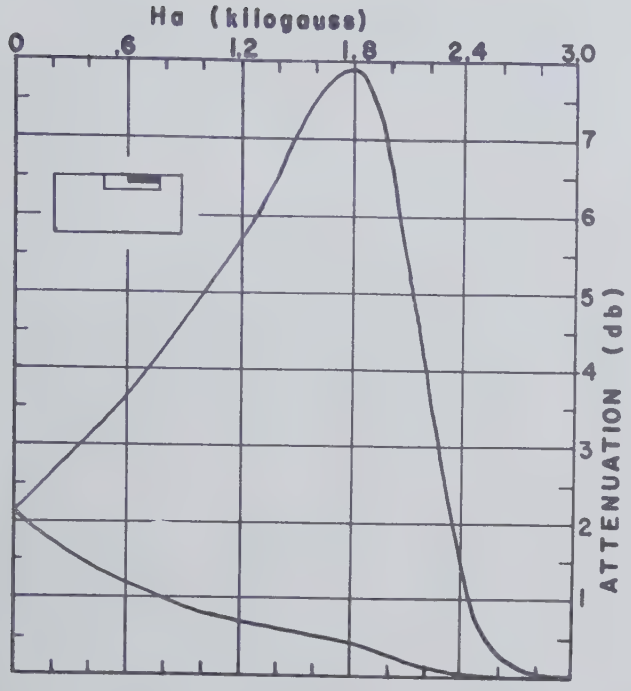

Fig. 5—Reverse and forward attenuation as a function of applied magnetic field for Ferramic R1 (0.125 inch×0.801 inch×4.00 inches) enclosed in Stycast K-12 (0.250 inch×1.602 inch×8.00 inches) at 1300 mc.

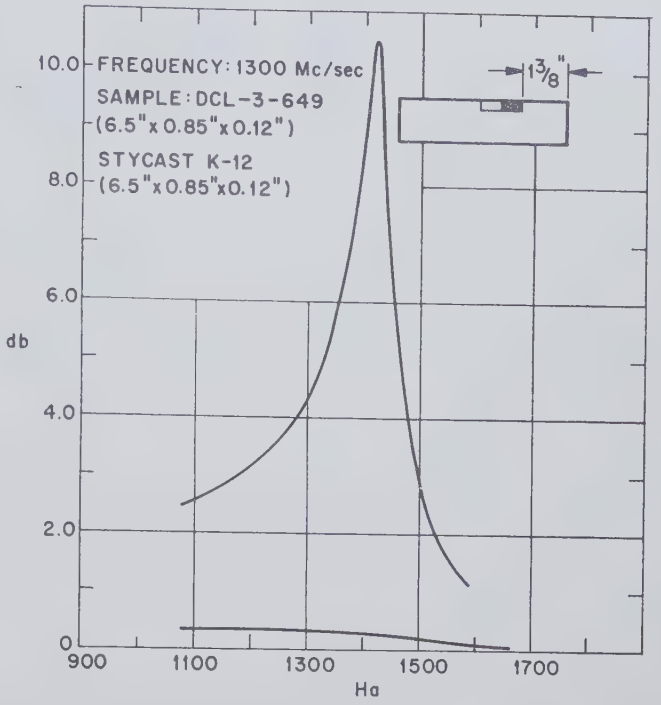

Fig. 7—Reverse and forward attenuation as a function of applied magnetic field for ferrite DCL-3-649 in waveguide dielectrically-loaded with Stycast K-12.

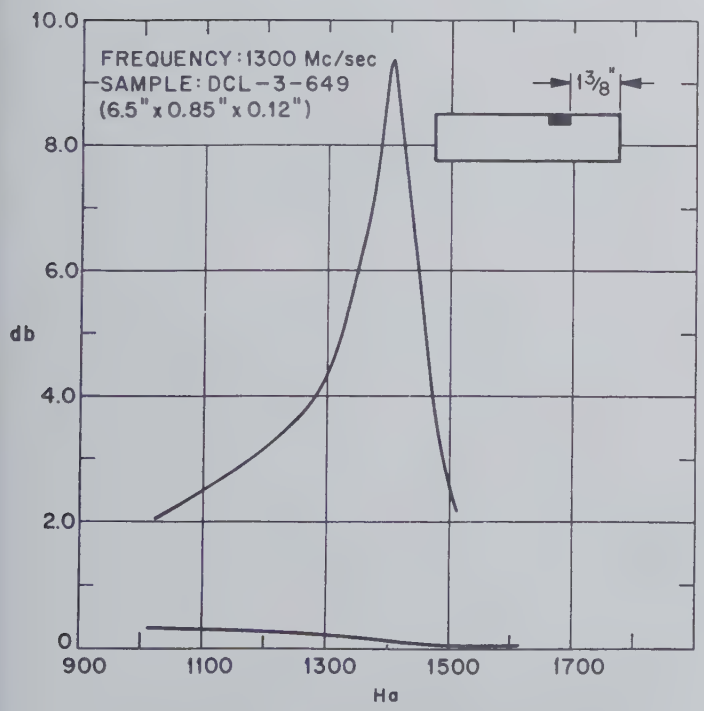

Fig. 6—Reverse and forward attenuation as a function of applied magnetic field for ferrite DCL-3-649.

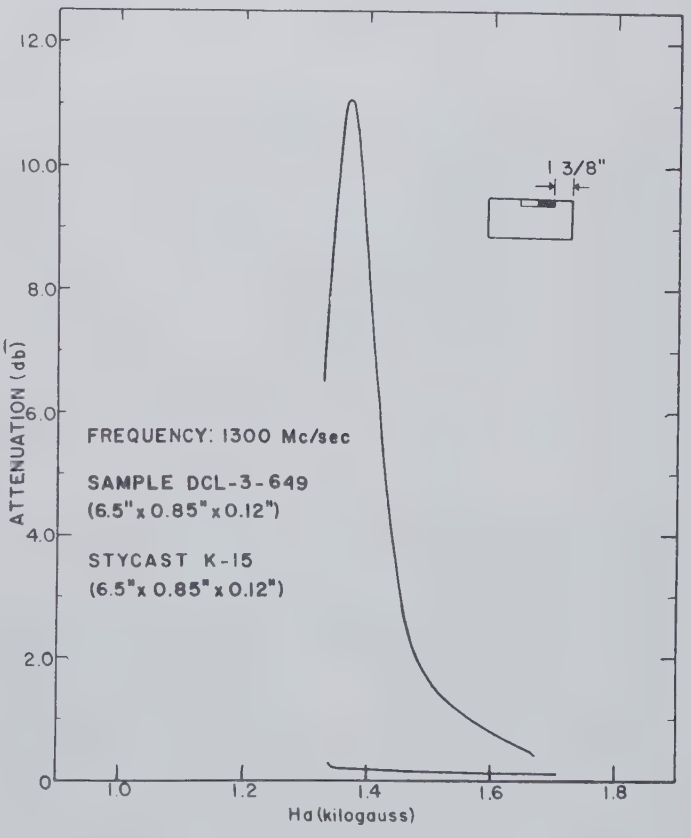

Fig. 8—Reverse and forward attenuation as a function of applied magnetic field for ferrite DCL-3-649 in waveguide dielectrically-loaded with Stycast K-15.

Measurements with Narrower Line-Width Ferrites

Dr. John Goodenough of these Laboratories kindly has supplied us with a ferrite which has a line width of one half to one third that of Ferramic R1. This Mn-Mg ferrite, DCL-3-649, has a saturation magnetization, $4\pi M$, of 1160 Gauss and a Curie temperature of 100°C. Although this low Curie temperature precludes use of this ferrite at high powers, the data presented here should point out the possibility of constructing low-frequency isolators with narrower line width materials.

A sample of this material, 6.5 inches long, consisting of three slabs placed end to end, was inserted in the same pinched-waveguide section described previously. The optimum reverse-to-forward ratio occurred when the sample was located $1\frac{3}{8}$ inches from the guide wall. The reverse loss for this geometry was 9.5 db and the forward loss was less than 0.20 db giving a ratio of approximately 50. (Fig. 6)

With Stycast K-12 loading, as shown in Fig. 2, the reverse loss increased to 10.5 db, but the forward loss also increased reducing the ratio to approximately 40. (Fig. 7)

Since narrower line-width ferrites would have larger rf permeabilities, dielectric loading of a higher dielectric constant was tried. Stycast K-15 produced a reverse loss of about 11 db and a forward loss small enough so that the ratio was greater than 70. (Fig. 8)

Measurement Techniques

Measurements were made with a bridge consisting of both coaxial and waveguide components as shown in Fig. 9. The attenuator section consisted of a vernier controlled resistor card moving across standard L-band waveguide and the phase shift was accomplished by the use of a variable length of coaxial line. Care was taken to eliminate reflections in the system, all waveguide to coaxial line transitions having a vswr of less than 1.05 at 1300 mc. The attenuator section was calibrated with a power meter and balance of the bridge could be obtained to a much higher accuracy than the attenuator calibration.

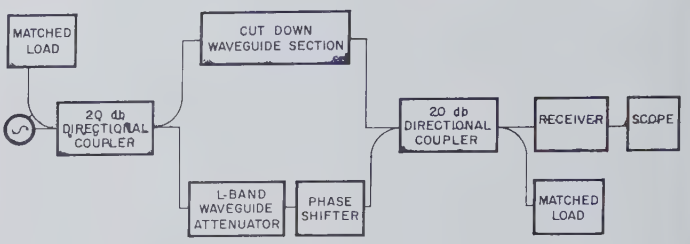

Fig. 9—Block diagram of microwave bridge used to measure attenuation in ferrite-loaded waveguide.

Conclusion

Using commercially available ferrite with the dielectric loading and favorable geometry it is possible to construct resonance isolators at frequencies as low as 1300 mc with a reverse to forward ratio of 10 and a reverse loss of less than 1 db. Narrower line width ferrites result in much larger ratios and these ratios are roughly inversely proportional to the square of the line width. With the advent of new narrow line width materials, such as yttrium-iron garnet, it should be possible to construct practical resonance isolators at even lower frequencies. However, rectangular waveguide will then become too unwieldy and probably it will be necessary to resort to physically smaller structures such as dielectrically loaded coaxial lines[4] or trough lines.[5]

[4] B. J. Duncan, L. Swern, K. Tomiyasu, J. Hannwacker, "Design considerations for broad-band ferrite coaxial line isolators," Proc. IRE, vol. 45, pp. 483–490; April, 1957.

[5] H. S. Keen, "Scientific Report on Study of Strip Transmission Lines," Airborne Instr. Lab. Rep. No. 2830-2; December 1, 1955.

An Electronic Scan Using a Ferrite Aperture Luneberg Lens System*

D. B. MEDVED†

Summary—Beam displacements up to ±30° have been observed in the radiation patterns from various ferrite-loaded waveguide apertures in transverse magnetic fields. The apertures are used as feeds for Luneberg lenses, and electrical lobing of narrow pencil beams is accomplished. The proposed use of a square waveguide ferrite-filled feed for a sequential lobing system is described.

Introduction

UNTIL recently, attempts to apply ferrites to the problem of electronic scanning have been limited to their indirect utilization as electrically variable phase shifters in corporate or sequential structure arrays,[1,2] A direct approach to the problem has been studied by Angelakos and Korman,[3] who have investigated the far-field radiation patterns from a ferrite-filled rectangular aperture at *X* band. They found that shifts in far-field beam maxima up to ±30° can be obtained by application of a transverse magnetic field. Wheeler[4] has reported the beam scattering from magnetized ferrite spheres in cylindrical waveguide apertures for possible application to an electronic conical scan.

At Convair, we have restricted our immediate goal to the development of a passive electronic tracking system with the following consequent simplifications:

1) Electrical beam lobing of the pencil beam is restricted to small squint angles (less than 3°).
2) The nonreciprocity of the Cotton-Mouton effect for the ferrite-filled aperture can be neglected.
3) The nonlinear behavior of ferrites at high power is not relevant.

In this paper, it is proposed that the electronic tracking be based on a sequential lobing system. This leads to use of waveguide geometries having lower symmetry than that required by a conical scanner.

Evaluation of Waveguide Apertures Containing Ferrites

We have studied the shift in the beam maxima of the far-field radiation patterns as a function of applied magnetic fields at ferrite-loaded apertures for three configurations.

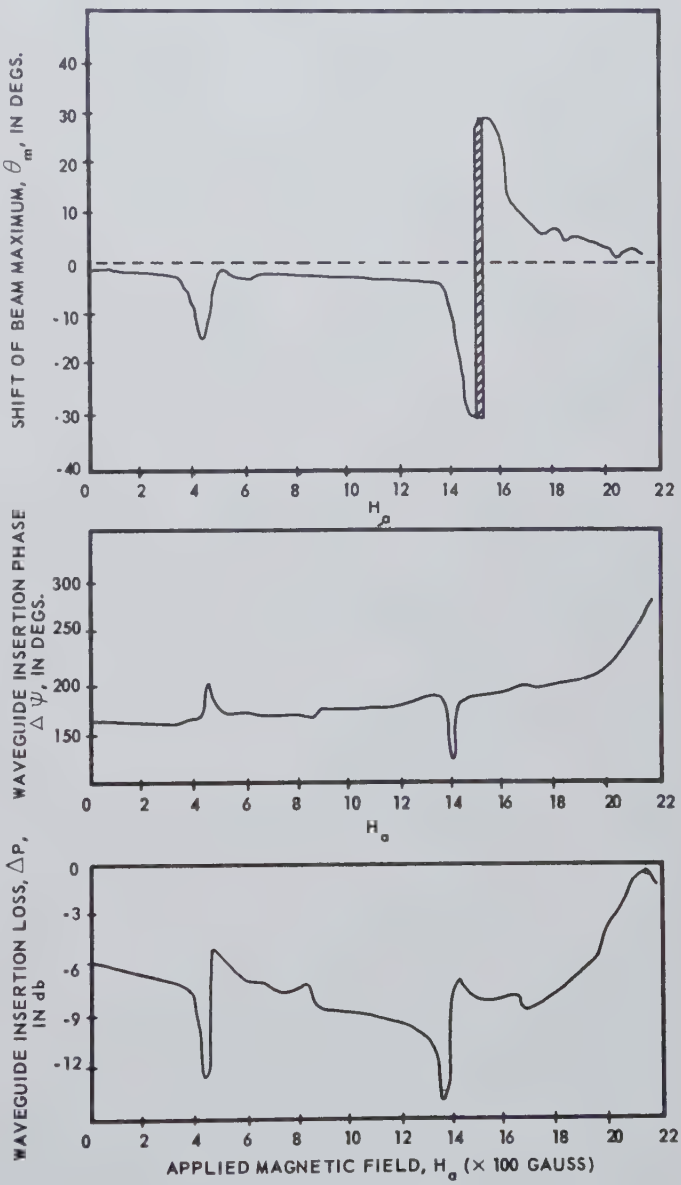

Fig. 1—Comparison of beam swing, θ_m, and waveguide characteristics for ferrite-filled rectangular guide.

The original geometry of Angelakos and Korman[3] [Fig. 4(a)] was studied for a ferrite sample $\frac{3}{8}$ inch thick (General Ceramics R-1) at a frequency of 9375 mc. Ultrasonic cutting techniques were used for shaping these and subsequent ferrite slabs for precise fit in the waveguide apertures. Beam lobing in the *H* plane up to ±30° for 60° beamwidths was observed. Fig. 1 (top curve) represents the shift in beam maximum, θ_m,[5] as a

* Manuscript received by PGMTT, September 5, 1957; revised manuscript received, October 8, 1957.
† Convair, Div. General Dynamics Corp., San Diego, Calif.
[1] *Proceedings of Third Symposium on Scanning Antennas*, Naval Res. Lab., Washington, D. C.; April, 1952.
[2] *Record of the Georgia Tech-SCEL Symposium on Scanning Antennas*, Georgia Inst. Tech., Atlanta, Ga.; December 18–19, 1956.
[3] D. J. Angelakos and M. M. Korman, "Radiation from ferrite-filled apertures," PROC. IRE, vol. 44, pp. 1463–1468; October, 1956.
[4] M. S. Wheeler, "Nonmechanical beam steering by scattering from ferrites," this issue, p. 38.
[5] Beam maximum position is defined as the average of the angular coordinates of the 3-db points.

function of applied field, H_a. This curve is in general agreement with the results of Angelakos and Korman for this thickness and frequency. It is shown here only for the interesting correlation with the two lower curves of Fig. 1. These are plots of relative insertion phase, $\Delta\psi$, and insertion loss, ΔP, for the identical ferrite sample in nonradiating waveguide. They were obtained by use of microwave interferometer techniques previously applied to investigation of dielectric constant. Significant changes in ΔP, $\Delta\psi$ occur for those regions of applied field producing large beam swings. This technique has been utilized to determine regions of appreciable beam shift for other thicknesses, frequencies, and ferrite materials without recourse to extensive measurement on the antenna pattern range. In addition, this observed correlation between the curves of Fig. 1 appears to give some credence to the assumption that the field distributions at the aperture plane are approximately those which, in principle, can be found from an analysis of the waveguide problem.[6,7] (This analysis has yet to be carried out for a finite slab filling the guide cross section.)

A second geometry investigated, also in rectangular X-band waveguide was that of the twin slab structure.[8,9] A typical aperture is shown in Fig. 2 (a 24-inch square ground plane is omitted). With this configuration, beam shifts up to 15° in the vicinity of 1500 Gauss were observed. Several variations of this twin slab geometry were studied in detail; the most interesting was one in

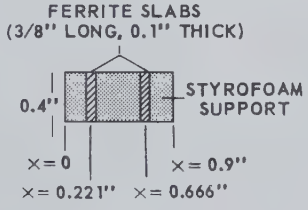

Fig. 2—Typical twin slab aperture.

which the spacing of the slabs was only 0.2 inch, the slab thickness 0.05 inch. In this case, beam shift up to ±35° with a corresponding loss in radiation amplitude of 1.08 db was observed in the neighborhood of 1600 Gauss. In the case of the completely filled aperture, beam shifts of this order have a corresponding loss in radiation amplitude, of at least 5 db and ranging up to 20 db and higher.

Finally, in order to remove the limitation of beam lobing to a single plane, a square waveguide system shown in Fig. 3 has been devised. The square waveguide is operated in either TE_{10} or TE_{01} modes as two independent apertures.[10] The direction of applied magnetic field is synchronized with the appropriate probe

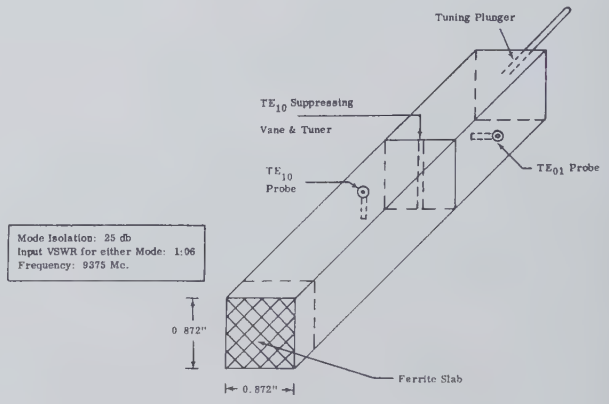

Fig. 3—Square waveguide use as a dual mode feed.

excitation. Mode isolation of about 25 db is obtained with the geometry used.[11] The ferrite slabs investigated do not introduce any observable additional cross-mode coupling. Beam shifts obtained with a single mode were analogous to those observed with the rectangular waveguide, although the details of the $\theta_m(H_a)$ function are quite different.

Electrical Lobing of Pencil Beams

Phase and amplitude determinations of the various aperture electric field distributions have been obtained using a second modification of the microwave interferometer.[12] Ferrite-loaded rectangular and square waveguide apertures have subsequently been used as feeds for a Luneberg lens (see Fig. 5).[13] The Luneberg lens is admirably suited for magnetic scanning since one is not concerned with an aperture blocking problem. The 3-db beamwidth with an 18-inch lens is 4.5°. A typical lobing pattern in the H plane obtained with this system is shown in Fig. 4 (deeper crossovers up to 3 db were obtained with the rectangular feed). In all cases, it was observed that as the squint angle increased, with consequently deeper crossovers, the sidelobe levels also increased. The patterns shown in Fig. 4 constitute a compromise between the opposing requirements of deep crossover and low side lobes. The side lobe increase is considered to be analogous to the coma lobes observed when one attempts large angle off-axis scan of paraboloid reflectors.

A continuous scan in the H plane has been observed with the monitoring equipment of Fig. 5. Rectangular waveguide was used as the feed for a 12-inch Luneberg.

[6] D. B. Medved, Second Bimonthly Progress Report, Convair RSR Project 1002; March 13, 1957.
[7] G. Tyras and G. Held, "Radiation from a Rectangular Waveguide Filled with Ferrite," URSI-IRE Joint Meetings, Commission 6; May 24, 1957.
[8] M. L. Kales, H. N. Chait, and N. G. Sakiotis, "A nonreciprocal microwave component," *J. Appl. Phys.*, vol. 24, p. 816; June, 1953.
[9] B. Lax, K. J. Button, and L. M. Roth, "Ferrite phase shifters in rectangular wave guide," *J. Appl. Phys*, vol. 25, p. 1413; November, 1954.
[10] D. Levine and W. Sichak, "Dual-mode horn feed for microwave multiplexing," *Electronics*, vol. 27, p. 162; September, 1954.
[11] This could be considerably improved by using a tee arrangement with appropriate matching posts.
[12] D. B. Medved, "An Electronic Scan Using a Single Ferrite Aperture," Convair Rep. ZN-309, pp. 19–21; May, 1957.
[13] J. Brown, "Microwave Lenses," Methuen & Co., Ltd., London, Eng., pp. 86–89; 1953.

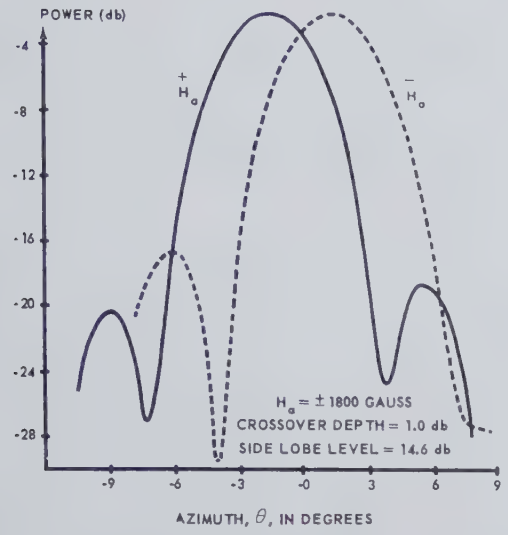

Fig. 4—Beam lobing patterns: 18-inch Luneberg lens fed by square waveguide.

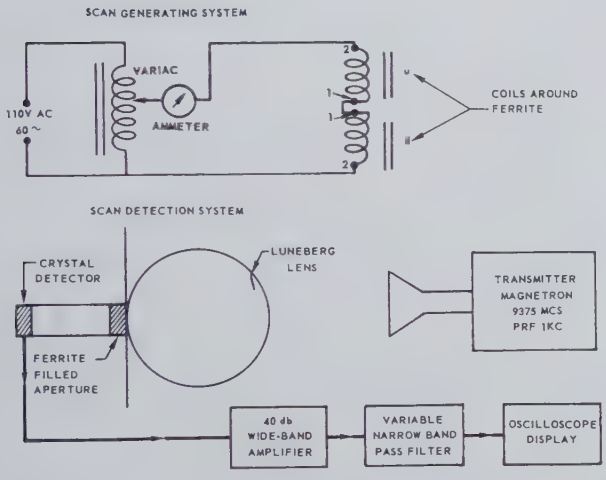

Fig. 5—Method for generation and detection of electronic scan.

Sine wave currents corresponding in peak value to $H_a = 1600$ Gauss were passed through the electromagnet coils at 60 or 400 cycles. The resulting pattern is thus sector-scanned in the H plane at the 60 or 400 cycle rate. An error signal effect is simulated by offsetting the receiver from the line-of-sight axis to the transmitter. The detected signal is amplified, filtered, and displayed on an oscilloscope. Maximum signal was observed at an 8° offset angle.

Sequential Lobing with Square Waveguide

A proposed sequential lobing system using ferrite filled square waveguide as a feed for a Luneberg lens is illustrated in Fig. 6. The square waveguide is operated essentially as two independent sources for TE_{10} and TE_{01} modes. The circles represent positions of beam maxima with appropriate rf E-field polarization indicated by the dashed arrows. Signals detected by the TE_{10} probe (beams 1 and 3) would be fed into an azimuth information channel, whereas tilt coordinate information is supplied by the crossover of beams 2 and 4. In the lower part of the figure, the time variation of electromagnet current necessary to produce the desired lobing sequence is plotted; *e.g.*, current in the coils labeled U-D with rf field corresponding to TE_{10} produces a shift of the beam to the right or left in the azimuth plane, depending on the magnetic field direction.

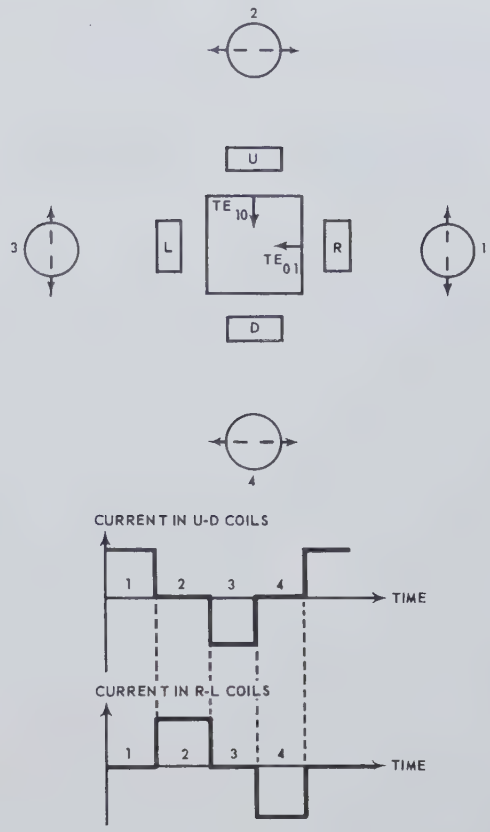

Fig. 6—Sequential lobing using square waveguide aperture.

The polarization sensitivity of the method may seem to present a serious limitation to use of this method. Consider for example, the reflected signal from a wing surface parallel to the E field of the TE_{01} mode. Information on the azimuth coordinates cannot be obtained under these conditions. However, if one considers the equivalent situation for conical scan, neither azimuth nor tilt coordinates can be obtained in the case that the nutating beam is polarized perpendicular to the wing. The difference in the two systems may be paraphrased by a choice of being at least half informed all the time or not informed at all some of the time concerning the target coordinates.

Acknowledgment

Most of the measurements were obtained with the technical assistance of R. R. Hanselman, R. W. Berg, and R. L. Norman. This work was supported by Convair's General Engineering Fund and in part by the Convair Office of Scientific Research.

Round Table Discussion on Design Limitations of Microwave Ferrite Devices

THE 1957 Annual PGMTT Meeting concluded on May 10 with a round table discussion on Design Limitations of Microwave Ferrite Devices. This discussion was moderated by Professor C. L. Hogan of Harvard University, and the panel members were Drs. J. O. Artman, H. J. Carlin, D. L. Fresh, G. S. Heller, R. C. LeCraw, H. Seidel, and P. H. Vartanian. The topics considered appropriate for discussion were: 1) high-power effects (nonlinearity), 2) low-frequency limits, 3) high-frequency limits, 4) anomalous propagation in ferrite loaded waveguides, 5) below-saturation behavior of ferrites, 6) "fast" ferrite devices (depending on relaxation time), 7) bandwidth problems, 8) materials and losses, and 9) high-speed magnetic field problems. An edited version of the recorded discussion is published on the following pages.

Dr. C. L. Hogan: Gentlemen, we now come to the close of a most interesting two-day session on the present state of the art in microwave ferrite devices. In this closing session I have with me on the platform seven experts in this field who have come prepared to discuss the various aspects of this subject and to answer, as well as they are able, any questions which you might like to put to them. (Seven panel members introduced to audience.)

Dr. B. Lax (M.I.T. Lincoln Laboratory): What are some of the low-frequency limitations of garnets as compared with ferrites?

Dr. Hogan: I believe that some of the potentialities of the yttrium garnet material at the low microwave frequencies are evident from Mr. Rodrigue's talk yesterday. The fundamental low-frequency limit of any nonreciprocal microwave ferrite device is related to the "width" of the ferromagnetic resonance line. To be sure, there are several practical low-frequency problems in addition to the problem of obtaining narrower resonance lines, but assuming for the moment that these problems can be solved, we find that the ultimate low-frequency limit is set by the line width of the material. In fact, one can easily calculate the highest front to back ratio that can be obtained in an isolator using a particular material from the line width of the material and the frequency of operation of the isolator. For a given material, the theoretical reverse to forward ratio of an isolator decreases as the frequency decreases. These calculations show that a line width less than 50 oersteds is required if a 10-db isolation per 1-db insertion loss is desired at approximately 200 mc. Thus, the yttrium garnet material promises to extend the low-frequency limit materially.

However, this narrow line creates a problem in itself. Suhl's theory of nonlinear effects in ferrites indicates that the narrower the resonance line, the lower the power level at which nonlinearities set in. Hence, even though garnets promise to make possible the extension of the low-frequency limit down to a few hundred megacycles, there will be many problems associated with their use at high power levels, and one will not have as much freedom in the choice of biasing magnetic fields and geometries as one has at higher frequencies with ferrites.

Dr. P. H. Vartanian Jr. (Microwave Engineering Laboratories): I think it should be pointed out that, excluding several of the broader line width materials, the garnet materials, as discussed in Mr. Rodrigue's paper, have, for the most part, saturation moments which are comparable to those exhibited by ferrites. For example, yttrium garnet has a saturation magnetization of approximately 1670 Gauss at room temperature. It is well known from considerations of Kittel's equation that certain geometries, such as longitudinally magnetized rods, cannot be used at low frequencies at or below ferromagnetic resonance unless the saturation moment of the ferrite is reduced. Consequently, geometry remains as one of the practical low-frequency problems. For example, a Faraday rotator using a rod of yttrium garnet cannot be made to operate below ferromagnetic resonance in L band. I think that low-frequency applications of garnets as well as ferrites will be limited for the most part to transversely magnetized slab geometry.

Dr. J. O. Artman (Harvard University): I would like to add that the low-field loss phenomenon is always present in these magnitudes of fields. Off-hand, I presume that the results will be pretty much the same in garnets as in ferrites and this ultimately will set a lower frequency limit in some kinds of devices.

Dr. Hogan: There is no reason why the saturation moment, and perhaps even the line width of a polycrystalline garnet, cannot be controlled by chemical methods in the same way as it is done in ferrites by adding aluminum and cobalt, as reported by Mr. Pippin yesterday.

Dr. G. S. Heller (M.I.T. Lincoln Laboratory): I would like to make another comment on this. The ferrite which I described, having a large back to front ratio at 1300 mc, had a saturation moment of 1160 Gauss and this is certainly not very low. In designing a resonance isolator the geometry helps you. Since a very thin flat slab can raise the ferromagnetic resonant

frequency very substantially and minimize low-field losses, it might not be too essential in some applications to get the saturation moment down to very low values.

Dr. Artman: If I may make one additional comment, one very nice thing about garnets is that the degree of valence is unambiguous; the ions are trivalent, and presumably, some of the other loss mechanisms that may exist in ferrites can not occur in the garnets.

Dr. Howard Scharfman (Raytheon Manufacturing Co.): Is it necessary to use very low anisotropy ferrites with such structures? As Dr. Heller pointed out, good performance in resonance isolators is possible at low frequencies by using high saturation magnetization ferrites with anisotropy fields of a few hundred oersteds.

Dr. Hogan: The yttrium garnet probably has a lower anisotropy than any ferrite except those that have Curie temperatures around room temperature. Yesterday Mr. Rodrigue pointed out that by using a mixture of holmium yttrium garnet, it is theoretically possible to get a zero anisotropy material. How well this will be realized rests upon experimental evidence.

T. N. Anderson (Airtron, Inc.): What is the lowest practical frequency limit for devices that has been reached so far using conventional ferrite materials?

Dr. Heller: Well, the best I have heard done is the *S*-band circulator made at Sperry, operating above resonance. I don't quite know what you mean by existing ferrites, but I believe this was an aluminate which has a low saturation moment. This isolator was built to work above resonance to get out of the zero field loss region and, of course, it makes the structure quite long, which likely increases the insertion loss. If one of the gentlemen from Sperry is here, perhaps he can answer it.

B. J. Duncan (Sperry Gyroscope Co.): In relation to this device, I will have to speak in complete generalities because it is classified by the military. I was quite interested, however, that the news got around so fast. I am somewhat inclined to take issue with the statement that it has to be very long. As far as the physical structure of the Sperry circulator is concerned, it's not a particularly short device, but if one considers the operating frequency it's not appreciably longer than a similar type *X*-band circulator operating below resonance. We did a little work with dielectrics to improve nonreciprocal phase shift, both per unit length and per unit loss, over that attainable with ferrites alone. The techniques utilized are similar to those described earlier by M. T. Weiss of Bell Labs. I think that about all I can say about its design features is that it is a device designed to operate above resonance. Undoubtedly everyone here knows that it is a high-power device, and that it has operated successfully over a moderate bandwidth in the *S*-band region.

Dr. E. Wantuch (Airtron, Inc.): I have tried to operate differential phase shift circulators below resonance and the lowest frequency that I have been able to design so far is around 5000 mc (*C* band). It operates below resonance and the geometry was optimized according to some of the comments made a few minutes ago. As far as resonance isolators are concerned, we have to separate them into high- and low-power. For military equipment in the low-frequency region, it goes without saying that most of these applications operate at fairly high power. You probably have all seen the picture that Ben Lax presented of Airtron's 10-inch long *S*-band resonance isolator capable of operation at the highest available *S*-band power, about 5 megw peak and 4000 watts average. I know that some of the people at Raytheon have been doing work on an *L*-band isolator and I think we should get Howard Scharfman up here to see whether he cares to say anything about it.

Dr. Scharfman: This is prerelease information, but it is true that Raytheon has successfully built an *L*-band isolator with a 10 to 1 back to front ratio. The unit handles peak power in excess of 1 megw and has a power absorption capability in excess of 300 watts average. These are minimum figures and I am sure the unit can handle more. Detailed specifications will be released very soon.

Dr. Wantuch: We have also worked on coaxial isolators with the help of Microwave Engineering Labs. and have successfully made coaxial isolators down to 1800 mc. These are not what you might call extremely high-power devices, but I think they would probably compare in power handling capabilities with the 1300-mc isolator that G. S. Heller has described.

Dr. Lax: A discussion on the nonlinear effects appears to be in order. In particular, I would be interested in hearing from Dr. Seidel on how such effects would influence his anomalous propagation where he claims there are high concentrations of electromagnetic fields.

Dr. H. Seidel (Bell Telephone Laboratories): As I indicated yesterday, we have examined some of these interference phenomena with respect to the application of high power and we certainly were able to disturb the appearance of these interferences significantly with rather small magnitudes of "high" power. I hope no one will object to my ambiguous choice of words, but I believe that the major point to Dr. Lax's question is that in these modes practically all the energy density of the guide is essentially bound to a surface with a consequent large enhancement of the magnetic field there. One finds, in fact, that the higher these modes are in mode number the more the tendency to confine the wave to the surface and, therefore, the greater the tendency for loss. Hence this leads to the statements I made earlier, that one can drive a ferrite, however "lossless," into an arbitrarily high state of loss.

The same mechanisms which drive the ferrite into this very high magnetic field state are obviously the same mechanisms which can induce the high power effects; and we have observed them. However, since these waves are so highly bound at the surface, there is a question of how far the high-power phenomenon will propagate transversely within the ferrite beyond this very

high density region. So far I don't have any information about this, although it would be rather interesting to determine whether these very highly concentrated fields can possibly nucleate high-power effects into the interior of the ferrite at powers lower than those for which they occur ordinarily.

Dr. R. C. LeCraw (Diamond Ordnance Fuze Laboratories): I would like to ask one of the members of the panel a question. I was under the impression that one of the possible advantages of the type of isolator you have been suggesting is that, in contrast with displacement isolators utilizing a resistance strip, the power would be dissipated within the entire volume of the ferrite rather than in a small thin strip. But did you not indicate that this is a surface phenomenon and that all the power dissipation would take place on the surface of the ferrite?

Dr. Seidel: Power dissipation does occur on the surface; however, one can get these propagations in arbitrarily small guide so that there need not be much more ferrite than just the surface. I believe that the ferrite can be made sufficiently small to produce these effects. There isn't too much of a heat transmission problem, I believe, because of the finite manner in which the energy is bound to a surface. It will have considerably higher power dissipation than a very thin film, but I am not sure just how much power one should actually attempt to dissipate.

Dr. H. J. Carlin (Polytechnic Institute of Brooklyn): I would like to ask whether it had been definitely established that some of this anomalous propagation could not be described by a complete set of TE and/or TM modes, that is, an ordinary mode description, and whether it was necessary to assume that this anomalous type of surface mode was necessary?

Dr. Seidel: I would say that these anomalous modes are part of a complete set and not an admixture of another part of a complete set. These modes will propagate under conditions where no other modes can propagate and one can ascribe propagation constants to these field distributions which are real. Since real propagation constants cannot be obtained from an admixture of cutoff modes, we must conclude that these anomalous modes are a linearly independent portion of a complete set.

Dr. Lax: There is one thing that disturbs me about this type of propagation. You are talking about it when the field is adjusted for resonance. I presume that, when you were talking about these high reverse-to-forward ratios due to bridging effects, you were on resonance.

Dr. Seidel: These are nonresonant effects which operate at relatively low fields, and these are not interference phenomena. They differ from the bridging phenomenon Crowe alluded to yesterday.

Dr. Lax: Nevertheless, one does obtain a large loss factor at these particular frequencies.

Dr. Seidel: We have built various types of "paradox isolators" (I guess that's as good a name for them as any, I was even thinking of using the name "Laxadox isolators") and actually we get fairly low losses in one direction and rather wide rejection of nominally large values in the opposed direction, essentially without reflection. I would like to elaborate, just for a moment, on what I feel might be the primary advantage of such devices. Resonance isolators, field displacement isolators, or the type of isolators that Bill Crowe talked about yesterday, depend on balancing techniques or circuit resonance. These are effects which can only be stimulated over a narrow band. The field displacement isolator is a device operating over a limited band where the field is essentially excluded from a dissipative medium. Faraday devices operating dispersively would tend to act this way too. The virtue of the sort of isolator which you have introduced in paradox form, Dr. Lax, is that the isolation occurs in principle over a very broad range, whereas transmission over this range is not restricted. I believe, therefore, that we may possibly be able to build relatively broad-band devices based on this sort of phenomenon, as opposed to the type of isolator which one builds on the other effects, namely operating on a balance which is theoretically perfect at only one frequency.

We have built some rather striking isolators based on these phenomena, although these are as yet not nearly as wideband or as lossless as I would hope. I feel that these structures represent not so much of an anomaly as a rather interesting and practical sort of mechanism for construction.

Dr. Vartanian: I wonder if Dr. Seidel would care to comment on the relationship between this anomalous propagation and the spinwave modes described by Suhl and Walker. Is there some kind of relationship between these two phenomena?

Dr. Seidel: It's unfair to call them the Suhl and Walker modes because in this particular area Suhl obtained one set of spinwave modes, Walker obtained another, and I believe I have obtained still another. Suhl involved himself with spinwave modes which relate to the exchange system and these are of extremely high wave numbers. I do not believe that the sort of modes which we get in the anomalous propagation relates to them. These modes may have wave numbers of the order of a micron wave length, which are of the order of crystallite dimensions and, therefore of the order of many thousands of lattice constants. On the other hand, the Suhl type of mode actually gets down to just the order of several lattice constants and it is of entirely different nature. Walker's modes I believe are somewhat similar to my own, except, that he treats them in a localized region. He shows that there are transversely propagating modes within a disk or sphere or some limited geometry. The modes I have referred to as "anomalous modes" are somewhat reminiscent of Walker's, but relate to a cylindrical waveguide distribution. Mechanisms dealt with are similar; Walker and I both employ only the dipolar features associated with

the ferrite and do not consider its exchange.

Dr. R. F. Soohoo (Cascade Research Corp.): If we assume both the waveguide and ferrite to be lossless, would the anomalous mode still have loss in it? Do you still have energy dissipated, and if so, where does the energy go?

Dr. Seidel: Technically, every medium must have some loss on an atomic level of description. In the treatments generally considered, an idealization is made of the medium to a continuum with a precessional character represented by the Polder tensor. Maxwell's equations are thermodynamically correct and there is no violation of thermodynamics within this framework of description of the medium in assigning a zero value to the damping parameter. I assume that the question asked relates to energy absorption in such a hypothetical medium. This type of absorption relates in turn to the Lax anomaly discussed earlier in which energy absorption might appear to occur in such an idealized dissipationless medium.

In answer to this question I feel that the "anomalous" modes represent a mechanism of energy loss in such a medium. We define a lossless medium to be a limiting case for one whose resonance line width approaches zero. Choosing any line width, however narrow, one may then always choose a mode of wave number of order greater than the reciprocal of the line width which absorbs energy from the medium. Essentially this implies that, however small the damping parameter, one may always find waves sufficiently slow to absorb energy. This description, however, fails when the wave numbers become atomistic, since they have no meaning within this sort of a description.

Philip Johnson (Signal Engineering Laboratories): During this conference there has been no discussion about the barium oxide type of magnet, in fact there hasn't been much since M. T. Weiss' paper of a few years ago. I was wondering if you think there is much hope for the barium oxide type device today?

Dr. Hogan: In the first place, it appears that all of the ferroxoplanar materials including Ferroxdure have been neglected by microwave engineers. Perhaps this is due to the fact that up to now there has not been great emphasis on the need for devices which operate at the extremely high frequencies where these materials will be most useful. There is no doubt that these materials offer unique advantages at the very high frequencies where very large magnetic fields are necessary to bias a ferrite to resonance. As a single crystal or as an oriented polycrystal, the high anisotropy fields in these materials can be used to materially reduce the applied field necessary for resonance. Since the family of ferroxoplanar materials promise to give us materials in which the anisotropy field can be controlled over wide limits, it appears that these materials will have a distinct advantage over the usual ferrites for most frequencies above *K* band. In addition, the limited data that has been taken on these materials indicate they can be prepared with extremely low dielectric loss.

Dr. Vartanian: I might add something to this. I believe that the Dutch at Phillips Research Laboratories are doing a considerable amount of work on this ferroxoplanar material, and about two months ago they were going to begin measuring its properties at microwave frequencies. I haven't heard anything since, however. Another interesting property of these materials seems to be that they will maintain a high permeability, which remains flat as a function of frequency all the way out to something like, say, 1200 mc. Typical values of permeability might be around 10 or so.

Dr. Artman: Another interesting thing about these materials (which may not have practical use) is that under certain simplified conditions in single crystals below magnetic saturation, the material is a gyrotropic resonator in a plane, but just a linear resonator in the third direction at a different frequency from that for gyrotropic resonance.

Leonard Swern (Sperry Gyroscope Co.): I would like to direct the panel's attention to fast switching type ferrite devices. I am wondering whether anybody can talk about, let's say, devices in the megacycle switching rate region, perhaps single-sideband modulators, and what material developments are required to really extend that region.

Dr. LeCraw: The subject of fast ferrite switching is an interesting area in which a lot of ferrite materials development needs to be done. I'm afraid, though, that your question is so broad I don't know where to start. For some of you who may not be aware of it, ferrite microwave switches have been made which can operate as fast as 5 mμsec switching time from an ON to an OFF state or vice versa. This limit was the limit of our viewing system. The actual limiting ferrite switching time is probably of the order of the spin-spin relaxation time, which is approximately 1 mμsec. But from this value all the way through the microsecond range, which you mentioned, there is a whole series of design problems. We have found that ferrites intrinsically can handle speeds as fast as 5 mμsec. From this speed range to much slower speeds one should know whether he is forced to use transverse fields or longitudinal fields, or whether he has a heavy duty cycle or low duty cycle, in order to discuss the design limitations.

I would like to say one thing further about materials development in connection with high-speed ferrite switching. I am speaking now of microwave switching and not of computers. One of the biggest problems is finding a ferrite which has good characteristics both at microwaves and over the frequency spectrum of the rise time that you are talking about. I believe very little has been done in this respect because most microwave design engineers are so concerned about insertion loss that they are unwilling to tolerate an extra db of insertion loss in order to obtain a ferrite with much lower hysteresis loss, for example, to minimize the area under one pulsing cycle.

John H. Rowen (Bell Telephone Laboratories): A switch designed at our laboratories is amenable to fast switching applications, but we were using it to switch a microwave relay where a millisecond was fast enough. I should point out that the same principle of operation was used in LeCraw's switch even earlier. LeCraw added a number of details which make it possible to produce a very fast switch. Both switches make use of an interference effect such that the current required to turn the switch off has a very broad characteristic. The switch is initially turned off, say with 100 ma of solenoid current, and stays turned off until it exceeds several hundred milliamperes. The virtue of this is that one can choose a steady-state value of current way up on the characteristic, and very early in the rising portion of the current cycle the switch will go into the OFF position. In this way you can get perhaps a factor of ten in improvement in switching time; *i.e.*, ten times the limiting speed of switching the ferrite itself. LeCraw achieved this sort of dependence in his switch through the use of irises. J. A. Weiss, through the use of different kinds of irises, has produced the same effect in a way that can lead also to a reasonably broad-band switch, for example, a switch which would operate over a band of 200 or 300 mc out of 6000 mc. However, as I said, we haven't carried out any extensive experiments on fast switching devices.

Dr. Vartanian: There is one rather basic problem to any high repetition rate ferrite switching scheme in which the direction of the magnetization is reversed or in which the ferrite is allowed to become unsaturated. This is that the hysteresis losses can cause a significant rise in the ferrite temperature which in turn can significantly degrade the switching characteristics. Consequently, it would seem desirable to operate high duty cycle switches with the ferrite remaining normally saturated, and let the switch operate as a result of a change in H rather than M.

Dr. Soohoo: I would like to say just a word about fast switching. Since the switching time or the speed at which it is switched depends among other things on the eddy currents, it seems that we have to concern ourselves with nearby metallic objects as well as the ferrite itself. For example, iron has resistivity of 10^{-5} ohm-cm while ferrite has resistivity of 10^{9} or so, which is 14 orders of magnitude higher. It seems to me the speed would be limited more by the waveguide and the winding nearby, for example, rather than by the intrinsic properties of the ferrite itself.

Dr. Wantuch: I won't go into any details here for fairly obvious reasons but we have designed ferrite switches as tr tube replacements. We have been able to switch in a tenth of a microsecond and the total power required for switching at several-hundred-kc rate has been about 10 watts average.

Dr. LeCraw: I would like to say a word about Dr. Soohoo's question. For very high-speed switches where you have to worry about skin depths and penetrations of waveguide, etc., we have had considerable success in putting the coil inside the waveguide very close to the ferrite, in fact within 1/16 of an inch of the ferrite, without appreciably perturbing the microwave fields. This is very advantageous from a pulse design standpoint and can appreciably diminish the effects of the waveguide walls and eddy currents.

Dr. Soohoo: We have built the Cacheris single-sideband modulator and found that a metallic coating on the inside of the waveguide substantially limits the field requirement. For instance, we found that a very bulky magnet was required for a K_u-band modulator.

John C. Cacheris (Diamond Ordnance Fuze Laboratories): We have designed several reflection type single-sideband modulators that shift the frequency of X-band signals by 20 kc using a magnetic field, rotating transverse to a ferrite differential half-wave section. With thin coatings of either cadmium or nickel plating we have minimized eddy current losses in the waveguide so that the rotating magnetic field is not appreciably attenuated. We have found that the ferrite, and its geometry, are the most important factors in obtaining the 180-degree differential-phase-shift with as low a value of magnetic field as possible, so that the modulating power is not too large. At X-band frequencies, the 200-oersted magnetic field can be rotated at 10 kc by applying approximately 18 watts in each pair of coils. At K_u band the magnetic field required will be larger, since the differential-phase-shift decreases with increasing frequency and the modulating power will be larger. The eddy current losses do not depend upon the microwave frequency. They depend upon the value of the magnetic field and should account for the same fraction of modulating power.

Dr. Seidel: I should like to ask Dr. Carlin a question. There are many types of representation of ferrite structures which are all equivalent. For instance, Tellegen represents the nonreciprocal character of the ferrite through a gyrator type of description. Haus has a nonreciprocal element, a four pole cascade element. Circulators are employed in describing ideal networks too. If you desire to describe a ferrite network through a minimum number of elements, what do you consider are the canonical elements for such a description?

Dr. Carlin: There are many circuit representations for linear nonreciprocal structures. For example, just recently, at the 1957 IRE National Convention, Mason presented another basic nonreciprocal element and there have been many others. So far as I know the only complete treatment of general linear nonreciprocal passive circuits in canonical configuration (*i.e.*, a treatment which shows that given any physically possible system it will always be possible to form an equivalent circuit out of preassigned building blocks) has been done in terms of usual reciprocal elements and the gyrator. With that as a basis, any other element you want to take as a building block to represent nonreciprocity must be shown capable of suitable combinations to form

the equivalent of a gyrator. As to which building block is most convenient, and gives the best equivalent circuits, I don't think I would know the answer to that. I would imagine that you would have to adapt your equivalent circuit representations to the problem at hand. In some instances current and voltage controlled sources might be most useful (these are active, however). In other instances a "gain-producing" black box has been used. The gyrator however has the theoretical advantage of being purely passive, and I may reiterate that any passive linear system may be represented in terms of gyrators and conventional bilateral elements.

Dr. Seidel: Could you go into just a little more detail on Mason's equivalent circuit?

Dr. Carlin: I heard Mason discuss the so-called gyristor at the IRE 1957 National Convention and, maybe I won't do justice to him, but it was something like this. Any nonreciprocal circuit can evidence nonreciprocity if it's at least a two-port, as it must have an input and an output. For this reason no nonreciprocal element is needed to represent a one-port. However, Mason uses what appears to be a one-port for his nonreciprocal building block. This two-terminal device works as follows. If it has a voltage V_A (terminals 1 to 2). the current I_A (1 to 2) is aV_A. If the same voltage is impressed from 2 to 1, the current from 2 to 1 is not I_A but $-I_A$. If you visualize a ground terminal as terminal 3, it is easy to see that with respect to voltages to this ground reference the device has an admittance matrix $Y_{11}=-Y_{22}=a$, $Y_{12}=-Y_{21}=a$. Thus this element is actually a nonreciprocal three-terminal two-port. Furthermore, it is not passive and can be represented as a gyrator shunted by a positive and negative resistor at its input and output, respectively.

Dr. Artman: I might mention that from a physical point of view it's immediately intuitive that you should have a two-port system. If you have an ordinary type of linear oscillator there is only one direction. Here something else happens in another (a perpendicular) direction, and really everything automatically follows from that.

Mr. Cacheris: What are the limitations of a single crystal as compared to polycrystalline materials when used in devices with regard to switching time, losses, etc.?

Dr. Hogan: The question, if I understand it correctly, is, "What are the potentialities and limitations of single crystal materials as compared to polycrystalline materials for various microwave devices?" Often in the past, single crystals sounded very promising for many types of microwave devices and I know of some development work being done where single crystal ferrites were used in several devices. Usually, however, the designer finally ended up using polycrystalline material, not only because it was cheaper and more reproducible, but because the polycrystalline material could be made with most of the desired properties and there seemed to be little reason to press for better materials.

However, many of the newer devices recently proposed (*i.e.*, harmonic generators, Suhl's amplifier, microwave detectors, and passive limiters) appear to be really practical only with the very narrowest resonance line width materials available and so it does seem that in the future single crystal ferrites and garnets will have more engineering importance than they have had up to the present. Before they can be used, however, it appears that much work will need to be done on methods of preparing the single crystal material. In most of these devices we need larger, more homogeneous crystals than are usually available today.

We really can't say much else in comparison except as a conjecture, since there is little data on single crystal material. Usually single crystal ferrites have much higher dielectric loss than polycrystalline ferrites, but this need not always be the case if we can learn to grow single crystals with the proper oxygen stoichiometry. Probably the magnetization in a single crystal can never be switched as fast as it can be in some of the specially prepared polycrystalline materials.

Dr. D. L. Fresh (Trans-Tech, Inc.): The potential need of large single crystals presents a serious problem to workers in the materials field. Whereas polycrystalline ferrites can be prepared utilizing standard ceramic methods of compacting oxide mixtures and kiln firing, single crystal preparation requires tedious and time-consuming techniques, which often involve elaborate equipment. The two techniques which have been investigated most extensively are precipitation from a melt and Verneuil's method. In the precipitation method the oxide constituents are combined with a flux and the mixture is melted by heating. Upon very slow cooling, crystals precipitate from the melt. Galt at Bell Telephone Laboratories used a method employing a flux of borax to prepare crystals of nickel ferrite and zinc-manganese ferrite. Garnet single crystals have been prepared by this method using lead monoxide as a flux. The main disadvantage to the precipitation method is the small size of the product, which is usually not more than several millimeters on an edge. A second disadvantage is the possibility of inclusion of impurities from the flux. Verneuil's method offers a means for growing larger single crystals. Here the oxide mixture is shaken into the flame of an oxygen-hydrogen torch. The mixture is sintered into a cone which collects on a refractory pedestal. The top of the cone melts and the pedestal is lowered gradually as the melted material builds up and in this way a crystalline boule is formed. Due to the high temperatures required in this method, it is very difficult to establish stoichiometry from the standpoint of oxygen content and, in some instances, metal content too, if volatile metallic constituents are involved. Such nonstoichiometry generally leads to a useless product because of a high dielectric loss. Verneuil's method has been employed in preparing the spinel type of ferrite, such as magnesium ferrite, but I am not aware of any work that has been done using this method on the gar-

nets. Such an effort might prove fruitful since the garnet crystal does not contain divalent metallic ions and therefore would be less susceptible to nonstiochiometry. If the need for large single crystals materializes, the two methods just discussed, as well as other methods such as zone melting and vapor deposition, should be thoroughly investigated. As Dr. Hogan remarked, there is definitely a lot to learn about growing single crystals before they will become available. I strongly endorse this sentiment.

Dr. Artman: I would like to make one additional comment, leaving aside the very difficult problems concerned with procuring these crystals. The analysis of many of these devices being discussed would be much more difficult because the specification of the properties of the medium would be somewhat more complicated due to the single crystal properties (which are in a sense averaged out when you speak about polycrystals). If I may, I would like to ask a question on another subject. Since the advent some years ago of ridged waveguide why, at least to my limited knowledge, have no isolators or other components been developed using this type of waveguide?

Dr. Wantuch: I would say that for ridge guide isolators you have some of the same problems you have without ridges. There is always the average power that you have to handle and I think there is nothing really different about ridged waveguide. I know we have made isolators covering 40 per cent or more in bandwidth with the same kind of ratios you have in ordinary rectangular waveguide configurations.

Dr. A. L. Aden (Sylvania Elec. Prod.): Sylvania has built isolators of several types using ridged waveguide. Using dielectric loaded ridged guide we have built isolators covering a bandwidth of 2 to 1. I think the reason that ridged waveguide is not used more commonly at the present time, however, is that the bandwidths currently achievable in rectangular waveguide structures are adequate to meet the needs of most systems applications. For example, Sylvania has built isolators with a bandwidth of 1.5 to 1 in dielectric loaded rectangular waveguide in all frequency bands from S through X band. In addition, recent, and as yet unpublished, work at the Sylvania Microwave Physics Laboratory has shown that with proper dielectric loading the bandwidth of a rectangular waveguide can be increased by a factor of approximately 1.7 over its empty waveguide bandwidth.

Dr. Seidel: I would like to ask a question of Dr. LeCraw. I know that both he and John Rowen have observed negative values of K''. Would he comment on its significance?

Dr. LeCraw: Let me say one thing first about K itself, the off-diagonal component of the permeability tensor. Some people take K as an intrinsically negative number and others take it as a positive number. This has caused some confusion as to whether the anomaly is a negative K'' or a positive K''. But either way the change of sign of K'' is the essential anomaly. There is no contradiction at all as far as absorbed power is concerned in the change of sign of K''. It is easy to show by integrating the power dissipated in a ferrite that K'' can have either sign. But μ'' cannot have either sign; it must be positive. As far as K'' changing sign, an important thing about this is that below saturation the μ and K are spatial averages of quantities which only have "point" meaning down inside a crystallite. Slides are often shown of μ and K, but below saturation these quantities don't have quite the same meaning as they do above saturation. The K'' changing sign means that the average of K'' over all the crystallites in the sample changes sign. These averages, of course, are the experimental quantities which are measured in any perturbation experiment. But it is a rather interesting effect in that below saturation the anti-Larmor sense of circular polarization is in general absorbed to a greater extent than the Larmor sense of polarization. Incidentally, the change in sign of K'' below saturation is an intrinsic loss property of the ferrite and should not be confused with the widely discussed energy concentration effects in the experiments of A. G. Fox of the Bell Telephone Laboratories. The situation reverses above saturation and everything is normal from then on out to arbitrarily large dc fields. The explanation of the effect is rather involved, and I hope it has been explained satisfactorily in an article which I have written recently. The effect should be very useful as a probe for studying domain structure and magnetization processes in ferrites.

Dr. Artman: I would like to make one slight comment; I think it's a little bit unfair to single out K'' as such. Again, going back to the basic model, the ferrite is a gyroscope and when you consider loss you have to consider gyroscopic precession. If you have some kind of a linear drive you have to, at least visually, break up the drive appropriately into two gyroscopic drives. True, on a glib basis some of these μ'' and K'' may drop out or something like that, depending upon the circumstances, but I think it would be best to keep, or try and keep, the physical picture in mind.

E. Schlomann (Raytheon Manufacturing Co.): I wonder if somebody could comment on the relative advantages and disadvantages of the new garnet amplifier and the solid-state maser.

Dr. H. E. D. Scovil (Bell Telephone Laboratories): At the moment both devices would appear to be quite expensive amplifiers *per se*, and it would seem that perhaps the main virtue of them would be what we hope is a low noise figure. At the present time the noise figures have not been measured.

There is good theoretical reason to believe that a two-state maser has low noise. Perhaps one should be somewhat more cautious with regard to the three-level solid-state device in so far as the large pumping power may mix in noise from some unknown nonlinearities. The ferrite device being essentially a reactive amplifier at first sight also has low noise; on the other hand there appears to be perhaps even a stronger possibility of mix-

ing in additional noise. We must await the noise measurements.

The ferrite device is capable of higher output powers than the maser and operates at room temperature. At the present stage the solid-state masers are low temperature devices.

Mr. Anderson: Could we get some suggestions for nomenclatures for these devices, three-level maser, two-level maser, the ferrite or garnet amplifier, so that maybe we could start using a common name?

Dr. Scovil: I believe the term "maser" should be restricted to devices utilizing a population inversion or negative temperature and that the various masers should be differentiated perhaps by a prefix indicating their method of operation; *e.g.*, ammonia beam maser, two-level maser, three-level maser, etc.

I think that the christening of the ferrite device is best left to Drs. Suhl and Weiss who have produced it. It does not fall in the category of negative temperature devices.

Dr. R. W. Damon (General Electric Co.): The principal reason for the great interest in resonance amplification devices lies in their potentiality as low noise amplifiers. Usually the term "noise" refers only to a fluctuating output observed in the absence of a signal, but, under some conditions, random variations in amplifier gain also should be considered. In this respect, the ferromagnetic amplifier might be at some disadvantage compared to the three-level paramagnetic device. The paramagnetic amplifier uses the driving oscillator only to create a saturation condition for a pair of energy levels. If the driving power is sufficiently large, fluctuations in the driving level have little effect on the degree of saturation and the gain is thus independent of small variations in driving power. The ferromagnetic amplifier, on the other hand, operates as a negative resistance device, obtained by driving a nonlinear reactance with power level above a certain instability threshold, and fluctuations in power level of the driving source will lead to fluctuations in gain.

Dr. Hogan: Well I have just been informed that in about 3 minutes the lights in this auditorium will be turned out, so I suggest we start on our way.

Correspondence

Note on Impedance Transformations by the Isometric Circle Method*

The isometric circle method is a graphical method of transforming a complex quantity by the linear fractional transformation. It has recently been applied to impedance transformations through bilateral two-port networks.[1] The purpose of this note is to show the connection between the isometric circle method and another graphical method called the "triangular" method, and also to present a useful formula for reflection-coefficient transformations through bilateral, lossless two-port networks.

The triangular method is described in an unpublished paper by Mason.[2] In this method it is assumed that one pair of corresponding values $Z_a \rightarrow Z_a'$ is known for the linear fractional transformation

$$Z' = \frac{aZ + b}{cZ + d}, \quad ad - bc = 1 \qquad (1)$$

where, for a fixed frequency, a, b, c, and d are complex constants. The values $Z' = O_i = a/c$ for $Z = \infty$, and $Z' = \infty$ for $Z = O_d = -d/c$ are known also. For an arbitrary impedance Z, the transformed impedance Z' is constructed by drawing the similar triangles O_dZ_aZ and $O_iZ'Z_a'$ in the complex impedance plane. See Fig. 1. The connection between the triangular method and the isometric circle method is shown in Fig. 1. In Fig. 1, the different operations of the isometric circle method (marked by arrows) are indicated by the points Z_1, Z_2, and Z', and the angle -2 arg $(a+d)$ is denoted by θ.

Impedance transformations through bilateral, lossless two-port networks can be performed by the equation

$$Z' = \frac{a'Z + jb''}{jc''Z + d'}, \quad a'd' + b''c'' = 1, \qquad (2)$$

where $a' = \text{Re } a$, $b'' = \text{Im } b$, $c'' = \text{Im } c$, and $d' = \text{Re } d$. Expressed in reflection coefficients,

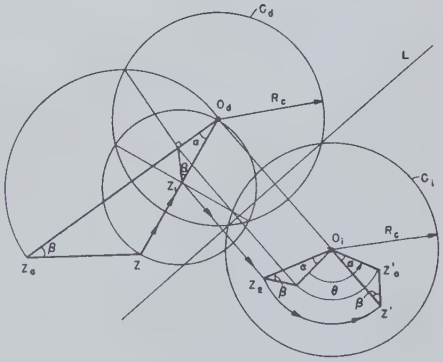

Fig. 1—Connection between the triangular method and the isometric circle method.

(2) takes the form

$$\Gamma' = \frac{A\Gamma + C^*}{C\Gamma + A^*}, \quad |A|^2 - |C|^2 = 1, \qquad (3)$$

where

$$A = (a' + d')/2 - j(b'' + c'')/2$$
$$C = (a' - d')/2 - j(b'' - c'')/2. \qquad (4)$$

A star indicates a complex conjugate quantity.

* Received by the PGMTT, October 4, 1957. This work was supported in part by the U. S. Army (Signal Corps), the U. S. Air Force (Office of Scientific Research, Air Research, and Development Command), and the U. S. Navy (Office of Naval Research).

[1] E. F. Bolinder, "Impedance and polarization-ratio transformations by a graphical method using the isometric circles," IRE TRANS., vol. MTT-4, pp. 176–180; July, 1956.

[2] S. J. Mason, "A Simple Approach to Circle Diagrams"; 1954.

We can write (3) in the form

$$\Gamma' = \frac{\Gamma \cosh \psi e^{j\phi_a} + \sinh \psi e^{-j\phi_c}}{\Gamma \sinh \psi e^{j\phi_c} + \cosh \psi e^{-j\phi_a}}, \quad (5)$$

where ψ, ϕ_a, and ϕ_c can easily be expressed in a', b'', c'', and d'.

The isometric circles of (5) are given by

$$\left.\begin{aligned} O_d &= -\coth \psi e^{-j(\phi_a+\phi_c)} \\ O_i &= \coth \psi e^{j(\phi_a-\phi_c)} \\ R_c &= 1/|\sinh \psi| \end{aligned}\right\}. \quad (6)$$

Eq. (5) has recently been used as a basis for an elementary study of impedance transformations through bilateral, lossless two-port networks.[3] A somewhat more complicated study of the same type of network has been performed by means of non-Euclidean hyperbolic geometry in the two-dimensional Cayley-Klein diagram.[4] Similarly, bilateral, lossy two-port networks have been studied by means of the Cayley-Klein model of the three-dimensional hyperbolic space[5].

E. Folke Bolinder
Res. Lab. of Electronics
Mass. Inst. Tech.
Cambridge, Mass.

[3] E. F. Bolinder, "Some applications of the isometric circle method to impedance transformations through lossless two-port networks," presented at the URSI-USA meeting in Washington, D. C.; May 22-25; 1957, and *Acta Polytech., Elec. Eng. Ser.*, to be published.

[4] ———, "Graphical methods for transforming impedances through lossless networks by the Cayley-Klein diagram," *Acta Polytech., Elec. Eng. Ser.*, vol. 7, no. 202; 1956.

[5] ———, "Impedance transformations by extension of the isometric circle method to the three-dimensional hyperbolic space," *J. Math. Phys.*, vol. 36, pp. 49–61; April, 1957.

On the Pressure Dependence of Microwave Crystal Rectifiers*

During the past couple of years, as a result of government interest, silicon microwave crystal rectifiers have not only decreased their noise figures but also have increased their resistance to adverse environments; *i.e.*, high burnout, high temperature, excessive humidity.

However, recent requirements have indicated a need for microwave crystal rectifiers which operate at low pressures; *i.e.*, high altitudes. Unfortunately, while there is no obvious reason to suspect any serious pressure dependence of any of the crystal parameters, there have been no quantitative operating measurements made as far as can be determined, except for the fact that radars do work in airplanes.

Therefore, in order that the current silicon microwave crystal rectifiers be characterized in so far as low pressure is concerned, a measurement of all the crystal parameters was performed in a reduced atmosphere.

All crystal measurements were made on a special test set which enables one to measure all the crystal parameters, primarily at the test frequency of 9375 mc under the established JAN conditions.[1] The conversion loss was measured by the usual modulation method. The noise temperature (ratio) was measured by comparing the noise power output of the crystal under test with the noise power output of a (equivalent) resistor. The vswr was measured with the standard slotted section, and the IF impedance by the use of an ac wheatstone-bridge type circuit operating at 1000 cps. The over-all noise figure of each crystal was measured by inserting a known amount of excess noise into the crystal at the signal frequency (9375 mc ± 30 mc) and determining the increase in output power.

The crystal mixer (holder) was placed in a bell jar which could be evacuated by a nearby fore-pump. The reduced pressure was measured with the aid of an attached, calibrated altimeter. The crystal was initially measured in this holder at normal conditions, measured at the desired pressure, and remeasured at the standard (initial) conditions. The results of the measurements are shown in Table I.

TABLE I

Results of Measurements of Microwave Crystal Rectifiers At Standard and Reduced Pressures
Initial Readings—Standard Pressure

Number	Pressure (mm Hg)	Rectified Current (ma)	Conversion Loss (db)	Noise Temperature (times)	IF Impedance (ohms)	VSWR	Over-all Noise Figure (db) F_{IF} = 3.2 db approx.
1	760	1.44	4.6	1.3	342	1.23	8.6
	15	1.28	4.9	1.3	361	1.39	8.4
	760	1.30	4.7	1.3	362	1.41	8.4
2	760	1.37	4.5	1.2	350	1.23	8.0
	15	1.33	4.6	1.2	359	1.28	8.2
	760	1.33	4.6	1.2	359	1.28	8.0
3	760	1.30	4.7	1.4	397	1.21	9.1
	15	1.30	4.7	1.4	399	1.22	9.0
	760	1.30	4 7	1.4	400	1.22	9.0
4	760	1.42	4.4	1.2	352	1.11	7.9
	15	1.39	4.5	1.2	356	1.16	8.0
	760	1.39	4.5	1.2	357	1.16	7.8
5	760	1.44	4.5	1.3	329	1.19	8.2
	15	1.44	4.6	1.3	331	1.19	8.2
	760	1.44	4.5	1.3	332	1.20	8.0
6	760	1.18	5.2	1.3	370	1.20	9.3
	15	1.16	5.5	1.3	375	1.20	9.1
	760	1.18	5.1	1.3	374	1.20	9.0
7	760	1.18	5.5	1.5	343	1.35	10.2
	15	1.14	6.0	1.5	346	1.36	10.2
	760	1.17	5.6	1.5	344	1.34	9.9
8	760	1.12	5.4	1.5	345	1.46	9.9
	15	1.12	5.5	1.6	349	1.47	10.1
	760	1.11	5.5	1.6	347	1.46	9.9
9	760	1.12	5.5	1.3	353	1.22	9.3
	15	1.12	5.6	1.3	357	1.22	9.3
	760	1.12	5.6	1.3	357	1.23	9.1
10	760	0.99	5.7	1.5	425	1.36	10.1
	15	1.00	5.8	1.5	424	1.37	10.2
	760	0.99	5.8	1.5	426	1.37	10.1

Table I shows that the crystal parameters were found to be essentially constant under reduced pressure and at standard pressure after the test when compared with initial measurements. Therefore, one can conclude that under the stated conditions (*i.e.*, MIL-E-1-C, JAN 1N23C, E or WE) up to an atmosphere of 85,000 feet (15 mm Hg) the cartridge type, JAN, silicon microwave crystal rectifiers show little or no degradation in performance due to a reduced pressure environment.

Acknowledgment should be given to W. Dworzak and G. E. Hambleton for assistance in setting up the test equipment, and to G. Hall for performing the measurements.

Wesley G. Matthei
U. S. Army Signal Eng. Labs.
Fort Monmouth, N. J.

* Received by the PGMTT, October 14, 1957.

[1] See 1N23C, E or WE Specifications issued by USASESA, Fort Monmouth, N.J.; also see Torrey and Whitmer, "Crystal Rectifiers," McGraw-Hill Book Co., Inc., New York, N. Y., ch. 9; 1948.

PGMTT News

1957 Annual PGMTT Meeting

The Annual PGMTT Meeting was held May 9–10 in New York, N. Y., at the Western Union Auditorium. Three hundred and six attended the outstanding program. Twenty-three technical papers were given, three of which had been invited.

Unusually keen interest in microwave ferrites, as evidenced by the incredible rate of research and development accomplished during the relatively short time ferrites have been in existence, was noted in the papers.

Highlighting the Annual Meeting was a Round Table Discussion on the design limitations of microwave ferrite devices. During the well-attended Annual Dinner it was announced that Dr. Robin I. Primich had been awarded the Microwave Prize. The technical papers and Round Table Discussion are featured in this issue.

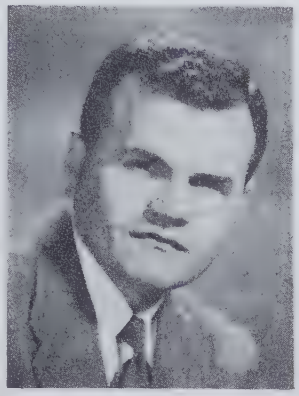

The Annual PGMTT Meeting was organized by T. N. Anderson (left) and opening remarks were made by W. L. Pritchard (right), Vice-Chairman, PGMTT Administrative Committee.

PGMTT members at the Annual Dinner were (left to right): Dr. A. A. Oliner, Jack A. Moore, Dr. Eugene Fubini, W. L. Pritchard, Dr. Seymour B. Cohn, Dr. P. H. Vartanian, and Leonard Swern.

Another Dinner group included (left to right): Leo B. Silber, Dr. Samuel Weisbaum, Patricia Loth, Dr. Kiyo Tomiyasu, and Theodore S. Saad.

Panel members of the Round Table Discussion on Design Limitations of Microwave Ferrite Devices were (left to right): Drs. D. L. Fresh, J. O. Artman, G. S. Heller, P. H. Vartanian, C. L. Hogan, Moderator, H. Seidel, R. C. Le Craw, and H. J. Carlin.

CALL FOR PAPERS FOR 1958 PGMTT NATIONAL SYMPOSIUM

Stanford University, Stanford, Calif., will be the scene on May 5–7 of the 1958 Symposium, sponsored by the National PGMTT with the San Francisco Section of the IRE acting as host. Dr. Arthur L. Aden is the Symposium Chairman.

Prospective authors have been invited to submit papers in the fields of microwave physics and applications, microwave components, and microwave theory and techniques, prior to January 15th, to Dr. Kiyo Tomiyasu, Chairman, Technical Program Committee, 601 California Avenue, Palo Alto, Calif.

Six invited papers will be presented:

"Solid State Microwave Amplifiers," Prof. Hubert Heffner, Stanford University

"Microwave Properties of Gas Discharges," Prof. Sanborn C. Brown, M.I.T.

"At the Frontiers in Radio Astronomy," Dr. Harold I. Ewen, Ewen-Knight Corp.

"The Present State of the Millimeter Wave Generation and Technique Art," Prof. Paul D. Coleman, University of Illinois

"Applications of the Nonlinear Properties of Ferromagnetic Resonance," Prof. C. Lester Hogan, Harvard University

"Design Considerations for High Power Microwave Filters," Dr. Seymour B. Cohn, Stanford Research Institute.

The technical sessions will be led by William W. Mumford, Bell Telephone Labs.; Samuel Sensiper, Hughes Aircraft Co.; John R. Whinnery, University of California; Theodore S. Saad, Sage Labs.; Donald D. King, Electronic Communications; and Tore N. Anderson, Airtron.

The Microwave Prize for the best paper published in these TRANSACTIONS will be announced at the banquet to be held on May 6th.

STEERING COMMITTEE

A. L. Aden, *Chairman*, Sylvania Microwave Physics Lab.
T. N. Anderson, Airtron
S. B. Cohn, Stanford Research Institute
W. A. Edson, General Electric Microwave Lab.
H. Heffner, Stanford University
P. D. Lacy, Hewlett-Packard Co.
J. L. Melchor, Microwave Engineering Labs.
T. Moreno, Varian Associates
W. H. Thon, Sylvania Microwave Tube Lab.
K. Tomiyasu, General Electric Microwave Lab.
J. R. Whinnery, University of California

SYMPOSIUM COMMITTEE

A. L. Aden, *Chairman*
K. Tomiyasu, *Chairman, Technical Program Committee*
T. Moreno, *Chairman, Finance Committee*
H. Schroeder, *Chairman, Local Arrangements Committee*, Sylvania Microwave Physics Lab.
G. H. Keitel, *Chairman, Publicity Committee*, General Electric Microwave Lab.

TECHNICAL PROGRAM COMMITTEE

K. Tomiyasu, *Chairman*
S. B. Cohn
E. M. T. Jones, Stanford Research Institute
P. D. Lacy
H. J. Shaw, Stanford University
P. H. Vartanian, Jr., Microwave Engineering Labs.
G. J. Wheeler, Sylvania Microwave Physics Lab.

HOTELS AND MOTELS*

Richeys Studio Inn, 4219 El Camino Real, Palo Alto
Holiday Inn, 1984 El Camino Real, Mountain View
Paso Del Norte Motel, 4238 El Camino Real, Palo Alto
Flamino Motel, 3398 El Camino Real, Palo Alto
Palo Alto Travelodge, 3255 El Camino Real, Palo Alto
El Rancho Palo Alto Motel, 3901 El Camino Real, Palo Alto
Algiers Motel, 2610 El Camino Real, Redwood City
Eldorado Motel, 3305 El Camino Real, Palo Alto
Sky Ranch Motel, 4234 El Camino Real, Palo Alto
Dinahs Motor Hotel, 4269 El Camino Real, Palo Alto
Presidents Hotel, University Avenue and Cowper, Palo Alto

* To simplify the work of the Local Arrangements Committee, no hotel or motel reservations will be made.

Contributors

D. I. Bolef

Dan I. Bolef was born in Philadelphia, Pa., on June 10, 1921. He was graduated from Pennsylvania State College with the degree of Bachelor of Science in physics in 1946. He received the Doctor of Philosophy degree in physics from Columbia University, New York, N. Y., in 1952.

Dr. Bolef was in the Army from 1943 to 1946. He was an instructor in physics in the Stevens Institute of Technology, Hoboken, N. J., from 1949 to 1950; from 1950 to 1953, he was an assistant professor of physics at The State University of New York Maritime College, Bronx, N. Y.

At the present time Dr. Bolef is in the physics department, Westinghouse Research Laboratories, Pittsburgh, Pa. Dr. Bolef's fields of interest are molecular beam studies of diatomic molecules, nuclear magnetic and nuclear quadrupole studies of solids, and electron paramagnetic resonance.

He is a member of Sigma Xi and the American Physical Society.

❖

H. E. Bussey

H. E. Bussey was born in Yankton, S. D., on September 14, 1917. He attended Yankton College and the George Washington University, Washington, D. C., receiving from the latter the Bachelor of Arts degree in mathematics in 1943, and the Master of Science degree in physics in 1951. He continued his studies at the Universities of Maryland and Colorado. His military service included the "A" meteorological course at the Massachusetts Institute of Technology, Cambridge, Mass., the radar-weather course at Seagirt, N. J., and duty as a weather engineering and a weather forecasting officer.

In September, 1946, Mr. Bussey joined the Central Radio Propagation Laboratory of the National Bureau of Standards, to do tropospheric propagation research. In 1951, he transferred to the Radio Standards Division of the same laboratory in the microwave dielectric and magnetic measurements project, and he has been project leader since 1956.

He is a member of the American Physical Society, American Meteorological Society, RESA, Commission I of the International Scientific Radio Union, and Sigma Pi Sigma.

G. W. Catuna

George W. Catuna was born in Waltham, Mass., on December 7, 1923. He attended public schools in Belmont, Mass. He was associated with radar and electronic computers during his service with the United States Army, from February, 1943, to February, 1946, and again from March, 1951, to December, 1952. Since 1952, he has been employed by the Lincoln Laboratory, M.I.T., Lexington, Mass., where he now holds the position of engineering aide in the Solid State Spectroscopy Group. Mr. Catuna is at present taking the electrical engineering course at the Lowell Institute of M.I.T.

❖

P. F. Chester

Peter F. Chester was born in London, England, in 1929. He was graduated with the B.Sc. degree in physics from London University, London, England; he received the Ph.D. degree from that University in 1953. From 1953 to 1954, he was a post-doctorate Fellow with the National Research Council, Ottawa, Ontario, Canada. From 1954 to the present time, Dr. Chester has been with the Low Temperature Group, Westinghouse Research Laboratories.

Dr. Chester's fields of interest are low temperatures, superconductivity, high-pressure phenomena, acoustoelectric effects in semiconductors, and nuclear and electron spin resonance.

Dr. Chester is a member of the Physical Society of London and the American Physical Society.

❖

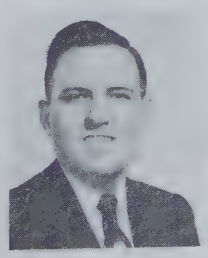

B. J. Duncan

Bobby J. Duncan (M'54) was born in Carrollton, Ga., on February 1, 1930. He received the B.S. degree in physics from Berry College, Rome, Ga., in 1950, and the M.S. degree in physics from Emory University, Atlanta, Ga., in 1951. While at Emory, he did research in microwave spectroscopy. He continued research in this same field while performing graduate work toward a doctorate in physics at the University of Florida, Gainesville, Fla., until 1952, at which time he joined the Sperry Gyroscope Company as a project engineer.

At Sperry he initially did research in applied microwave spectroscopy. Subsequently, he was associated with research and development projects on microwave ferrites, special radar systems, radar countermeasures techniques, and obstacle avoidance equipment. More recently he has worked almost exclusively in the field of microwave ferrite research and components applications. At present, he is a senior engineer and group leader of the microwave ferrite research and advanced development group at the Clearwater, Fla., plant of the Microwave Electronics Division.

❖

D. A. Fleri

Dominic A. Fleri was born in Brooklyn, N. Y., on November 8, 1931. He received the B.S. degree in physics from the Polytechnic Institute of Brooklyn, Brooklyn, N. Y., in 1953. He is currently attending evening sessions at New York University, New York, N. Y., where he is completing the requirements for the M.S. degree in physics. He joined the Sperry Gyroscope Company in June, 1953, but was called to active duty with the U. S. Army Signal Corps in February, 1954. During his two years of military service, he was assigned primarily as an electronics instructor at the Signal School, Fort Monmouth, N. J.

He returned to Sperry in January, 1956, and since then has been engaged in microwave ferrite investigations in the Applied Physics Section of the Microwave Electronics Division, Great Neck, N. Y.

❖

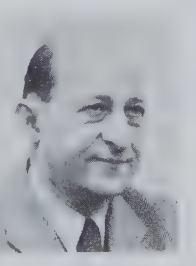

L. Goldstein

Ladislas Goldstein (SM'55–F'56) was born February 6, 1906, in Dombrad, Hungary. He received the B.S. degree in physics from the College of the City of Nagyvarad in 1924, and the M.S. degree in Paris, France, in 1928. He was a fellow from 1929 to 1934, receiving the D.Sc. degree in nuclear physics in 1937.

Dr. Goldstein was an assistant instructor in radium, in Paris, from 1934 to

1937; 1937–1940, a research associate and a fellow of the National Center Research of France; 1940–1941, a research associate at the Institute of Atomic Physics in Lyon; 1942–1944, director of the laboratories at Canadian Radium and Uranium Corp.; 1944–1945, a research worker with the Admiralty Research Laboratories in England, and 1945–1951, a research physicist with the Federal Telecommunication Laboratory. In 1951, he became a professor of electrical engineering at the University of Illinois, Urbana, Ill.

In April, 1956, he received the IRE Fellow Award for his work in the field of microwave gaseous electronics. He has concentrated his efforts in the field of nuclear physics. He has worked on the use of gas discharge phenomena in microwave physics, microwave propagation through media containing free electronics, infrared radiation detection, and the application of ionizing radiations of radioactive substances.

Dr. Goldstein is a member of the Physical Society.

❖

D. S. Heim (S'55) was born in Niles, Mich. on July 15, 1930. He received the degree of Bachelor of Science from the University of Michigan, Ann Arbor, Mich., in 1957, and at the present time Mr. Heim is employed by the University of Michigan as a research assistant in the Electronic Defense Group, where he is engaged in microwave research.

D. S. Heim

Mr. Heim is a member of the American Physical Society.

❖

Gerald S. Heller was born on September 5, 1920, in Detroit, Mich. He received the Bachelor of Science degree in physics in January, 1942, from Wayne University, Detroit, Mich.

G. S. Heller

From 1942 to 1945, he was a staff member of the Radiation Laboratory at Massachusetts Institute of Technology. For one year during this period, he was a member of the Australian Group of the Radiation Laboratory at the Radio Physics Laboratory in Sydney, Australia.

After leaving M.I.T., he was a fellow in applied mathematics at Brown University, where he received the Sc.M. degree in applied mathematics in 1946, and the Ph.D. degree in physics in 1948. Dr. Heller remained at Brown until 1954 as Assistant Professor of physics and worked in theoretical acoustics.

Since 1954, he has been a member of the Microwave Section of the Solid-State Group at the Lincoln Laboratory, M.I.T.

❖

C. Lester Hogan (SM'54) was born on February 8, 1920, in Great Falls, Mont.

In 1942, he received the B.S. degree from Montana State College; in 1947, the M.S. degree from Lehigh University, and in 1950, the Ph.D. degree in physics. Harvard University conferred an honorary M.A. degree upon him in 1954.

C. L. Hogan

Following his graduation from Montana State College, Mr. Hogan became a research engineer with the Anaconda Copper Mining Company. From 1943 to 1946, he served as a lieutenant (jg) with the U. S. Naval Reserve.

Mr. Hogan became an instructor in physics at Lehigh University in 1947. He left that position in 1950 to join the technical staff at Bell Telephone Laboratories, and in 1953, he was named a subdepartment head.

In 1954, he became associate professor of applied physics at Harvard University, Cambridge, Mass., and, in 1957, a Gordon McKay Professor of Applied Physics.

His research interest is the application of ferrites and semiconductors to microwave transmission systems.

He is a member of the American Physical Society, Sigma Xi, Phi Kappa Phi, and Tau Beta Pi.

❖

Benjamin Lax was born in Hungary on December 29, 1915. He received the B.M.E. degree from Cooper Union, New York, N. Y., in 1941 and the Ph.D. degree in physics from Massachusetts Institute of Technology, Cambridge, Mass., in 1949.

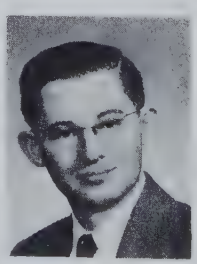

B. Lax

During World War II, he served with the U. S. Signal Corps and the Air Force; he was stationed during 1944–1946 at the M.I.T. Radiation Laboratory carrying on radar development.

In 1946, he became a radar consultant for the Sylvania Electric Products Company, Boston, Mass., and later that year joined the staff of the Air Force Cambridge Research Center. At the same time, he enrolled as a graduate student in physics at M.I.T. He carried on research in microwave gas discharges until November, 1949, when he became a member of the Solid State Group at the Lincoln Laboratory and researched semiconductors and microwave aspects of ferrites. In May, 1953, he was appointed head of the Ferrites Group, which carried on research in the field of ferrites and semiconductors at microwave frequencies. In July, 1955, he was named leader of the Solid State Group, which carries on fundamental and applied work on semiconductors and ferrites. He became associate division head in charge of solid state research at Lincoln Laboratory in March, 1957.

Dr. Lax is a Fellow of the American Physical Society and of Sigma Xi.

❖

David B. Medved (SM'56) was born February 21, 1926, in Philadelphia, Pa. Following service in the Navy from 1944 to 1946, he attended the University of Pennsylvania from which he received the B.A. degree in chemistry in 1949. From 1949 to 1951 he was with the Research Division of Philco Corp., where he engaged in research on color centers, semiconductors, and electron physics. He received the M.S. degree in physics from the University of Pennsylvania in 1951 and the Ph.D. degree in physics in 1955.

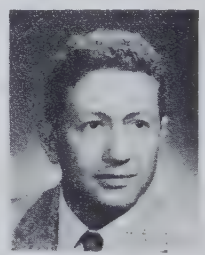

D. B. Medved

While at the University of Pennsylvania, he worked on hydrothermal crystal growth and photoconductivity and chemisorption in zinc oxide semiconductor. Dr. Medved joined Convair's Radiation Systems Section in October, 1954 and has been engaged in research on microwave scanners, radomes, and solid-state devices. He presently is on the staff of the Physics Group at Convair.

Dr. Medved is a member of Sigma Xi and the American Physical Society.

❖

Conrad E. Nelson (A'52) was born on December 4, 1927, on Long Island, N. Y. He received the B.S. degree in electrical engineering from the University of California at Los Angeles in 1949. In 1952, Mr. Nelson was graduated from the three-year Advanced Engineering program at the General Electric Company, Schenectady, N. Y., and continued for three years at GE, Syracuse,

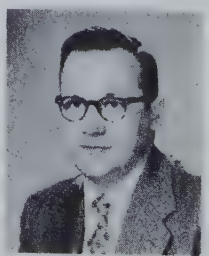

C. E. Nelson

N. Y., doing advanced development of microwave components. Since 1955, Mr. Nelson has been in the Electronics Department of the Microwave Laboratory, Hughes Research Laboratories, Culver City, Calif.

He has been a registered professional engineer in New York since 1955.

❖

John E. Pippin was born in Kinard, Fla., on October 7, 1927. He served in the U. S. Navy during 1945 and 1946, and entered Georgia Institute of Technology, Atlanta, Ga., in September, 1946. He received the B.E.E. degree (Cooperative plan) in 1951 and the Master of Science in Electrical Engineering degree in 1953, both from Georgia Tech. His undergraduate work periods were spent at the Western Electric Company in Burlington, N. C., and Radio Station WSB in Atlanta, Ga. While working for the Master's degree (1951–1953), he worked as a research engineer at the Georgia Tech Experiment Station, with a group studying a fundamental problem in radar tracking.

J. E. Pippin

In 1953, Mr. Pippin entered Harvard University, where he is currently completing work for the Ph.D. degree in applied physics. He is a member of the magnetic materials group at Harvard, which is concerned with the microwave properties of ferrites, garnets, and other magnetic oxides.

He is a member of Sigma Xi, Tau Beta Pi, and Eta Kappa Nu.

❖

Harold Rapaport (M'54–SM'56) was born in Pittsburgh, Pa., in 1922. He received the B.S. degree in physics in 1947 from the University of Pittsburgh, Pittsburgh, Pa., and the M.E.E. degree from the Polytechnic Institute of Brooklyn, Brooklyn, N. Y., in 1956.

H. Rapaport

From 1947 to 1949, he was a graduate assistant and instructor in engineering physics and electrical measurements at the University of Pittsburgh. His experience includes a year as an engineer with the Electronics Research Laboratory at the University of Pittsburgh where he worked on electron tube properties and devices, and several years as an engineer in the Tube Division of the Westinghouse Electric Corporation where he did research and development on high vacuum power tubes.

From 1952 to 1956 he was employed at the Microwave Research Institute, Polytechnic Institute of Brooklyn, as research associate and project engineer on research and development in microwave components and ferrite devices. In 1957, Mr. Rapaport joined the Surface Communications Systems Laboratory of the Radio Corporation of America where he is currently engaged in systems planning.

Mr. Rapaport is a member of Sigma Xi. He was co-editor with M. Wind of the "Handbook of Microwave Measurements" and was on the Editorial Board of the "Handbook of Electronic Measurements."

❖

G. P. Rodrigue was born on June 19, 1931, in Paincourtville, La. He attended Southwestern Louisiana Institute in 1948–1949 and received the B.S. and M.S. degrees in physics from Louisiana State University in 1952 and 1954, respectively. During the summer of 1954, he worked with the power transistor development group at Bell Telephone Laboratories. Since entering the Division of Engineering and Applied Physics at Harvard University in 1954, he has worked towards the Ph.D. degree in applied physics on a Fellowship awarded by the Union Carbide and Carbon Corp., and is a member of the magnetic materials group investigating the microwave properties and applications of magnetic oxides. He held a teaching fellowship while a graduate student at both Louisiana State and Harvard Universities.

G. P. Rodrigue

Mr. Rodrigue is a member of Sigma Pi Sigma and an associate member of Sigma Xi.

❖

H. E. D. Scovil was born on July 25, 1923, in Victoria, B. C., Canada. He received the Bachelor of Arts degree from the University of British Columbia in 1948, the Master of Arts degree in 1949 from the same University, and the Doctor of Philosophy degree in 1951 from Oxford University, Oxford, England.

H. E. D. Scovil

Mr. Scovil was a Nuffield Research Fellow at Oxford from 1951 to 1952. He worked as assistant professor at the University of British Columbia from 1952 to 1955.

For the past two years, he has been employed as a member of the technical staff at Bell Telephone Laboratories, Murray Hill, N. J. Mr. Scovil's work is concerned with solid-state devices.

❖

C. B. Sharpe (S'46–A'52) was born in Windsor, Ont., Canada, on April 8, 1926. He attended Northwestern University, Evanston, Ill., and the University of Michigan, Ann Arbor, receiving the B.S. degree in electrical engineering from the latter in 1947. He received the S.M. degree from Massachusetts Institute of Technology, Cambridge, Mass., in 1949 and the Ph.D. degree from the University of Michigan in 1953, both in electrical engineering. From 1953 to 1955, he served as assistant project officer in the guided missile branch of the U. S. Navy Bureau of Ordnance and as a technical aide in the Office of Naval Research.

C. B. Sharpe

Since returning to the University of Michigan in 1955, he has held the title of assistant professor of electrical engineering. As a faculty consultant at the Electronic Defense Group, he is presently doing microwave research in the field of solid-state devices.

Mr. Sharpe is a member of Tau Beta Pi and Sigma Xi.

❖

Leon A. Steinert was born in Shattuck, Okla., on May 2, 1930. He attended La Sierra College, Arlington, Calif., where he received the B.A. degree in physics in 1952. In 1956, he received the M.S. degree in physics from the University of Colorado, Boulder, Colo.

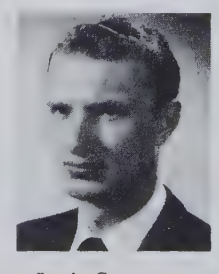

L. A. Steinert

During most of 1953, he was associated with the National Bureau of Standards, Washington, D. C., working in the Resistance Measurements Section. In September, 1953, he began graduate studies in physics and mathematics and served as a part time instructor in physics at the University of Colorado.

Since June, 1956, Mr. Steinert has been associated with the Microwave Physics Section of the National Bureau of Standards Laboratories, Boulder, Colo. He has been connected generally with dielectric and magnetic measurements and presently is

engaged in the study of measurements of ferrite characteristics.

Mr. Steinert is an associate member of RESA.

❖

F. J. Tischer, for a biography and photograph please see page 77 of the January, 1957, issue of these TRANSACTIONS.

❖

Myron S. Wheeler (A'43–M'55) was born in Pittsburgh, Pa., in 1920. He received the B.S. degree from Pennsylvania State University, University Park, Pa., in 1942 and the M.S. degree from Stevens Institute of Technology, Hoboken, N. J., in 1946. Since 1942, he has been with the Westinghouse Electric Corporation working on microwave tubes at the Bloomfield Lamp Division and on microwave circuits and antennas at the Air Arm Division. During the war, he was engaged in development work on fm, cw magnetrons, frequency reference cavities, and tr devices. More recently he has been in development work on radar antennas and other electromechanical devices.

M. S. WHEELER

He has assisted the IRE on the Papers Review Committee and the Antennas and Waveguides Committee. Mr. Wheeler is a member of Sigma Tau and Eta Kappa Nu.

❖

Walter L. Whirry (S'54–M'56) was born in McMinnville, Ore., on January 21, 1933. He received the Bachelor of Science degree in electrical engineering in 1955 and the Master of Science degree in electrical engineering in 1956 from the California Institute of Technology, Pasadena, Calif.

W. L. WHIRRY

From 1955 to 1956, Mr. Whirry was employed as a teaching assistant at the California Institute of Technology. Since June, 1956, he has been engaged in microwave component development as a member of the technical staff in the Microwave Laboratory, Hughes Research Laboratories, Culver City, Calif.

Mr. Whirry is a member of Tau Beta Pi.

❖

Werner P. Wolf was born in Vienna, Austria, on April 22, 1930. He received the B.A. degree in physics at Oxford University in 1951 and the M.A. and D.Phil. degrees in 1954. He continued with research and teaching work at Oxford during 1955 and 1956 and then spent a year at Harvard University in the Division of Engineering and Applied Physics as a research fellow. He is currently at Oxford University on an I.C.I. Fellowship. Dr. Wolf's research has dealt with the properties of paramagnetic salts at very low temperatures and their applications to cooling by adiabatic demagnetization. He has also worked on the ferrimagnetic resonance of rare earth garnets and the theory of ferromagnetic anisotropy.

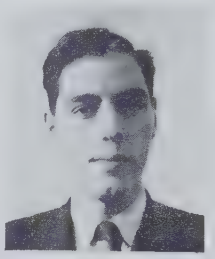

W. P. WOLF

Membership Roster

of the

IRE Professional Group

on

Microwave Theory and Techniques

November 5, 1957

Roster of PGMTT Members

Listed by IRE Regions and Sections, as of November 5, 1957

Region 1

Binghamton

Maslak, Michael
Van Horn, J. F.
Wheeler, N. D.

Boston

Abel, Fred
Adams, G. J.
Alexander, H. C.
Allen, D. C.
Alter, R. S.
Altman, J. L.
Altshuler, E. E.
Anderson, A. F.
Angulo, C. M.
Apsokardos, E.
Arlinsky, M. L.
Armstrong, D. G.
Astulfi, S. O.
Atchley, D. W., Jr.
Barker, H. R., Jr.
Barrett, R. M.
Bayliss, R. E.
Beauregard, W. G.
Benson, E. D.
Bergmann, S. M.
Bergstad, P. A.
Bers, Abraham
Blacksmith, Philipp, Jr.
Blaisdell, Arthur
Blanchard, R. L.
Bliss, Z. R.
Bloom, L. J.
Bloom, M. I.
Bobroff, D. L.
Borts, R. B.
Bougas, A. C.
Braden, R. S.
Brady, M. M.
Brown, D. F.
Brown, N. J.
Brunton, R. H., III
Buckley, E. F.
Butler, L. H.
Cahill, T. C.
Callaghan, E. P.
Cannon, J. H.
Carr, K. L.
Carter, G. E., Jr.
Cary, T. R., Jr.
Cayer, R. E.
Chapell, H. F.
Chase, D. G.
Child, J. W.
Chow, Yutze
Chu, Tse-Hou
Clark, N. F.
Cohen, Albert
Colbourne, R. H.
Cole, B. R.
Collins, R. M.
Crandell, P. A.
Crowley, D. J., Jr.
Cuming, W. R.
Cunningham, J. E.
Czarapata, A. H.
Czeropski, W. P., Jr.
Dandreta, William
Danforth, W. C., Jr.
Day, A. R.
Devane, M. E.
Dibiase, A. F.
Dombrowski, G. E.
Dominick, F. J.
Duffy, J. M.
Dunbar, E. E.
Duncan, K. W.
Duross, C. J.
Edelberg, Seymour
Eisenstadt, B. M.
Eklund, A. M.
Ewen, H. I.
Faflick, C. E.
Faigen, I. M.
Falconer, Stanley
Fallows, E. M.
Fast, Saul
Favaloro, C. J.
Feldman, E. J.
Fischer, R. F.
Fisk, E. B.
Fitzgerald, W. D.
Fock, H. W.
Foss, D. W.
Francis, E. A.
Fricker, S. J.
Friis, R. W.
Fritsch, P. C.
From, W. H.
Fulton, D. A.
Galagan, Steven
Galejs, Janis
Gildea, T. L.
Glynn, J. J.
Goldberg, H. B.
Goldman, E. M.
Goldstein, Irving
Graham, J. S.
Graham, J. W.
Gregory, J. G.
Gregory, Nicholas
Gronroos, Eino
Gunn, K. C. C.
Haddad, S. G.
Hadge, Eugene
Hall, R. T.
Hall, W. M.
Hamilton, E. A., Jr.
Hammond, G. H.
Hardsog, H. N.
Harkless, L. B.
Hart, J. J., Jr.
Haus, H. A.
Hecht, B. P.
Heins, Harold
Hellenbrand, C. M.
Helm, G. D.
Hevesh, A. H.
Hiatt, R. E.
Hogan, C. L.
Holmes, K. O.
Howe, S. E.
Huang, Chaang
Ironfield, Richard, Jr.
Jacobson, R. E.
James, G. E.
Jayne, A. W.
Jenkinson, J. V.
Johnson, S. L.
Karazia, R. J.
Karplus, Edward
Kasparian, G. D., Jr.
Kay, A. F.
Kazules, A. J.
Keane, L. M.
Keren, David
Kim, Y. S.
King, R. P.
Klemm, G. H.
Kline, Jack
Kohler, H. M.
Kostriza, J. A.
Krulee, R. L.
Lanciani, D. A.
Land, H. R.
Laughlin, M. J.
Leake, B. W.
Lehr, C. G.
Lessin, Irving
Lester, D. R.
Lewis, F. D.
Lieber, Morris
Lippincott, Southard
Loewenthal, Morton
Long, R. G.
Lucas, E. J.
MacEwan, Alexander, Jr.
Mack, R. A.
Mack, R. B.
Manahan, J. F.
Mann, A. M.
Margolin, M. C.
Martin, J. E.
Mayer, Alex
McCarthy, D. J.
McCormack, R. L.
McCoubrey, A. O.
McCoy, A. M., Jr.
McGeoch, C. R., Jr.
McLeod, W. W., Jr.
Mennella, R. A.
Mercer, W. R.
Meyer, M. A.
Michelson, Max
Miller, S. J.
Mingins, C. R.
Moats, R. R.
Mohr, M. C.
Monell, F. B.
Morgenthaler, F. R.
Murphy, E. J.
Myers, O. C., Jr.
Nans, E. A., Jr.
Nelson, A. A.
Nichols, A. J.
O'Hara, F. J.
Osepchuk, J. M.
Paananen, R. A.
Packert, D. E.
Parke, N. G., III
Pascalar, H. G.
Pathe, J. F.
Pease, M. C., III
Pease, R. L.
Peeler, G. D. M.
Peters, J. D., Jr.
Philips, C. M.
Pippin, J. E.
Plumb, D. R.
Polachowski, B. A.
Pollack, Dale
Pomeroy, A. F.
Potts, T. J., Jr.
Pritchard, W. L.
Purdy, W. E.
Querido, H. B.
Ramsey, W. H.
Rawlinson, P. E.
Reed, John
Reem, G. M., II
Rey, T. J.
Riblet, H. J.
Ricardi, L. J.
Richter, Edwin
Riegelhaupt, N. H.
Ripple, E. G.
Rivers, R. A.
Rizzi, P. A.
Roat, W. F.
Roberts, L. S.
Rodman, A. K.
Rodrigue, G. P.
Roediger, F. E.
Rojak, F. A.
Rosato, F. J.
Rotman, W.
Row, R. V.
Rubin, Samuel
Rutledge, P. D.
Ruze, John
Ryan, J. W., Jr.
Saad, T. S.
Salzberg, Edward
Scharfman, Howard
Schmidt, R. A.
Schramm, M. W., Jr.
Schwab, W. C.
Schwarzkopf, D. B.
Segal, Sumner
Serba, E. W.
Shafer, C. G.
Sheingold, L. S.
Sheldon, D. L.
Sherburne, A. E.
Silverman, Elliot
Simmons, A. J.
Simon, D. H.
Sinclair, D. B.
Skolnik, M. I.
Sletten, C. J.
Smith, C. L.
Smith, H. A.
Smith, N. L., III
Smith, R. D.
Smith, R. L.
Smith, R. V.
Smith, W. R.
Smoll, A. E.
Smullin, L. D.
Snay, R. J.
Soderman, R. A.
Soorsoorian, S. A.
Sotiropoulos, Arthur
Spencer, R. C.
Stacey, J. M.
Stanney, W. J.
Stein, Seymour
Stern, M. M.
Stewart, R. F.
Stockman, Harry
Stone, M. L.
Stratoti, A. R.
Straus, T. M.
Street, E. L.
Strum, P. D.
Tahan, E. N.
Teich, W. W.
Tenenholtz, Robert
Thomas, H. J., Jr.
Thompson, E. D.
Tucker, Nathaniel
Tyler, E. M.
Ulm, E. H.
Vafidaes, B. C.
Vant, L. M.
Wade, C. E.
Walker, R. M.
Wall, R. B.
Walsh, J. E.
Walsh, W. P.
Wang, S. C.
Wantuch, Ernest
Weiner, Gerald
Westbrook, E. P.
Whelpton, J. P.
White, D. A.
White, D. H.
Willenbrock, F. K.
Wing, Jack
Wolfe, R. W.
Wolfson, J. A.
Woodward, J. H.
Yee, T. G.
Yoshida, Shinichiro
Zettler, W. R.
Zucker, F. J.

Buffalo-Niagara

Ayer, D. R.
Bachman, C. G.
Backard, M. J.
Bartnik, J. C.
Borkowski, C. J.
Bouchard, J. G. F.
Buranich, G. F.
Butler, J. L.
Clougherty, J. F.
Earl, H. D.
Fandl, R. F.
Frost, A. D.
Goulder, M. E.
Horvath, J. O.
Kell, R. E.
Kellerman, R. E.
Leonard, D. J.
Lowe, W. R., Jr.
Melvin, D. W.
Michalski, Richard
Misek, V. A.
Newton, D. J., Jr.
Nuckolls, R. G.
Page, R. S.
Pelton, F. M.
Pothier, R. G.
Price, E. L., Jr.
Sarkees, Y. T.
Schlichter, E. S.
Smith, C. N.
Snyder, W. W.
Sommers, D. J.
Stengel, C. J., Jr.
Stone, A. P.
Talbot, R. D.
Wagner, R. W.
Welch, D. P.
Weller, D. B.
Wenzel, J. H.
Widmann, L. C.
Wolf, E. H.

Connecticut Valley

Andrews, W. J.
Artuso, N. F.
Barlow, Kenneth
Bolus, J. J.
Breden, W. W.
Brown, C. A.
Cutler, M. A.
Dickon, A. J.
Getsinger, W. J.
Lamb, J. J.
Landers, J. J.
Lovell, B. W.
Mahar, T. F.
Marchand, Nathan
Merrill, John
Migliaro, B. J.
Ostendorf, Bernard
Pannullo, F. T.
Petrucelly, V. J.
Pryor, W. L., Jr.
Reich, H. J.
Simko, R. S.
Sontheimer, C. G.
Stoker, W. C.
Thayer, D. C.
Van Delft, R. N.
Warner, E. J.

Elmira-Corning

Barney, W. H., Jr.
Blair, W. E.
Cox, G. L.
Duhl, John E.
Gerard, W. A.
Guyer, E. M.
Henry, A. B.
Hostetler, C. L.
Keeton, T. G.
Larson, R. G.
Lempert, Joseph
Okress, E. C.
Upshaw, Vert

Ithaca

Bryant, N. H.
Charton, P. W.
Eastman, L. F.
Ingalls, C. E.
Kantor, Gideon
Maresca, T. J.
Matt, Sol
Mayer, H. F.
Shurer, Florian
Stanton, J. W.
Surtes, M. J.
Swana, J. J.
Travis, J. B., Jr.

Rochester

Baldwin, L. D.
Chesna, John
Edighoffer, E. A.
Eisaman, Leo C.
Evans, J. E.
Gutzmer, R. F.
Heit, J. C.
Jermyn, T. A.
Mazel, L. G.
Morrison, R. F., Jr.
Ramos, A. S.
Raymond, R. S.
Schiff, Seymour
Shalloway, A. M.
Valmore, E. W.

Rome-Utica

Augustine, J. A.
Baldridge, B. H.
Chrestien, C. A.
Cruickshank, J. E.
DeMesme, T. A.
Grimm, R. S.
Handelsman, Morris
Krull, D. M.
Malowicki, Edward
Miller, C. R.
Orear, E. R.
Rodriguez, P. T.
Romanelli, P. A.
Scott, E. C.
Smith, S. L.
Vaccaro, Joseph
Vogelman, J. H.
Ward, J. W.
Warrick, A. C.
Winn, O. H.

Schenectady

Allen, C. C.
Amoth, V. W.
Anderson, J. M.
Babits, V. A.
Blume, A. E.
Boyd, M. R.
Branch, G. M., Jr.
Bristol, T. R.
Burkett, F. T.
Cohoon, R. L.
Curtis, T. P.
Dehn, R. A.
Elder, T. A.
Feiker, G. E., Jr.
Griffin, G. J., Jr.
Grover, F. W.
Harris, H. D.
Johnson, R. E.
Keenan, P. P.
Matthews, E. W., Jr.
Maurer, J. W.
Mayer, C. B.
McNary, B. D.
Miglore, Carmine
Mihran, T. G.
Newsom, W. L.
Oshima, M.
Owens, O. G.
Peters, P. H., Jr.
Quine, J. P.
Rankin, A. E.
Raschke, R. R.
Speray, M. R.
Stein, H. H.
Teare, W. H.
Truax, C. J.
Turrentine, R. E.
Vaughan, J. R. M.
Watson, R. P.
Wilbur, D. A.

Syracuse

Anderson, A. F.
Benfey, R. L.
Biele, R. J.
Caffrey, T. P.
Carson, R. E.
Cheng, D. K.
Cohen, Arthur
Conger, W. H.
Cook, G. V.
Cuccarese, E. A.
Demaree, G. A.
Doolittle, W. T., Jr.
Drum, J. J.
Eber, L. O., Jr.
Evans, H. J.
Fitzmorris, S. R.

Gildersleeve, R. E.
Grimm, H. H.
Grisetti, R. S.
Gruenberg, Harry
Habermann, Rudolph, Jr.
Healy, D. W., Jr.
Heidrich, A. J.
Hesler, J. P.
Hu, Ming-Kuei
Hurley, D. T.
Hwang, Y. C.
Jacobs, G. B.
Johnson, A.
Kassler, Raymond
Kenyon, S. W.
Kinney, R. V.
Kinsey, R. R.
Kluender, E. C.
Knox, R. L.
Kuhn, D. H.
Lambert, J. M.
LePage, W. R.
Leppanen, K. E.
Linker, J. B., Jr.
Manwarren, T. E.
Martin, H. R.
Mather, D. L.
Mayo, B. R.
McCoy, D. R.
Michalek, A. R.
Mullen, E. B.
Neelands, L. J.
Nester, W. H.
Place, J. F.
Poppe, J. R.
Rosen, Samuel
Smith, D. L.
Smith, Jack
Smith, W. F., Jr.
Strawn, R. K.
Tessier, H. J. R.
Totten, H. Q.
Vahle, Julius
Vandeven, D. W.
Veley, H. N.
Whistler, W. T.
Williamson, J. C.
Zeisler, M. D.

Region 2

Long Island

Agree, Irvin
Ahman, A. J.
Albanese, V. J.
Angevine, R. A.
Arams, F. R.
Arfin, Bernard
Aronowitz, Leonard
Auerbach, Martin
Bachman, H. L.
Badoyannis, G. M.
Barash, L. F.
Barry, A. C.
Basil, Alexander
Bauer, W. C.
Beamer, F. E.
Becker, J. E.
Berlly, Edward
Bernstein, George
Bertan, L. L.
Biss, Rita-Ellen P.
Blanco, M. G.
Blass, Judd
Bloom, G. M.
Bogner, B. F.
Bogner, R. D.
Bourke, W. A.
Breese, M. E.
Brenner, Milton
Briskin, H. B.
Brounstein, Arnold
Bruns, E. A.
Calatabianca, J. W.
Capellupo, F. V.
Carter, P. S.
Casper, Stuart
Chaikin, Marvin
Chang, W. H. K.
Cheney, A. G.
Chubb, Elliott
Churchill, D. B.
Cohen, A. L.
Cohen, Harold
Cohen, S. A.
Collins, Kenneth
Cornes, R. W.
Cortizas, A. P.
Crosby, M. G.
Dagavarian, H. O.
D'Agostino, J. V.
Damm, G. W.
Daum, Alfred
Day, W. B.
DeSize, L. K.
Dettinger, D.
Devine, J. H., Jr.
DiToro, M. J.
Dobson, D. A.
Dong, H. L. H.
Dong, J. G.
Dorato, P. E.
Dorne, Arthur
Doundoulakis, G. J.
Eberle, E. E.
Eckert, G. F.
Egan, W. G.
Elefant, Jack
Engle, D. C.
Ettenberg, Morris
Farber, Herman
Fisch, Jerome
Fleming, P. L.
Forker, L. W.
Forster, E. W.
Freed, Arthur
Friedman, E. D.
Fromm, W. E.
Fubini, E. G.
Fucci, Salvatore
Gallagher, J. H.
Gamble, J. H.
Garretson, G. M.
Gebhardt, J. W.
Gethin, S. A.
Glass, H. W.
Goldberg, Julius
Goldstein, Siegfried
Goldstone, L. L.
Goldstone, L. O.
Gorelick, George
Gould, R. V.
Greenberg, D. R.
Greene, J. C.
Griemsmann, J. W. E.
Gutman, J. H.
Hall, J. D.
Hana, T. C.
Hanfling, J. D.
Hannan, P. W.
Hanover, A. M.
Hanratty, R. J.
Hansell, C. W.
Hanulec, J. D.
Harges, M. T.
Harrison, R. I.
Haussig, Lester
Heacock, W. J., Jr.
Heiss, W. H.
Hellmann, R. K.
Hendler, A. J.
Hershler, Abe
Hittner, Charles
Hoffman, H. L.
Hronek, R. L.
Hunt, H. W.
Jaffe, D. L.
James, A. V.
Jasik, Henry
Jaworowski, E. V.
Jorge, Arlindo
Juhas, L. A.
Kant, Milton
Kaplan, Martin
Kaplan, R. A.
Katzelnick, Harold
Kaye, Murray
Kearney, J. W.
Keim, D. Y.
Kent, L. I.
Kiesling, J. D.
Kishinsky, L. S.
Kleinberger, Robert
Knothe, C. H.
Kraemer, E. H.
Krayer, Gus
Kudo, Yoshito
Kurz, F. A.
Kuskowski, L. J.
Laird, J. A., III
LaRosa, Richard
Learned, Vincent
Lebenbaum, M. T.
Lee, T. K.
Leibowitz, Bernard
Lencine, L. A.
Lepic, R. E.
Lerner, David
Levine, B. I.
Liebert, F. R.
Ligori, Joseph
Lory, John
Losee, W. B., Jr.
Loth, P. A.
Lowman, R. V.
Lyons, J. F., Jr.
Magenheim, Bertram
Malech, R. G.
Mariotti, P. G.
Marotta, A. R.
Marston, R. S.
Martin, A. R.
Martin, E. E.
Marzoli, Armando
Maurer, S. J.
McBee, W. D.
McCristall, J. A.
McEvoy, J. A.
McFarland, J. E.
Menaker, D. S.
Merrill, J. L., Jr.
Mieher, W. W.
Milukas, V. V.
Mouier, Georges
Murphy, R. B.
Neiland, A. C.
Nigro, A. F.
Noji, T. T.
Novick, Murray
Odessey, P. H.
Offutt, W. B.
Okwit, Seymour
Olthuis, R. W.
Oranges, D. F.
Orazio, A. F.
Osherowitz, J. M.
Oswald, Henry
Ottenberg, E. C.
Packard, K. S., Jr.
Packer, Leroy
Paolantonio, Anthony
Paterno, Philip M.
Pelner, Nathan
Perini, H. R.
Peterson, H. O.
Peterson, P. R.
Petrossian, George
Phanos, Stephen
Pleasure, Myron
Prew, H. E.
Price, R. C.
Prihar, Zvi
Redlien, H. W., Jr.
Regis, Robert
Resnick, Sander
Reymann, Joseph, Jr.
Reynolds, M. R.
Rickert, H. H.
Rinkel, S. A.
Robinson, H. L.
Rosen, Bernard
Rothman, H. S.
Rubin, S. W.
Russell, D. H.
Satre, W. I., Jr.
Saunders, C. L.
Savalli, F. P.
Scherer, R. L.
Schiffres, Paul
Schindler, J. P.
Schmidt, E. R.
Scholer, R. M.
Selbmann, R. W.
Sferrazza, P. J.
Shameson, Leon
Shepherd, J. E.
Sherry, R. S.
Shizume, P. K.
Shnitkin, Lothar
Sieminski, Edward
Silverstein, Irving
Simmonds, Jules
Skipper, L. C.
Skwarek, F. J.
Smith, C. I.
Sonnenschein, A. H.
Speakman, E. A.
Spector, Norman
Spencer, N. A.
Spillane, L. R.
Stephenson, J. G.
Stevens, Stanley
Stokes, B. C.
Strong, J. J., Jr.
Sullivan, D. J.
Sutkin, Seymour
Suttenberg, Stewart
Swenson, C. F.
Swern, Leonard
Tames, Joel
Tanenbaum, M. S.
Taub, J. J.
Tenenbaum, Frank
Tiger, H. S.
Torgow, E. N.
Vaher, Eo
Varza, George
Vaupel, G. E.
Waller, W. E.
Warren, R. J.
Wathen, R. L.
Weber, I. J.
Weibel, G. E.
Weichardt, H. H.
Wengenroth, R. D.
Whalen, A. D.
Wheeler, H. A.
Whipple, G. D.
Williams, F. H.
Wilson, L. B.
Wind, Moe
Winzemer, A. M.
Woods, W. C., Jr.
Yarnall, W. M.
Young, V. J.
Zanichkowsky, Martin
Zeidner, Sidney
Zellers, J. E., Jr.

New York

Altschuler, H. M.
Ammirati, Salvatore
Armstrong, R. W.
Arnold, J. W.
Aviv, D. G.
Bady, Isidore
Baker, L. C.
Banner, Leonard
Barker, D. R.
Beck, A. C.
Berger, R. M.
Berlin, Jack
Binzer, Carl
Birnbaum, Joseph
Bland, G. F.
Bowlby, R. E.
Brathwaite, Augustus
Brenner, Adolph
Bresler, A. D.
Carlin, H. J.
Cassidy, J. J.
Cedarholm, J. P.
Chanzit, Lawrence
Chays, Seymour
Chen, Tsung-Shan
Chomet, Marc
Clemens, G. J.
Cloud, P. R.
Cohen, M. M.
Cohen, Morris
Cohen, Morton
Coltun, Louis
Cooper, Marvin
Cooper, Nathan
Corbell, P. I., Jr.
Cosentino, A. A.
Costa, M. J.
Creel, J. D.
Crevello, A. A., Sr.
Cuccia, J. F.
Daly, R. T.
D'Angelo, Felix
Dawson, R. W.
De Loach, B. C., Jr.
Deoul, Neal
Deschamps, G. A.
Di Fusco, F. J.
Dobbs, R. C.
Douglas, R. H.
Drosin, A. B.
Dunford, William
Dusio, E. W.
Egan, G. E.
Ellen, N. A.
Espersen, George
Fair, R. D.
Feehan, J. D.
Felsen, L. B.
Ferri, R. I.
Finke, H. A.
Fleisher, Harold
Flower, R. A.
Fox, A. G.
Fox, Jerome
Franco, A. G.
Fraser, J. T.
Freudenberg, Boris
Friis, H. T.
Fruhner, E. T.
Gamertsfelder, G. R.
Gannett, D. K.
Garman, R. L.
George, D. E.
Giannattasio, A. R.
Giordano, A. B.
Goldmuntz, L. A.
Golden, Donald
Goldsmith, A. N.
Goldstein, Abe
Goodall, W. M.
Govinsky, Walter
Gronner, Alfred
Guenther, Richard
Gussak, Murray
Hackett, A. J.
Hahn, Steven
Harris, Lawrence
Hartnett, J. J.
Hearn, R. B.
Heise, E. R.
Higgins, W. T.
Hoffmann, W. H.
Hollander, Sidney
Honig, A. R.
Honig, W. M.
Horowitz, Louis
Isaacson, H. B.
Kagan, Herman
Kahn, W. K.
Kaiser, E. J.
Kaplan, L. J.
Kaplowitz, Morris
Karp, J. R.
Kasper, H. W.
Keller, E. W.
Kibler, L. U.
Kilgore, G. R.
King, A. P.
Klein, Alfred
Klipper, Harold
Klug, S. H.
Korewick, John
Kowalsky, John
Krevsky, Seymour
Kullback, Irving
Kummer, W. H.
Kurzrok, R. M.
Lamensdorf, C. M.
Lavi, Yeshayahu
Lebowitz, R. A.
Leibowitz, M. R.
Lesman, Edward
Levey, Lawrence
Levine, Seymour
Lewis, W. M.
Lipetz, Nathan
Lippin, Gerard
Liverios, D. T.
Mack, Alfred
Maedel, G. F.
Malloy, E. J.
Mansky, Leonard
Martin, J. E.
Mateer, K. W.
Matthei, W. G.
Mazziotti, I. J.
McLaughlin, N. C.
McVey, A. B.
Menhennett, G. H.
Mercado, Manuel
Meserole, W. E.
Meslener, G. J.
Messina, Joseph
Milazzo, Salvatore
Miller, S. E.
Murgia, J. C.
Nielsen, Peter
Ohm, E. A.
Oliner, A. A.
Orefice, Gaetano
Orenstein, Nathan
Oswald, H. J.
Parisier, Maurice
Plishner, P. J.
Ploussios, George
Pokorny, G. E.
Popper, J. N.
Posklensky, David
Rabinowitz, Martin
Rabinowitz, S. J.
Radner, M. A.
Ragland, R. M.
Rapaport, Harold
Reder, F. H.
Rivera, J. J.
Rolfs, J. C.
Rolnik, J. A.
Rood, R. S.
Rosenthal, S. W.
Rudin, Stuart
Rudner, B. S.
Rugge, R. A.
Rusinow, Kalman
Ryan, J. J.
Rymaszewski, E. J.
Sachs, G. I.
Safran, Paul
Sakitt, Mark
Saltzman, Henry
Sardo, William
Sawelson, A. I.
Schafer, J. P.
Schenck, H. H.
Schetzen, Martin
Schlesinger, S. P.
Schneider, Seymour
Schreiner, K. E.
Schwartz, Leonard
Schwartz, Samuel
Schwartzman, Leon
Sharpless, W. M.
Sherry, J. J.
Shubel, E. J.
Simon, Harold
Slobodin, Leo
Smithline, Herbert
Soreny, E. V.
Spratt, E. L.
Stavis, Gus
Stearns, J. H.
Stein, V. J.
Stern, Emanuel
Stern, Ernest
Stern, R. M.
Sterzer, Fred
Stewart, C. E.
Stillman, Morton
Stock, D. J. R.
Stuart, W. D.
Sweet, L. O.
Szekely, Zoltan
Thomas, R. O.
Topper, Leo
Turner, E. H.
Ungar, S. G.
Unger, Hans-Georg
Victor, H. W.
Viola, R. D.
Wallace, Marcel
Walton, J. S. V.
Wang, M. T.
Weber, Ernst
Weinstein, H. W.
Weiss, M. T.
Weller, Leonard
Westheimer, Manfred
Wing, Omar
Winkelstein, R. A.
Winkler, Arthur
Wu, W. I. L.
Zareh, Mahmood
Zenchoff, Philip
Zimet, M. M.
Zuzolo, P. R.

Northern New Jersey

Abrams, Irving
Albrecht, H. W.
Anderson, T. N.
Arditi, Maurice
Ashbrook, J. M.
Augenblick, H. A.
Basinger, E. G.
Beltz, W. F.
Benenson, C. A.
Blanchard, R. J.

Bollman, J. H.
Bradburd, E. M.
Bridges, T. J.
Brown, A. T., III
Brown, C. R.
Brown, D. J.
Callanan, W. F.
Carlson, E. S.
Casabona, A. M.
Chartoff, Maurice
Chisholm, D. A.
Cimorelli, J. T.
Clavier, A. G.
Cocchiaro, Michael
Cohan, Lloyd
Comstock, R. L.
Cox, A. L.
Crowell, M. H.
Davis, M. G.
Dayem, A. H.
De Bell, J. M., Jr.
Dehoney, R. J.
De Paola, G. E.
De Rosa, L. A.
Dipple, W. M.
Dishal, Milton
DiStadio, Dominic
Doba, Stephen, Jr.
Dorney, P. E.
Drexler, Jerome
Dulac, J. P. P.
Engelmann, H. F.
Engler, C. F.
Evans, N. L., Jr.
Fay, C. E.
Fessler, W. H.
Filo, J. P.
Foley, R. M.
French, H. A.
Fulmer, R. J.
Furrer, C. G.
Geiger, R. H.
Gewartowski, J. W.
Giger, A. J.
Glass, L. H.
Glomb, W. L.
Goldman, Hyman
Green, M. W.
Greenquist, R. E.
Haenichen, J. C.
Hafemeister, E. F.
Hammer, Harry
Hansen, J. A.
Harkless, E. T.
Harris, W. T.
Harvey, J. B.
Hasbrouck, R. T.
Havstad, Harald
Heney, J. F.
Henry, T. J.
Hensel, M. L.
Hewitt, W. H., Jr.
Hines, M. E.
Hodowanec, Gregory
Horneck, J. F.
Houghton, E. W.
Ingalls, David
Jacobs, B. H.
Jacobs, G. W.
Jordan, D. R.
Kelmis, K. J.
Kinaman, E. W.
Klein, Melvin
Klein, M. S.
Kolts, R. C.
Kompfner, Rudolph
Kovach, Leslie
Kramer, A. S.
Kreer, J. G., Jr.
Kulesha, K. J.
Kups, E. F.
Kuras, H. F.
Lamb, J. M.
Laport, E. A.
Larena, S. F.
Lenker, J. N.
Levin, R. M.
LeVine, D. J.
Lindenberg, N. L.
Lorentzen, R. R.
Lundburg, F. J.
MacVeety, R. C., Jr.
Malloy, J. J.
Marchese, T. J.
Martin, J. F. P.
Mathews, D. E.
Mattingly, R. L.
Maunsell, H. I. G.
McClelland, W. R.
McCrory, J. R.
McDowell, H. L.
McEntee, J. A., Jr.
McEwan, A. W.
Meier, W. L.
Moltz, A. J.
Moreno, C. N.
Morgan, S. P.
Mottram, E. T.
Mount, Ellis
Mueller, P. L.
Mulligan, J. H., Jr.
Mumford, W. W.
Nebel, C. N.
Nicodemus, K. L.
Nielsen, A. H.
Noll, J. C.
Nowogrodzki, Markus
Olin, R. P.
Osborn, P. H.
Ostlund, E. M.
Panter, P. F.
Pattan, B. A.
Peck, J. L.
Perenic, L. J.
Perkins, C. B., Jr.
Perry, I. D.
Petrich, L. G.
Pickholtz, R. L.
Pike, Neal
Pincus, Leonard
Poarch, M. F.
Price, A. C., Jr.
Quickel, T. E.
Reed, S. C.
Reiser, M. W.
Robertson, G. H.
Robertson, J. P.
Rowen, J. H.
Salzer, R. M.
Samson, R. L.
Sansalone, F. J.
Schacher, D. L.
Schafersman, R. L.
Scheibner, J. F.
Schmidt, C. R.
Schumacher, H. L.
Schumann, L. C.
Shangraw, C. C.
Shotliff, L. A.
Sichak, William
Simkovich, J. R.
Southworth, G. C.
Spanos, W. M.
Sproul, P. T.
Stahl, P. D.
Stebbins, M. D.
Steinhoff, Reynold
Stinehelfer, H. E., Sr.
Sullinger, W. B.
Talpey, R. G.
Tatsuguchi, Isamu
Treuhaft, M. A.
Tulchin, Henry
Vaccaro, F. E.
Vaughan, C. B.
Von Aulock, W. H.
Wakefield, P. R.
Ware, P. M., Jr.
Weber, R. M.
Wehrle, A. W.
Welber, Irwin
Wheeler, G. W.
White, R. E.
Wickliffe, P. R., Jr.
Williams, N. T.
Winter, J. W.
Wolkstein, H. J.
Young, C. B., Jr.
Zayac, F. R.
Zweibel, Joseph

Princeton

Beam, W. R.
Belohoubek, E. F.
Braden, R. A.
Epstein, Jess
Ernst, W. P.
Ginsberg, L. H.
Gottschalk, W. M.
Hamilton, K. E.
Hautzik, R. M.
Heald, M. A.
Heckscher, J. L.
Heim, C. W.
Hensperger, E. S.
Houser, B. E.
Kihn, Harry
Klopfenstein, R. W.
Knechtli, R. C.
Levine, Sam
Miller, Robert
Norman, F. H.
Olin, I. D.
Polk, Charles
Rankin, J. B.
Sirkis, M. D.
Snyder, C. L.
Westneat, A. S., Jr.
Woodward, O. M., Jr.

Atlanta

Berry, G. C.
Crozier, H. W.
Duggan, R. S., Jr.
Fellers, R. G.
Garrett, W. O.
Hayes, R. D.
Hildreth, H. J.
Hollis, J. S.
Hooke, G. P.
King, T. R.
Krusberg, R. J.
Long, M. W.
McClung, W. C.
McCombs, J. W.
McIntyre, R. T.
Meadows, H. E., Jr.
Moseley, R. E.
Peifer, W. A.
Rochat, V. E.
Smith, R. T.
Swygert, W. E., Jr.
Thomason, J. G.
Thompson, R. F.
Williams, R. E.

Baltimore

Ap Rhys, T. L.
Baida, Seymour
Barthel, D. R.
Brannon, D. L.
Brodwin, M. E.
Cassedy, E. S., Jr.
Cerva, C. H.
Choncholas, J. J.
Claborn, K. D.
Clark, F. K., Jr.
Clark, M. C.
Clark, T. H.
Cohn, Marvin
Cole, E. B., Jr.
Davis, R. J.
De Andrade, W. C.
Dempsey, M. E.
Drake, J. E.
Dullinger, A. G., Jr.
Eby, J. T.
Evans, G. E.
Friedman, D. S.
Gerwig, C. H., Jr.
Goodman, S. N.
Grauling, C. H., Jr.
Hamer, E. G.
Hanks, H. C., Jr.
Harris, H. N.
Herwald, S. W.
Hoffmanner, G. H.
Hom, W. R.
Izzo, A. J.
Jackson, H. L.
Jones, G. R.
Jones, R. E.
King, D. D.
Koether, G. H., Jr.
Krakau, W. S.
Kudo, F. M.
La Bree, C. T.
Lilly, B. R.
Lowe, W. H.
Maxwell, D. J.
May, H. A.
McBride, J. F.
McDonough, J. T.
Meador, A. B., Jr.
Moskowitz, Charles
Owen, J. Q.
Packard, R. F.
Pipkin, J. E.
Pratt, Amasa
Rutstein, H. S.
Sanner, G. E.
Sartorio, D. R.
Scanga, W. A.
Schmid, Otto, Jr.
Schrank, H. E.
Schutz, Harald
Sefton, H. B., Jr.
Seman, A. E., Jr.
Shaw, G. D.
Shelor, E. G., Jr.
Sichelstiel, B. A.
Silva, F. A.
Singer, L. M.
Smith, E. L., Jr.
Sorrell, P. A.
Stout, G. P.
Tellier, Jacob
Thompson, J. E.
Trinter, V. E.
Valenzuela, G. R.
Vierling, H. D.
Visher, W. A.
Wallace, B. E., Jr.
Watson, T. E.
Watts, H. M.
Wentworth, F. L.
Wheeler, M. S.
Willey, R. E.
Wiltse, J. C., Jr.
Woodyard, R. H.
Young, Leo

Central Florida

Apriletti, C. A.
Barkes, R. L.
Bivans, R. W.
Blanton, J. E.
Clarke, R. L.
Doughty, S. D.
Dunavant, W. E.
Frerking, H. W.
Garrott, W. L.
Gray, A. R.
Haaland, C. M.
Horton, W. H.
Jones, A. E.
Lally, P. M.
Little, P. R.
Lowrie, R. W.
McMath, D. C., Jr.
McMurrough, R. W.
Miller, L. S.
Moline, J. C.
New, C. H.
Parkes, D. A.
Pelchat, G. M.
Rhoads, A. S., Jr.
Rhodes, D. R.
Rich, C. E.
Silas, L. W.
Steele, W. L.
Tomberlin, J. L.
Walter, E. R.
West, K. A.
Williams, D. A.
Wing, A. H., Jr.
Winters, B. C.
Wren, A. W., Jr.

Florida West Coast

Abremski, M. C.
Bailey, R. L.
Bellare, David
Duncan, B. J.
Grimes, E. S., Jr.
Henning, R. E.
Horner, G. F.
Peacock, W. T., Jr.
Rosenzvaig, J. E.
Schugel, J. A.
Sloan, S. C., Jr.
Wells, J. D.
White, E. L.
Willert, A. F.

Huntsville

Kingery, M. K.
Lowery, H. R.
Schumann, Fred

Miami

Lampkin, G. F.
Neely, E. H.
Roque, Leonard
Smith, R. L.
Smith, S. B.

North Carolina

Balden, J. M.
Barron, J. I.
Baynard, J. S., Jr.
Bezera, Gabriel
Harris, R. H.
Hirner, J. A.
Howard, T. E.
Lee, R. E., Jr.
Mann, J. H.
Minor, M. J.
Purnell, L. S.

Northwest Florida

Clifton, C. L.
Grafe, R. W.
Haskell, H. B.
Hill, W. W.
Jones, C. M.
Saffer, R. A.
Sites, F. J.

Philadelphia

Abeyta, Isaac
Allerton, G. L.
Anderson, W. G.
Arnold, P. H.
Bargellini, I. P. L.
Bazan, S. J.
Beardwood, J. T., III
Beaver, J. A., Jr.
Beck, M. R.
Bennett, W. P.
Benson, S. E.
Bicking, H. P.
Booth, A. T., Jr.
Bowman, D. F.
Boyer, N. W.
Bradford, C. E.
Bradley, W. E.
Brennan, J. B., III
Brett, G. F.
Brough, J. R.
Cantafio, L. J.
Chadwick, P. S.
Chronister, W. M.
Ciletti, V. J.
Clark, F. R.
Clasen, C. P.
Coburn, J. M.
Colby, N. C.
Combellack, E. M.
Cooley, C. C., Jr.
Crosby, D. R.
Dahlberg, R. S., Jr.
Daniels, A. J.
Davis, C. E.
Eachus, Iredell, Jr.
Eberle, Harry
Elder, H. E.
Fast, Herbert
Fink, E. A.
Fiore, R. E.
Follensbee, W. R.
Fong, T. T.
Forbes, E. J.
Fricke, R. H.
Friend, A. W.
Gans, J. S.
Garrett, L. B., Jr.
Gazen, Louis
Goblick, T. J., Jr.
Goldstone, B. J.
Grace, J. W.
Graham, D. J., Jr.
Greenfield, Alexander
Gumacos, Costantine
Haimowitz, Bernard
Hamm, N. G.
Hanft, Herbert
Hawthorne, E. I.
Heidgen, Bernard, Jr.
Heskett, Harry
Hewitt, E. C.
Hockeimer, H. E.
Hoffman, N. N.
Honda, Hajime
Hricko, R. M.
Jacobs, Ernest
Jarecki, S. J.
Jayne, F. B.
Johnson, O. E.
Kall, A. R.
Kelly, P. J.
Kiel, J. H.
King, W. C.
Klavens, N. I.
Knapschaefer, D. H.
Kressman, J. H.
Kritikos, H. N.
Latham, N. D.
Laurent, G. J.
Lawton, R. S.
Lewis, E. S.
Lindsay, J. E.
Lisicky, A. J.
Lombardini, P. P.
Luciw, Wolodymyr
Mapes, R. G.
Marucci, D. L.
Mathwich, H. R.
McCracken, L. G., Jr.
Messenger, G. C.
Milewski, C. A.
Millet, M. R.
Munson, I. K.
Osbahr, B. F.
Paiss, M. H.
Peterson, C. E.
Quan, Kuo-Kong
Reisener, W. C., Jr.
Reiss, H. R.
Ringland, R. S.
Rodman, M. D.
Roop, R. W.
Saloom, J. A.
Sayer, T. C.
Sazynski, Paul
Schach, Saul
Scholz, K. W.
Schumacher, R. T.
Schwartz, A. J.
Schwartz, R. F.
Schwartzberg, H. L.
Senulis, R. E.
Shenoy, R. P.
Sheppard, W. H.
Sims, R. L.
Smith, R. M.
Smyton, S. A.
Solomon, Saul
Sos, John
Spitzer, E. E.
Stauffer, J. W.
Sterner, F. L.
Stokes, P. F.
Story, T. H.
Sumerlin, W. T.
Thompson, L. E.
Thowless, E. A.
Titefsky, E. J.
Trachtenberg, J. M.
Twist, G. A.
Venters, D. C.
Ver Wys, G. A.
Walker, H. R.
Warren, W. L.
Williams, A. J., Jr.
Wing, D. H.
Wolin, Samuel
Wood, M. H.
Young, C. R.
Zebrowitz, Stanley

Virginia

Dial, E. W.
Fadeley, J. H.
Fossum, T. T.
Grymes, J. R., Jr.
Harris, O. R.
Hastings, C. E.
Keast, P. M.
McGahey, E. W., Jr.
Miller, C. L.
Pellock, L. E.
Taylor, M. L.
Webb, W. R.
Welch, A. A.

Washington, D.C.

Adams, J. T.
Alde, R. O.
Algor, M. M.
Allen, D. A.
Allen, P. J.
Anderson, H. W.
Anderson, R. J.
Arnett, H. D.
Bass, C. A.
Bawer, Robert
Beck, E. A.

Bernstein, Benjamin
Bickart, T. A.
Birochak, Edward
Bolt, C. A., Jr.
Bostick, B. E.
Bowie, D. M.
Brimberg, M. M.
Brown, S. R.
Buckley, R. O.
Burkhardt, R. H.
Cacheris, J. C.
Cannon, R. E., Jr.
Carr, L. H.
Celander, Bengt
Chadwick, G. G.
Chait, H. N.
Chen, Y. M.
Cheston, T. C.
Chi, A. R.
Clair, J. D.
Cleckner, D. C.
Conley, J. W.
Cook, F. W.
Cooper, H. W., III
Crenshaw, A. N., Jr.
De Vore, Charles
Diehl, L. G.
Dropkin, H. A.
Everhard, F. U , Jr.
Feild, S. C., Jr.
Fink, Charles
Flynn, J. E.
Ford, R. R.
Francis, C. J.
Gabriel, W. F.
Gager, W. B.
Garver, R. V.
Gerlach, H. W. A.
Gessner, R. J.
Goldberg, Harold
Gould, W. I., Jr.
Grantham, R. E.
Griffith, K. E.
Guhne, R. D.
Hanyok, Andrew
Hastert, D. D.
Henry, V. F.
Herman, Julius
Herring, R. A., Jr.
Hockensmith, R. P.
Hoffman, Murray
Houseman, E. O., Jr.
Irby, R. F.
Isaacson, Sheldon
Katzin, Martin
Keating, Thomas, Jr.
Kefalas, G. P.
Kelley, J. R.
Kirshner, J. M.
Klamm, G. E.
Kohler, H. W.
Koppl, W. J.
Kuhnle, R. C.
Lally, J. F.
Lay, L. L.
Liss, F. T.
Livingstone, R. H.
Lockwood, E. H.
Marks, M. M.
Marsh, E. V.
McGill, J. A., Jr.
Mendus, W. M.
Miller, J. W.
Moore, C. G., Jr.
Ornstein, Edward
Ould, R. S.
Pan, P. M.
Parker, C. F., Jr.
Pavlos, Pete
Peyton, P. B., Jr.
Pitsenberger, J. W.
Polak, Henri
Portmann, P. A.
Ports, D. C.
Potter, R. S.
Puro, W. O.
Pyle, E. J., Jr.
Pyles, W. S.
Quigley, C. E.
Ray, H. A., Jr.
Read, A. H.
Redden, M. S., Jr.
Regardh, C. B.
Reggia, Frank
Renner, J. J.
Reynard, A. I.
Richardson, D. J.
Ringenbach, M. E.
Rozak, D. T.
Rueger, L. J.
Rutz, E. M.
Sakiotis, N. G.
Salisbury, L. L., Jr.
Savarese, R. T.
Schreyer, S. D.
Settersten, R. A.
Shamp, D. J.
Shapiro, Gustave
Shelton, J. P., Jr.
Silins, Andrejs
Smith, Charles
Smith, R. J.
Sorger, G. U.
Stahl, B. E.
Staley, I. B.
Stastny, G. F.
Stelter , L. R.
Stewart, R. B.
Stitch, B. D.
Stone, R. O.
Sumoski, A. W.
Tai, J. H. Y.
Thompson, R. T., Jr.
Tozzi, L. M.
Turnage, H. C.
Uglow, K. M., Jr.
Vann, W. L.
Verela, A. A.
Waldschmitt, J. A.
Wanselow, R. D.
Ward, H. T., Jr.
Weinschel, B. O.
West, R. G.
White, D. R. J.
Whitney, F. G.
Wigington, R. L.
Wilson, L. M.
Witte, J. J.
Wolff, E. A.
Worne, B. E.
Wright, S. T.
Yee, D. K.
Youmans, A. B.
Young, H. D.
Young, H. M.

Region 4

Akron

Burke, J. T.
Di Caudo, V. J.
Greenwood, R. E.
Hakes, T. H.
Iler, K. R.
Ingalls, R. S.
Kelley, C. M.
Klever, W. O.
Mathis, H. F.
Neuwirth, K. R.
Pressel, P. I.
Strang, J. R.
Thompson, R. B.
Vaughan, T. J.
Welch, G. H.
White, W. C.
Zurcher, L. A.

Central Pennsylvania

Files, W. D.
Geronimo, M. B.
Hall, F. T., Jr.
Herlt, B. G., Jr.
Herman, E. B.
Holter, D. H., Jr.
Key, J. T., Jr.
Lopez, A. F.
Norris, R. S.
O'Connor, H. C., Jr.
Passow, R. L.
Smith, J. P.
Thompson, F. C.
Welch, C. L.
Wolfe, R. E.

Cincinnati

Bereskin, A. B.
Blasberg, L. A.
Dalins, Ilmars
Dutton, C. E.
Gruber, J. R.
Kelling, D. G.
Kuecken, J. A.
MacKinnon, A. J.
Marshall, D. A.
Sang, W. W.
Seward, G. J.
Ward, D. L.
Weaver, C. W.
Zupansky, Milo

Cleveland

Ackerman, E. K.
Banshak, W. G.
Bird, J. R.
Braschwitz, H. J.
Busher, R. E.
Davison, Beaumont
Elze, R. P.
Gunderman, R. J.
Jacques, G. E.
Kragle, R. J.
Plonsey, Robert
Schneider, R. F.
Scott, E. P.
Smetana, Jerry

Columbus

Albright, R. E.
Baechle, J. R.
Blake, R. E.
Boone, E. M.
Brown, D. M.
Bulman, W. E.
Carter, C. J.
Chen, Fang-Shang
Chu, Ta-Shing
Cosgriff, R. L.
Crawford, R. W.
Damon, E. K.
Dawirs, H. N.
Falkenbach, G. J.
Ferguson, R. E.
Hayden, J. R.
Hines, J. N.
Jones, E. A.
Kennaugh, E. M.
Kennedy, Peter
Kirschbaum, H. S.
Kisha, Alex
Ko, H. C.
Kouyoumjian, R. G.
Levis, C. A.
Masters, R. W.
Nash, R. T.
Pang, T. C.
Perry, R. C.
Peters, Leon, Jr.
Richmond, J. H.
Rife, W. E.
Stoutenburg, D. V.
Taylor, R. C.
Thurston, M. O.
Tice, T. E.
Tischer, F. J.
Troyan, J. F.
Uenohara, Michiyuki
Ward, R. C.
Webster, R. E.
Yaw, D. F.

Dayton

Dunn, V. E.
Feist, W. E.
Godwin, S. J.
Gross, E. H.
Kurtz, A. W.
Littell, C. C., Jr.
Simopoulos, N. T.
Vanderpool, H. D.
Waugh, R. E.
Whittenberger, J. S.

Detroit

Amick, R. H.
Arrowsmith, Robert
Black, J. R.
Breymaier, R. W.
Brown, L. R.
Bryant, J. H.
Chute, G. M.
Crane, R. B.
Crimmins, J. W.
Doll, R. E.
Fischl, Robert
Fleig, W. J.
Friedberg, I. S.
Harmon, S. T.
Heim, D. S.
Hershenov, Bernard
Highstrete, B. A.
Hodge, W. H.
Hok, Gunnar
Holland, L. N.
Hoop, R. E.
Jankowski, Joseph, Jr.
Johnson, S. M.
Jones, H. E.
Keeney, M. G.
Kordos, R. W.
Larson, Richard W.
Larson, Ronal W.
Lawrence, B. T.
Le Baron, G. M.
Miller, M. H.
Mollard, W. N.
Nichols, A. D.
Peltzer, R. G.
Quin, W. J.
Ray, D. C.
Ristow, H. E.
Rollin, R. A., Jr.
Rowe, J. E.
Rykala, T. P.
Sharpe, C. B.
Smith, A. E.
Sobol, Harold
Strand, John
Taras, S. M.
Von Tersch, L. W.
Winters, L. C.
Wong, Andrew
Wooster, A. F.

Emporium

Golla, E. F.
Kelley, D. J.

Pittsburgh

Apostolakis, G. C.
Bozer, Ruchan
Courtney, J. E.
Flaherty, J. M.
Forrester, A. T.
Haun, R. D., Jr.
Kadak, Eugene
Klotzbaugh, G. A.
Oshea, R. P.
Peters, J. E.
Ralston, W. P.
Reissig, G. W.
Reynolds, M. T.
Schatz, E. R.
Spenik, John
Tanner, J. E.
Thompson, J. H.
Veselovsky, L. R.
Vogeley, C. E., Jr.

Toledo

Butler, J. A.
Wott, H. W.

Williamsport

Horrigan, J. B.
Sibley, R. C.
Simmons, W. J., Jr.

Region 5

Cedar Rapids

Anderson, R. L.
Coble, R. B.
Duhamel, R. H.
Frewaldt, E. W.
Johnston, D. H., Jr.
Lister, L. R.
Loupee, B. J.
Ore, F. R.
Sawvelle, E. V.
Steffes, R. M.
Tector, R. J.
Thompson, W. J.
Ulstad, M. S.
Ware, L. A.
Weeks, R. R.

Chicago

Akerman, Steve
Allen, C. R.
Allen, P. G.
Anderson, C. J.
Anton, A. J.
Arnow, C. L.
Austin, G. E.
Barrick, W. E.
Beam, R. E.
Becker, R. C.
Beneke, E. H.
Brittain, G. H.
Brown, J. S.
Buckler, R. A.
Burmeister, M. A.
Carlson, D. A.
Carrel, R. L.
Cassettari, Francisco
Castor, R. W.
Chen, Chen-Lin
Chien, R. T.
Clavier, P. A.
Cohn, G. I.
Coleman, P. D.
Corcoran, V. J.
Crotty, R. E., Jr.
Damm, G. J.
Del Vento, J. M.
Dennis, R. J.
Dervishian, Edward
Dichtl, R. J.
Dirsa, E. F.
Dougal, A. A.
Druz, W. S.
Duncan, J. W.
Dyson, J. D.
Emery, W. L.
Ernst, E. W.
Flesher, G. T.
Freymodsson, J. B.
Fuglestad, K. R.
Gallagher, J. A.
Gardner, B. H.
Gerber, H. L.
Gershon, J. J.
Gillespie, N. R.
Goldstein, Ladislas
Goodrich, P. D.
Graham, F. A.
Graziano, Victor
Haack, William, Jr.
Hargis, R. N.
Hedvig, T. I.
Hemminger, D. H.
Herling, D. L.
Horde, J. W.
Hu, A. Y.
Hupert, J. J.
Jauniskis, K. P.
Karas, W. P.
Kenyon, R. J.
Kiver, M. S.
Kott, W. O.
Kowitz, A. E.
Krahe, L. R.
Kuhn, N. J.
Kvitek, G. L.
Li, Tingye
MacAskill, R. B., Jr.
Maciszewski, A. H.
Magnuski, Henry
Mahrous, Haroun
Maier, R. H.
Marshall, F. R.
Mayes, P. E.
McCarrell, S. G.
McMullen, C. W.
Mittra, Rajjeshwar
Moore, R. A.
Morgan, R. E.
Needle, J. S.
Pakan, J. J.
Parkinson, J. A.
Peach, L. C.
Peterson, J. W.
Pettegrew, J. B.
Pichler, R. H.
Polich, W. J.
Rabowsky, Irving
Raef, A. J.
Rao, K. V. N.
Risky, F. A.
Robinson, D. E.
Roszkowski, G. J.
Ruzicka, B. J.
Samocki, C. J.
Saxe, R. E.
Sayles, H. L.
Scherer, P. J.
Schinski, D. L.
Segal, A. A.
Shewan, William
Shuba, J. P.
Skaperdas, D. O.
Sladek, N. J.
Sladkey, R. J.
Smierciak, E. S.
Spencer, W. H.
Stafford, J. J.
Thomas, G. E.
Thomas, R. G.
Travis, William
Ulaszek, J. J., Jr.
Uyetani, Bob
Voorhaar, F. R.
Weber, K. C.
Weeks, W. L.
Westerlund, C. T.
White, E. S.
White, R. F.
Williams, J. T.
Win, S. M.
Woodbury, H. L.
Yang, R. F. H.
Ye, J. W. F.
Yuen, P. C.

Evansville-Owensboro

Johnson, A. L.
Walker, R. J.

Fort Wayne

Artman, R. L.
Coles, D. K.
Cooper, M. J.
Dees, J. W.
Dye, N. E.
Ecker, J. L.
Fisher, C. C.
Gough, L. E.
Gramer, E. E., Jr.
Hambrock, H. E.
Helderman, T. E.
Hessler, John, Jr.
Hively, R. R.
Hutchison, D. P.
Jensen, C. W.
Killion, D. G.
Mast, P. L.
McFadden, J. H.
Richards, G. A.
Rogers, G. E.
Sessler, J. G.
Skidmore, C. E.
Terry, C. B.
Wallace, C. E., Jr.

Indianapolis

Bolle-Kramer, D. M.
Clark, R. E.
Cory, N. L.
Dalton, R. C.
Gaskins, G. L.
George, R. H.
Hayt, W. H., Jr.
Justus, J. R.
Schultz, F. V.
Spencer, R. L.

Louisville

Fitzmayer, L. H.
Morris, C. R.
Scheer, D. J.

Milwaukee

Gessner, Urs
Haugen, M. G.
Howell, J. F.
Ishii, Koryu
Jilbert, R. T.
Kerske, J. F.
Nieburh, K. E.
Scheibe, E. H.
Schlicke, H. M.
Scott, K. J.
Swift, W. B.
Taus, H. G.
Van Bladel, J. G.

Omaha-Lincoln

Bernard, P. G.
Beshore, P. S.
Borcher, E. J.
Elwell, W. G.
Hyde, C. M.
Runyon, R. E.
Staley, J. D.

South Bend-Mishawaka
Dunlap, K. H.
Floering, K. S.
Marshall, R. E.
Modesitt, M. B.
Pilcher, R. M.

Twin Cities
Badaker, Harriett
Bonstrom, D. B.
Born, V. A.
Grosz, W. S.
Haxby, B. V.
Holte, J. E.
Kanda, A. F.
Nysturn, A. M.
O'Dea, O. B.
Raabe, H. P.
Rickett, R. J.
Robertson, A. J. L.
Sikorski, J. W.
Snyder, W. D.
Webster, J. W.
Yeager, R. L.

Region 6

Alamogordo-Holloman
Fix, O. W.
Lux, M. O.
MacDonald, H. J.
Nicholson, Taft
Warnock, R. L.

Beaumont-Port Arthur
Acker, W. M.

Dallas
Armstrong, F. L.
Bailey, R. W.
Bondy, M. A.
Bullock, M. W.
Carr, W. B.
Coats, R. P.
Dyke, Ed
Earhart, C. E.
Fisher, L. M.
Flowers, B. R.
Forsyth, P. G.
Hallford, B. R.
Hertel, Paul, Jr.
Lee, Chwan-Chang
Logan, J. J.
Maxwell, J. W.
McMillin, J. M., Jr.
Pippenger, D. E.
Pittman, P. D., Jr.
Reynolds, P. R.
Sanford, A. L.
Schafer, N. B.
Shuffler, R. M.
Stanton, A. N.
Stone, R. M.
Strom, L. D.
Vilbig, J. L., Jr.
Weedfall, W. W.

Denver
Beatty, R. W.
Bell, B. G.
Burkhard, D. G.
Bussey, H. E.
Case, W. E.
Cook, E. E.
Daniels, W. H.
Estin, A. J.
Foley, W. V.
Grove, W. C.
Harrington, R. D.
Howell, R. G.
Kennedy, R. N.
Lance, H. W.
Larson, R. E.
Pierpont, H. F.
Revilla, A. G.
Richardson, J. M.
Rickerson, W. B.
Rinn, B. R.
Rumfelt, Anne
Schafer, G. E.
Spano, A. J.
Tary, J. J.
Thompson, M. C., Jr.
Wait, J. R.
Wang, C. S.

El Paso
Foster, M. J.
Haas, H. W.
Harrison, H. C.
Henry, D. G.
Kidwell, R. P.
Rojas, H. A. M.
Roth, F. P.
Taylor, L. S.
Tipton, R. B.
Welch, C. M.

Fort Worth
Brooks, J. L.
Brust, M. F.
Bryan, K. W.
Carmouche, C. L.
Cook, A. B.
Harman, D. G.
Hodges, T. R.
James, B. O.
Langston, J. W.
McClanahan, M. E.
Roy, F. J.
Sivernell, R. B.
Speairs, M. F.
Van Hoozer, C. H.
Ward, E. B.

Houston
Brown, H. K.
Caplan, R. S.
Hauschild, R. L.
McElroy, J. D.
Salas, R. E.
Swearingen, J. E.
Swearingen, J. L.

Kansas City
Anderson, R. W.
Bahm, D. H.
Basham, Ray
Chinn, F. T.
Dalton, R. C.
Guthrie, J. E.
Hax, D. H.
Jackman, C. A
Johnson, G. L.
Johnson, P. G.
Lane, C. A.
Verhyden, L. C.
Wilcox, J. V.

Little Rock
Cannon, W. W.
Kettler, E. W., Jr.
McNully, J. L.
Nider, M. E.
Stahlkopf, J. V.

Lubbock
Farmer, P. E.
Gray, Thomas, Jr.

New Orleans
Craig, G. H.
Hulteen, C. K.
Rust, J. J.

Oklahoma City
Dunlap, B. A.
Herriott, J. K., Jr.
Hoole, C. R.
Wood, G. J.

St. Louis
Ashworth, B. W.
Augustine, R. J.
Brennan, R. D.
Cummings, G. M.
Hardy, J. W., III
Hirsch, O. C.
Kaiser, R. L.
Lechtreck, L. W.
Lienhard, O. W.
McHoney, L. M.
McPherson, W. R.
Meyer, C. J.
Mohrman, R. F.
Mosley, C. E.
Mueller, T. E.
Reiniger, R. A.
Robel, M. C.
Skitek, G. G.

San Antonio
Barquist, W. S., Jr.
Bell, R. L.
Block, E. H.
Douglas, J. H.
Economy, Richard
McHugh, E. L.
O'Brien, B. B.
Pease, L. A.
Wangler, R. B.
Weber, L. C.

Shreveport
Randolph, A. M.
Strickland, E. C.
Thomas, O. D., Jr.

Tulsa
Bennett, D. W.
Cheney, J. F.
Draheim, L. H.
Ewing, T. N.
Morrow, J. E.
Phillips, H. W.
Silverman, Daniel
Sykora, G. E.

Wichita
Egbert, G. W., Jr.
Jones, D. E.
Klatt, W. K.
Smith, Tom

Region 7

Albuquerque-Los Alamos
Allen, L. J.
Ames, J. R.
Arnot, G. A., Jr.
Bittner, B. J.
Connell, J. C.
Crook, G. S.
Dike, S. H.
Eckhoff, R. W.
Fagan, Peter
Finch, H. D.
Fossum, D. E.
French, Gene
Glass, R. E.
Grover, R. K.
Hampton, D. J.
Hayes, Bernard
Jackson, H. J.
Jones, M. C.
Kellom, A. W.
Kudrna, K. L.
Lincoln, R. A.
Noble, R. P.
O'Nan, R. L.
Ray, H. K.
Scharrer, R. G.
Senter, C. H.
Smith, D. A.
Weingarthen, D. H.
Widenhoefer, N. C.

China Lake
Courtney, J. D.
Creusere, M. C.
Deyoe, D. C.
Poulson, W. A.

Fort Huachuca
Lowy, W. M.
Marshall, R. W.
Paul, B. W.

Los Angeles
Aaron, B. D.
Adcock, M. D.
Ajioka, J. S.
Albrecht, Albert
Alpine, P. E.
Anderson, D. B.
Anderson, G. R.
Anderson, S. E.
Andrew, V. J.
Arciuch, J. P.
Arrowsmith, E. B.
Ashcraft, W. D.
Asmus, J. F.
Babcock, D. F.
Bagi, R. R.
Bailey, F. W.
Baird, W. H.
Baker, B. W.
Barkson, J. A.
Barnes, J. G.
Bates, D. J.
Batson, D. D.
Bauman, H. W.
Bedrosian, Edward
Beekman, R. E.
Begovich, N. A.
Bekey, Ivan
Benbrooks, L. A.
Bennett, R. G.
Berry, D. C.
Bessette, Andrew
Blackwell, M. B.
Blatchford, Dean
Bobrow, E. N.
Bock, M. J.
Bonney, L. A.
Boreham, J. F.
Boutin, C. U.
Bowers, E. O.
Boyd, C. D.
Boyle, S. R.
Brandon, E. T.
Bredon, A. D.
Breece, R. C.
Brewer, C. P.
Bridges, W. B.
Brown, David
Brown, F. W.
Brunn, K. R.
Buchanan, H. R.
Bucher, F. X.
Buczek, C. J.
Burton, J. R.
Butts, L. E.
Campbell, F. L.
Capranica, R. R.
Carey, G. D.
Carlile, R. N.
Carr, J. W.
Chandler, C. W.
Chang, Bansun
Chernin, M. G.
Child, C. H.
Christoffers, W. H.
Clapp, R. W.
Clarke, F. H., Jr.
Clavin, Alvin
Clunis, Kenneth
Coling, F. L.
Considine, J. M.
Cooper, P. V.
Cordray, R. E.
Cornell, J. R.
Cowan, C. F.
Cox, H. N.
Cox, W. F.
Craven, W. A., Jr.
Criss, G. B.
Currie, M. R.
Curtis, C. W.
Dain, H. W.
Dalley, D. G.
Davis, E. F.
Davis, J. I.
Davis, K. S.
De Cristoforo, E. J.
Deininger, C. F.
Derington, V. E.
Dexter, G. W.
Dobbertin, W. H.
Doll, C. L.
Donnelly, R. W.
Dorratcague, P. E.
Duda, R. O.
Dunn, C. E.
Duvall, W. E.
Dvoracek, F. H.
Eatough, C. D.
Elliott, R. S.
Ellis, A. R.
Endler, H. M.
Fafarman, Alfred
Fahnestock, R. J.
Feeney, J. E.
Fenn, W. H.
Fernandey, Ferdinand
Ferrel, D. W.
Fisher, M. K.
Fonda-Bonardi, Giusto
Foster, H. E.
Francis, T. F.
Frankos, D. T.
Fraser, M. R.
Fredericks, R. W.
Frieburg, H. E.
Friedman, J. A.
Friedman, Percy
Futterman, Meyer
Gage, N. C.
Gallagher, H. E.
Gannaway, Robertson
Gardner, F. M.
Gee, L. C.
George, Nick, Jr.
Gibbons, T. J.
Gibbs, L. C.
Gill, D. A.
Ghose, R. N.
Giddis, A. R.
Gillespie, E. S.
Gleason, M. J.
Gola, A. S.
Gottier, R. L.
Grabowski, K. P.
Graham, D. R.
Griffiths, R. W.
Guinane, J. E.
Gustafson, L. A.
Hadden, F. A.
Hagerty, R. J.
Hajic, E. J.
Hall, R. D.
Hansen, R. C.
Harmon, J. J.
Harrington, V. L.
Hata, F. T.
Hatcher, E. C., Jr.
Helland, J. C.
Hershberger, W. D.
Hetland, George, Jr.
Hewitt, G. E.
Hicks, A. R.
Higa, W. H.
Hiller, E. R., Jr.
Hodson, W. G.
Hoff, Knut
Holdsworth, D. M.
Holland, J. E.
Holley, A. E.
Horning, T. D.
Hovda, R. E.
Hudspeth, Tom
Hughes, W. A.
Hutcheon, R. S.
Hyneman, R. F.
Ittleson, J. S.
Jackson, J. A.
Jamison, R. S.
Joerger, J. C.
Jones, L. E.
Kalstrom, R. D.
Kaprielian, Z. A.
Kasai, G. S.
Kaufman, Irving
Keiser, J. A.
Kelso, J. M.
Kemanis, Gunars
Kern, W. W.
Kimmel, R. O.
Kinaga, Thomas
King, H. E.
Kiser, A. J.
Kitabayashi, Tomotsu
Klapper, Eric
Koontz, R. H.
Kopulsky, Sam
Kovensky, D. J.
Kramer, A. G.
Krausz, Robert
Kreinheder, D. E.
Krill, C. K.
Kriz, K. H.
Krogh, R. A.
Kroy, W. H., Jr.
Kurtz, L. A.
Lambert, D. W.
Lance, A. L.
Leng, R. B.
Lepoff, J. H.
Linnes, K. W.
Lockhart, E. H.
Loop, H. L.
Lopez, R. L.
Louie, P. Y.
Louie, William
Lovick, Edward, Jr.
Lund, W. W., Jr.
Lundquist, C. R.
Lym, V. W.
Machlis, Jerome
Magid, Milton
Maguire, W. W.
Majka, C. J.
Mallison, J. A.
Margerum, D. L.
Margolin, A. R.
Markin, Joseph
Mathison, R. P.
Matthaei, G. L.
Martin, D. P.
Martin, W. R.
Masuda, H. B.
Maxum, B. J.
McCann, J. G.
McClure, D. H.
McCone, G. L.
McDowell, D. E.
McElwee, J. F.
McFarlane, M. D.
McWilliams, J. D.
Mead, J. A.
Metter, R. E.
Metzger, H. W.
Meyer, D. R.
Mickelson, J. R.
Milham, R. F., Jr.
Miller, G. B.
Mizell, M. H.
Moise, N. L.
Mongan, A. J.
Moore, J. A.
Morse, J. H.
Morton, W. B., Jr.
Mueller, W. M.
Muhlstein, R. W.
Mumma, J. W.
Munushian, Jack
Murray, R. E.
Nelson, C. E.
Nevins, J. E., Jr.
Newton, W. P.
Noorland, Martinus
Notvest, R. A.
Oleesky, S. S.
Oltman, H. G., Jr.
Omiya, E. S.
Orr, J. A.
Oshiro, F. K.
Otoshi, T. Y.
Pamler, R. G.
Parisky, R. N.
Parzl, R. C.
Paul, P. F.
Paulson, E. T.
Peringer, Paul
Perry, W. C.
Pinol, D. G.
Polzin, E. M.
Potter, P. D.
Powell, R. M.
Proctor, D. W.
Pruett, D. W.
Purdum, L. C.
Randall, G. M.
Reed, R. H.
Reese, R. F.
Roberts, P. S.
Robinson, Percy
Roehl, E. R.
Royal, D. E.
Rumsey, W. E., Jr.
Sabisky, E. S.
Saltzman, Harold
Samuels, A. H.
Samuelson, H. R.
Sassman, R. W.
Schaefer, W. C.
Schaffer, Alvin, Jr.
Scharp, G. A.
Seaton, A. F.
Sedin, J. W.
Seeley, E. W.
Seltzer, L. J.
Sensiper, Samuel
Shahan, Onnig
Shapiro, S. S.
Sheldon, P. H.
Shigemoto, J. M.
Shimabukuro, F. I.
Signer, R. M.
Silence, N. C.
Silva, L. M.
Sims, J. L.
Sion, Elio
Sisson, A. R.
Smith, R. D.
Smith, R. G.

Snyder, W. A.
Spoor, L. C.
Stark, Louis
Stegen, R. J.
Steinkolk, R. B.
Stodder, D. J.
Stone, R. E.
Street, N. C.
Strumwasser, Eric
Struve, L. M.
Sur, John
Swan, R. L.
Symonds, R. J.
Tampico, Joseph
Tang, Raymond
Tarot, Alfred
Tasker, R. B.
Thomas, D. L.
Tomikawa, K. B.
Tondreau, H. J.
Tornheim, Harold
Trainer, R. F.
Trapp, R. R.
Tudor, J. E.
Uebele, G. S.
Underberger, G. M.
Valette, H. C.
Vallar, T. F.
Vernon, F. L., Jr.
Von Lanken, J. R.
Wachowski, H. M.
Wada, J. Y.
Walcek, E. J.
Walkup, L. A.
Walsh, B. L.
Walters, A. W.
Ward, B. M., Jr.
Warhurst, J. W.
Wayman, J. M.
Webb, P. S.
Weglein, R. D.
Wehner, R. S.
Weil, F. M.
Wells, R. E.
Wershoven, G. A.
Whirry, W. L.
Wildman, A. J.
Willis, M. R.
Wills, J. D.
Wiseman, S. D.
Wolking, D. H.
Wong, Lem
Wood, G. D.
Wood, J. R.
Woster, S. H., Jr.
Young, C. W.
Zamites, C. J.
Zboril, F. R.

Phoenix

Blair, L. R.
Boekelheide, A. W.
Burns, J. J.
Carter, P. M.
Echols, R. A.
Funk, R. E.
Ham, N. C.
Hickman, J. E.
Jurich, Samuel
Knight, W. H.
Lindsay, J. D. G.
Murray, P. W.
Nicholas, J. C.
Noon, J. R.
Robertson, S. D.
Schaffner, Gerald
Solem, R. J.
Stearns, W. P.
Sterns, W. G.
Warriner, Ben
Wilkinson, C. O.

Portland

Brock, E. G.
Calnon, D. C., Jr.
Dyke, W. P.
Hashizume, G. K.
Hawley, G. K.
McCutcheon, S. R.
Menegat, M. M.
Miller, F. E.
Richardson, W. E.
Sleeth, J. D.
Surdam, E. L.
Tabshy, S. J.

Sacramento

Dunkel, H. D.
Fuller, G. R.

Salt Lake City

Anderson, D. W.
Bowen, M. J.
Delore, G. E.
Haegele, R. W.
Hansen, C. F.
McLaughlin, J. W.
Nicholes, G. H.

San Diego

Abbey, Kirk
Ayers, J. L.
Babbitz, H. B.
Bergant, G. G.
Boyce, W. E. L.
Chang, G. M.
Chazotte, M. M., Jr.
Derenthal, R. J.
Dickstein, H. D.
Dobyne, J. C., Jr.
Hartin, W. J.
Honer, R. E.
Hopkins, R. U. F.
Humphrey, R. D.
Kaestner, P. C.
Keener, M. A.
Kluck, J. H.
Medved, D. B.
Moore, W. E.
Mulvey, J. X., Jr.
Phillips, C. E.
Proctor, David
Ratkevich, A. E.
Schick, H. F.
Siegel, William
Simmons, J. M., Jr.
Small, B. I.
Taylor, W. G.
Thomas, H. A.
Thomas, J. J.
Trogdon, W. H.
Trolese, L. G.
Undesser, Karl
Wilson, W. R.
Wolfe, G. W.
Wooley, G. J.
Youngberg, B. E.

San Francisco

Abraham, W. G.
Addleman, L. A.
Adelson, M. B.
Aden, A. L.
Agadoni, C. A.
Allen, M. A.
Allen, S. E., Jr.
Allen, T. L., Jr.
Allison, J. E.
Anderson, C. T.
Anderson, J. S.
Andrews, J. V.
Angelakos, D. J.
Armstrong, R. S.
Arnold, C. A.
Arnold, D. T.
August, Gerald
Ayers, W. R.
Ayers, W. P.
Barbano, Normand
Barkoczy, A. B.
Barnes, C. W., Jr.
Barnes, F. S.
Barnett, E. F.
Batten, H. W.
Beaver, W. L.
Benson, Stanley
Bert, J. E.
Birdsall, C. K.
Blumberg, Martin
Booth, R. E.
Borghi, R. P.
Bostwick, W. E.
Boyer, B. E.
Brinton, R. L.
Brunn, John
Bunn, H. L.
Buss, R. R.
Butterfield, F. E.
Carnhan, C. W.
Carter, P. S., Jr.
Caryotakis, George
Chan, W. W.
Chang, Nein-Chih
Chang, W. S. C.
Chodorow, Marvin
Clifton, J. K.
Clinton, W. R.
Coale, F. S.
Cogshall, P. D.
Cohn, S. B.
Connor, T. J.
Contos, P. A.
Cool, L. R.
Craig, R. A.
Crane, Milton
Cumming, R. C.
Cushing, T. D.
Damonte, J. B.
Davis, L. W.
De Grasse, R. W.
Detwiler, R. D.
Dill, G. D.
Dimmick, R. R.
Dinapoli, F. C.
Di Napoli, G. W.
Disman, Murray
Dodds, Wellesley
Dow, D. G.
Dunbar, A. S.
Dunn, D. A.
Eallonardo, C. M.
Eaves, H. H.
Edson, W. A.
Edwards, B. N.
Eggers, R. E.
Eisenberg, Morris
Elam, J. M.
Engler, C. G.
Enos, R. M.
Fank, F. B.
Feeney, W. G.
Ferri, Giuseppe
Feuchtwang, T. E.
Fitzpatrick, J. P.
Fong, Arthur
Fontana, Jorge
Forrer, M. P.
Foster, C. P., Jr.
Franks, R. E.
Gamara, N. J.
Geppert, D. V.
Gerig, J. S.
Gerling, J. E.
Gilden, Meyer
Gillard, C. W.
Ginzton, E. L.
Golde, Hellmut
Goodman, D. H.
Grace, D. J.
Graham, R. E.
Grande, V. J.
Granger, J. V. N.
Groberg, L. R.
Grow, R. W.
Gunn, T. L.
Guthrie, E. E.
Hagopian, R. H.
Hand, B. P.
Harman, W. A.
Heffner, Hubert
Helgesson, A. L.
Hennies, S. R.
Henschke, R. A.
Hiestand, N. P.
Hightower, W. D.
Hlavka, L. F.
Hochman, Daniel
Holaday, R. E.
Honey, R. C.
Horton, M. C.
Hsu, Jen
Huffman, G. A.
Hunter, L. W.
Hunton, J. K.
Hurst, S. R.
Jaffe, J. S.
Jaynes, E. T.
Jepsen, R. L.
Johnson, L. B.
Jones, E. M. T.
Kaisel, S. F.
Kavanaugh, J. C.
Kebby, M. H.
Keitel, G. H.
Kino, G. S.
Kirstein, P. T.
Klamm, C. F., Jr.
Kluver, Billy
Kohl, W. H.
Kootsey, J. M.
Kotzebue, K. L.
Kovalevski, N. N.
Krenz, J. H.
Kreutzer, M. L.
Lacy, P. D.
Lagerstrom, R. P.
LaRue, A. D.
Lebacqz, J. V.
Levy, M. C.
Lim, Alfred
Lind, J. N.
Linden, D. A.
Lindley, J. P.
Lohr, Dieter
Ludovici, B. F.
Luebke, W. R.
Lundstrom, O. C.
Mace, J. C.
Main, W. F., Jr.
Maltzer, Irving
Mannas, R. G.
Markum, J. A., Jr.
Mathers, G. C.
Maudens, L. C.
Mays, A. S.
McCullough, J. A.
McEuen, A. H.
McKee, L. H.
Meader, H. W.
Medina, M. A.
Melchor, J. L.
Menneken, C. E.
Milazzo, Ciro, Jr.
Mizuhara, Albert
Moe, C. R.
Monson, J. E.
Moreno, Theodore
Morita, Tetsu
Mueller, M. T.
Murphy, E. J.
Nalos, E. J.
Nelson, B. E.
Nemirow, D. M.
Newman, H. L.
Nikonenko, P. V.
Nitz, I. C.
Norris, N. J.
Novick, Gabriel
Oliver, B. M.
Olson, F. A.
Olte, Andrejs
Orrick, R. L., Jr.
Palmquist, N. B., Jr.
Pantell, R. H.
Parker, J. F.
Patch, C. S.
Patience, D. L.
Peters, D. W.
Peters, R. L.
Peterson, C. J.
Phillips, R. M.
Price, V. G.
Prickett, R. J.
Proctor, E. K., Jr.
Prommer, Alfred
Rawlins, R. E.
Reis, C. S.
Reynolds, Walter, Jr.
Rierson, J. W.
Riley, R. B.
Rosenthal, H. A.
Ross, T. A.
Roumbanis, Theodore
Rowley, J. J.
Rudee, Elliott
Ruetz, J. A.
Ryan, A. H.
Ryland, B. G.
Rynn, Nathan
Sagawa, S. S.
St. Clair, M. W.
Sanders, R. B.
Savarin, Alex
Schauers, C. J.
Schiffman, B. M.
Schreiner, R. W.
Schrumpf, D. A.
Schumacher, F. M.
Seiden, P. E.
Senise, J. T.
Serang, A. M.
Shaw, H. J.
Sherk, P. M.
Shimizu, J. K.
Siegman, A. E.
Singer, J. R.
Sklar, Howard
Sloan, D. H.
Smith, P. G.
Smullin, W. B.
Snyder, R. D., Jr.
Sonkin, Simon
Spangenberg, Karl
Steele, C. W.
Stinson, D. C.
Sutherland, R. I.
Teeter, W. L.
Tetenbaum, S. J.
Thon, W. H.
Thornburg, R. O.
Thornton, D. D.
Tomiyasu, Kiyo
Valdes, L. B.
Valles, B. V.
Vane, A. B.
Vartanian, P. H., Jr.
Vea, T. H.
Vehn, R. E.
Vinding, J. P.
Waldman, M. D.
Watkins, D. A.
Watson, G. G.
Watson, W. H.
Weed, G. E.
Welch, W. J.
Westall, C. L.
Wharton, C. B.
Wheeler, G. J.
Whinnery, J. R.
White, D. W.
White, F. M., Jr.
Whitmer, R. F.
Whitten, C. L.
Wholey, W. B.
Wightman, B. A.
Wilds, R. B.
Williams, W. F.
Winkler, R. H.
Wood, F. B.
Worley, O. C.
Yadavalli, S. V.
Yee, K. S.
Zitelli, L. T.

Seattle

Arens, V. R.
Armstrong, C. W.
Belenski, J. D.
Biggs, A. W.
Burns, G. A.
Bystrom, Albin, Jr.
Christie, L. F., Jr.
Coughlan, G. B.
Dalby, T. G.
De Groot, E. B.
Egbert, H. F.
Guy, A. W.
Hasserdjian, G. K.
Held, Gedalia
Herr, M. D.
Janes, H. P., Jr.
Kieburtz, R. B.
Kiskaddon, W. V.
Larson, L. A.
Leonard, P. W.
Lidovitch, S. B.
Lillie, W. A.
Loski, R. R.
Lundquist, F. E.
Metter, R. E.
Mitchell, H. R.
Morris, C. R.
Oakes, G. K.
Quirk, W. J.
Reynolds, D. K.
Short, R. C.
Siddons, W. J.
Smith, A. E.
Tighe, R. F.
Ware, D. R.
Waterman, H. B.

Territory of Hawaii

Chang, D. C.
Harada, Saburo
Higa, Koken
Hill, R. R.

Tucson

Bundy, R. C.
Carpenter, R. L., Jr.
Dale, G. G.
Gravell, A. J.
Hessemer, R. A., Jr.
Leifheit, S. E.
Marston, E. J.
Ream, S. M.
Wilde, Ned

Region 8

Bay of Quinte

Chambers, R. G.
Chisholm, R. M.
Mitchell, T. E.
Swan, C. B.
Waller, M. J.

Hamilton

Balmain, K. G.
Conquest, E. A.
Hedgecock, N. E.
Lyons, K. C.
Matthies, J. G.
McLennan, E. A.
Samson, J. F.

London

Dearle, R. C.
Seifert, W. J.
Thomas, Arthur
Tull, E. H.

Montreal

Adkar, C. K.
Anderson, L. K.
Arsenault, Leo
Beaulieu, J. A.
Birman, Gerhard
Bonneville, Sydney
Bosisio, R. G.
Burtnyk, Nestor
Campbell, A. F.
Collin, R. E.
Cox, J. R. G.
Cummins, J. A.
Dion, Andre
Fabiszewski, Henry
Glegg, K. C. M.
Haberl, J. F.
Hansard, H. H.
Heroux, Leo
Hryhorijiw, Wolodymyr
Jackson, K. A.
Jamshedji, J. S.
Kingan, A. J.
Kubina, S. B.
Lavoie, J. L.
L'Heureux, L. J.
Libera, F. A.
Mockler, T. P.
Moore, E. J.
Nadon, Leo
Parent, G. J. C.
Postema, G. B.
Price, C. C.
Reeves, Rene
Roloff, W. T.
Sankey, Charles
Savard, J. Y.
Surtees, W. J.
Taylor, N. J.
Tiberghien, C. M. J., Jr.
Vaillancourt, R. M.
Weytze, D. W.
Whitmore, E. J.

Newfoundland

Au, G. D.
Haycock, Alfred, Jr.
Moseley, S. V.
Tibbett, J. E.

Northern Alberta

Hall, T. W.
Usher, Roy

Ottawa

Adey, A. W.
Beneteau, P. J.
Carroll, D. V.
Corbett, L. V.
Covington, A. E.
Craven, J. H.
Cumming, W. A.
Fawcett, G. M.
Gagne, R. R. J.
Henderson, J. T.
Hurd, R. A.

Kalra, S. N.
Klein, E. J.
McCord, J. T.
McCormick, G. C.
Medd, W. J.
Miller, G. A.
Moorcroft, D. R.
Nikkel, R. F.
Steele, K. A.
Turner, J. B.
Waugh, J. B. S.
Wilcox, D. A.
Wittke, P. H.

Regina

Kavadas, A. D.
Smith, S. K.

Southern Alberta

Davis, A. P.
Johnston, C. W.
Lundrigan, E. G.
Smith, M. F.

Toronto

Aagesen, John
Auld, B. A.
Baart, J. G.
Banner, W. G.
Barclay, A. P. H.
Baron, H. D.
Bell, A. R.
Bohn, E. V.
Bridgman, J. M.
Buckles, F. G.
Bull, T. R.
Byers, H. G.
Dalzell, T. D.
Dmitrevsky, Sergej
Elliott, A. W. D.
Farrell, G. L.
Fredericks, M. J.
Green, M. E.
Hackbusch, R. A.
Hewit, H. O.
Hyde, Geoffrey
Lang, G. R.
Martens, G. O.
Matthews, R. P.
McLeod, J. W.
Moore, A. D.
Murray, R. L. A.
Noakes, Frank
Nordstrand, R. B.
Penner, R. J.
Robinson, R. A.
Sengupta, D. L.
Sinclair, George
Snitke, J. A.
Stewart, A. C.
Stone, D. G.
Tamagi, T. T.
Tang, D. D.
Teng, Toivo
Tomicio, Nicholas
Van Den Ende, Hendrik
Vural, Bayram
Walley, B. C.
Wang, C. P.
Wisenden, G. A.
Wray, D. G.
Yachimec, Peter
Yen, J. L.

Winnipeg

Campbell, D. C.
Campbell, J. F.
Gunston, F. H.
Kowalik, Harry
Shaver, H. B.

Military Overseas

Aulbach, C. E.
Ballard, J. L.
Bowler, J. A.
Cheney, F. H.
Duncan, H. H.
Engelbrecht, R. S.
Fozdar, J. K.
Gallup, G. B.
Graf, E. A.
Grimme, H. J.
Harcar, A. R.
Harris, C. E.
Hurlbut, G. N.
Iwai, K. G.
Johnson, C. W.
Kirkland, F. B.
Liston, Jack
Lovitt, S. A.
Madsen, J. F.
Mathews, C. A., Jr.
Mergy, E. A. E.
Moss, K. S., Jr.
Perry, W. S., Jr.
Polgar, M. S., Jr.
Roy, L. B.
Sloman, F. A.
Snyder, Norman
Valge, Juri
White, Walter, Jr.

Foreign

Buenos Aires

Pinasco, S. F.

Israel

Shekel, Jacob
Spector, J. O.
Tamir, Theodor
Weissberg, Ephraim

Rio de Janeiro

Girard, P. A.
Sa, M. A. M.

Tokyo

Aoi, Saburo
Fujii, Tadakuni
Harashima, Osamu
Hariu, Tokyo
Hayasi, Syuiti
Ibuka, Masaru
Imai, Haruzo
Ishikawa, Denji
Ishikawa, Takeji
Iwakata, Hideo
Iwasawa, Hiroshi
Kano, Tetuo
Kawano, Tadasu
Kitsuregawa, Takashi
Kohno, Shishu
Konomi, Mitsugu
Kumagai, Toshiro
Kuroiwa, Yutaka
Makimoto, Toshio
Matsumaru, Katsu
Matsuyuki, Toshitada
Mikuma, Fumio
Minozuma, Fumio
Mita, Shigeru
Miyakoshi, Kazuo
Mizuma, Masaichiro
Morita, Kazuyoshi
Morita, Kiyoshi
Morita, Masasuke
Murakami, Ichiro
Mushiake, Yasuto
Nakagami, Minoru
Nakahara, Fujio
Nemoto, Tadao
Niguchi, Koichiro
Nishizawa, Jun-Ichi
Niwa, Yasujiro
Ohkoshi, Takanori
Okabe, Takahiro
Okada, Minoru
Okamura, Sogo
Omori, Shunichi
Owaki, Kenichi
Owaku, Shuzo
Saito, Shigebumi
Sato, Teiji
Shintani, Takeshiro
Sugi, Masao
Suzuki, Michio
Taki, Yasuo
Tanabe, Yoshitoshi
Taniguchi, Fusao
Tanimura, Isao
Tomono, Masami
Tomota, Miyaji
Uchida, Hidenari
Yamashita, Kanehiro
Yamazaki, Takashi
Yasuda, Ichiji

Other Countries

Alaska

Ordonia, J. M.

Australia

Honnor, W. W.
Sanders, R. J.
Willoughby, E. O.

Austria

Zemanek, Heinz

Belgium

Buys, W. L.
Desirant, M. C.
Gewillig, M. R.
Vanwormhoudt, M. C.

Bermuda

Harries, J. H. O.

Brazil

Caicoya, J. I.
Grant, F. W.
Muller, F. R.
Tai, C. T.

Burma

Naing, H. M.

Ceylon

Adikaram, K. B.

Colombia

Cuevas, Alfonso

Cuba

Arnaud, J. P.
Bode, M. C.
Guiral, R. L.
Montes, J. V.
Pages, E. V.
Pella, Anibal

Denmark

Christensen, C. L.
Fomsgaard, Kurt
Gronlund, M. P. S.
Hansen, G. K. F.
Ingerslev, F. H. B.
Larsen, B. F.
Nag, D. S.
Sorensen, E. V.
Sorensen, N. E.
Toft, S. C.

England

Ash, E. A.
Brown, John
Cullen, A. L.
Dawes, J. E.
Forte, S. S.
Halsey, J. E.
Harris, K. E.
Jackson, Willis
Kelliher, M. G.
Laverick, Elizabeth
Macnee, D. H.
Parsons, A. N.
Rantzen, H. B.
Rouse, F. W. D.
Rubenstein, Gerald
Siddiqi, M. I.
Sodomsky, K. F.
Townsend, F. H.

Finland

Ivars, R. E.

Formosa (Taiwan)

Hian-Yao, Ong
Wang, Chun-Chuan

France

Baron, Jean
Berline, S. D.
Blassel, P. P.
Calon, A. E.
Ferrier, P. A.
Fuks, Alexandre
Ghertman, Jean
Guenard, P. R. G.
Guyot, L. F.
Kerbec, M. J.
Labin, Emile
Leblond, A. F.
Loeb, J. M.
Mandel, Paul
Prache, P. M.
Simon, J. C.
Sirel, Michel
Voge, J. P.
Warnecke, R. R.
Weill, Henri

Germany

Borgnis, F. E.
Busch, C. W.
Meyer, E. W.
Schnupp, Peter
Severin, H. K. F.
Uhrmann, A. M.
Von Trentini, Giswalt
Zinke, Otto

Greece

Kariambas, Nicolas

Hong Kong

Hsu, Hsiung

Iceland

Frimannsson, Hordur

India

Bhattacharyya, B. K.
Chatterjee, A. K.
Daruvala, D. J.
Jain, J. D.
Misra, Harihar
Raman, S.
Rao, K. L.

Iraq

Bunyan, S. A.

Italy

Catorci, B. P.
Derossi, A. D.
De Vito, G. R.
Egidi, Claudio
Fagnoni, Elio
Floriani, Virgilio
Genta, Dino
Koch, Renato
Monti-Guarnieri, I. G.
Palandri, G. L.
Stracca, G. B.
Vergani, Angelo

Korea

Hwang, I. Y.

Lebanon

Hoffman, J. D.

Mexico

Chora, L. M.
Diaz, J. S.
Espinoza, C. E. F.
Gilberto, H. R.
Higuera-Mota, H. R.
Joaquin, D. S.
McGee, W. F., Jr.
Mendez, E. D.
Rodriguez, Eugenio
Zepeda, Salvador

Netherlands

Alma, G. H. P.
Gudmansen, P. E.
Hheijboer, R. J.
Nijenhuis, Willem
Op Den Orth, J. M.
Seeger, C. L.
Tellegen, B. D. H.
Zijlstra, Paul

Norway

Bostad, J.
Eliassen, K. E.
Gaudernack, L. F.
Jenssen, Matz
Tangvik, Svein
Wessel-Berg, Tore

Scotland

Campbell, C. K.
Maclean, D. J. H.

Singapore

Hock, T. C.

South Africa

Zawels, Jakob

Sweden

Aurell, C. P.
Backmark, Nils
Bolinder, E. F.
Elfving, A. L.
Fagerlind, S. G.
Granqvist, C. E.
Haard, Bertil
Hvatum, Hein
Josephson, B. A. S.
Joste, S. V.
Lindstrom, Gunnar
Lofgren, E. O.
Persson, N. I. E.
Roll, Anders
Sivers, C. H. V.

Switzerland

Bonanomi, J. A.
Braun, A. F.
Brumm, I. G.
Epprecht, G. W.
Gaumann, Tino
Gloor, Bruno
Guanella, Gustave
Hagger, H. J.
Holtz, R. F.
Lang, G. J.
Lapostolle, P. M.
Schneider, M. V.
Tank, Franz
Walder, Emil

USSR

Martjushov, K. I.
Shmakov, P. V.

Venezuela

Alamo-Segovia, J. A.
Arreaza, R. G.
Carter, Jack
Elguezabal, I. I.
Guia-Monasterio, A. E.
Guitian, J. E.
McBain, H. F.
Torrealba, Juan

Airtron inc. presents the latest specifications on some of its newest, advanced-design microwave ferrite components

0.360 X 0.220 O.D. WAVE GUIDE SIZE

FERRITE ISOLATOR 100 KW
(WR-28 GUIDE SIZE)

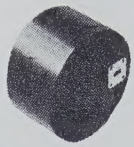

FREQUENCY RANGE: ..... 34.5 - 35.9 KMC
ISOLATION: ..... 20 db min.
INSERTION LOSS: ..... 1 db max.
INPUT VSWR: ..... 1.15 max. with matched load
POWER HANDLING CAPABILITY: .... 100 KW peak at 30 psig.
100 watts average into
a 2 to 1 load mismatch

ARA-133 WAVE GUIDE SIZE

X-BAND FERRITE RIDGED WAVE GUIDE ISOLATOR
(ARA-133 GUIDE SIZE)

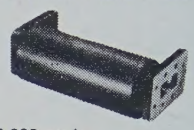

FREQUENCY RANGE: ..... 7050 to 10,800 mc/s
ISOLATION: ..... 10 db minimum
INSERTION LOSS: ..... .5 db maximum
INPUT VSWR: ..... 1.15 maximum with matched load
POWER HANDLING CAPABILITY: ..... 400 watts average into a
2 to 1 load mismatch

1.250 X .625 O.D. WAVE GUIDE SIZE

FERRITE MINIATURE ISOLATOR 300 KW
(WR-112 GUIDE SIZE)

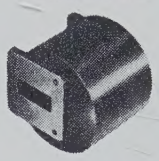

FREQUENCY RANGE: ..... 8500 to 9600 mcs.
ISOLATION: ..... 15 db min.
INSERTION LOSS: ..... 0.5 db max.
INPUT VSWR: ..... 1.10 max. with matched load
POWER HANDLING CAPABILITY: .... 300 KW peak at 30 psig;
300 watts average into
a 2 to 1 load mismatch

3.000 X 1.500 O.D. WAVE GUIDE SIZE

FERRITE MINIATURE ISOLATOR 400 KW
(WR-284 GUIDE SIZE)

FREQUENCY RANGE: ..... 2700 - 2900 MCS
ISOLATION: ..... 15 db minimum
INSERTION LOSS: ..... 0.5 db maximum
INPUT VSWR: ..... 1.10 maximum with matched load
POWER HANDLING CAPABILITY: .... 400 KW peak
400 watts average
with matched termination

2.000 X 1.000 O.D. WAVE GUIDE SIZE

FERRITE ISOLATOR 350 KW
(WR-187 GUIDE SIZE)

FREQ. RANGE (mc/s)	ISOLATION db (min.)	INSERTION LOSS db (max.)	INPUT VSWR (max.)	POWER CAPACITY	
				PEAK	AVERAGE
5400 to 5650	15	.5	1.15	350 KW	350 watts
5400 to 5900	10	.5	1.10	350 KW	300 watts

1.000 X .500 O.D. WAVE GUIDE SIZE

MINIATURE FERRITE PHASE DIFFERENTIAL DUPLEXERS
(WR-90 AND WR-112)

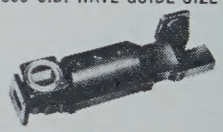

FREQUENCY RANGE: _____ 8500-9600 mc/s
TRANSMITTED INSERTION LOSS: _____ .4 db
RECEIVED INSERTION LOSS: _____ .5 db
MAGNETRON INPUT VSWR: _____ 1.15
ANTENNA INPUT VSWR: _____ 1.15
LOAD TO MAGNETRON ISOLATION: _____ 25 db
MAGNETRON TO RECEIVER ISOLATION: _ 25 db
POWER HANDLING CAPABILITIES: _____ WR-90 — 250 kw peak; 300 watts average @ 20 psia pressure. 200 kw peak — 300 watts average @ 15 psia. WR-112 — 600 kw peak; 600 watts average @ 30 psia pressure.

1.50 X .750 O.D. WAVE GUIDE SIZE

FERRITE ISOLATORS FOR MICROWAVE RELAY
(WR-137 GUIDE SIZE)

FREQUENCY RANGE: ..... 5925 to 6425 mcs.
ISOLATION: ..... 40 db min.
INSERTION LOSS: ..... 1 db max.
INPUT VSWR: ..... 1.15 max.
POWER HANDLING CAPABILITY: 10 watts average; 10 KW peak into
a 2 to 1 load mismatch

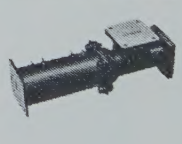

Numerous other ferrite designs are available upon request such as the ferrite attenuator, RF switch, and mixer-ferrite duplexer shown above.

1.50 X .750 O.D. WAVE GUIDE SIZE

BROAD BAND FERRITE TEST ISOLATORS

Waveguide Size (O.D.)	Frequency Range (KMC)	Isolation (DB) (Minimum)	Insertion Loss (DB) (Maximum)	Input VSWR (Maximum)	Average Power (Watts)
.360 x .220	26.5–40.0	30	1.0	1.15	5
.500 x .250	18.0–26.5	30	1.0	1.15	10
.702 x .391	12.4–18.0	30	1.0	1.15	10
1.00 x .500	8.2–12.4	30	1.0	1.15	15
1.25 x .625	7.05–10.0	30	1.0	1.15	15
1.50 x .750	5.85–8.2	30	1.0	1.15	20
2.00 x 1.00	3.95–5.85	25	1.0	1.15	20
3.00 x 1.50	2.60–3.95	20	1.0	1.15	25

Airtron inc.

1122 W. Elizabeth Ave., Linden, New Jersey
Airtron, Cambridge (Ferrite) Division Cambridge, Mass.
Foreign Affiliates:
Airtron Canada, Ltd., Toronto, Canada
W. H. Sanders (Electronics) Ltd., Stevenage Herts, England
Sivers Lab., Hagersten, Sweden

INSTITUTIONAL LISTINGS

The IRE Professional Group on Microwave Theory and Techniques is grateful for the assistance given by the firms listed below, and invites application for Institutional Listing from other firms interested in the Microwave field.

COLLINS RADIO CO., Cedar Rapids, Iowa
Complete Industrial Microwave, Communication, Navigation and Flight Control Systems

HUGHES AIRCRAFT COMPANY, Culver City, Calif.
Radar Systems, Guided Missiles, Antennas, Radomes, Tubes, Solid State Physics, Computers

MARYLAND ELECTRONIC MANUFACTURING CORPORATION, College Park, Md.
Development and Production of Microwave Antennas and Waveguide Components

MICRODOT, INC., South Pasadena, Calif.
Microminiature Coaxial Connectors, Cables, and Assemblies

MICROWAVE TUBE LAB., SYLVANIA ELECTRIC PRODUCTS, INC., 500 Evelyn Ave., Mountain View, Calif.
Traveling-Wave Tubes, Backward Wave Oscillators (Helix and Oscillators), Klystrons

NATIONAL INSTRUMENT CO., INC., 23 E. 26 St., New York, N. Y.
Wide-Band Microwave Equipment, Simulated Flight Instruments, Lobe Switches, Custom Built Precision Apparatus

WEINSCHEL ENGINEERING CO. INC., Kensington, Md.
Attenuation Standards, Coaxial Attenuators and Insertion Loss Test Sets

WHEELER LABORATORIES, INC., 122 Cutter Mill Road, Great Neck, N. Y.
Consulting Services, Research & Development, Microwave Antennas & Waveguide Components

The charge for an Institutional Listing is $50.00 per issue or $140.00 for four consecutive issues. Applications for Institutional Listings and checks (made out to the Institute of Radio Engineers) should be sent to Mr. L. G. Cumming, Technical Secretary, Institute of Radio Engineers, 1 East 79th Street, New York 21, N. Y.

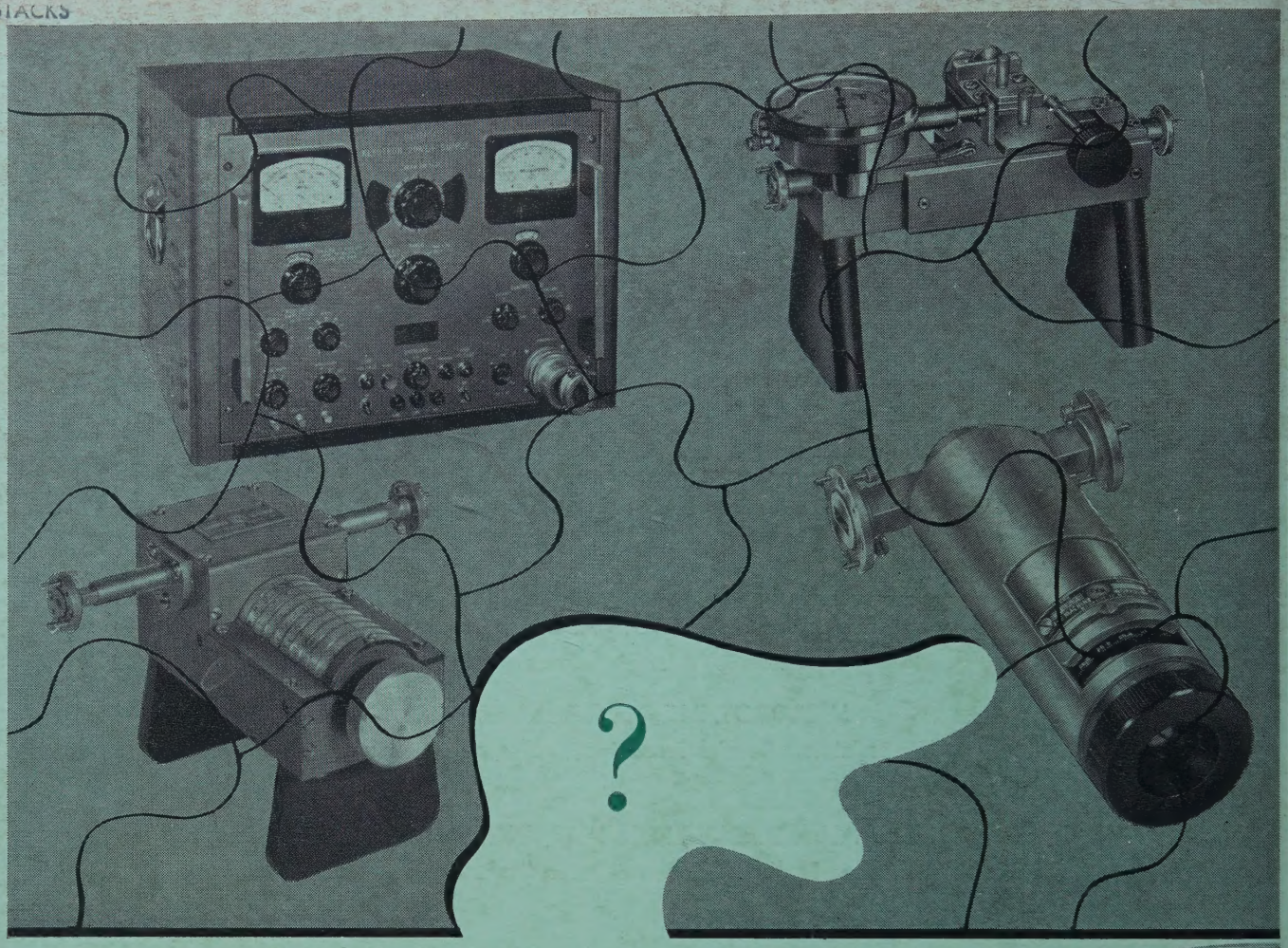

NEED DELIVERY?

Call...

Representatives:

AHMCO **BOEING FIELD** **KING CITY AIRPORT** **SEATTLE 8, WASH.**	WASHINGTON OREGON
A & M ASSOC. **1145 19th ST., N.W.** **WASHINGTON, D. C.**	WASHINGTON, D. C.
HYTRONIC **MEASUREMENTS INC.** **1295 S. BANNOCK ST.** **DENVER 23, COLORADO**	COLORADO NEW MEXICO UTAH WYOMING
KADELL SALES ASSOC. **5875 N. LINCOLN ST.** **CHICAGO 45, ILLINOIS**	ILLINOIS INDIANA WISCONSIN
VAN GROOS CO. **21051 COSTANSO ST.** **WOODLAND HILLS, CALIF.**	CALIFORNIA ARIZONA
SZUCS INT'L CORP. **50 BROAD STREET** **NEW YORK 4, N. Y.**	EXPORT

ELECTRONICS & X-RAY DIVISION · F-R MACHINE WORKS, INC. ·

FXR

for **Precision Microwave Test Equipment**

Electronics & X-Ray Division

F-R MACHINE WORKS, Inc.
Woodside 77, N. Y.
AStoria 8-2800